Total Synthesis of the Δ^{13}-9-Isofurans: A Stereodivergent Approach

By

Zachary Ryan Austin

Dissertation

Submitted to the Faculty of the

Graduate School of Vanderbilt University

in partial fulfillment of the requirements

for the degree of

DOCTOR OF PHILOSOPHY

in

Chemistry

October 31, 2021

Nashville, Tennessee

Approved:

Gary A. Sulikowski, Ph.D.

Brian Bachmann, Ph.D.

Steven Townsend, Ph.D.

James West, Ph.D.

"If you can't do what you imagine, then what is imagination to you?"

- *Kid Cudi*

Acknowledgements

I would like to begin by thanking my advisor Dr. Gary Sulikowski for taking a chance on me and constantly striving to make me a better chemist. This dissertation would not be possible without his guidance and patience. Gary taught me that patience and critical thinking are necessary to be a synthetic chemist and that these skills will prepare me for life. In addition to an academic mentor, Gary was always there for discussions about life and moving forward. I am forever grateful for your mentorship.

I am greatly appreciative of my committee Dr. Brian Bachmann, Dr. Steven Townsend, and Dr. James West. Their guidance and probing questions during committee meetings always led to an increased understanding of my project and a renewed energy for continued learning within the field.

For creating an exciting atmosphere within the laboratory to learn and grow as chemists, I am appreciative of all lab members past and present. I want to thank Dr. Brendan Dutter and Dr. Katherine Chong for your friendship and guidance. Dr. Robert Davis is a perpetual source of support and believed in me when I didn't at times. Our long talks about life keep me pushing forward. Dr. Jennifer Kimbrough was the best benchmate I could have asked for. Her support as a coworker and as a friend means more than she knows. Dr. Jason Hudlicky is someone I truly admire for his perseverance and work ethic. He was also a great distraction when I needed a laugh. Dr. Christopher Fullenkamp was a great source of chemistry advice and always instilled confidence. Dr. Quinn Bumpers and I came to Vanderbilt in the same year and grew as chemists and friends over the years. He was always available whether I needed help or someone to attend a concert. Dr. Alex Allweil has been a great friend and I am glad that we were able to finish graduate school together. I would like to thank Cal Larson for his discussions and hard work on our shared project. I know you will do well in your career.

Graduate school is a challenging endeavor and I would not have survived without the help of a certain few. Dr. Berk Ellis was a great friend throughout. He was always there when I wanted to grab dinner or relax over a round of golf. Caleb West has been my best friend since freshman year of high school. We've been through everything together and I wouldn't be where I am today without him. The West family has been a constant source of support and love for over a decade. To Mrs. Allison, I love you and miss you. I know you would be proud.

None of this would be possible without my family. My parents have given me everything I have ever needed to succeed and have always supported me. The advice and love provided from them means the world to me. My brother John is there for me when I need a laugh or just to talk. He is not only a best friend, but is also the most giving person I know. Thank you to my family. This dissertation is dedicated to you.

Table of Contents

List of Tables

List of Figures

List of Schemes

List of Abbreviations

2,2-DMP	2,2-dimethoxypropane
9-BBN	9-borbicyclo[3.3.1]nonane
AA	arachidonic acid
Ac	acetyl
AcOH	acetic acid
Ac_2O	acetic anhydride
BMPR2	bone morphogenic protein receptor type 2
BsCl	benzenesulfonyl chloride
CBS	Corey-Bakshi-Shibata
d	doublet
Da	Dalton
DCC	dicyclohexylcarbodiimide
DDQ	2,3-dichloro-5,6-dicyano-1,4-benzoquinone
DIAD	diisopropyl azodicarboxylate
DIBAL-H	diisobutylaluminum hydride
DMAP	4-dimethylaminopyridine
DMF	dimethylformamide
DMP	Dess-Martin periodinane
ELOVL5	elongation of very long chain fatty acids protein 5
Et	ethyl
Et_2O	diethyl ether
EtOAc	ethyl acetate
FADS1	fatty acid desaturase 1
FADS2	fatty acid desaturase 2
g	gram
GC-MS	gas chromatography-mass spectrometry
GPR55	G protein-coupled receptor 55
H_2O_2	hydrogen peroxide
ImH	imidazole
IsoF	isofuran
IsoP	isoprostane
KHMDS	potassium bis(trimethylsilyl)amide
L	liter
LAH	lithium aluminum hydride
LC/MS	liquid chromatography / mass spectrometry
LRMS	low resolution mass spectrometry
m	multiplet
M	molar concentration
m-CPBA	meta-chloroperoxybenzoic acid
Me	methyl
MeCN	acetonitrile
MHz	megahertz
mol	mole
Ms	methanesulfonate

NaHMDS	sodium bis(trimethylsilyl)amide
n-BuLi	*n*-butyllithium
NCS	N-chlorosuccinimide
NEt_3	triethylamine
PAH	pulmonary arterial hypertension
PCC	pyridinium chlorochromate
$PGF_{2\alpha}$	prostaglandin $F_{2\alpha}$
PGG_2	prostaglandin G_2
PhH	benzene
PhMe	toluene
PMVEC	pulmonary microvascular endothelial cell
PNBA	4-nitrobenzoic acid
p-TSA	para-toluenesulfonic acid
ROS	reactive oxygen species
s	singlet
SAD	Sharpless asymmetric dihydroxylation
SAE	Sharpless asymmetric epoxidation
t	triplet
TBACl	tetrabutylammonium chloride
TBAF	tetrabutylammonium fluoride
TBDPSCl	*tert*-butyldiphenylchlorosilane
TBS	*tert*-butyldimethylsilyl
TEMPO	2,2,6,6-Tetramethylpiperidinyloxy
Tf_2O	trifluoromethanesulfonic anhydride
TFA	trifluoroacetic acid
THF	tetrahydrofuran
$TMSCHN_2$	(trimethylsilyl)diazomethane
TMSCl	trimethylsilyl chloride
TP	thromboxane A_2 receptor
TrCl	trityl chloride

Chapter 1: Autoxidation of Arachidonic Acid Under Oxidative Stress

Arachidonic Acid

Arachidonic acid (AA) is a non-essential fatty acid obtained through foods or the desaturation and chain elongation of linoleic acid.[1] AA is integral to cellular membrane structure, modulates various ion channels and enzymes, and serves as a precursor to a number of physiologically important secondary metabolites, known collectively as eicosanoids. These eicosanoids are produced through enzymatic metabolism as well as non-enzymatic autoxidation processes. For the majority of the period in which AA metabolites have been studied, enzymatically produced eicosanoids were thought to be the only ones of physiological relevance. However, in the past few decades eicosanoids produced via autoxidative pathways have come to the forefront of discussion. This resulted from the discovery that large amounts of isoprostanes (structurally similar to prostaglandins) were formed in vivo in humans and shown to possess biological activity.[2] More recently, the formation of another family of non-enzymatic eicosanoids known as the isofurans was observed.[3] The free radical conditions under which these compounds are formed, known as oxidative stress, have been linked to numerous disease states including cardiovascular disease, diabetes, cancer, neurodegenerative diseases, chronic kidney disease, pulmonary arterial hypertension, etc.[4–6] As such, the isoprostanes and isofurans serve as crucial tools for the assessment of these disease states and are believed to serve physiological roles.

Biosynthesis of Arachidonic Acid from Linoleic Acid

The primary sources of arachidonic acid from food are poultry, fish, and various other forms of meat. As a result, it is vital for herbivores and vegetarians to obtain arachidonic acid via

biosynthesis from linoleic acid, which is abundant in many nuts and seeds.[1] The production of arachidonic acid begins with desaturation of linoleic acid by fatty acid desaturase 2 (FADS2) to γ-linolenic acid (Scheme 1.1).[7] Enzymatic chain elongation of γ-linolenic acid by way of fatty acid

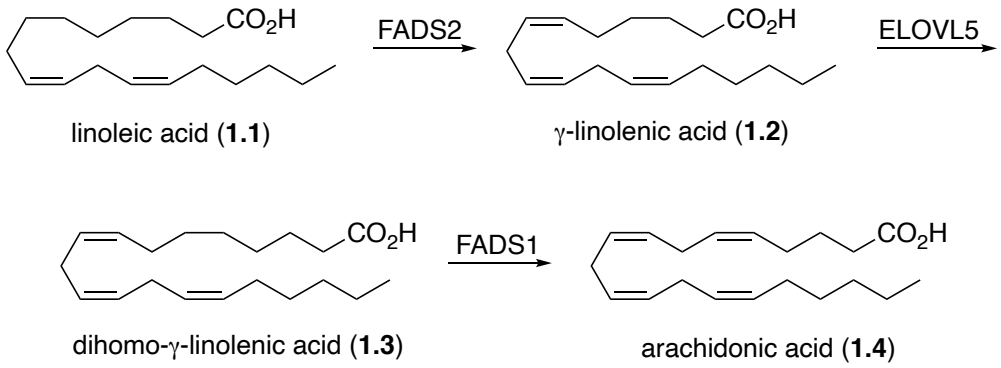

Scheme 1.1 Biosynthesis of arachidonic acid from linoleic acid.

elongase 5 (ELOVL5) extends the carbon chain to the requisite twenty carbons. In a final desaturation step, fatty acid desaturase 1 (FADS1) installs the fourth *cis*-double bond to yield arachidonic acid which can be taken up as phospholipids in the cellular membrane.

Reactivity of Arachidonic Acid

Polyunsaturated fatty acids, such as arachidonic acid, display a much greater reactivity toward free-radical intermediates than their mono-unsaturated and saturated fatty acid counterparts. This results from the presence of multiple double bonds creating bis-allylic sites within the fatty acid rendering these positions susceptible to hydrogen atom abstraction. This abstraction is the primary step in the autoxidative metabolism of all polyunsaturated fatty acids.[2] In the case of arachidonic acid, there are three bis-allylic positions at carbon numbers 7, 10, and 13 (Figure 1.1). Porter and co-workers have estimated the bond dissociation enthalpy (BDE) of these three C-H bonds to be in the 78-80 kcal/mol range, which is approximately 10 kcal/mol lower

in energy than the allylic C-H bonds present in monounsaturated fatty acids, such as oleic acid.[8] This process of lipid autoxidation in biological systems can be initiated by free radicals generated

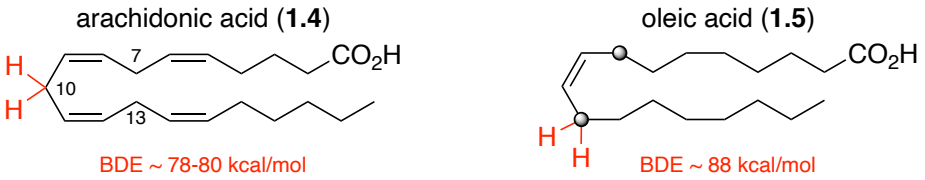

Figure 1.1 BDE of C-H bonds in polyunsaturated and mono-unsaturated fatty acids.

through exogenous means (smoking, UV-light, air pollution, etc.) or endogenous systems (NADPH oxidase, xanthine oxidase, leakage from the electron transport chain, etc.).[9] The major source of these radicals is in the form of reactive oxygen species, otherwise known as ROS. Once initiated, the bis-allylic radicals propagate upon reaction with molecular oxygen to generate peroxyl radicals. The rate of this oxygen addition is correlated to the local concentration of oxygen in the tissues or organs. Therefore, the autoxidation products formed from arachidonic acid are dependent on physiological state. This is apparent in the formation of two of the classes of compounds associated with autoxidation via ROS: isoprostanes and isofurans.

Isoprostanes

Isoprostanes have been known as products of autoxidation of AA since the 1970s. However, the first class of known as the F_2-isoprostanes were discovered and characterized in 1990 by Morrow and co-workers as autoxidation products observed in vivo in human and rat plasma / urine as a result of oxidative stress.[10] This class of isoprostanes were named F_2-isoprostanes in accordance with prostaglandin nomenclature as their cyclopentane functionality and unsaturated side-chains corresponded to the enzymatically formed prostaglandin F_2 (PGF_2)

series. In addition to the F_2-isoprostanes, isoprostanes bearing synonymous ring substitution patterns to other prostaglandins have been observed (Figure 1.2).

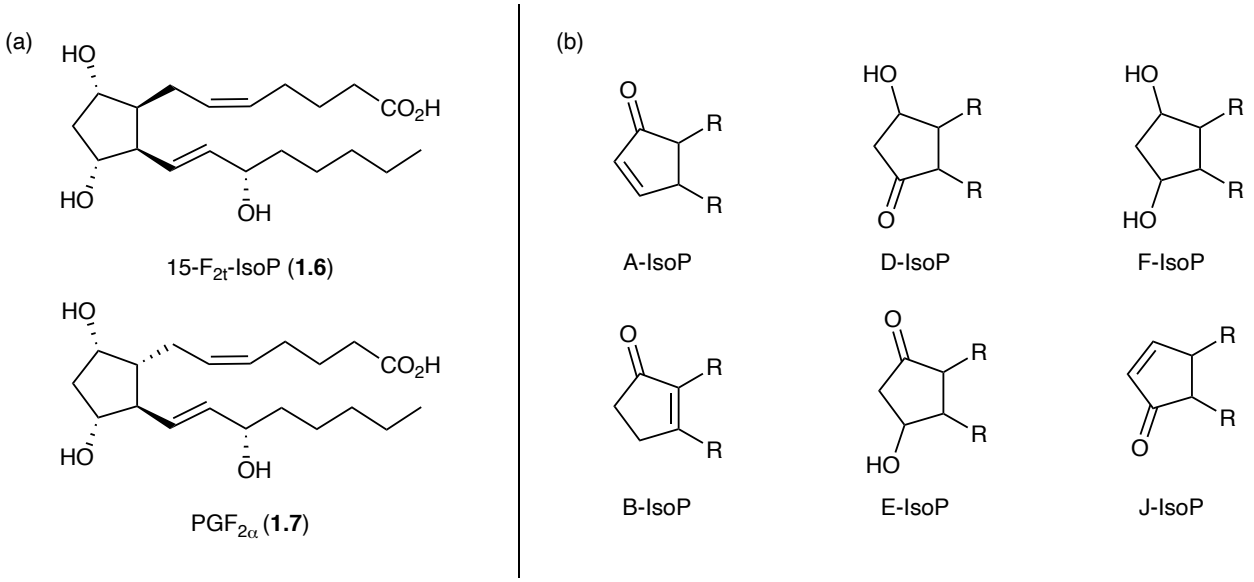

Figure 1.2 (**a**) 15-F_{2t}-isoprostane and prostaglandin $F_{2\alpha}$. (**b**) Isoprostane ring type nomenclature derived from prostaglandins.

Autoxidative Production of F_2-Isoprostanes

The F_2-isoprostane family consists of four constitutional isomers: 5-F_2-IsoPs, 8-F_2-IsoPs, 12-F_2-IsoPs, and 15-F_2-IsoPs (Figure 1.3).

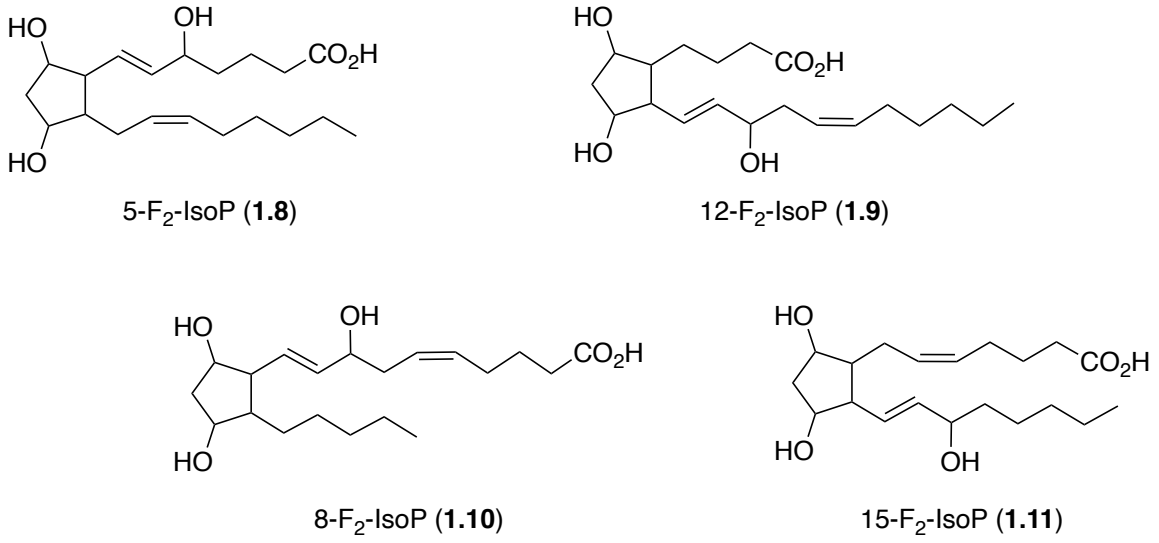

Figure 1.3 Four F_2-isoprostane constitutional isomers.

Formation of these IsoPs begins with the radical abstraction of hydrogen from one of three bis-allylic positions (*vide supra*) by a radical source, such as ROS (Scheme 1.2). Reaction of the newly formed radical intermediates **1.12-1.14** with an equivalent of oxygen generates peroxy radical intermediates **1.15-1.18**. Upon 5-exo-trig cyclization to form endoperoxides **1.19-1.22**, another 5-exo-trig radical cyclization occurs forming the cyclopentane ring of the isoprostanes. The alkyl sidechains are shown in the energetically favorable equatorial orientation which leads to *cis*-orientation after cyclization. The resulting carbon radical is trapped with another equivalent of oxygen generating PGG_2-like intermediates **1.23-1.26**. Reduction of the peroxide intermediate produces the corresponding four F_2-isoprostane isomers **1.8-1.11** (Figure 1.3). Of these four isoprostanes, the 5-F_2-isoprostanes (**1.8**) and the 15-F_2-isoprostanes (**1.11**) are produced in the greatest amounts. This is believed to be a result of the tendency of the peroxyl radical precursors to **1.24** and **1.25** to further cyclize and oxidize to dioxolane-isoprostanes.[11]

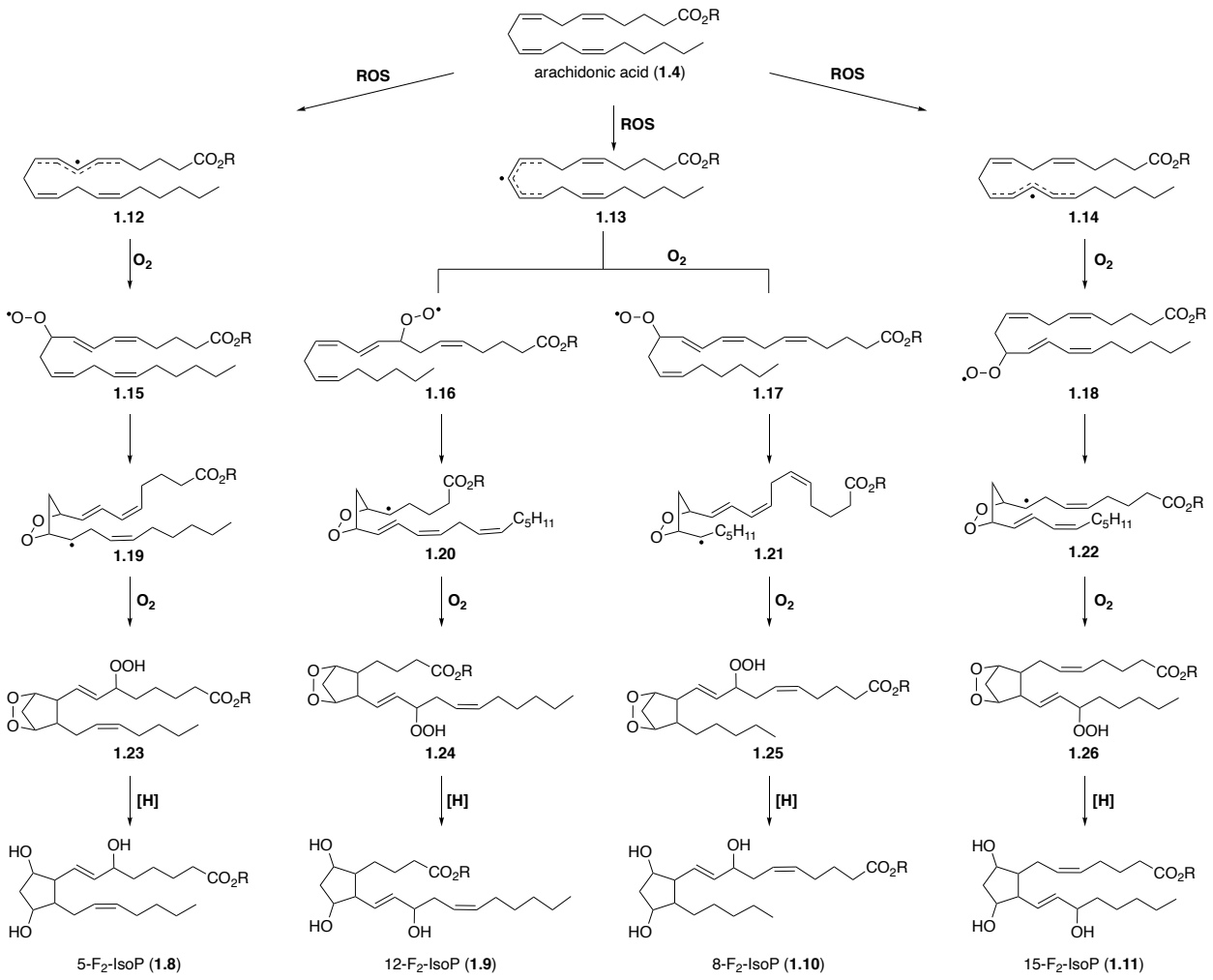

Scheme 1.2 Autoxidative formation of four F_2-isoprostane constitutional isomers.

Discovery of the Isofurans

In 2002, Roberts and Fessel, reported the discovery of a novel class of non-enzymatically produced eicosanoid metabolites termed isofurans (IsoF).[3] Upon oxidation of AA in vitro, a set of compounds distinct from the isoprostanes were observed using GC-MS. Characteristics such as a similar retention time and a mass of 16 Da higher than the isoprostandes led to the postulation that these novel autoxidation products were structurally related, possessing an additional oxygen atom.

Treatment of these compounds with various reagents in an attempt to elucidate their structure resulted in the conclusion that the functionality distinctive from the isoprostanes was in the form of a furan ring leading to their isofuran parent name. Isotopic labeling studies further confirmed this assumption and provided two possible pathways to the formation of the isofurans: the cyclic peroxide cleavage pathway and the epoxide hydrolysis pathway.[3] These pathways result in the production of 8 constitutional isomers of the isofurans (Figure 1.4) each possessing 5 stereocenters leading to a total of 256 individual isofuran isomers.

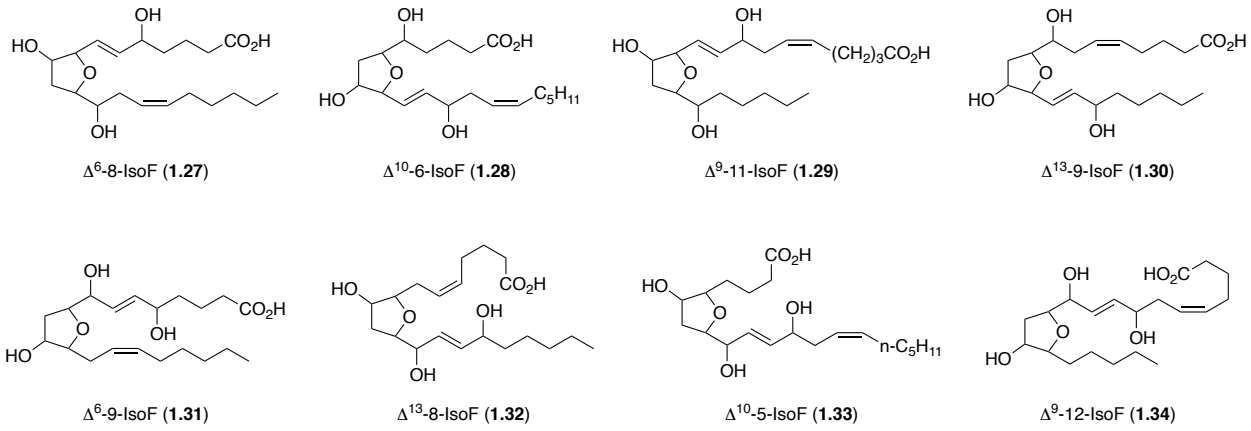

Figure 1.4 Eight isofuran constitutional isomers.

Isofuran Nomenclature

In 2003, Roberts and coworkers proposed a unified nomenclature of the isofuran family of compounds, an extension of their previously described isoprostane nomenclature.[12] Due to the large number of stereoisomers, it was important to establish a system of naming in which each isomer could readily be differentiated. Following eicosanoid nomenclature precedent, carbon numbering begins with the carboxylic acid moiety (Figure 1.5a). The relative orientation of the alkyl chains of the furan is denoted as anti (A) or syn (S). The relative orientation of the furan hydroxyl group and the neighboring alkyl chain is denoted as cis (C) or trans (T). Following assignment of relative orientations, Δ^n is utilized to signify the lowest carbon number of the *E*-

alkene (n), then the lowest carbon number of the furan ring followed by the IsoF suffix. The default stereochemistry of the sidechain alcohols is (*S*). Any deviation from this default stereochemistry is denoted with carbon number followed by the prefix "epi". If the stereochemistry at the first carbon of the furan is (*R*), then the entire name is prefaced with the prefix "*ent*" and the default stereochemistry of the sidechain alcohols becomes (*R*). From the two proposed pathways of isofuran production, two classes of isofurans emerge: the alkenyl and enediol isofurans. The

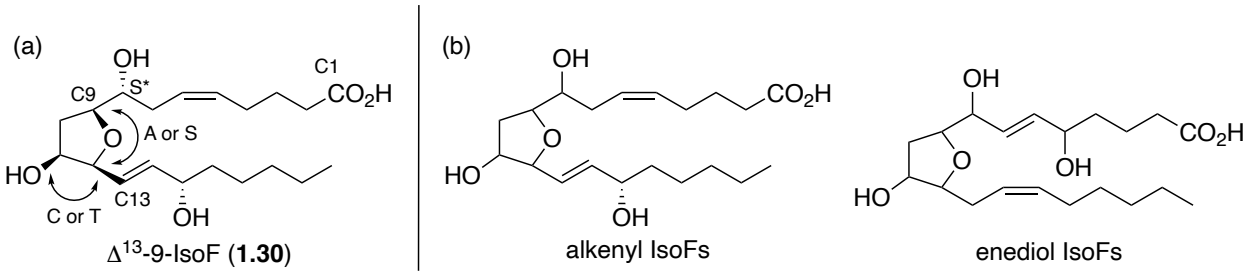

Figure 1.5 Isofuran nomenclature established by Roberts and coworkers: (**a**) Guideline to naming individual isofuran isomers. (**b**) Alkenyl and enediol isofurans are the two classes distinguished by the location of the furanyl alcohol in relation to the allyl alcohol sidechain.

alkenyl isofurans are characterized by the proximal relation of the ring alcohol to the *E*-alkene. The enediol isofurans are recognizable due to the ring alcohol being distal to the sidechain possessing the *E*-alkene.[2] Each of these classes is comprised of 4 constitutional isomers.

Autoxidative Production of Isofurans

Cyclic Peroxide Cleavage Pathway The autoxidation of AA in the presence of $^{18}O_2$ and $H_2{}^{18}O$ yielded a distribution of isotopically labeled isofurans providing two distinct pathways to their formation. The first pathway, known as the cyclic peroxide cleavage pathway incorporated $^{18}O_2$ solely from isotopic oxygen gas. Scheme 1.3 demonstrates the proposed pathway generated from these results.

Beginning with free or esterified arachidonic acid, a free-radical (ROS) abstracts a hydrogen from one of three bis-allylic positions (Scheme 1.3). This radical intermediate reacts with molecular oxygen to form endoperoxides **1.19**-**1.22**, which are present in both this pathway and the isoprostane autoxidative pathway. The presence of these common intermediates has important physiological implications, which will be discussed in the role of these compounds as biomarkers of oxidative stress. At higher levels of oxygen concentration, reaction of these radical intermediates with molecular oxygen to form diperoxides **1.35**-**1.38** interrupts the intramolecular cyclization necessary for isoprostane formation. A single electron reduction of the endoperoxide

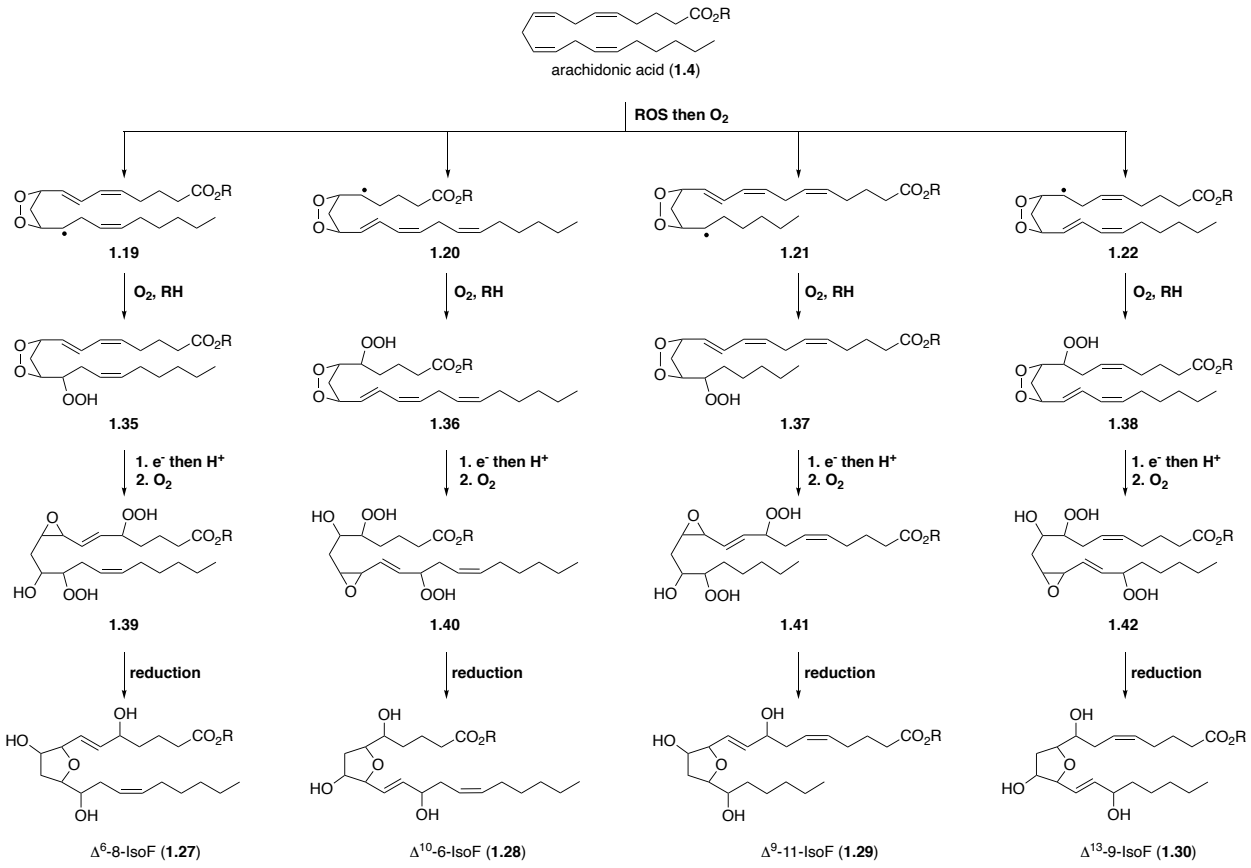

Scheme 1.3 Cyclic peroxide cleavage pathway formation of alkenyl isofurans.

moiety is followed by a 3-exo-trig radical cyclization to generate the epoxides. The newly formed allyl radical traps another equivalent of oxygen to form epoxides **1.39**-**1.42**. Subsequent intramolecular cyclization and reduction affords each of the alkenyl-IsoFs.

Epoxide Hydrolysis Pathway The second mechanism of isofuran production is referred to as the epoxide hydrolysis pathway in which 3 atoms of oxygen are introduced via molecular oxygen, and the final oxygen atom is delivered through epoxide hydrolysis (as determined through isotopic labeling). This pathway is responsible for the formation of a portion of the alkenyl-isofurans and all of the enediol-isofurans.[13]

In a similar manner to the other autoxidation pathways of AA, a free-radical (ROS) abstracts 1 of 3 bis-allylic hydrogens and the newly formed radical reacts with molecular oxygen to form endoperoxides **1.19** and **1.22** (Scheme 1.4). Cleavage of the endoperoxide moiety allows for formation of the diepoxide followed by reaction with molecular oxygen to give diepoxy hydroperoxides **1.43** and **1.44**. Hydrolysis of a single epoxide produces epoxy diols **1.45**-**1.48** from which a 5-exo or 5-endo-tet cyclization provides the furan core. Ensuing reduction of the hydroperoxide furnishes Isofurans **1.27** and **1.30**-**1.32**. Isofurans **1.28**, **1.29**, **1.33**, and **1.34** are also produced in a similar manner.

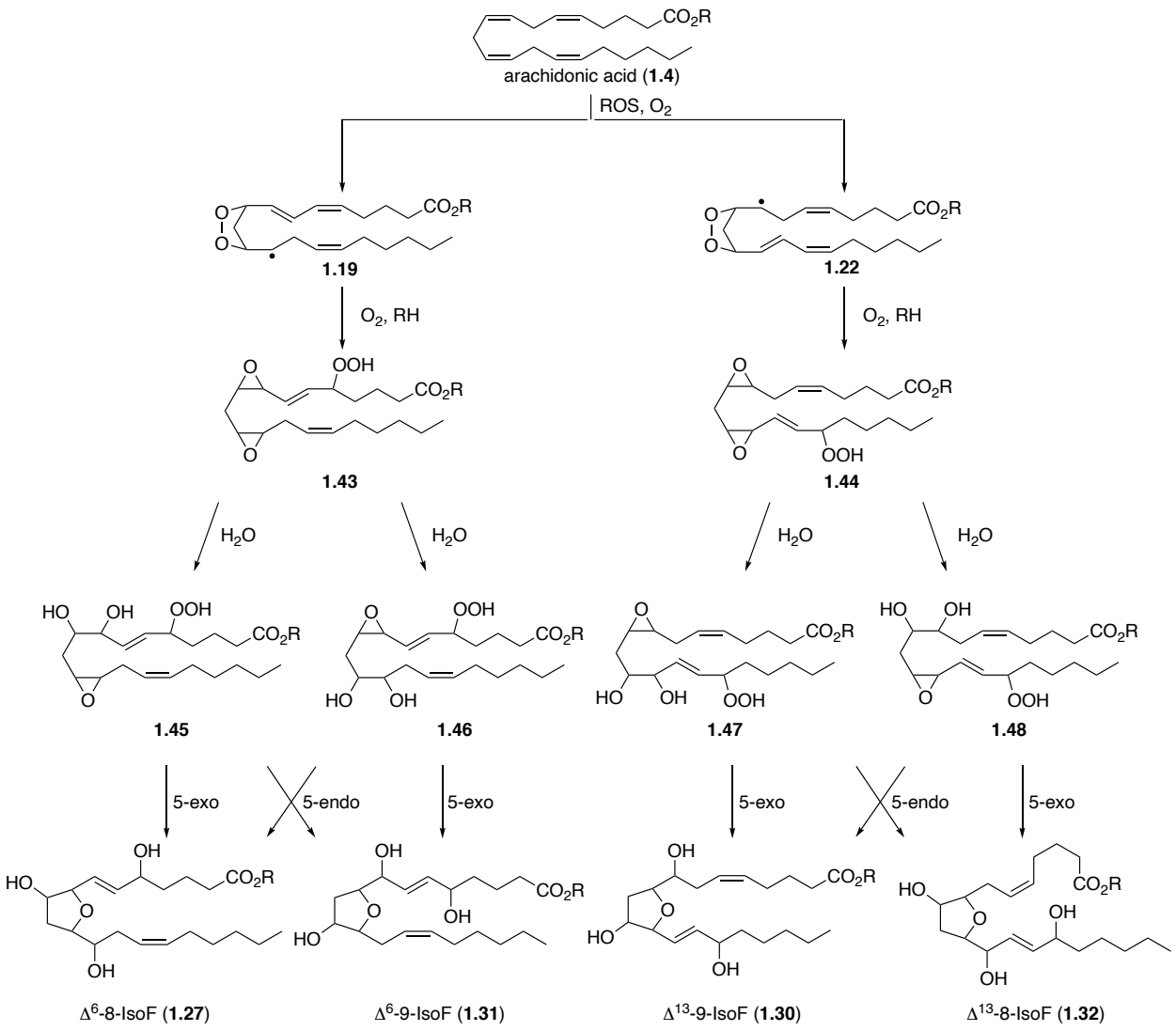

Scheme 1.4 Epoxide hydrolysis pathway production of the 8 isofuran regioisomers (4 shown).

Autoxidation of AA in the Context of Oxygen Concentration

As previously mentioned, a common radical intermediate (i.e. **1.22**) exists between the autoxidative formation of F_2-isoprostanes and isofurans. Roberts and coworkers hypothesized that due to the competitive rate of oxygen addition to radical cyclization, increasing levels of oxygen

tension could positively modulate the formation of isofurans (Scheme 1.5). As a result, they performed a series of experiments to determine the extent to which oxygen concentration determines the ratio of isofurans to isoprostanes.[3] Upon *in vitro* oxidation of AA at various levels of oxygen tension, it was observed that 21% ambient oxygen was the point at which isoprostane formation plateaued. As expected, the formation of isofurans increased until 100% ambient oxygen

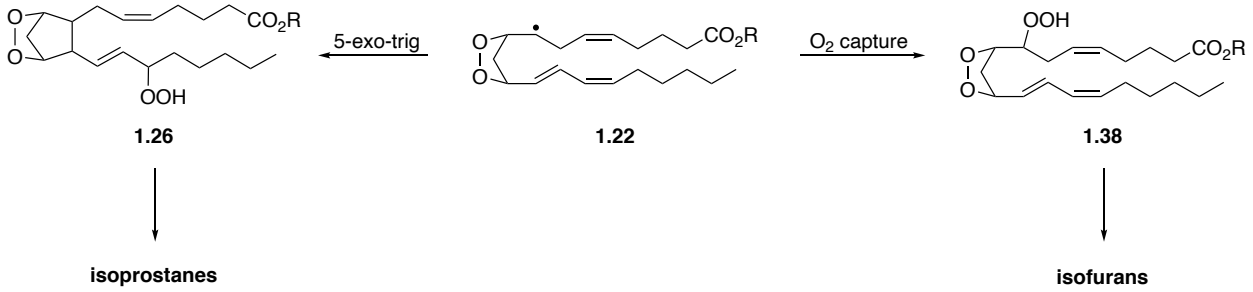

Scheme 1.5 Isoprostane / isofuran formation dependence on oxygen concentration.

was reached. The *in vivo* autoxidation product ratios supported this observation in rats. In rats treated with carbon tetrachloride (CCl_4), which is known to induce oxidative injury, the ratios of isofurans to isoprostanes in the liver were much lower than more highly oxygenated organs, such as the kidney and brain hippocampus. As a result of the production of isofurans in response to oxidative stress, it is hypothesized that using isofurans in addition to isoprostanes will serve as a more complete assessment of oxidative injury in the context of disease.

Isoprostanes as Clinical Biomarkers of Oxidative Stress

Within a decade of their characterization, the F_2-isoprostanes became widely regarded as reliable biomarkers as relates to assessing oxidative stress in vivo. This designation was a result of several defining factors of this particular class of isoprostanes. These include F_2-IsoP's stability, detectability under normal physiological conditions in every biological tissue and fluid, increased

production under conditions of oxidative stress, regulated production via antioxidants, and their formation is independent of lipid content of a patient's diet.[14–16] The combined result of these characteristics is a stable biomarker that is capable of the precise identification of oxidative stress with minimal invasiveness. According to a study funded by the National Institutes of Health, F_2-isoprostanes serve as the most accurate biomarker of oxidative stress *in vivo* via urine and plasma analysis.[17] However, recent literature has demonstrated that the utilization of F_2-IsoPs' for this purpose is a complex process due to convoluting factors such as the measurement of free F_2-isoprostane as opposed to esterified F_2-isoprostane and the untangling of F_2-isoprostane single isomers produced non-enzymatically as opposed to those produced via cyclooxygenase enzymes.[18] The resolution of these issues is of great value as the use of F_2-isoprostanes in a clinical setting could aid in antioxidant-based therapy.

There are a large number of oxidative stress-associated diseases for which F_2-IsoP's serve as valuable biomarkers. In a large meta-analysis performed by van't Erve and coworkers, 50 health conditions and environmental factors were ranked in order of the extent to which oxidative stress is involved in the pathogenesis of disease.[19] 15-F_{2t}-IsoP, the most commonly used F_2-IsoP biomarker, showed the largest increase in conditions such as cystic fibrosis, pulmonary arterial hypertension, chronic renal insufficiency, Rett syndrome, autism disorder, congestive heart failure and others. Further analysis is required on other F_2-IsoP isomers, yet this work provides a starting point for the assessment and treatment of these diseases most correlated to oxidative stress.

In these disease states most affected by oxidative stress, the use of IsoFs as biomarkers should theoretically serve as a more accurate index (*vide supra*). Comparison of the ratios of these two classes of compounds in a physiological context would provide valuable insight to treating patients sustaining oxidative injury.

References

(1) Tallima, H.; El Ridi, R. *J. Adv. Res.* **2018**, *11*, 33–41.

(2) Jahn, U.; Galano, J.-M.; Durand, T. *Angew. Chem. Int. Ed.* **2008**, *47* (32), 5894–5955.

(3) Fessel, J. P.; Porter, N. A.; Moore, K. P.; Sheller, J. R.; Roberts II, L. J. *Proc. Natl. Acad. Sci.* **2002**, *99*, 16713–16718.

(4) Liguori, I.; Russo, G.; Curcio, F.; Bulli, G.; Aran, L.; Della-Morte, D.; Gargiulo, G.; Testa, G.; Cacciatore, F.; Bonaduce, D.; Abete, P. *Clin. Interv. Aging* **2018**, *13*, 757–772.

(5) Schleicher, E.; Friess, U. *Kidney Int.* **2007**, *72*, S17–S26.

(6) Uttara, B.; Singh, A.; Zamboni, P.; Mahajan, R. *Curr. Neuropharmacol.* **2009**, *7* (1), 65–74.

(7) Hanna, V.; Hafez, E. *J. Adv. Res.* **2018**, *11*, 23–32.

(8) Pratt, D.; Mills, J.; Porter, N. A. *J. Am. Chem. Soc.* **2003**, *125*, 5801–5810.

(9) Yin, H.; Xu, L.; Porter, N. A. *Chem. Rev.* **2011**, *111*, 5944–5972.

(10) Morrow, J. D.; Hill, K. E.; Burk, R. F.; Nammour, T. M.; Badr, K. F.; Roberts II, L. J. *Proc. Natl. Acad. Sci.* **1990**, *87*, 9383–9387.

(11) Yin, H.; Morrow, J. D.; Porter, N. A. *J. Biol. Chem.* **2004**, *279*, 3766–3776.

(12) Taber, D. F.; Fessel, J. P.; Roberts, L. J. *Prostaglandins Other Lipid Mediat.* **2004**, *73*, 47–50.

(13) Roberts, L. J.; Fessel, J. P. *Chem. Phys. Lipids* **2004**, *128*, 173–186.

(14) Roberts, L. J.; Morrow, J. D. *Free Radic. Biol. Med.* **2000**, *28*, 505–513.

(15) Burk, R.. *Biochim. Biophys. Acta BBA - Gen. Subj.* **1983**, *757*, 21–28.

(16) Richelle, M.; Turini, M. E.; Guidoux, R.; Tavazzi, I.; Métairon, S.; Fay, L. B. *FEBS Lett.* **1999**, *459*, 259–262.

(17) Kadiiska, M. B.; Gladen, B. C.; Baird, D. D.; Germolec, D.; Graham, L. B.; Parker, C. E.; Nyska, A.; Wachsman, J. T.; Ames, B. N.; Basu, S.; Brot, N.; FitzGerald, G. A.; Floyd, R. A.; George, M.; Heinecke, J. W.; Hatch, G. E.; Hensley, K.; Lawson, J. A.; Marnett, L. J.; Morrow, J. D.; Murray, D. M.; Plastaras, J.; Roberts, L. J.; Rokach, J.; Shigenaga, M. K.; Sohal, R. S.; Sun, J.; Tice, R. R.; Van Thiel, D. H.; Wellner, D.; Walter, P. B.; Tomer, K. B.; Mason, R. P.; Barrett, J. C. *Free Radic. Biol. Med.* **2005**, *38*, 698–710.

(18) Milne, G. L. *Redox Biol.* **2017**, *12*, 897–898.

(19) van ’t Erve, T. J.; Kadiiska, M. B.; London, S. J.; Mason, R. P.. *Redox Biol.* **2017**, *12*, 582–599.

Chapter 2: Physiological Roles of F_2-Isoprostanes and Isofurans

Reactive Oxygen Species

Before discussing the physiological roles of autoxidatively produced AA metabolites, it is important to identify the sources of reactive oxygen species (ROS) within the body, their role as signaling molecules, and their deleterious effects in the context of oxidative stress. Even though ROS are present under normal physiological conditions, oxidative stress occurs when there is an imbalance between these species and the antioxidant mechanisms meant to regulate them. There are three main molecules associated with ROS. These include hydrogen peroxide, superoxide, and the hydroxyl radical. Each of these are the byproduct of oxygen reacting with electrons from oxidative metabolism processes within the cell.[20]

H_2O_2 is generated through the dismutation of superoxide by superoxide dismutases (SODs), along with other oxidases, and serves as an important signal transduction molecule in redox biology. The ability of H_2O_2 at low concentrations to oxidize cysteine residues in proteins allows for allosteric changes altering protein function.[21] This oxidation of thiolate anions at nanomolar concentration results in the formation of cysteine sulfenic acid or disulfide residues regulating key processes such as inflammation, aging, circadian rhythm, tissue repair, etc.[22,23] However, at higher levels of H_2O_2 irreversible oxidation of cysteine residues occurs resulting in the formation of sulfinic and sulfonic acids. This irreversible protein damage is an example of oxidative damage triggered by H_2O_2.

A second form of ROS is superoxide, denoted as $O_2^{\cdot-}$. This species serves as a source of H_2O_2 production and is generated from the one-electron reduction of molecular oxygen via NADPH oxidases (NOXs) or electron transport chain (ETC) within the mitochondria.[21,24] Similar

to H_2O_2, superoxide can act as a signaling molecule through various methods, although to a lesser extent, in relation to processes such as cell survival or autophagy.[25] However, superoxide is more strongly associated with oxidative stress than signal transduction. Upon reaction with iron-sulfur cluster containing proteins, superoxide oxidizes the [4Fe-4S] centers allowing for release of iron and damage / inactivation of these proteins.

While superoxide itself is not directly responsible for the oxidative damage to polyunsaturated lipids or DNA, it is responsible for the release of iron that catalyzes the production of hydroxyl radicals through Fenton-like reaction with H_2O_2.[26] This third form of ROS is the most destructive of the three species discussed. Hydroxyl radicals are highly reactive and oxidatively damage polyunsaturated lipids, proteins, DNA, and other biomolecules without discrimination. The formation of these free radicals leads to a large increase in autoxidative metabolites present in disease states associated with oxidative stress.

Physiology of F_2-Isoprostanes

In addition to being valuable indicators of oxidative stress, F_2-isoprostanes have proven to possess biological activity. 15-F_{2t}-IsoP (**1.6**) is the most widely studied isoprostane and has demonstrated vasoconstrictive properties in numerous tissues and vascular systems. This process is predominantly mediated by thromboxane A_2 (TP) receptors.[27,28] In addition to vasoconstriction, 15-F_{2t}-isoprostane has also been shown to induce mitogenic signaling in uterine vascular smooth muscle cells via a protein kinase cascade.[29] In human whole blood, 15-F_{2t}-isoprostanes inhibited platelet aggregation mediated by TP receptors. However, in platelet-rich plasma 15-F_{2t}-IsoP exhibited potentiation of platelet aggregation induced by TP receptor agonists, yet did not prove to possess proaggregatory characteristics alone.[30] This class of isoprostanes has been associated

with various other physiological responses, yet their role in the disease states for which they are biomarkers remains relatively unclear. Understanding the contribution of autoxidatively formed AA products to disease states related to oxidative stress is necessary to mature this field of study.

Isofurans in the Context of PAH

Pulmonary Arterial Hypertension The right ventricle of the heart is responsible for circulating venous blood to the lungs for oxygenation.[31] Pulmonary arterial hypertension (PAH) is a fatal disease involving an increased resistance to this blood flow, defined as ≥25 mmHg resting pulmonary arterial pressure.[32] Several factors lead to this increased resistance such as endothelial dysfunction, thrombosis, vascular stiffening, and vascular remodeling leading to a decrease in lumen diameter.[33,34] This process of increased resistance in the pulmonary arterial system is believed to ultimately prove fatal due to progressive right heart failure or sudden death.[35]

Oxidative stress is a notable characteristic of PAH at the cellular level including abnormal proliferation of pulmonary endothelial cells and smooth muscle cells.[36,37] Associated vasoconstriction is labeled as one of the integral elements in the beginning stages of PAH.[38] Along with an angiogenic increase in endothelial and smooth muscle cells, the increase in ROS production results in lipid peroxidation yielding a number of autoxidative products. F_2-isoprostane and isofuran formation have both been found to increase in patients with PAH.[39,40] Even with the abundance of observations pertaining to the PAH phenotype, the understanding of the root molecular causes behind this disease remain unclear.[41]

Isofuran Mechanism of Action Hypothesis Isofurans are the preferred lipid peroxidation products formed in PAH due to the large amount of oxygen present within the lungs and mitochondrial dysfunction associated with the pathogenesis of this disease. These two factors

result in an excess of oxygen and ROS. Isofurans have been demonstrated to act as an agonist for the endocannabinoid receptor GPR55, which leads to activation of members of the Rho-GTPase family responsible for cytoskeletal organization. Abnormal signaling within this pathway can result in cystoskeletal defects associated with heritable PAH derived from a mutation in bone morphogenic protein receptor type 2 (BMPR2).[42] Fessel, West, and coworkers have also shown in rat brains that isofurans can promote endothelial cell proliferation and an increase in angiogenesis. Pulmonary microvascular endothelial cells (PMVECs) possessing the BMPR2 mutation also exhibited angiogenic tube formation in a similar manner as PMVECs treated with isofurans. Additionally, isofurans demonstrated the ability to restrict intracellular trafficking of various receptors in a manner similar to the BMPR2 mutation.[43] These findings lead to the hypothesis that isofurans formed in excess in the lungs target GPR55 and induce the same underlying abnormalities observed in PAH pathogenesis. Synthesis of a large number of individual isofuran isomers is needed for further examination of this hypothesis.

References

(20) Auten, R. L.; Davis, J. M. *Pediatr. Res.* **2009**, *66*, 121–127.

(21) Schieber, M.; Chandel, N. S. *Curr. Biol.* **2014**, *24*, R453–R462.

(22) Rhee, S. G. *Exp. Mol. Med.* **1999**, *31*, 53–59.

(23) Sies, H. *J. Biol. Chem.* **2014**, *289*, 8735–8741.

(24) Brand, M. D. *Exp. Gerontol.* **2010**, *45*, 466–472.

(25) Chen, Y.; Azad, M. B.; Gibson, S. B. *Cell Death Differ.* **2009**, *16*, 1040–1052.

(26) Fridovich, I. *J. Biol. Chem.* **1997**, *272*, 18515–18517.

(27) Janssen, L. J. *Chem. Phys. Lipids* **2004**, *128*, 101–116.

(28) Cracowski, J.-L.; Devillier, P.; Durand, T.; Stanke-Labesque, F.; Bessard, G. *J. Vasc. Res.* **2001**, *38*, 93–103.

(29) Miggin, S. M.; Kinsella, B. T. *Biochim. Biophys. Acta BBA - Mol. Cell Res.* **2001**, *1539*, 147–162.

(30) Cranshaw, J. H.; Evans, T. W.; Mitchell, J. A. *Br. J. Pharmacol.* **2001**, *132*, 1699–1706.

(31) Naeije, R.; Manes, A. *Eur. Respir. Rev.* **2014**, *23*, 476–487.

(32) Galiè, N.; Humbert, M.; Vachiery, J.-L.; Gibbs, S.; Lang, I.; Torbicki, A.; Simonneau, G.; Peacock, A.; Vonk Noordegraaf, A.; Beghetti, M.; Ghofrani, A.; Gomez Sanchez, M. A.; Hansmann, G.; Klepetko, W.; Lancellotti, P.; Matucci, M.; McDonagh, T.; Pierard, L. A.; Trindade, P. T.; Zompatori, M.; Hoeper, M. *Eur. Respir. J.* **2015**, *46*, 903–975.

(33) Culley, M. K.; Chan, S. Y. *J. Clin. Invest.* **2018**, *128*, 3704–3715.

(34) Epstein, F. H.; Gibbons, G. H.; Dzau, V. J. *N. Engl. J. Med.* **1994**, *330*, 1431–1438.

(35) Tonelli, A. R.; Arelli, V.; Minai, O. A.; Newman, J.; Bair, N.; Heresi, G. A.; Dweik, R. A. *Am. J. Respir. Crit. Care Med.* **2013**, *188*, 365–369.

(36) Sakao, S.; Tatsumi, K.; Voelkel, N. F. *Respir. Res.* **2009**, *10*, 95.

(37) He, S.; Zhu, T.; Fang, Z. *Int. J. Hypertens.* **2020**, *2020*, 1–10.

(38) Reis, G. S.; Augusto, V. S.; Silveira, A. P. C.; Jordão, A. A.; Baddini-Martinez, J.; Neto, O. P.; Rodrigues, A. J.; Evora, P. R. B. *Pulm. Circ.* **2013**, *3*, 856–861.

(39) Cracowski, J.-L.; Cracowski, C.; Bessard, G.; Pepin, J.-L.; Bessard, J.; Schwebel, C.; Stanke-Labesque, F.; Pison, C. *Am. J. Respir. Crit. Care Med.* **2001**, *164*, 1038–1042.

(40) Hemnes, A. R.; Rathinasabapathy, A.; Austin, E. A.; Brittain, E. L.; Carrier, E. J.; Chen, X.; Fessel, J. P.; Fike, C. D.; Fong, P.; Fortune, N.; Gerszten, R. E.; Johnson, J. A.; Kaplowitz,

M.; Newman, J. H.; Piana, R.; Pugh, M. E.; Rice, T. W.; Robbins, I. M.; Wheeler, L.; Yu, C.; Loyd, J. E.; West, J. *Eur. Respir. J.* **2018**, *51*, 1702638.

(41) Fessel, J. P.; Flynn, C. R.; Robinson, L. J.; Penner, N. L.; Gladson, S.; Kang, C. J.; Wasserman, D. H.; Hemnes, A. R.; West, J. D. *Am. J. Respir. Cell Mol. Biol.* **2013**, *49*, 778–787.

(42) Johnson, J. A.; Hemnes, A. R.; Perrien, D. S.; Schuster, M.; Robinson, L. J.; Gladson, S.; Loibner, H.; Bai, S.; Blackwell, T. R.; Tada, Y.; Harral, J. W.; Talati, M.; Lane, K. B.; Fagan, K. A.; West, J. *Am. J. Physiol.-Lung Cell. Mol. Physiol.* **2012**, *302*, L474–L484.

(43) Sehgal, P. B.; Mukhopadhyay, S. *Am. J. Respir. Cell Mol. Biol.* **2007**, *37*, 31–37.

Chapter 3: Previous Syntheses of Autoxidative Products

Selected Total Syntheses of 15-F_2-Isoprostanes

The total syntheses of F_2-isoprostanes have provided valuable tools for the assessment of oxidative damage related to the pathogenesis of various diseases. An emphasis on the utilization of 15-F_2-isoprostane regioisomers has been established due to a greater abundance *in vivo* than 8-F_2-isoprostane and 12-F_2-isoprostane.[44] The 5-F_2-isoprostane isomers are produced in similar amounts to the 15-series, yet lack the relative physiological activity lessening their utility in disease assessment.[45] As a result, various total syntheses of the 15-F_2-isoprostanes have been selected and are presented below. The key 15-F_2-isoprostane syntheses fall into three general categories according to Jahn and coworkers: biomimetic cyclization, attachment of both sidechains to a cyclopentene core, or a two-step cyclization/attachment of a single side-chain.[2]

Corey (1984) In an effort to develop a biomimetic approach to enzymatically-derived $PGF_{2\alpha}$, Corey and coworkers synthesized the first published 15-F_2-IsoP.[46] The compound was termed 8-*epi*-$PGF_{2\alpha}$ due to the *cis*-orientation of the side chains (prostaglandin side chains are oriented as *trans*) and because this work was performed several years prior to the discovery of isoprostanes. Beginning from orthoester **3.1**, the carbon framework was extended via copper-catalyzed coupling with propargyl iodide **3.2** followed by dihydroxylation and semi-reduction to produce diol **3.3** (Scheme 3.1). Removal of the orthoester and subsequent methyl ester formation was followed by cleavage of the diol with lead tetraacetate to afford aldehyde **3.4**. Installation of the remaining carbon framework was accomplished through addition of the acetylide of enyne **3.5**. Lindlar catalyzed semihydrogenation afforded the tetraene in the desired *Z*-geometry. Mesylation

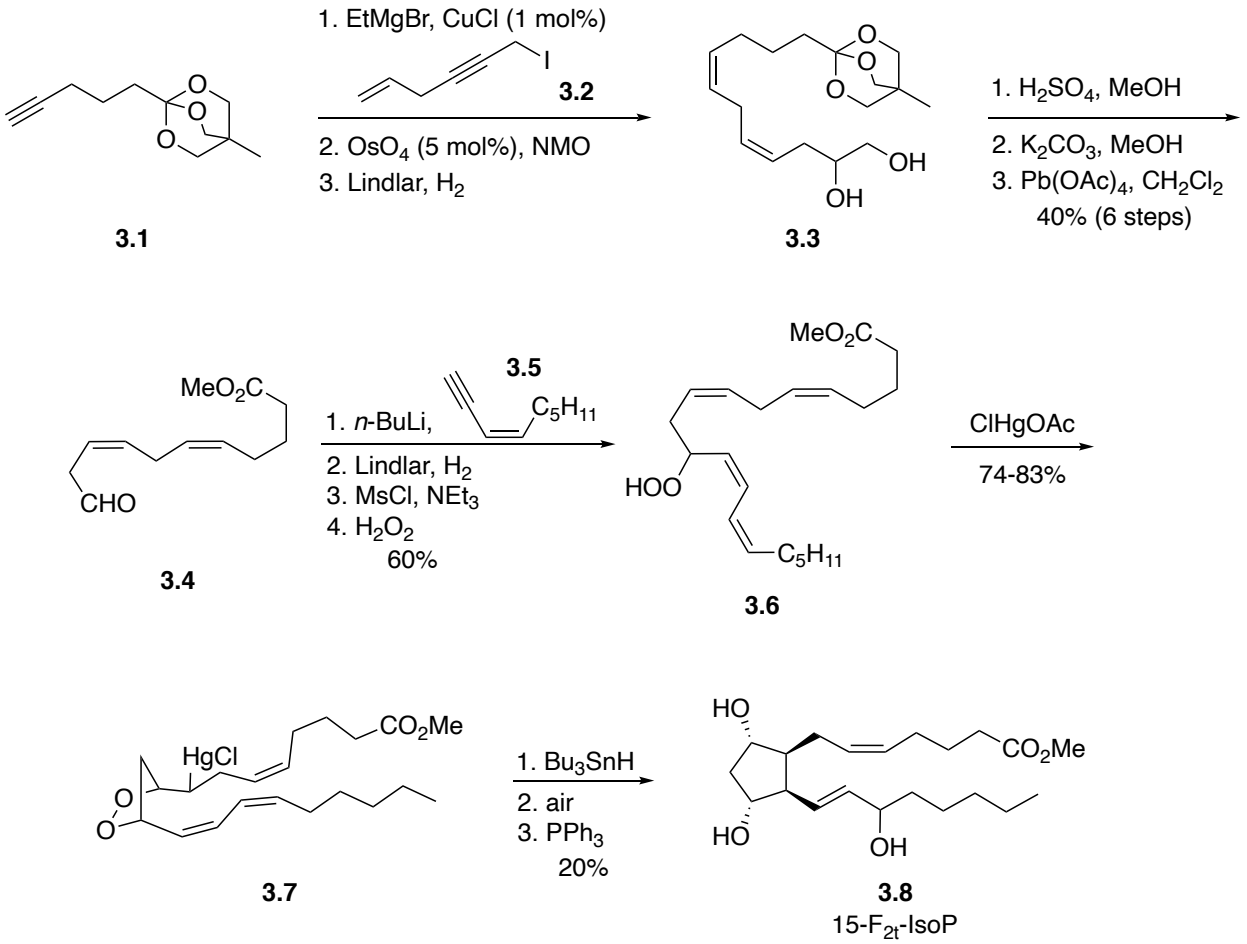

Scheme 3.1 Corey's synthesis of 15-F_{2t}-IsoP.

and displacement of the secondary alcohol with hydrogen peroxide set the stage for the pivotal peroxymercuration step. Treatment of **3.6** with mercury(II) chloroacetate generated endoperoxide **3.7**. This organomercurial intermediate served as a viable substrate for the biomimetic cyclization considering treatment with tributyltin hydride generated the radical necessary for 5-exo-trig cyclization seen in isoprostane formation. Subsequent reaction with air allowed for quenching of the radical intermediate with oxygen and treatment with triphenylphosphine reduced the PGG-like diperoxide to afford 15-F_{2t}-IsoP as a 1:1 mixture of epimers.

Larock (1991) Merely months after the initial reporting of the discovery of the isoprostanes, Larock and coworkers reported a concise total synthesis of 15-F_{2c}-IsoP.[47] Utilizing an intermolecular palladium coupling reaction, 15-F_{2c}-IsoP was synthesized in just four steps. Beginning from alcohol **3.9**, treatment with palladium acetate, ethyl vinyl ether, and enone **3.10** initiates a three-component intermolecular coupling to set the stereochemistry around the cyclopentane core and install the enone side chain (Scheme 3.2). This sequence begins with an

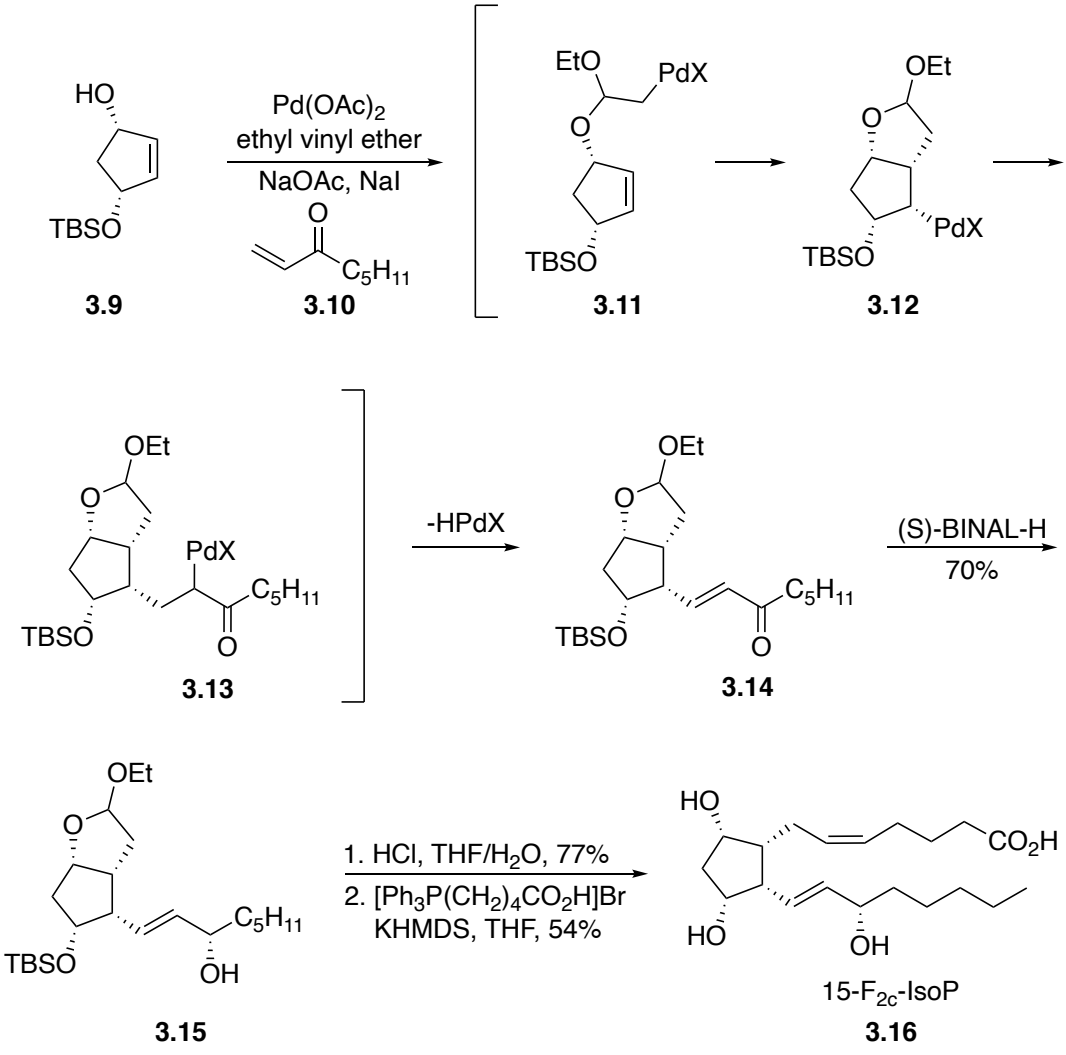

Scheme 3.2 Larock's synthesis of 15-F_{2c}-IsoP via a palladium coupling.

oxypalladation step to form **3.11** which then undergoes cis insertion to the cyclopentene. Organopalladium intermediate **3.12** was not susceptible to β-hydride elimination due to the relative stereochemistry of the silyl ether, which allowed for the final coupling with enone **3.10** to produce **3.14** in good yield. Stereoselective reduction of the enone using (S)-BINAL-H gave the desired allyl alcohol **3.15**. Subsequent hydrolysis and Wittig olefination provided 15-F_{2c}-IsoP **3.16**.

Snapper (2002) In an effort to provide facile access to each of the 15-F_2-IsoP isomers, Snapper and coworkers utilized a stereodivergent ring-opening metathesis/cross-metathesis strategy.[48] [2+2] photocycloaddition of **3.17** with acetylene provided a 1.8:1 mixture of exo **3.18** to endo **3.19**, which creatively installed the isoprostane *cis* stereochemistry (Scheme 3.3). Reduction of this inseparable mixture of bicyclo[3.2.0]heptenones using DIBAL-H gave varying stereochemical results. While the reduction of **3.19** yielded good stereoselectivity (~9:1 syn/anti dihydroxylated **3.21**), the reduction of **3.18** produced a modest selectivity of ~2.5:1 syn/anti **3.20**.

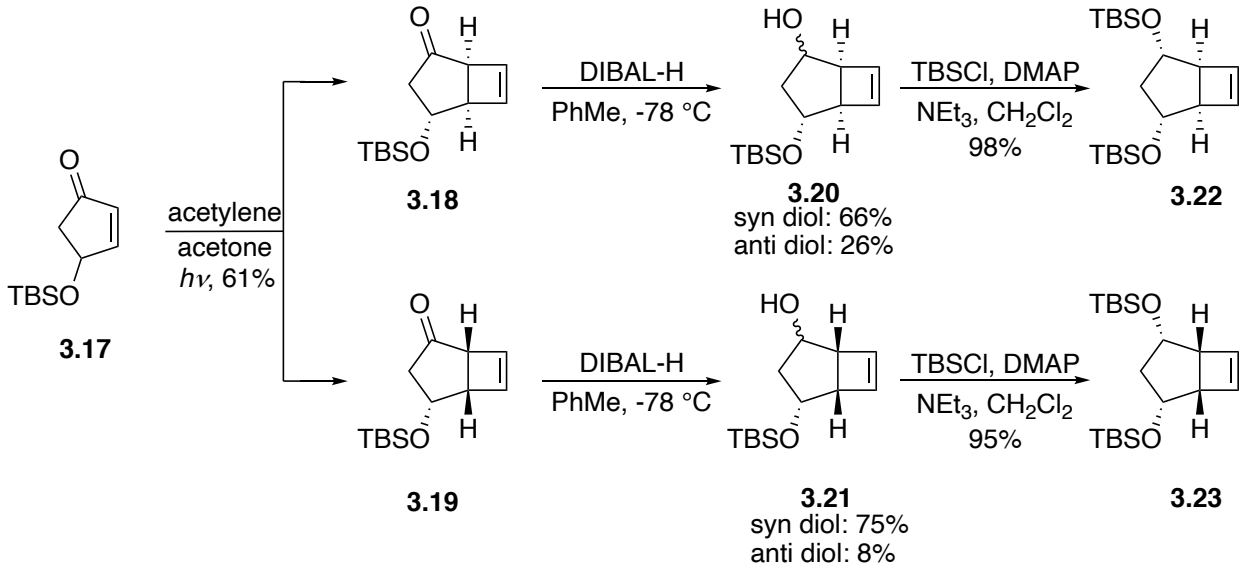

Scheme 3.3 Snapper's use of a [2+2] photocycloaddition to set cyclopentane stereochemistry.

Each of these stereoisomers proved separable. Bis-silylation of syn-**3.20** and syn-**3.21** occurred in high yields to provide **3.22** and **3.23**, respectively. Utilizing this photocyclization strategy provided a point of divergence for the synthesis of 15-F_{2c}-IsoP and 15-F_{2t}-IsoP series.

Ring-opening metathesis of **3.22** and **3.23** using Grubbs second generation catalyst in the presence of octen-3-ol afforded a near-equivalent mixture of *Z* and *E*-olefin isomers (Scheme 3.4). This issue was resolved through the employment of a PCC oxidation followed by catalytic iodine-mediated isomerization to the desired *E*-olefin. Obtaining a racemic mixture of **3.26** and **3.27** from this metathesis route created a second point of stereodivergence by producing both sets of stereoisomers (silyl ethers α and β) for each of the 15-F_{2c} and 15-F_{2t} series.

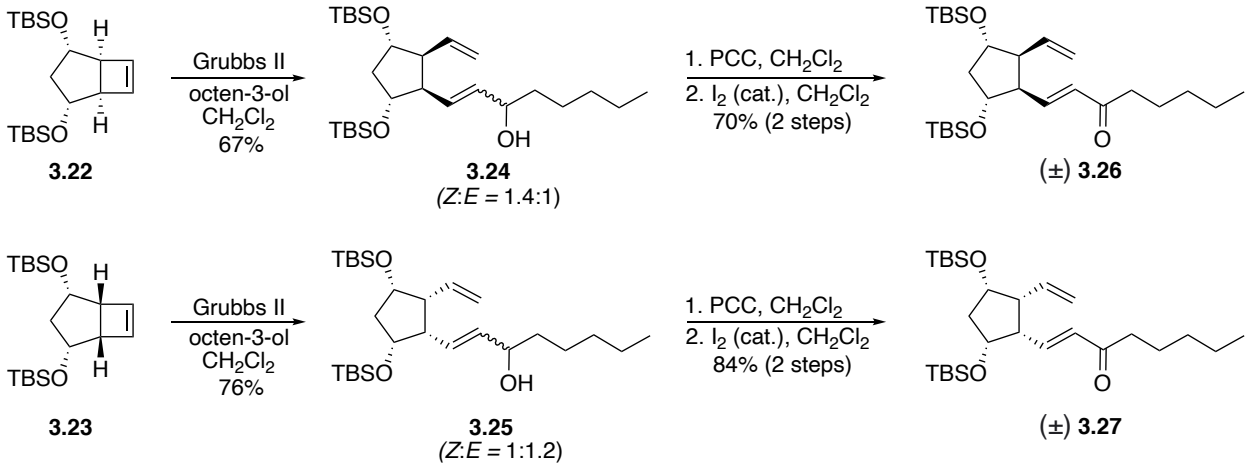

Scheme 3.4 Snapper's ring-opening/cross metathesis strategy for installing IsoP enone sidechain

Distinct strategies were required for the resolution of racemic **3.26** and **3.27**. For the resolution of **3.26** (15-F_{2t} series), the utilization of Corey-Bakshi-Shibata (CBS) reduction with (*S*)-2-Methyl-CBS-oxazaborolidine provided separable diastereomers **3.28** and **3.29** in high enantiomeric excess (Scheme 3.5). Each of these isomers was then subjected to PCC oxidation and subsequent CBS reduction with (*R*) or (*S*)-2-Methyl-CBS-oxazaborolidine to install the final stereocenter for each of the four possible 15-F_{2t}-IsoP isomers.

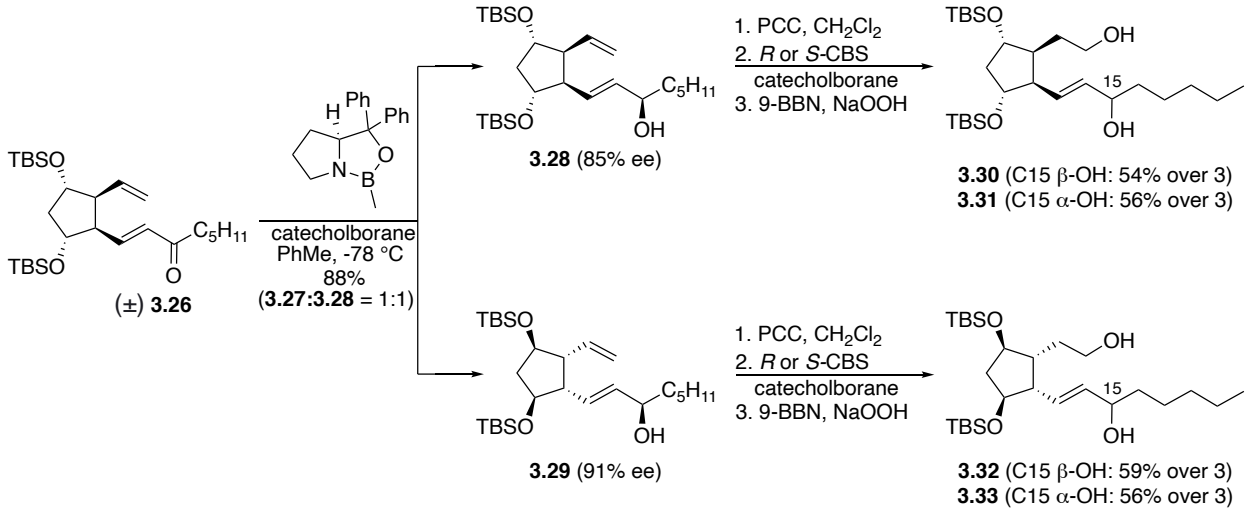

Scheme 3.5 Snapper's resolution of the 15-F_{2t}-IsoP series.

Once separated, these individual isomers were further elaborated via hydroboration-oxidation to afford diols **3.30-3.33**. Selective oxidation of the primary alcohol of each of these compounds was achieved upon treatment with TEMPO under phase-transfer conditions (Scheme 3.6). Treatment of the resultant aldehydes **3.34**-**3.37** with the requisite Wittig salt provided the fully elaborated carboxylic acid sidechain in good *Z*-stereoselectivity. Final desilylation of the cyclopentane diols afforded each of the four 15-F_{2t}-IsoP isomers.

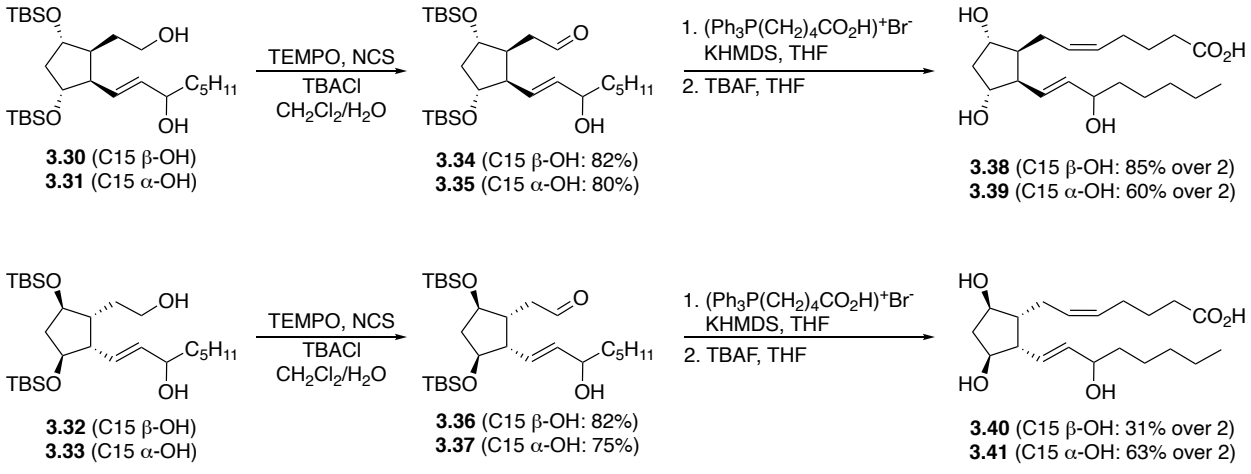

Scheme 3.6 Snapper's completion of the 15-F_{2t}-IsoP series.

Unlike the 15-F_{2t} series, CBS reduction of racemic enone **3.27** to resolve the 15-F_{2c} series proved unfruitful due to poor ee (less than 30%). Alternatively, the formation of mandelate esters allowed for separation and elaboration of the single enantiomers. Sodium borohydride reduction of racemic **3.27** afforded separable mixtures of racemic **3.42** and **3.43** (Scheme 3.7). Each of these mixtures were esterified with (*R*)-*O*-acetylmandelic acid chloride which allowed for separation of the enantiomerically enriched isomers. Subsequent removal of the ester functionality and hydroboration-oxidation provided enantiomerically pure diols **3.44-3.47**.

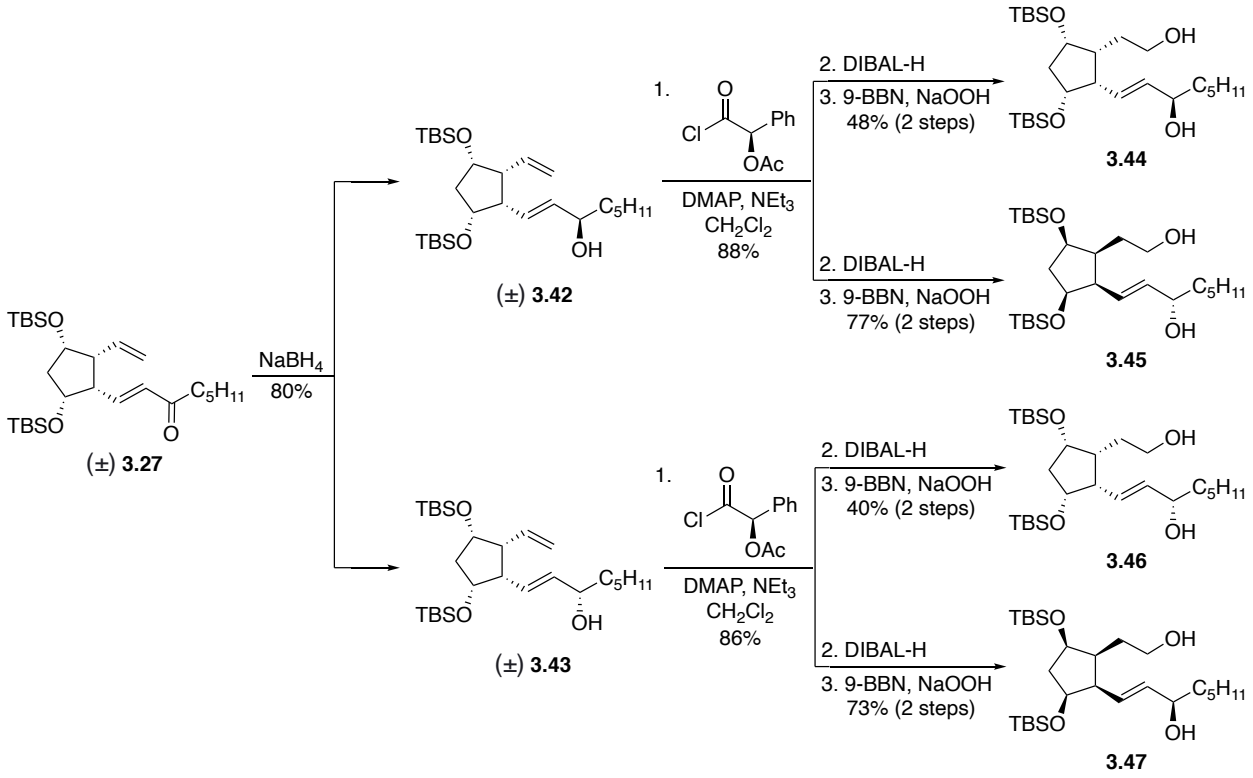

Scheme 3.7 Snapper's resolution of the 15-F_{2c}-IsoP series.

The completion of the 15-F_{2c} series was executed in a parallel manner to the 15-F_{2t} series. Selective oxidation of the primary alcohol of compounds **3.44-3.47** using TEMPO followed by Wittig olefination and desilylation yielded the remaining members of the 15-F_2-IsoP family **3.16**

and **3.52**-**3.54** (Scheme 3.8). This stereodivergent approach to the 15-F_2-isoprostanes was the first reported synthesis of all eight isomers and provided facile access to each.

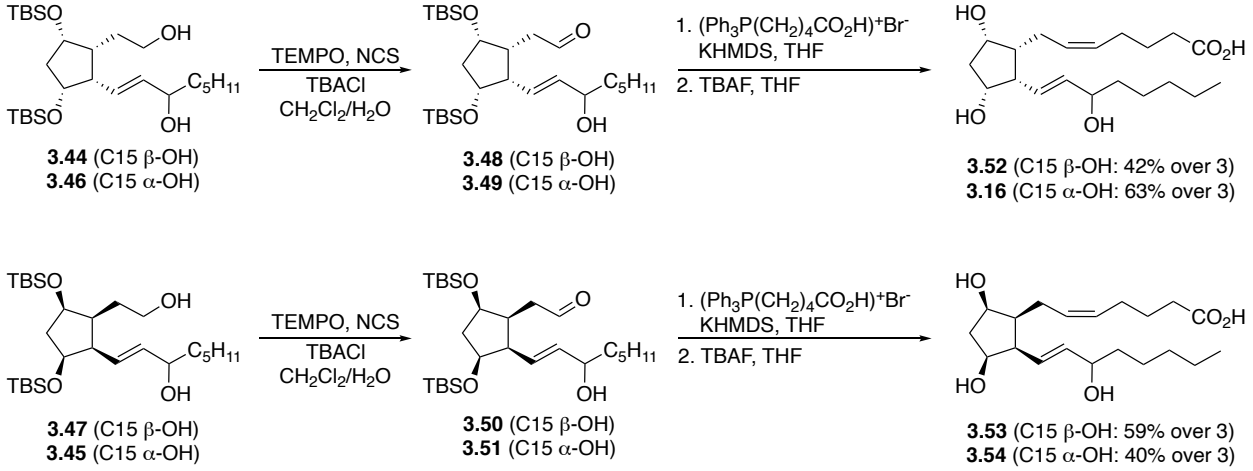

Scheme 3.8 Snapper's completion of the 15-F_{2c}-IsoP series.

Selected Total Syntheses of Δ^{13}-9-Isofurans

The isofurans are made up of eight of constitutional isomers each possessing five stereocenters leading to a total of 256 isomers. Little is known about the biological profile of these compounds meaning that rapid access to individual isomers is of high importance.

Taber (2004) Due to the physiological activity and role as biomarkers of the isoprostanes, Taber set out to synthesize the isofurans beginning with the regioisomer most closely related to the prostaglandins: the Δ^{13}-9-isofurans. In 2004, he reported the synthesis of both C15-epimers of 8-epi-SC-Δ^{13}-9-IsoF.[49] Beginning with sorbaldehyde **3.55**, bromination via the silyl enol ether followed by quenching with diol **3.56** resulted in dimethyl acetal **3.57** (Scheme 3.9). The allyl bromide underwent subsequent copper-mediated coupling with propargyl alcohol to afford eneyne **3.58**. After multiple failed attempts at reduction of the alkyne using Red-Al, Na/NH_3, and Li/1,3-

diaminopropane (allene formation), LAH in diethyl ether was discovered to produce the desired triene **3.59** in moderate yield. From this triene, Taber envisioned a series of oxidation steps in preparation for the key furan formation. Sharpless asymmetric epoxidation provided the desired epoxide followed by formation of benzenesulfonate **3.61**. Sharpless asymmetric dihydroxylation

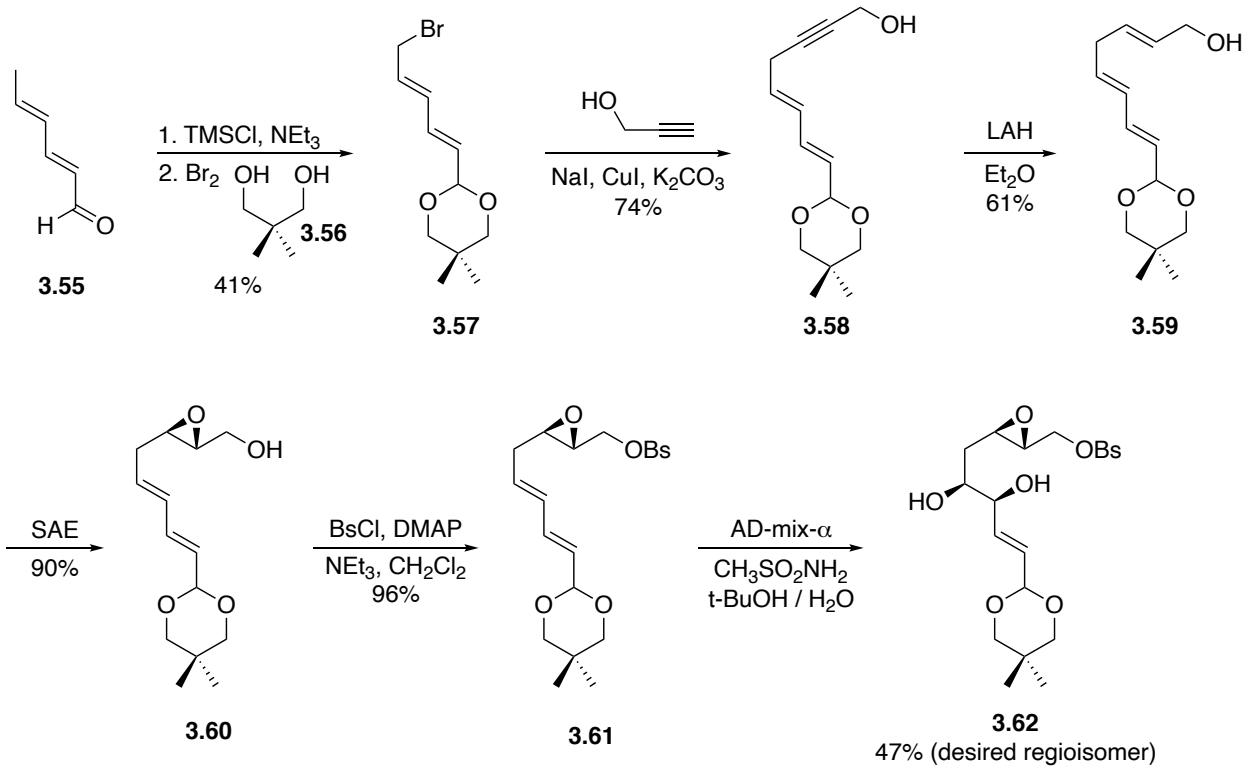

Scheme 3.9 Taber's synthesis of the cascade cyclization precursor.

gave the appropriate diol regioisomer in 47% yield. Fortuitously, the undesired diol was easily recycled to epoxy alcohol **3.60** upon an orthoester formation/thermal fragmentation sequence.

Treatment of **3.62** with potassium carbonate in methanol resulted in a cascade cyclization setting the stereochemistry of the furan ring and forming the epoxide to be used for installation of the carboxylic acid sidechain (Scheme 3.10). Silylation of the furanyl alcohol was used to stifle intramolecular addition to the epoxide. This was followed by the nucleophilic opening of the epoxide using the lithium acetylide of 5-hexynenitrile in the presence of a Lewis acid. Subsequent

reduction of the alkyne to the *cis*-olefin using P-2 nickel catalyst and removal of the dimethyl acetal provided aldehyde **3.65**. Installation of the remaining carbon framework occurred via Grignard addition of pentylmagnesium bromide. Silylation of the secondary alcohols prior to this nucleophilic addition proved useful in the separation of epimers **3.66** and **3.67**. Removal of the silyl groups and hydrolysis of the nitrile afforded SC-Δ^{13}-9-isofurans **3.68** and **3.69**. The methyl ester of each compound was synthesized to allow for a more facile characterization.

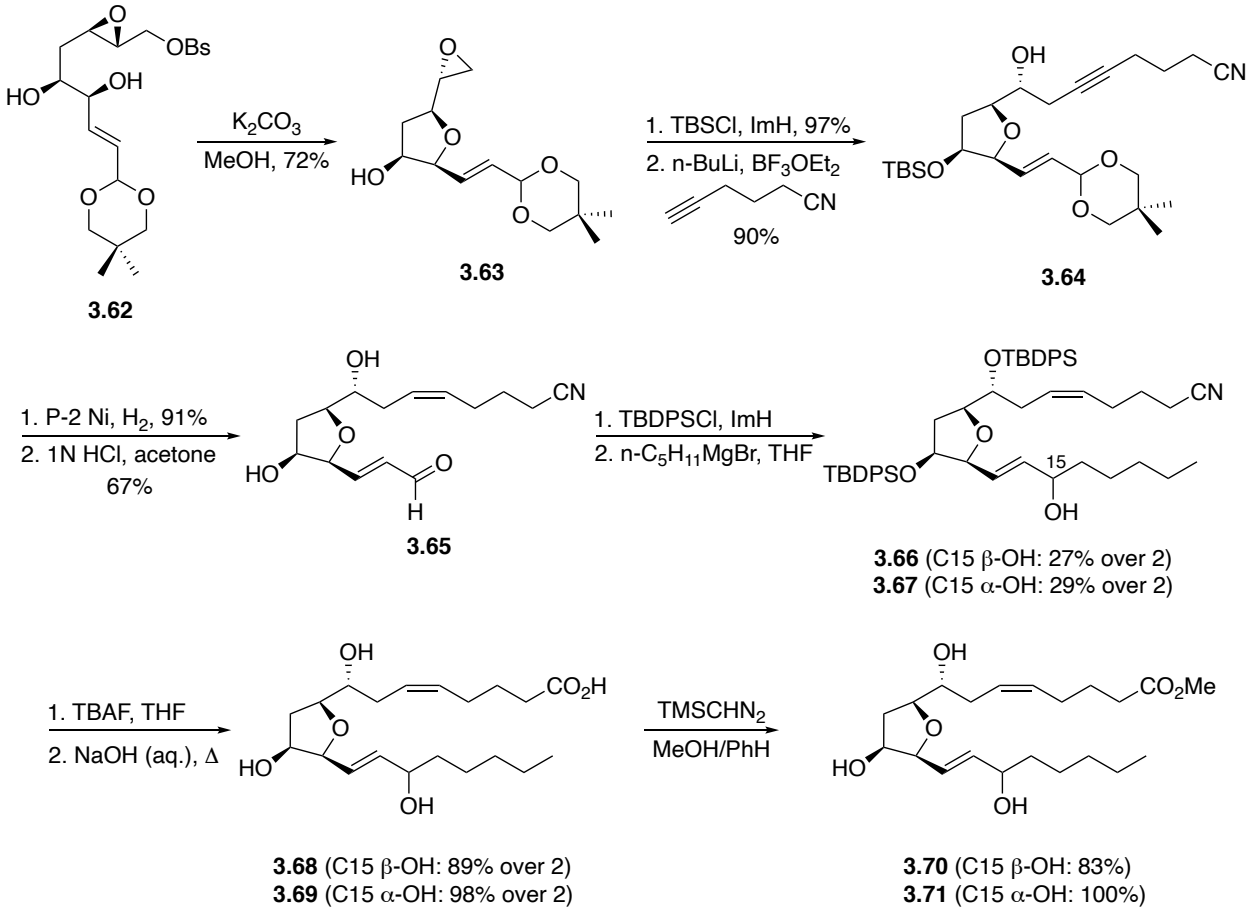

Scheme 3.10 Taber's synthesis of 8-epi-SC-Δ^{13}-9-IsoF and 8-epi-15-epi-SC-Δ^{13}-9-IsoF (2004).

Taber (2009) Following up their 2004 synthesis of diastereomeric isofurans **3.68** and **3.69**, the Taber group devised a new route to the Δ^{13}-9-isofurans enabling confirmation of previously inconsistent biological activities.[50] This new route also aimed to combat issues with regioselectivity present in the 2004 synthesis. Methyl bromocrotonate **3.72** was treated with lithium aluminum hydride to afford the allyl alcohol **3.73** (Scheme 3.11). Using parallel conditions to the 2004 synthesis, a copper-mediated displacement of the bromide with propargyl alcohol resulted in a 2 to 1 mixture of S_N2 to S_N2' products, which proved to be inseparable. Subsequent alkyne reduction with lithium aluminum hydride produced a 2:1 mixture of inseparable dienes **3.76** and **3.77**. Formation of the monotrityl ether allowed for isolation of the desired regioisomer **3.78**, which was to serve as the first point of stereodivergence in this route. Sharpless asymmetric

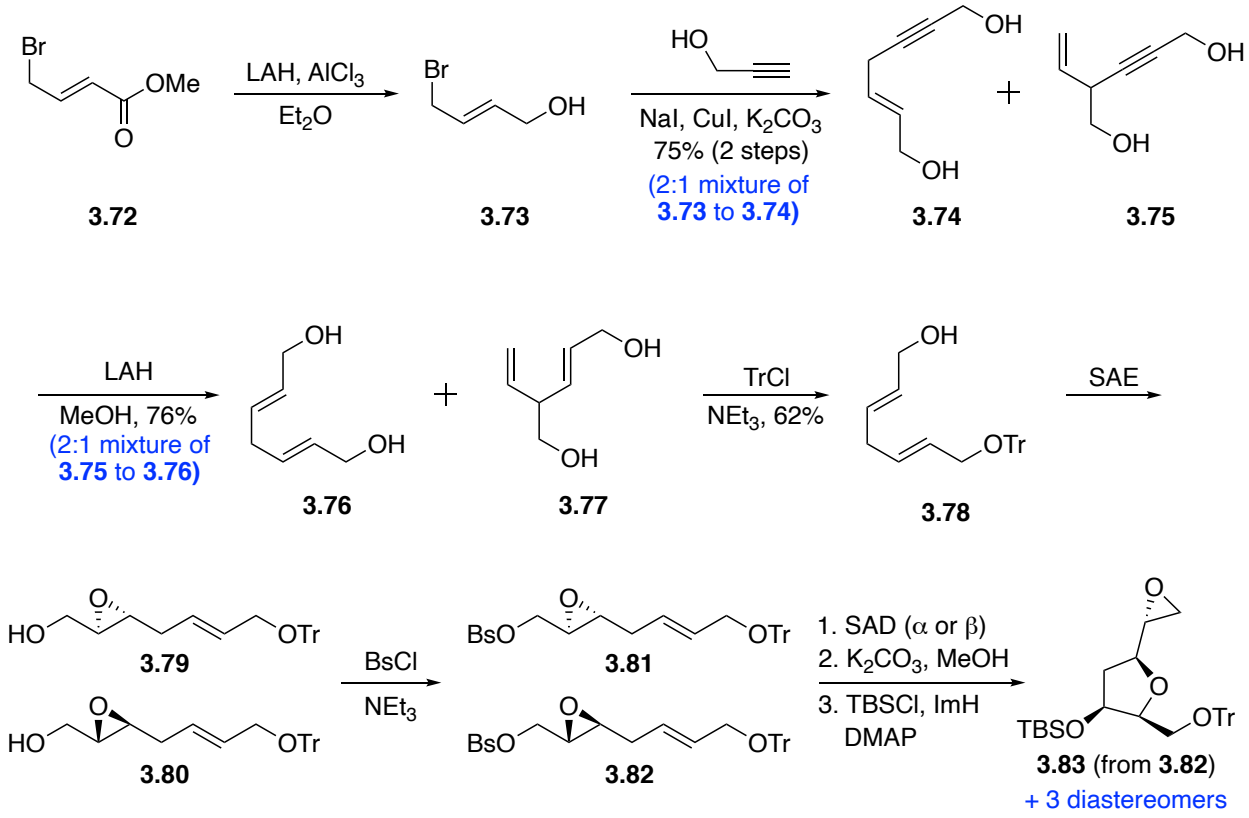

Scheme 3.11 Taber's synthesis of the furan core.

epoxidation using either L-DET or D-DET provided the α- and β-epoxyalcohols **3.79** and **3.80**. Conversion of the primary alcohol to a good leaving group was necessary for the ensuing furan cyclization. Sharpless asymmetric dihydroxylation using AD-mix-α or AD-mix-β on each of the epoxides **3.81** and **3.82** resulted in a second point of stereodivergence in that four epoxydiols were formed. These crude diols were subsequently treated with potassium carbonate in methanol to promote the 5-exo-tet cyclization required for furan formation. The ring alcohol was then silylated allowing for separation of any diastereomeric impurities from the asymmetric dihydroxylation and preventing intramolecular attack of the newly formed epoxide, which was observed in the 2004 synthesis.

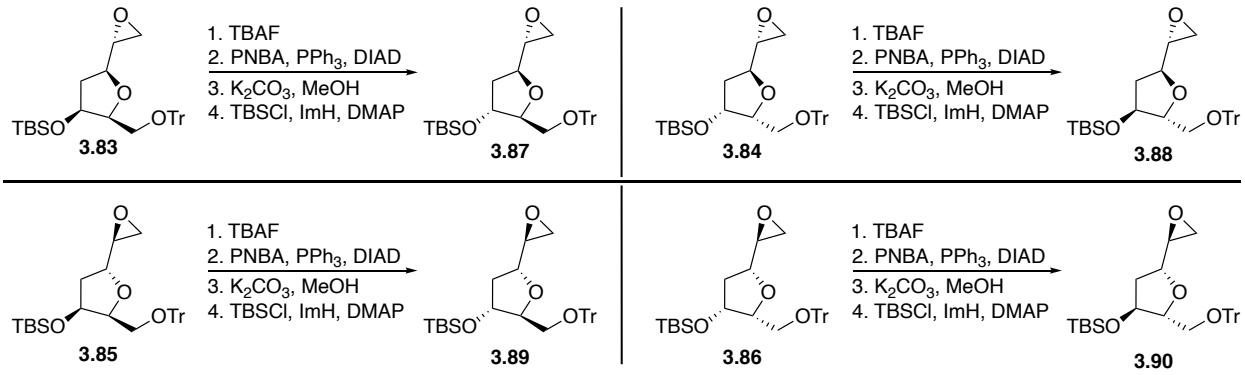

Scheme 3.12 Taber's use of Mitsunobu reaction to access to further furanyl diastereomers.

From each of these four furan cores **3.83**-**3.86**, Taber and coworkers were able to derive additional furanyl diastereomers **3.87**-**3.90** via Mitsunobu reaction to invert the ring alcohol stereochemistry (Scheme 3.12). This diversification strategy was central to accessing each of the 32 stereoisomers of the Δ^{13}-9-IsoF family.

From epoxide **3.83**, nucleophilic addition of the requisite hexynl chain installed the northern carbon framework (Scheme 3.13). An oxidation-reduction sequence gave inversion of the C8 stereocenter giving access to syn isomers at C8 and C9. The remaining furanyl epoxides **3.84**-

3.90 were carried out in parallel sequences. Use of P-2 nickel catalyst in the presence of hydrogen gas furnished the *cis*-olefin. Silylation of the secondary alcohol followed by deprotection of the primary trityl ether provided alcohol **3.93**. Oxidation with Dess-Martin periodinane and subsequent Horner-Wadsworth-Emmons olefination afforded the complete carbon framework via enone **3.94**. Luche reduction at C15 gave a nearly equivalent epimeric mixture, which proved to be separable, providing the final point of stereodivergence. Desilylation and hydrolysis of the nitrile furnished isofurans **3.68**-**3.69**.

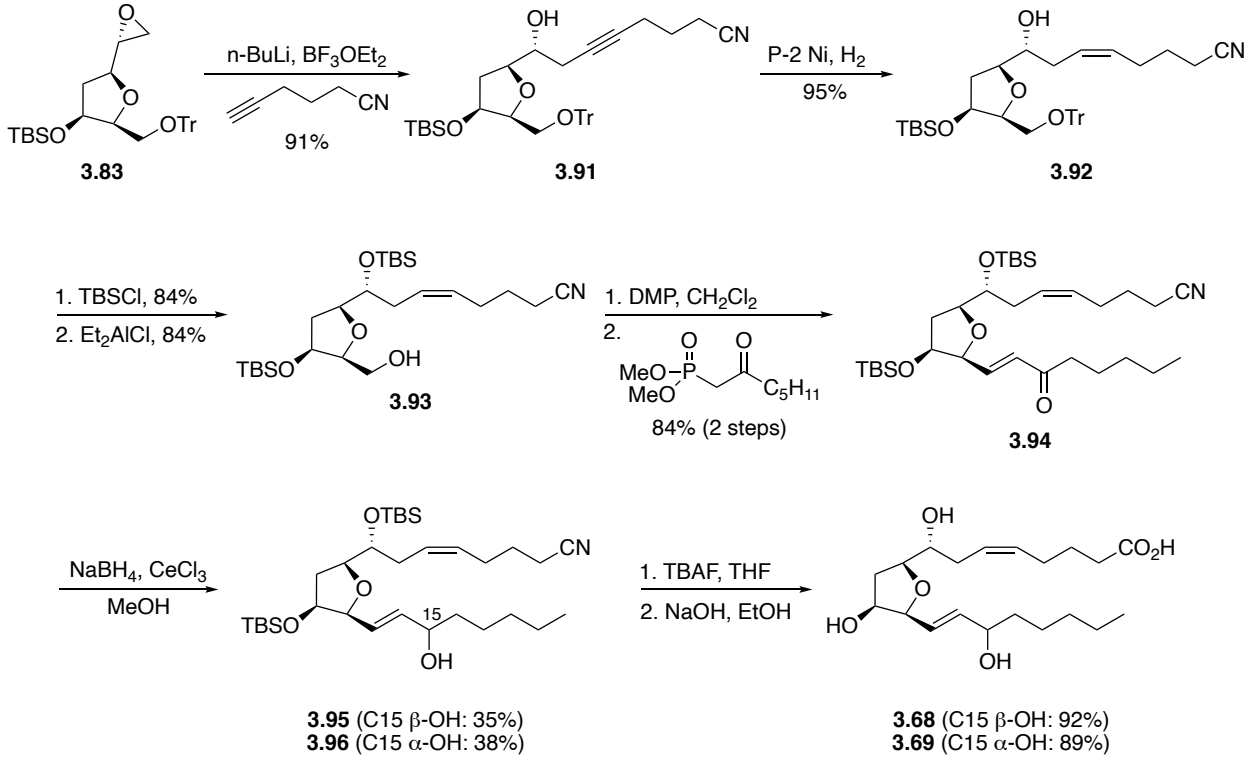

Scheme 3.13 Taber's synthesis of 8-epi-SC-Δ^{13}-9-IsoF and 8-epi-15-epi-SC-Δ^{13}-9-IsoF (2009).

References

(44) Waugh, R. J.; Morrow, J. D.; Roberts II, L. J.; Murphy, R. C. *Free Radic. Biol. Med.* **1997**, *23*, 943–954.

(45) Marlière, S.; Cracowski, J.-L.; Durand, T.; Chavanon, O.; Bessard, J.; Guy, A.; Stanke-Labesque, F.; Rossi, J.-C.; Bessard, G. *Br. J. Pharmacol.* **2002**, *135*, 1276–1280.

(46) Corey, E. J.; Shih, C.; Shih, N.-Y.; Shimoji, K. *Tetrahedron Lett.* **1984**, *25*, 5013–5016.

(47) Larock, R. C.; Lee, N. H. *J. Am. Chem. Soc.* **1991**, *113*, 7815–7816.

(48) Schrader, T. O.; Snapper, M. L. *J. Am. Chem. Soc. 124*, 10998–11000.

(49) Taber, D. F.; Pan, Y.; Zhao, X. *J. Org. Chem.* **2004**, *69*, 7234–7240.

(50) Taber, D. F.; Gu, P.; Li, R. *J. Org. Chem.* **2009**, *74*, 5516–5522.

Chapter 4: A Stereodivergent Synthesis of Δ^{13}-9-Isofurans

Stereodivergent Strategy Towards the Δ^{13}-9-Isofurans

Accessing the full spectrum of isofuran isomers through total synthesis requires careful strategic analysis. Stereodivergent synthetic routes have proven to facilitate the production of isomerically pure compounds of an isomeric series of synthetic targets in an efficient manner.[51] This has been applied in earlier eicosanoid synthetic programs, such as the previously discussed routes by Snapper and Taber.[48–50]

In the case of the Δ^{13}-9-isofurans, there are a total of 32 compounds (16 racemic diastereomers). We envisioned a stereodivergent route using starting materials from the chiral pool to facilitate incorporation of two of the five stereocenters (Figure 4.1). Using L-tartaric acid, D-tartaric acid, 2-deoxy-L-ribose, or 2-deoxy-D-ribose would allow for the stereocenters C11 and C12 of the furan ring to be in place from the beginning of the synthetic route. Elaboration to alkynes **4.1**-**4.4** utilizing previously utilized chemistry from the Sulikowski lab should provide valuable intermediates for the advancement of the stereodivergeent strategy.[52] Chain elongation and reduction of the alkyne to a cis or trans alkene (in no particular order) would provide suitable substrates for a stereospecific epoxidation followed by cyclization to furnish stereocenters C8 and C9 in a second stereochemical diversification. The described strategy would give access to each of the 16 possible stereochemical combinations around the furan core. A late-stage stereodiversification to install the final allylic alcohol stereocenter (not shown) should give access to all 32 isomers of the Δ^{13}-9-IsoF family. For the work described in this thesis, L-tartaric acid was utilized to synthesize 4 of the 32 isomers.

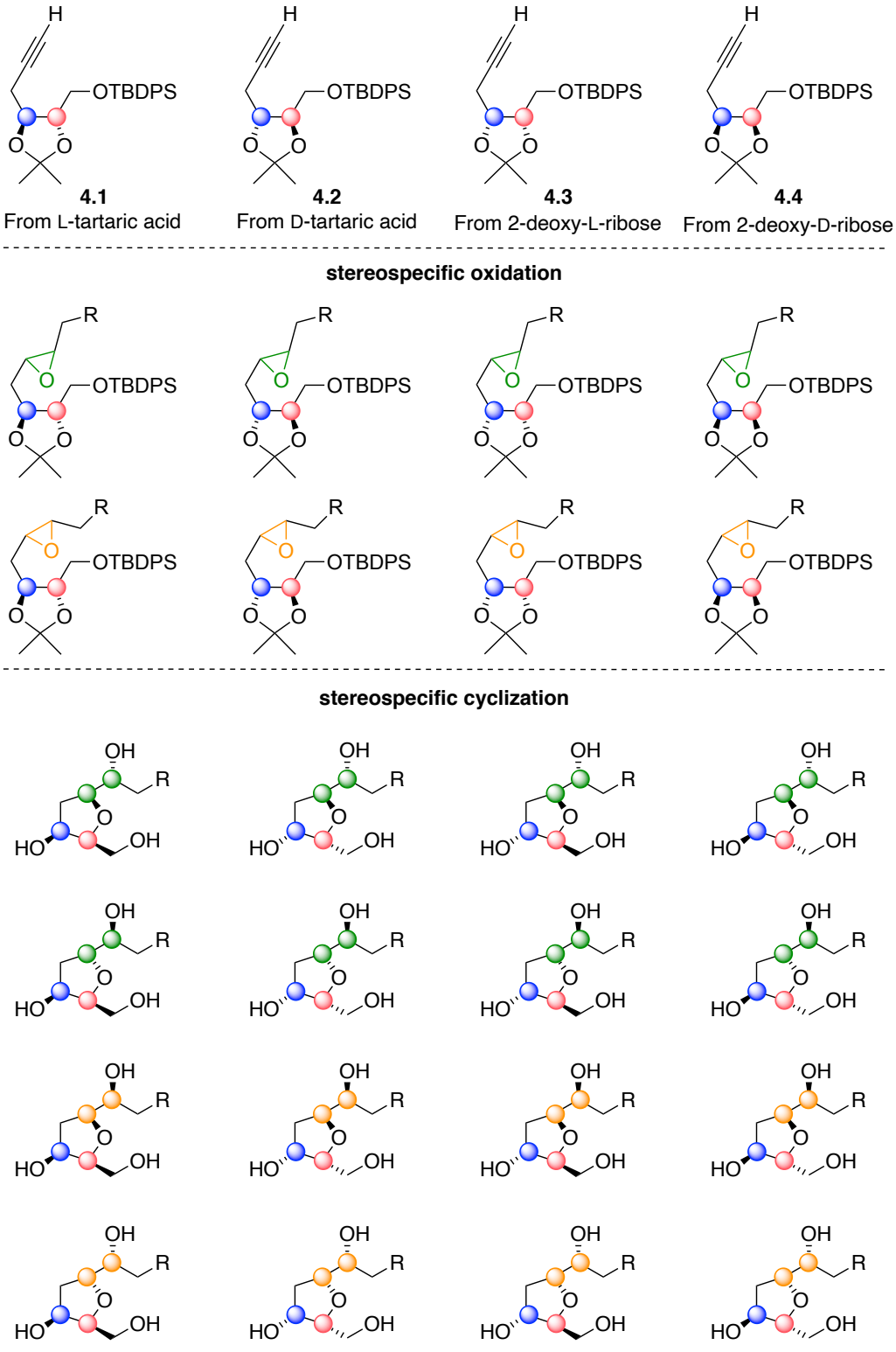

Figure 4.1 Stereodivergent approach to each of the 16 furan isomers of the Δ^{13}-9-IsoFs.

Synthesis of the SC and AC-Δ[13]-9-Isofurans

Our synthetic route to 4 of the SC and AC-Δ[13]-9-isofurans began from L-tartaric acid as a means of implementing the stereocenters at C11 and C12 from the outset (Scheme 4.1). In addition to serving as an important starting point in our stereodivergent strategy, this starting material was also highly economical (2.5 kilograms can be purchased for nearly 10 cents per gram).

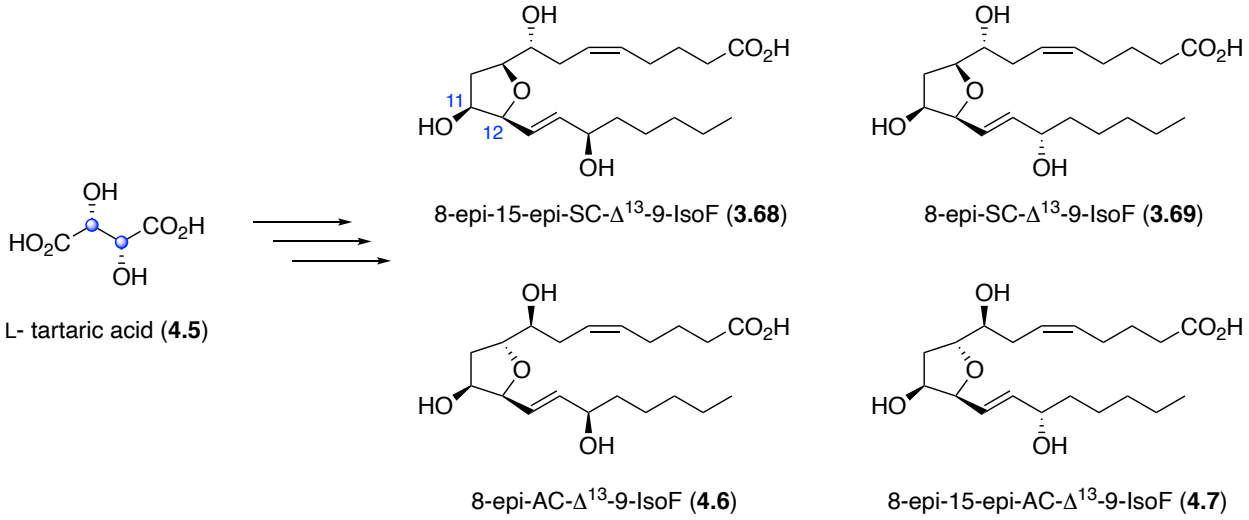

Scheme 4.1 L-tartaric acid as a valuable starting material in route to the SC and AC-Δ[13]-9-IsoFs.

The first stage of our synthesis involved installing the necessary trans alkene that would later serve as the site of the non-stereoselective epoxidation. Beginning from **4.5**, a one-pot Fisher esterification and acetonide protection of the diol furnished diester **4.8** in excellent yield using a known procedure (Scheme 4.2).[53] Following the same source, a subsequent reduction with LAH revealed diol **4.9** in moderate yield. Use of a Soxhlet apparatus to extract the inorganic precipitate upon workup proved to marginally improve the yield, yet was often not efficient due to the large amount of precipitate produced. Vacuum distillation allowed for large amounts of **4.8** and **4.9** to be purified with relative ease. Monosilylation of **4.9** with TBDPSCl resulted in desymmetrization allowing for functional group interconversion of the remaining free alcohol. In order to install the

desired alkyne, conversion of the primary alcohol **4.10** to a highly reactive leaving group was necessary. Previous work from our group reported in the thesis of Dr. Robert Davis outlined the failed attempts to form **4.12** via displacement of the corresponding primary halides and mild sulfonate esters (tosylate and mesylate). These attempts either resulted in no reaction or allene formation. Following the procedure of Mukai and coworkers, triflation of the primary alcohol was immediately followed by displacement with acetylide.[54] Triflate **4.11** proved to be minimally stable with regards to silica gel chromatography and storage for any prolonged amount of time. As

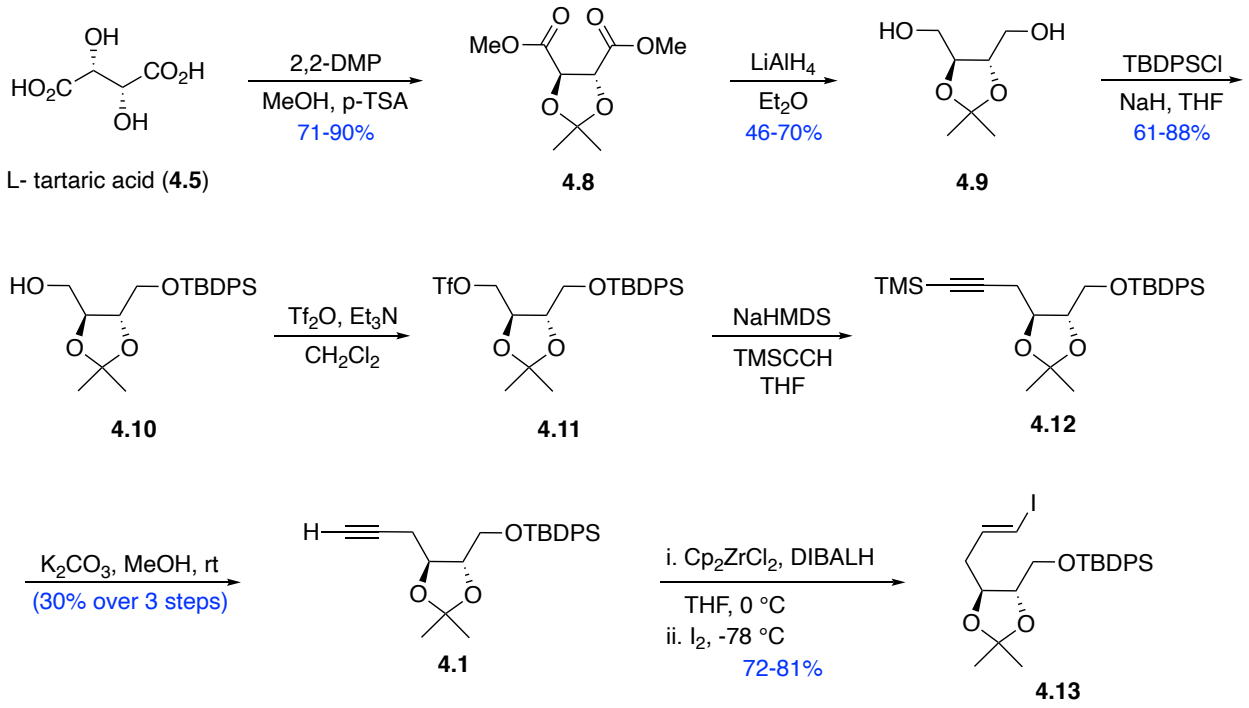

Scheme 4.2 Installation of the desired *E* olefin geometry.

a result, rapid purification via flushing through silica gel was required to achieve pure product followed by immediate treatment with the sodium acetylide or freezing in benzene for storage. Use of NaHMDS as a base for the deprotonation of TMS acetylene was not optimal, yet proved to be sufficient and avoided chloride displacement of the triflate observed upon the use of n-BuLi resulting in an inseparable mixture of halide and the desired alkyne **4.12**. This was thought to be

the result of excess lithium chloride present from the formation of n-BuLi. Desilylation of **4.12** revealed alkyne **4.1** to be used as a functional handle for the elongation of the carbon framework and installation of the desired olefin geometry. Hydrozirconation followed by iodine quench using an *in-situ* preparation of Schwartz's reagent established by Negishi allowed for preparation of vinyl iodide **4.13** as the trans diastereomer.[55] This freshly generated reagent showed marked improvement over commercially sourced Schwartz's reagent.

With the olefin geometry established, the next priority was to install the northern carbon chain (carboxylic acid). Vinyl iodide **4.13** provided a fitting substrate for palladium-mediated carbomethoxylation to afford enoate **4.14** (Scheme 4.3).[56] Reduction of the ester to the allyl alcohol followed by Appel halogenation furnished allyl chloride **4.16**.[57] This served as a suitable electrophile for a copper-mediated alkyne displacement to provide enyne **4.17**, effectively installing the carbon framework of the carboxylic acid chain.[58] Following unsuccessful attempts

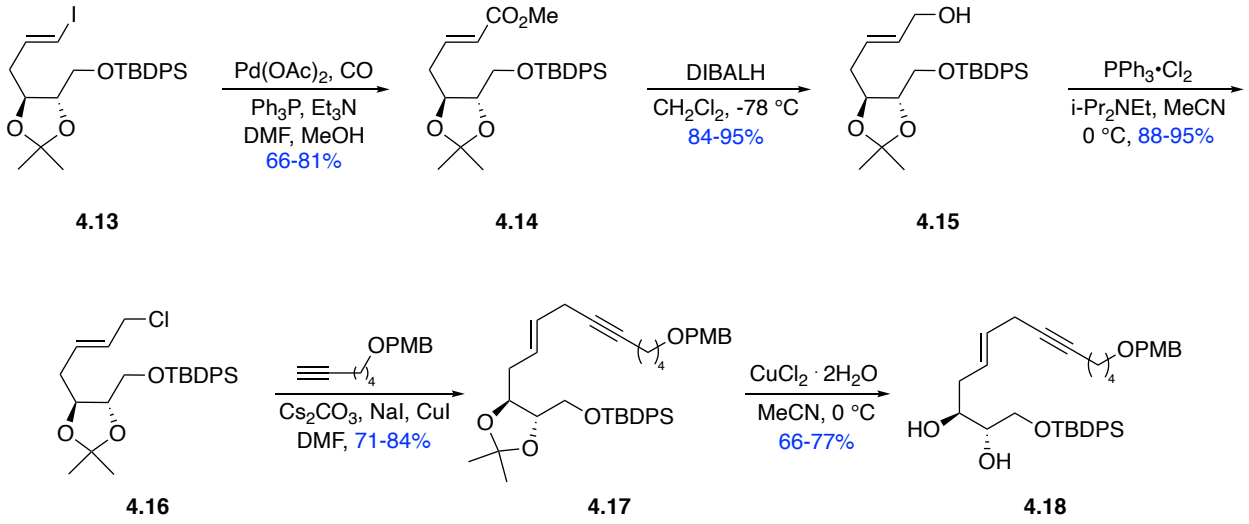

Scheme 4.3 Synthesis of the northern side chain of the Δ^{13}-9-IsoFs.

to remove the acetonide protecting group under standard acidic conditions such as TFA and HCl, copper (II) chloride dihydrate was shown to unveil diol **4.18**, when maintained at 0 °C.

With **4.18** in hand, a pivotal point in our stereodivergent strategy was approaching. The epoxidation of the *trans* alkene and subsequent furan cyclization would serve to install 2 of the remaining 3 stereocenters of the Δ^{13}-9-IsoFs. For maximum stereodiversification, a non-stereoselective epoxidation was selected in hopes of conserving steps and separating the isomers at a later point. This epoxidation of the *E* alkene was effected with m-CPBA to give a nearly 1:1 mixture of diastereomers **4.19** (Scheme 4.4). Subsequent treatment with TFA induced a stereospecific 5-exo-tet cyclization to form the furan ring. Fortuitously, the furans **4.20** and **4.21** were readily separable and the routes to the SC and AC-Δ^{13}-9-IsoFs were carried out in a parallel manner. The stereochemistry of the furans was confirmed by Mosher ester analysis of the secondary alcohol at C8.

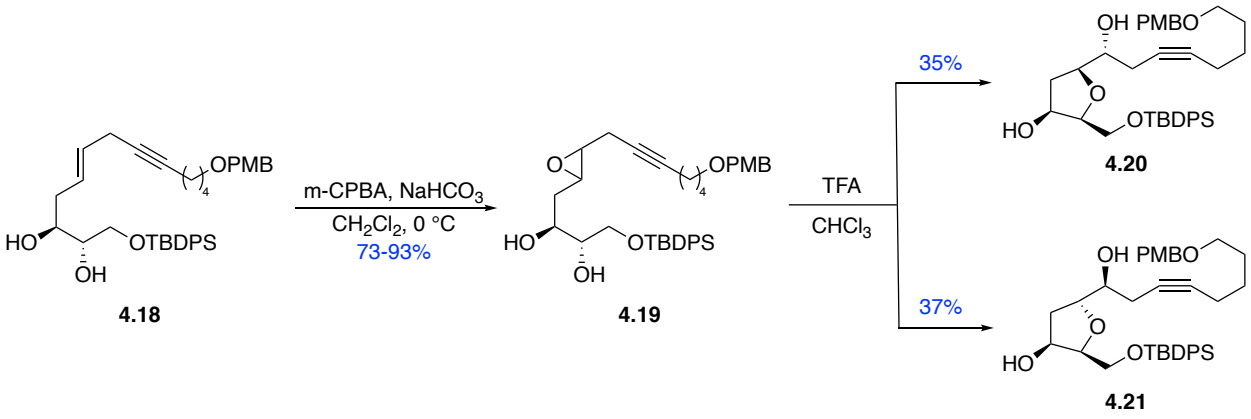

Scheme 4.4 Epoxidation / cyclization sequence to afford readily separable furan isomers.

After separation of isomeric furans **4.20** and **4.21**, functionalization of the newly-installed upper sidechain to closer resemble the carboxylic acid sidechain present in Δ^{13}-9-IsoFs became the focus. Each of the isomers **4.20** and **4.21** were protected as the diacetate (Scheme 4.5). Oxidative removal

of the PMB protecting group revealed the primary alcohols **4.23** and **4.28**. Upon treatment

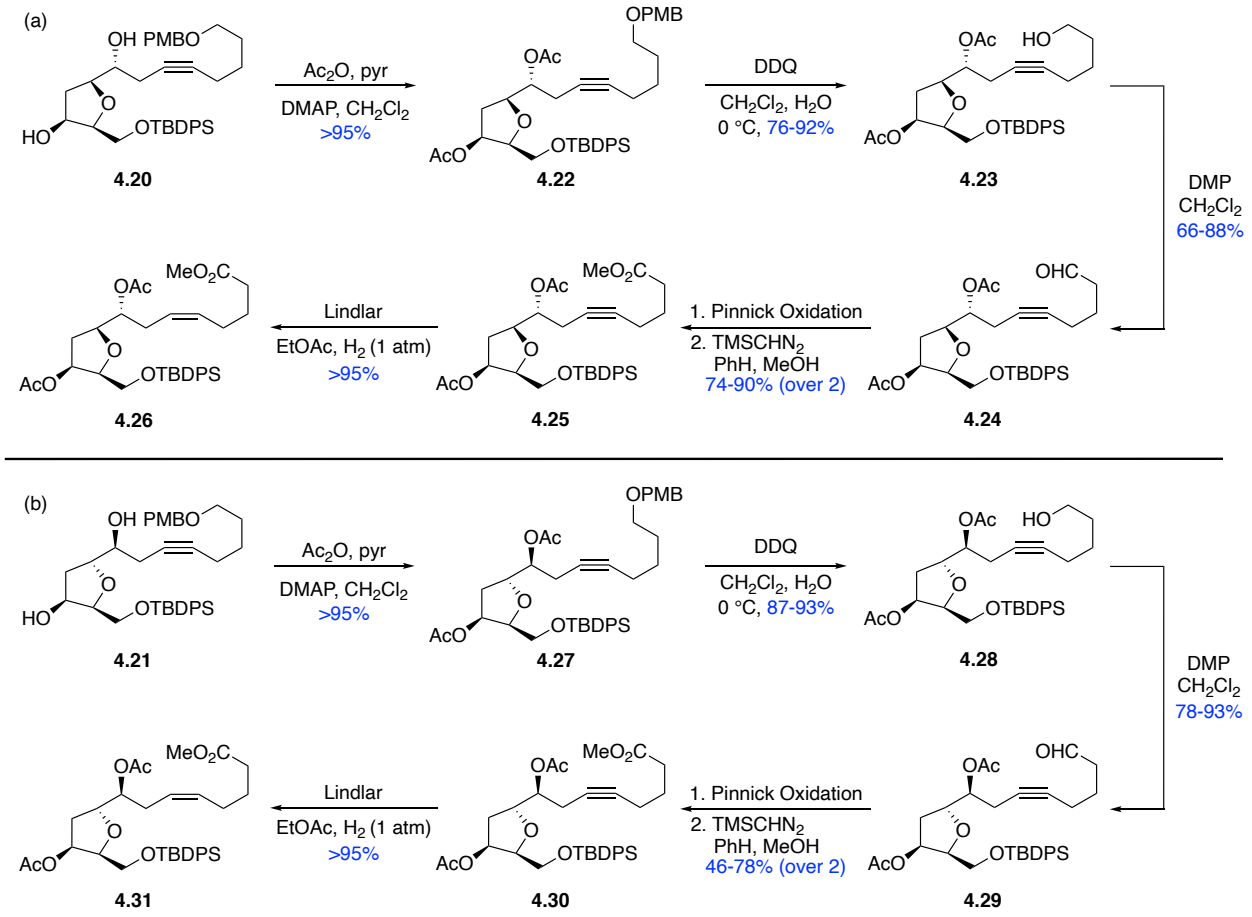

Scheme 4.5 Northern sidechain manipulation of (a) SC isomers and (b) AC isomers.

with Dess-Martin periodinane, alcohols **4.23** and **4.28** were readily converted to the aldehyde which underwent subsequent Pinnick oxidation to the carboxylic acid.[59,60] The crude carboxylic acid was then protected as the methyl ester using TMS diazomethane. With the desired oxidation state at C1 in hand, semireduction of the alkyne to the requisite *Z* alkene was accomplished via hydrogenation in the presence of Lindlar catalyst to afford alkenes **4.26** and **4.31**.

With the upper carboxylic acid sidechain installed, completion of the remaining carbon framework became the next obstacle to the total synthesis of these metabolites. Removal of the TBDPS protecting group with TBAF alone resulted in acyl migration from the neighboring acetate

to the *in situ* generated alkoxide (Scheme 4.6). As a result, acetic acid was implemented to buffer the reaction and inhibit this undesired side product. Alcohols **4.32** and **4.36** were oxidized with

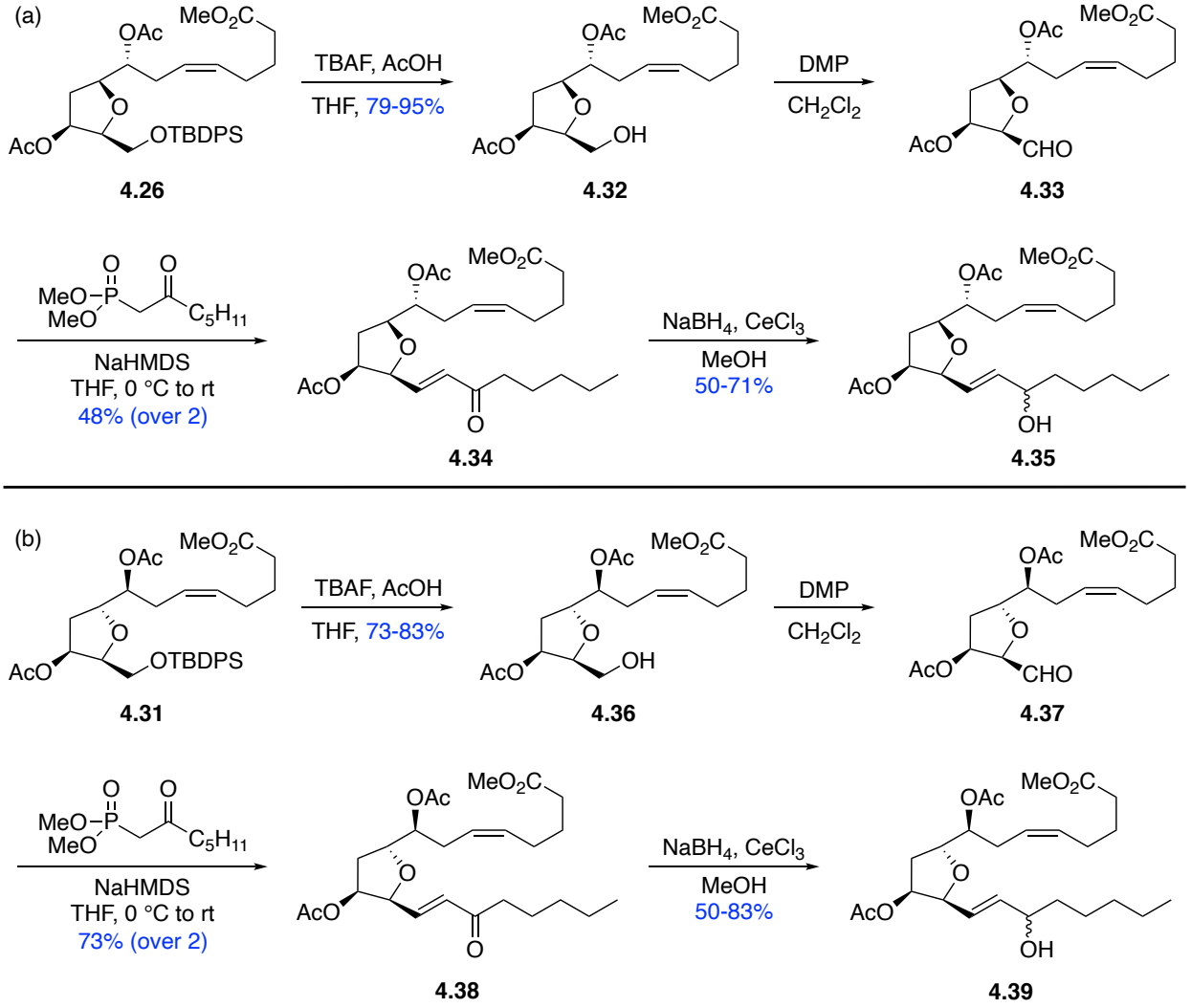

Scheme 4.6 Installation of the lower sidechain for (a) SC isomers and (b) AC isomers.

Dess-Martin periodinane followed by Horner-Wadsworth-Emmons olefination to provide the entire 20-carbon framework in the form of enones **4.34** and **4.38**. Similar to the epoxidation-cyclization sequence earlier in the synthetic route, we hoped to stereodiversify via symmetric reduction of these enones and separate at a later step. Luche reduction of the enone afforded a near 1:1 mixture of epimeric alcohols for the SC series (**4.35**) and the AC series (**4.39**). These mixtures

proved to be inseparable by column chromatography. Therefore, separation of these epimers through use of an enzymatic resolution was investigated.

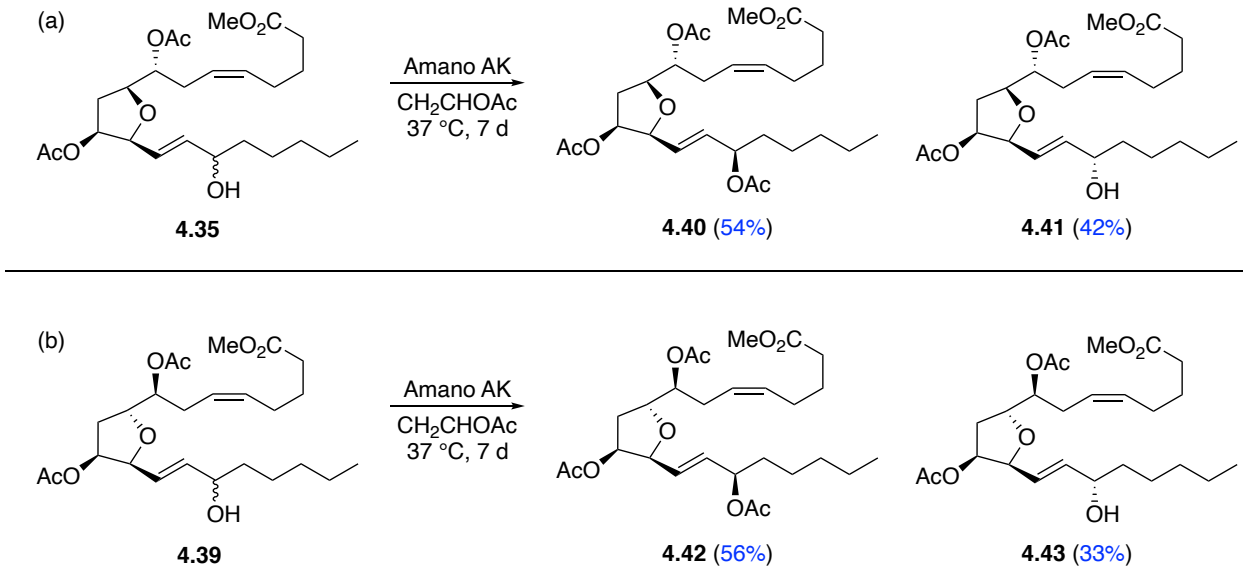

Scheme 4.7 Enzymatic resolution of C15 epimers (a) SC isomers and (b) AC isomers.

Investigation of multiple lipases, such as Amano AK, Amano SD, and Candida Antartica gave mixed results. Amano SD and Candida Antartica resulted in recovery of the epimeric mixture and partial resolution, respectively. Amano AK was able to selectively acetylate the (*R*) epimer at physiological temperature in the presence of powdered molecular sieves after 7 days (Scheme 4.7). This esterification allowed for facile separation of the mixture using column chromatography. Global deprotection of these 4 isomers via deacetylation and subsequent saponification afforded the Δ^{13}-9-isofurans **3.68**, **3.69**, **4.6**, and **4.7** (Scheme 4.8).

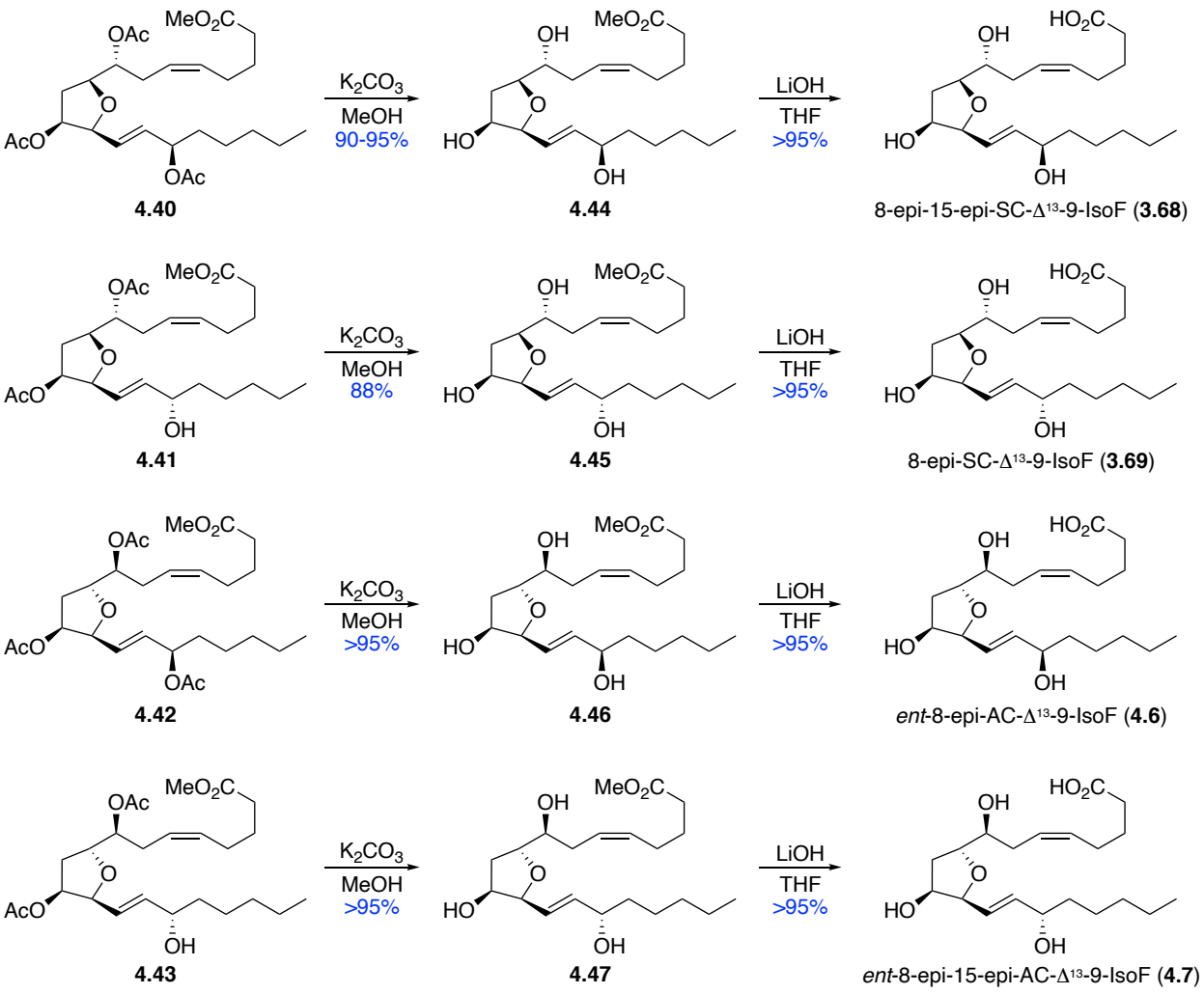

Scheme 4.8 Deprotection to afford 4 of 32 possible Δ^{13}-9-IsoFs.

Mosher Ester Analysis

Our synthetic route towards the production of isofurans **3.68**, **3.69**, **4.6**, and **4.7** provided multiple opportunities for stereochemical assignment using Mosher ester analysis.[61] Using the model presented by Hoye, the absolute configuration of the stereocenters in question could be determined (Figure 4.2).[62]

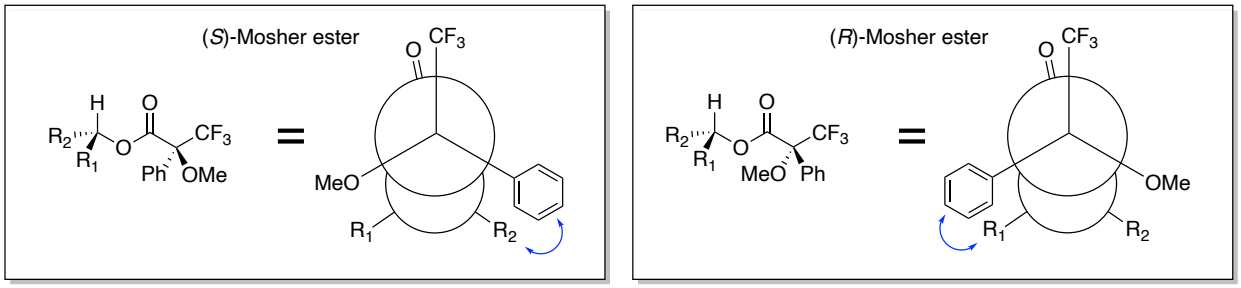

Figure 4.2 Model presented by Hoye for Mosher ester determination of stereochemistry

Due to anisotropic shielding by the phenyl group, protons in the R_2 side of the model for the (*S*)-Mosher ester will be more upfield than protons in the R_2 side for the (*R*)-Mosher ester. Alternatively, protons in R_1 of the (*R*)-Mosher ester will be more upfield than protons in R_1 of the (*S*)-Mosher ester. Therefore, a Δ-value can be assigned for which $\Delta = \delta_S - \delta_R$. Protons in R_2 will have a $\Delta < 0$ and protons in R_1 will have a $\Delta > 0$.

The first stereochemical assignment to be made was the stereocenters at C8 and C9 resulting from the epoxidation-cyclization sequence. Due to the presence of multiple free alcohols, a strategy for the selective esterification at C8 had to be implemented (Scheme 4.9). Desilylation of the silyl ether allowed for acetonide protection of the secondary alcohol at C11 and the newly formed primary alcohol at C13. The binding of these two alcohols left the secondary alcohol at C8

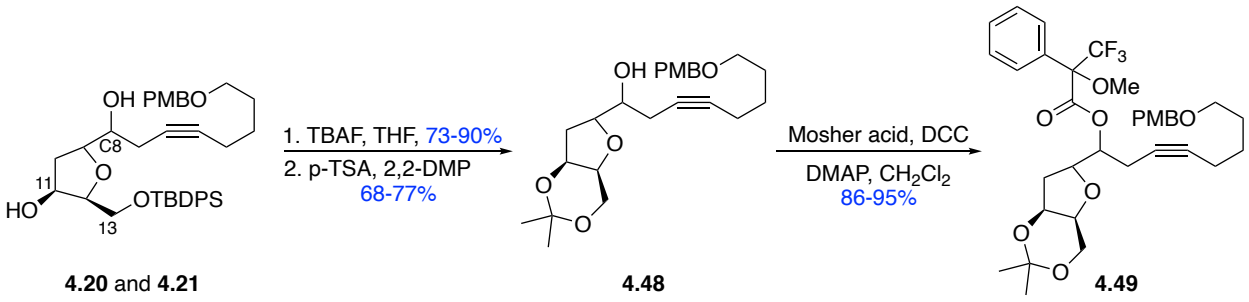

4.20 and **4.21** **4.48** **4.49**

Scheme 4.9 Formation of Mosher ester at C8.

as the sole site for esterification. Coupling of **4.48** with either (*R*) or (*S*)-Mosher acid using DCC provided the necessary compounds for analysis of the stereochemistry at C8. The ^{1}H NMR spectra were analyzed and the ppm values of the protons attached to carbons neighboring C8 were recorded (Tables 4.1 and 4.2).

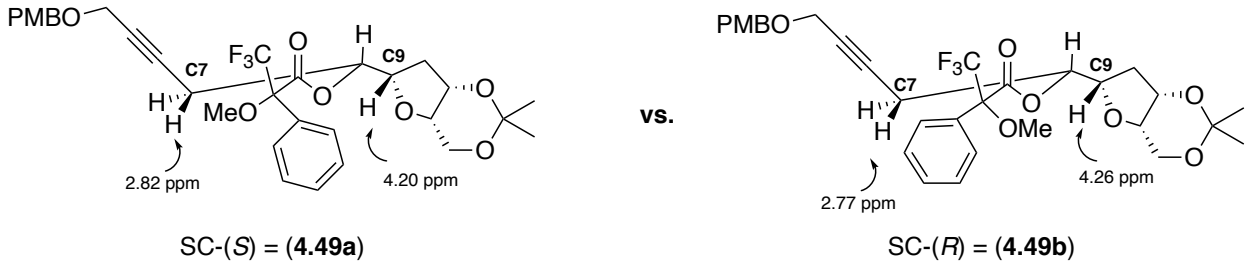

Figure 4.3 Assignment of stereochemistry at C8 using Mosher ester analysis for SC series.

Protons	**$\Delta\ \delta_H$ (4.49a-4.49b)**
H(7)	0.05 ppm
H(9)	-0.06 ppm

Table 4.1 Data obtained for Mosher ester analysis at C8 for SC series.

Based on the relative ^{1}H NMR shifts at C7 and C9 correlating to the (*R*) and (*S*) Mosher esters, the absolute stereochemistry at C8 for **4.49a** and **4.49b** was determined to be (*R*). Resulting from the stereospecific cyclization onto the trans epoxide, the stereocenter at C9 would therefore be (*S*) meaning that **4.49a** and **4.49b** belong to the SC-isofuran series.

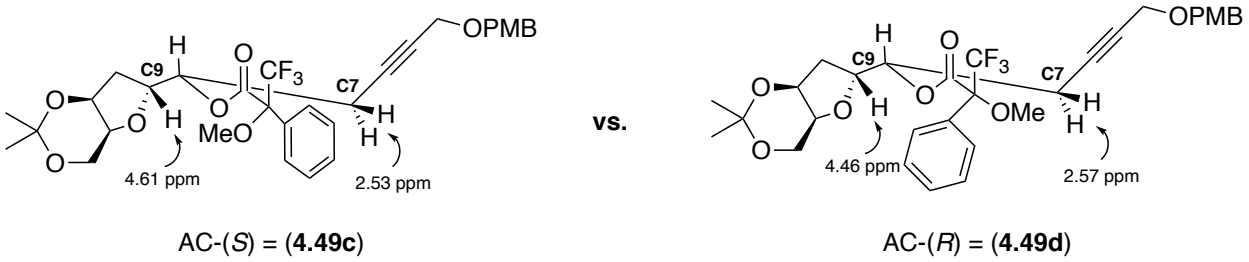

Figure 4.4 Assignment of stereochemistry at C8 using Mosher ester analysis for AC series.

Protons	**$\Delta\ \delta_H$ (4.49c-4.49d)**
H(7)	-0.04 ppm
H(9)	0.15 ppm

Table 4.2 Data obtained for Mosher ester analysis at C8 for AC series.

Based on the relative ^{1}H NMR shifts at C7 and C9 correlating to the (*R*) and (*S*) Mosher esters, the absolute stereochemistry at C8 for **4.49c** and **4.49d** was determined to be (*S*). This indicates the stereochemistry at C9 is (*R*), which leads to the conclusion that **4.49c** and **4.49d** belong to the AC-isofuran series.

Following enzymatic resolution using Amano AK lipase, a second Mosher ester analysis was performed to determine the absolute stereochemistry at C15. The use of diastereomerically

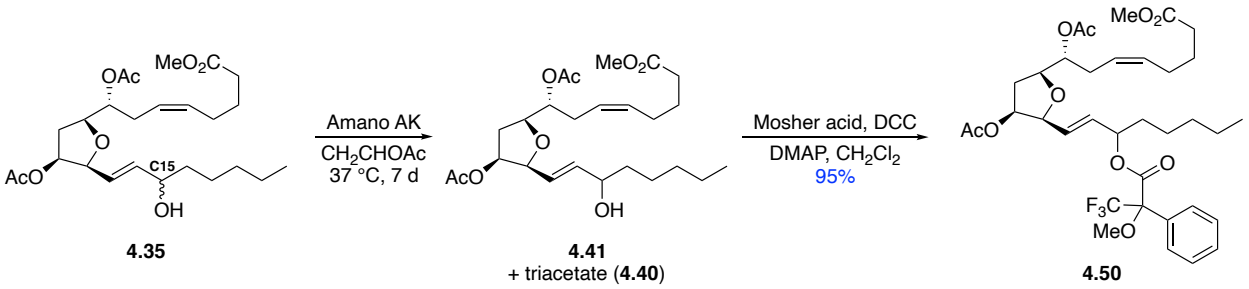

Scheme 4.10 Formation of Mosher ester at C15.

enriched diacetate **4.41** allowed for facile esterification without further protecting group manipulation (Scheme 4.10). DCC was used to couple **4.41** with (*R*) and (*S*)-Mosher acid to produce compounds **4.50a** and **4.50b**, respectively. Comparison of the chemical shifts at C13, C14, and C16 for **4.50a** and **4.50b** provided the stereochemistry at C15 (Table 4.3).

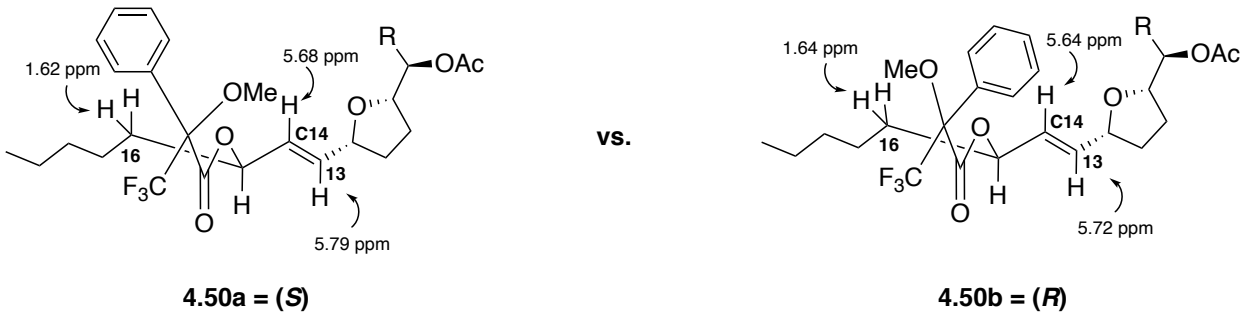

4.50a = (*S*) **4.50b = (*R*)**

Figure 4.5 Assignment of stereochemistry at C15 using Mosher ester analysis.

Protons	**$\Delta\ \delta_H$ (4.50a-4.50b)**
H(13)	0.07 ppm
H(14)	0.04 ppm
H(16)	-0.02 ppm

Table 4.3 Data obtained for Mosher ester analysis at C15.

Based on analysis of the ^{1}H NMR chemical shifts of the compounds **4.50a** and **4.50b**, the absolute stereochemistry at C15 was determined to be (*S*). This would indicate that the triacetate **4.40** produced from the enzymatic resolution possessed (*R*) stereochemistry at C15. Due to the minimal amount of material present at this point in our synthetic route, the Mosher ester analysis was only performed on the SC isofuran series. It was extrapolated that the stereochemistry of the epimer acetylated via enzymatic resolution was identical for the AC series.

Conclusion

Through the employment of a stereodivergent strategy, 4 members of the Δ^{13}-9-IsoF family were synthesized in 27 total steps (longest linear sequence). In collaboration with the laboratory of Dr. James West, studies to ascertain the biological activities of the individual isomers are ongoing in hopes unveiling the role of these autoxidative products in the context of PAH.

Experimental Methods

General Procedure. All glassware used for non-aqueous reactions was flame dried under vacuum. Reactions conducted at ambient temperature were run at approximately 23 °C unless otherwise noted. Reactions were monitored by analytical thin-layer chromatography performed on Analtech silica gel GF 250 micron plates. The plates were visualized with UV light (254 nm) and either potassium permanganate, ceric ammonium molybdate, or p-anisaldehyde followed by charring with a heat-gun. Flash chromatography utilized 230-400 mesh silica from Sorbent Technologies or Silica RediSep Rf flash columns on a CombiFlash Rf automated flash chromatography system. Solvents for extraction, washing and chromatography were HPLC grade. Nuclear magnetic resonance (NMR) spectra were acquired on a 400 MHz Bruker AV-400 FT-NMR spectrometer at ambient temperature. ^{1}H and ^{13}C NMR data are reported as values relative to $CDCl_3$.^{1}H chemical shifts are reported in δ values in ppm. Data are reported as follows: chemical shift, multiplicity (s = singlet, d = doublet, t = triplet, q = quartet, br = broad, m = multiplet), integration, coupling constant (Hz). ^{13}C chemical shifts are reported in δ values in ppm. Low resolution mass spectra were obtained on an Agilent 1200 series 6130 mass spectrometer with electrospray ionization. Yields were reported as isolated, spectroscopically pure compounds.

Materials. All reagents and solvents were commercial grade and purified prior to use when necessary. All reagents unless otherwise stated were purchased from Sigma Aldrich, Oakwood Chemical, or Strem Chemicals. All reactions were performed under argon atmosphere unless otherwise stated. Diethyl ether (Et_2O) and dichloromethane (CH_2Cl_2) were dried by passage through a column of activated alumina using an MBraun MB-SPS dry solvent system. Tetrahydrofuran (THF) was distilled from sodium with benzophenone as indicator prior to use.

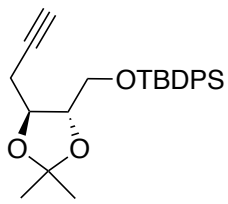

4.1: To a solution of alcohol **4.10** (1.95 g, 4.86 mmol) in CH_2Cl_2 (81 mL) at -20 °C was added NEt_3 (2.0 mL, 15 mmol) followed by trifluoromethanesulfonic anhydride (1.2 mL, 7.3 mmol). The resulting solution was allowed to stir at -20 °C for 45 min, quenched with satd. aq. $NaHCO_3$ (20 mL). The aqueous layer was extracted with CH_2Cl_2 (3 x 30 mL). The combined organic extracts were washed with brine (20 mL), dried ($MgSO_4$), filtered, and concentrated *in vacuo*. The residue was quickly filtered through a silica gel plug (10:1 hexanes/EtOAc) to afford 2.24 g of crude triflate used immediately in the next reaction.

To a solution of trimethylsilyl acetylene (1.2 mL, 8.4 mmol) in THF (23 mL) cooled to -10 °C was added a solution of NaHMDS (6.3 mL, 1M in THF) dropwise and the resulting solution was maintained at that temperature for 45 min. A solution of the crude triflate (2.24 g, 4.2 mmol) in THF (10 mL) was added and the reaction mixture was warmed to room temperature, stirred for 20 h and quenched with satd. aq. NH_4Cl (20 mL). The aqueous layer was extracted with Et_2O (3 x 40 mL). The combined organic extracts were washed with brine (30 mL), dried ($MgSO_4$), filtered and concentrated *in vacuo*. The residue was filtered through a silica plug (10:1 hexanes/EtOAc) to afford 1.42 g of crude trimethylsilyl alkyne (1.42 g, 2.95 mmol) and dissolved in MeOH (4.2 mL). To the methanol solution was added K_2CO_3 (0.408 g, 2.95 mmol) and the reaction mixture was stirred for 24 h. The reaction mixture was concentrated *in vacuo* and partitioned between water (30 mL) and Et_2O (30 mL). The aqueous layer was extracted with Et_2O (3 x 30 mL). The combined organic extracts were washed with brine (20 mL), dried ($MgSO_4$), filtered, and concentrated *in vacuo*. The residue was purified by flash column chromatography (gradient: 20:1 to 10:1 hexanes/EtOAc) to afford 0.821 g (41% over 3 steps) of **4.1** as a clear oil: R_f 0.55 (10:1

hexanes/EtOAc); ^{1}H NMR (400 MHz, $CDCl_3$) δ 7.68 (m, 4H), 7.40 (m, 6H), 4.13 (m, 1H),3.94 (m, 1H), 3.82 (m, 2H), 2.56 (m, 2H), 1.99 (t, *J* = 2.68 Hz, 1H), 1.42 (d, *J* = 11 Hz, 6H), 1.07 (s, 9H); ^{13}C NMR (100 MHz, $CDCl_3$) δ 135.8, 133.3, 129.9,127.8, 109.3, 80.5, 80.0, 76.0, 70.5, 64.1, 27.3, 27.2, 23.1, 19.4.

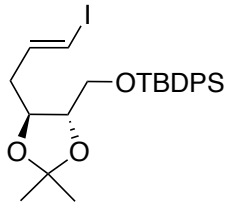

4.13: To a suspension of $ZrCp_2Cl_2$ (1.98 g, 6.78 mmol) in THF (15 mL) at 0°C was added DIBAl-H (6.8 mL, 1.0 M in hexanes, 6.8 mmol). The resulting suspension was maintained for 30 min and a solution of **4.1** (2.52 g, 6.17 mmol) in THF (3.1 mL) was added dropwise. The reaction mixture was allowed to warm to room temperature and stirring continued for 90 min. The solution was cooled to -78 °C, a solution of iodine (2.03 g, 8.01 mmol) in THF (9.2 mL) was added dropwise and the resulting solution was stirred for 30 min. The reaction was quenched with 1 N HCl. The aqueous layer was extracted with Et_2O (3 x 10 mL). The combined organic extracts were washed with $Na_2S_2O_3$ (10 mL), $NaHCO_3$ (10 mL), brine (10 mL), dried ($MgSO_4$), filtered and concentrated *in vacuo*. The residue was purified by flash column chromatography (gradient: 20:1 to 10:1 hexanes:EtOAc) to afford 2.64 g (80%) of iodide **4.13** as a colorless oil: R_f 0.61 (10:1 hexanes/EtOAc); $[\alpha]^{23}_D$ –13.2 (*c* 1.0, $CHCl_3$); ^{1}H NMR (400 MHz, $CDCl_3$) δ 7.66 (m, 4H), 7.40 (m, 6H), 6.56 (m, 1H), 6.10 (d, *J* = 14.5 Hz, 1H), 4.01 (m, 1H), 3.74 (m, 3H), 2.36 (m, 2H), 1.38 (d, *J* = 9.5 Hz, 6H), 1.06 (s, 9H); ^{13}C NMR (100 MHz, $CDCl_3$) δ 142.1, 136.0, 130.2, 128.1, 109.3, 80.4, 77.6, 77.4, 64.4, 39.6, 27.6, 27.2, 19.6; LRMS calculated for $C_{25}H_{33}IO_3Si$ $[M+Na]^+$ m/z 559.1, measured LC/MS (ESI) R_t 1.55 min, m/z 559.4 $[M+Na]^+$.

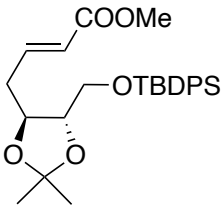

4.14: To a solution of iodide **4.13** (2.60 g, 4.83 mmol) in DMF (19 mL) was added triethylamine (1.35 mL, 9.68 mmol), palladium acetate (33 mg, 0.15 mmol), triphenylphosphine (76 mg, 0.29 mmol), and MeOH (7.8 mL). The mixture was purged with carbon monoxide for 10 min and stirred under an atmosphere of carbon monoxide at room temperature for 72 h. The reaction was diluted with Et_2O (20 mL) and water (10 mL). The aqueous layer was extracted with Et_2O (3 x 10 mL) and the combined organic extracts were washed with brine (20 mL) dried ($MgSO_4$), filtered, and concentrated *in vacuo*. The residue was purified by flash column chromatography (gradient: 20:1 to 4:1 hexanes/EtOAc) to afford 1.66 g (73%) of enoate **4.14** as a pale yellow oil: R_f 0.33 (20:1 hexanes/EtOAc); $[\alpha]^{23}_D$ -11.2 (*c* 1.0, $CHCl_3$); ^{1}H NMR (400 MHz, $CDCl_3$) δ 7.68-7.63 (m, 4H), 7.46-7.36 (m, 6H), 7.00 (ddd, *J* = 7.1, 7.1, 15.6 Hz, 1H), 5.91 (d, *J* = 15.7 Hz, 1H), 4.11-4.06 (m, 1H), 3.80-3.73 (m, 6H), 2.61-2.54 (m, 1H), 2.48-2.40 (m, 1H), 1.40 (s, 3H), 1.37 (s, 3H), 1.06 (s, 9H); ^{13}C NMR (100 MHz, $CDCl_3$) δ 166.8, 144.8, 135.8, 133.18, 133.15, 130.00, 129.97, 127.9, 123.4, 109.2, 80.4, 77.2, 64.1, 51.6, 35.9, 27.4, 27.1, 27.0, 19.4; LRMS calculated for $C_{27}H_{36}O_5Si$ $[M+Na]^+$ m/z 491.2, measured LC/MS (ESI) R_t 2.60 min, m/z 491.0 $[M+Na]^+$.

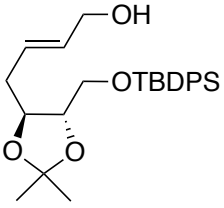

4.15: To a solution of enoate **4.14** (2.48 g, 5.29 mmol) in CH_2Cl_2 (16 mL) at -78 °C was added diisobutylaluminum hydride (11 mL, 1.0 M in hexanes, 11 mmol). The mixture was maintained at that temperature for 90 min, quenched with MeOH (ca. 5-10 drops) until gas evolution ceased, poured over satd. aq. Rochelle's salt (30 mL), and stirred for 16 h. The aqueous layer was then extracted with CH_2Cl_2 (3 x 10 mL) and the combined organic extracts were washed with dried ($MgSO_4$), filtered, and concentrated *in vacuo*. The residue was purified by flash column chromatography (gradient: 4:1 to 1:1 hexanes/EtOAc)

to afford 2.10 g (90%) of **4.15** as a clear oil: R_f 0.20 (4:1 hexanes/EtOAc); $[\alpha]^{23}_D$ +16.0 (*c* 1.0, $CHCl_3$); ^{1}H NMR (400 MHz, $CDCl_3$) δ 7.70-7.66 (m, 4H), 7.46-7.37 (m, 6H), 5.74-5.72 (m, 2H), 4.09-4.03 (m, 3H), 3.78-3.75 (m, 3H), 2.47-2.32 (m, 2H), 1.42 (s, 3H), 1.39 (s, 3H), 1.08 (s, 9H); ^{13}C NMR (100 MHz, $CDCl_3$) δ 135.8, 133.3, 132.0, 129.94, 129.90, 128.1, 127.9, 108.9, 80.7, 77.9, 64.2, 63.6, 36.1, 27.5, 27.1, 27.0, 19.4; LRMS calculated for $C_{26}H_{36}O_4Si$ $[M+Na]^+$ m/z 463.2; measured LC/MS (ESI) R_t 1.1 min, m/z 463.5 $[M+Na]^+$.

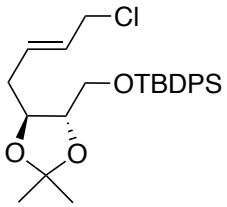

4.16: To a solution of **4.15** (2.10 g, 4.77 mmol) in MeCN (28 mL) at 0 °C was added diisopropylethylamine (2.6 mL, 15 mmol). The reaction mixture was stirred for 10 min, then dichlorotriphenylphosphorane (4.85 g, 14.3 mmol) was added and the reaction was maintained at 0 °C for 40 min. The solution was then loaded directly onto a silica gel column and purified by flash column chromatography (4:1 hexanes/EtOAc) to afford 1.95 g (89%) of **4.16** as clear oil: R_f 0.80 (4:1 hexanes/EtOAc); $[\alpha]^{23}_D$ -13.8 (*c* 1.0, $CHCl_3$); ^{1}H NMR (400 MHz, $CDCl_3$) δ 7.69-7.66 (m, 4H), 7.46-7.38 (m, 6H), 5.84-5.77 (m, 1H), 5.72-5.65 (m, 1H), 4.06-4.00 (m, 3H), 3.78-3.74 (m, 3H), 2.47-2.32 (m, 2H), 1.41 (s, 3H), 1.38 (s, 3H), 1.07 (s, 9H); ^{13}C NMR (100 MHz, $CDCl_3$) δ 135.8, 133.30, 133.28, 131.2, 129.97, 129.94, 128.8, 127.9, 108.9, 80.6, 77.7, 64.2, 45.1, 35.9, 27.5, 27.2, 27.0, 19.4; LRMS calculated for $C_{26}H_{35}ClO_3Si$ $[M+Na]^+$ m/z 481.2; measured LC/MS (ESI) R_t 1.46 min, m/z 481.4 $[M+Na]^+$.

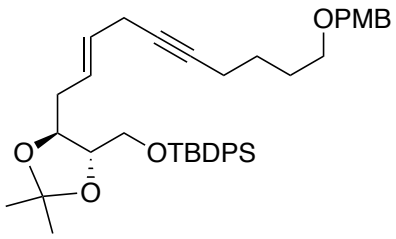

4.17: To a solution of **4.16** (1.95 g, 4.25 mmol) in DMF (16 mL) was added Cs_2CO_3 (2.77 g, 8.49 mmol), NaI (1.33 g, 8.88 mmol), CuI (0.914 g, 4.80 mmol), and PMB-protected hexyne (1.16 g, 5.31 mmol). The resulting suspension was maintained for 48 h

or until judged complete by TLC. The copper salts were filtered and washed with Et_2O (20 mL). The aqueous layer was extracted with Et_2O (3 x 30 mL) and the combined organic extracts were washed with brine (20 mL), dried ($MgSO_4$), filtered, and concentrated *in vacuo*. The residue was purified by flash column chromatography (gradient: 50:1 to 20:1 hexanes/EtOAc) to afford 2.28 g (84%) of **4.17** as a clear oil: R_f 0.20 (20:1 hexanes/EtOAc); $[\alpha]^{23}_D$ -12.6 (*c* 1.0, $CHCl_3$); ^{1}H NMR (400 MHz, $CDCl_3$) δ 7.69-7.66 (m, 4H), 7.45-7.36 (m, 6H), 7.25 (d, *J* = 8.6 Hz, 2H), 6.87 (d, *J* = 8.6 Hz, 2H), 5.73-5.66 (m, 1H), 5.48 (dt, *J* = 5.5, 15.2 Hz, 1H), 4.42 (s, 2H), 4.06-4.02 (m, 1H), 3.80-3.75 (m, 6H), 3.44 (t, *J* = 6.4 Hz, 2H), 2.88-2.87 (m, 2H), 2.42-2.29 (m, 2H), 2.21-2.16 (m, 2H), 1.73-1.66 (m, 2H), 1.60-1.55 (m, 2H), 1.40 (s, 3H), 1.38 (s, 3H), 1.06 (s, 9H); ^{13}C NMR (100 MHz, $CDCl_3$) δ 159.3, 135.8, 133.4, 130.9, 129.90, 129.86, 129.4, 128.1, 127.9, 126.9, 113.9, 108.7, 82.0, 80.7, 77.8, 77.6, 72.7, 69.7, 64.2, 55.4, 36.1, 29.1, 27.5, 27.2, 27.0, 25.9, 22.3, 19.4, 18.8; LRMS calculated for $C_{40}H_{52}O_5Si$ $[M+H]^+$ m/z 641.4, measured LC/MS (ESI) R_t 1.57 min, m/z 641.6 $[M+H]^+$.

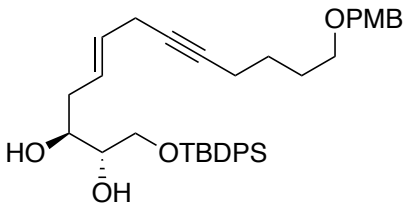

4.18: To a solution of **4.17** (2.28 g, 3.56 mmol) in MeCN (83 mL) at 0 °C was added copper (II) chloride dihydrate (6.06 g, 35.6 mmol). The reaction mixture was maintained at that temperature for 6 h, quenched with satd. aq. $NaHCO_3$ (10 mL) and extracted with EtOAc (3 x 15 mL). The combined organic extracts were washed with brine (10 mL), dried ($MgSO_4$), filtered, and concentrated *in vacuo*. The residue was purified by flash column chromatography (gradient: 7:1 to 1:1 hexanes/EtOAc) to afford 1.57 g (73%) of diol **4.18** as a clear oil: R_f 0.30 (3:1 hexanes/EtOAc); $[\alpha]^{23}_D$ -3.0 (*c* 1.0, $CHCl_3$); ^{1}H NMR (400 MHz, $CDCl_3$) δ 7.69-7.65 (m, 4H), 7.46-7.37 (m, 6H), 7.25 (d, *J* = 8.6 Hz, 2H), 6.87 (d, *J* = 8.6 Hz, 2H), 5.74-5.66 (m, 1H), 5.50 (dt,

J = 5.4, 15.2 Hz, 1H), 4.42 (s, 2H), 3.81-3.77 (m, 4H), 3.75-3.71 (m, 2H), 3.59-3.55 (m, 1H), 3.45 (t, J = 6.4 Hz, 2H), 2.89 (m, 2H), 2.70 (d, J = 6.1 Hz, 1H), 2.66 (d, J = 4.2 Hz, 1H), 1.74-1.67 (m, 2H), 1.61-1.54 (m, 2H), 1.07 (s, 9H) ; ^{13}C NMR (100 MHz, $CDCl_3$) δ 159.3, 135.70, 135.66, 133.0, 132.9, 130.8, 130.1, 129.4, 128.4, 128.0, 127.2, 113.9, 82.2, 77.6, 72.8, 72.7, 71.6, 69.7, 66.4, 55.4, 36.7, 29.1, 27.0, 25.8, 22.2, 19.3, 18.8; LRMS calculated for $C_{37}H_{48}O_5Si$ $[M+H]^+$ m/z 601.3, measured LC/MS (ESI) R_t 1.46 min, m/z 601.0 $[M+H]^+$.

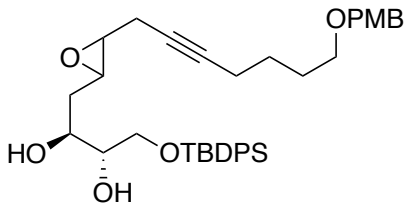

4.19: To a solution of diol **4.18** (1.57 g, 2.61 mmol) in CH_2Cl_2 (26 mL) at 0 °C was added m-CPBA (0.70 g, 3.1 mmol, 77% by weight) and $NaHCO_3$ (263 mg, 3.14 mmol). The reaction mixture was maintained at 0 °C for 5 h, or until judged complete by TLC, and diluted with water (20 mL). The aqueous layer was extracted with CH_2Cl_2 (3 x 15 mL). The combined organic extracts were washed with brine (10 mL), dried ($MgSO_4$), filtered, and concentrated *in vacuo*. The residue was purified by flash column chromatography (gradient: 4:1 to 2:1 hexanes/EtOAc) to afford 1.50 g (93%) of **4.19** as an 1:1.2 mixture of inseparable diastereomers as a pale yellow oil: R_f 0.33 (2:1 hexanes/EtOAc); ^{1}H NMR (400 MHz, $CDCl_3$) δ 7.68-7.64 (m, 4H), 7.46-7.38 (m, 6H), 7.26-7.23 (m, 2H), 6.88-6.86 (m, 2H), 4.42 (s, 2H, major), 4.41 (s, 2H, minor), 3.97-3.90 (m, 1H), 3.81-3.71 (m, 5H), 3.65-3.60 (m, 1H, minor), 3.58-3.55 (m, 1H, major), 3.45 (t, J = 6.4 Hz, 2H, major), 3.44 (t, J = 6.4 Hz, 2H, minor), 3.09-3.06 (m, 1H, major), 3.04-3.01 (m, 1H, minor), 2.90-2.84 (m, 2H), 2.58-2.52 (m, 1H), 2.46-2.35 (m, 1H), 2.19-2.15 (m, 2H), 2.01-1.94 (m, 1H, major), 1.87-1.81 (m, 1H, minor), 1.74-1.62 (m, 2H), 1.59-1.50 (m, 2H), 1.07 (s, 9H); ^{13}C NMR (100 MHz, $CDCl_3$) δ 159.3, 135.71, 135.66 (isomers), 133.0, 132.9 (isomers), 132.83, 132.78 (isomers), 130.8, 130.7 (isomers), 130.1, 129.39, 129.37 (isomers), 128.0, 113.9, 82.5, 74.74,

74.72 (isomers), 73.5, 73.3 (isomers), 72.7, 70.1, 69.8 (isomers), 69.7, 66.2, 65.9 (isomers), 56.7, 56.4 (isomers), 55.8, 55.7 (isomers), 55.4, 35.8, 35.5 (isomers), 29.0, 27.0, 25.68, 25.67 (isomers), 22.4, 22.3 (isomers), 19.34, 19.33 (isomers), 18.7; LRMS calculated for $C_{37}H_{48}O_6Si$ $[M+Na]^+$ m/z 639.3, measured LC/MS (ESI) R_t 1.21 min, m/z 639.0 $[M+Na]^+$.

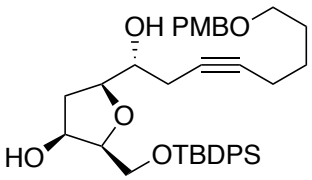

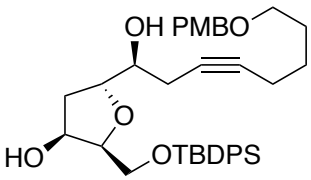

4.20 and 4.21: To a solution of epoxide **4.19** (1.50 g, 2.43 mmol) in $CHCl_3$ (61 mL) was added trifluoroacetic acid (0.19 mL, 2.4 mmol) and reaction maintained at room temperature for 1 h. Triethylamine (0.34 mL, 2.4 mmol) was added to the reaction mixture was concentrated *in vacuo*. The residue was purified by flash column chromatography (gradient: 3:1 to 1:1 hexanes/EtOAc) to afford 0.525 g (35%) of **4.20** and 0.548 g (37%) of **4.21** as clear oils. Stereochemical assignments of diols **4.20** and **4.21** were based on NMR analysis of Mosher esters derived from secondary alcohols at C8.

4.20 R_f 0.33 (1:1 hexanes/EtOAc); $[\alpha]^{23}_D$ +2.9 (*c* 1.0, $CHCl_3$); ^{1}H NMR (400 MHz, $CDCl_3$) δ 7.72-7.67 (m, 4H), 7.45-7.36 (m, 6H), 7.25 (d, *J* = 8.6 Hz, 2H), 6.87 (d, *J* = 8.6 Hz, 2H), 4.42 (s, 2H), 4.38-4.36 (m, 1H), 4.15 (dt, *J* = 3.7, 9.1 Hz, 1H), 4.01 (dd, *J* = 5.8, 10.8 Hz, 1H), 3.95-3.89 (m, 2H), 3.81-3.78 (m, 4H), 3.45 (t, *J* = 6.3 Hz, 2H), 2.40-2.15 (m, 5H), 2.01 (ddd, *J* = 1.4, 4.1, 14.0 Hz, 1H), 1.72-1.65 (m, 2H), 1.60-1.53 (m, 2H), 1.06 (s, 9H); ^{13}C NMR (100 MHz, $CDCl_3$) δ 159.3, 135.8, 135.7, 133.2, 133.1, 130.8, 130.0, 129.4, 127.91, 127.90, 113.9, 82.9, 82.6, 80.0, 75.8, 72.7, 72.2, 71.3, 69.6, 63.1, 55.4, 34.7, 29.0, 27.0, 25.8, 24.4, 19.3, 18.7; LRMS calculated for $C_{37}H_{48}O_6Si$ $[M+Na]^+$ m/z 639.3, measured LC/MS (ESI) R_t 2.57 min, m/z 639.0 $[M+Na]^+$.

4.21 R_f 0.22 (1:1 hexanes/EtOAc); $[\alpha]^{23}_D$ -5.8 (*c* 1.0, $CHCl_3$); ^1H NMR (400 MHz, $CDCl_3$) δ 7.73-7.66 (m, 4H), 7.47-7.38 (m, 6H), 7.25 (d, *J* = 8.6 Hz, 2H), 6.87 (d, *J* = 8.6 Hz, 2H), 4.59-4.57 (m, 1H), 4.42 (s, 2H), 4.32 (td, *J* = 5.0, 8.1 Hz, 1H), 4.00-3.94 (m, 3H), 3.83-3.78 (m, 4H), 3.44 (t, *J* = 6.4 Hz, 2H), 2.39-2.37 (m, 2H), 2.19-2.15 (m, 2H), 2.07-2.04 (m, 2H), 1.72-1.65 (m, 2H), 1.60-1.53 (m, 2H), 1.06 (s, 9H); ^{13}C NMR (100 MHz, $CDCl_3$) δ 159.3, 135.8, 135.7, 132.9, 132.7, 130.8, 130.1, 129.4, 128.01, 127.98, 113.9, 82.9, 81.6, 80.3, 75.8, 74.1, 72.7, 71.4, 69.7, 63.4, 55.4, 36.0, 29.0, 26.9, 25.8, 23.9, 19.3, 18.7; LRMS calculated for $C_{37}H_{48}O_6Si$ $[M+Na]^+$ m/z 639.3, measured LC/MS (ESI) R_t 2.57 min, m/z 639.0$[M+Na]^+$.

General acetylation of diols 4.22 and 4.27 To a solution of diol **4.20** (0.525 g, 0.851 mmol) in CH_2Cl_2 (17 mL) was added acetic anhydride (0.32 mL, 3.4 mmol), pyridine (0.68 mL, 8.5 mmol) and 4-dimethylaminopyridine (cat.). The resulting solution was maintained for 16 h, concentrated *in vacuo* and the residue purified by flash column chromatography (2:1 hexanes/EtOAc) to afford diacetate in 83-90% yield as a clear oil.

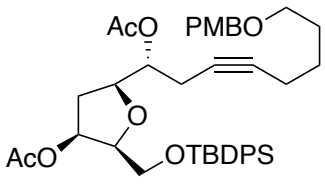

4.22: R_f 0.85 (2:1 hexanes/EtOAc); $[\alpha]^{23}_D$ +5.6 (*c* 1.0, $CHCl_3$); ^1H NMR (400 MHz, $CDCl_3$) δ: 7.66-7.64 (m, 4H), 7.43-7.36 (m, 6H), 7.25 (d, *J* = 8.6 Hz, 2H), 6.87 (d, *J* = 8.6 Hz, 2H), 5.38-5.36 (m, 1H), 4.94-4.89 (m, 1H), 4.42 (s, 2H), 4.17-4.11 (m, 1H), 4.08-4.04 (m, 1H), 3.83 (d, J = 6.3 Hz, 2H), 3.80 (s, 3H), 3.44 (t, J = 6.4 Hz, 2H), 2.58-2.43 (m, 2H), 2.36 (ddd, *J* = 6.0, 8.5, 14.5 Hz, 1H), 2.16-2.13 (m, 2H), 2.03 (s, 3H), 1.98 (s, 3H), 1.91 (ddd, *J* = 1.3, 4.4, 14.5 Hz, 1H), 1.71-1.64 (m, 2H), 1.58-1.51 (m, 2H), 1.03 (s, 9H); ^{13}C NMR (100 MHz, $CDCl_3$) δ: 170.6, 170.2, 159.3, 135.7, 135.6, 133.6, 133.4, 130.8, 129.9, 129.3, 127.9, 113.9, 82.2, 82.1, 77.5, 75.3, 73.6, 73.0, 72.7, 69.7,

61.8, 55.4, 35.0, 29.0, 26.9, 25.8, 21.6, 21.2, 19.3, 18.7; LRMS calculated for $C_{41}H_{52}O_8Si$ $[M+H]^+$ m/z 701.3, measured LC/MS (ESI) R_t 2.98 min, m/z 701.0 $[M+H]^+$.

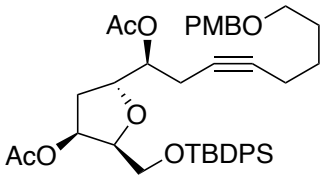

4.27: R_f 0.85 (2:1 hexanes/EtOAc); $[\alpha]^{23}_D$ +20.6 (*c* 1.0, $CHCl_3$); ^1H NMR (400 MHz, $CDCl_3$) δ 7.65-7.63 (m, 4H), 7.44-7.35 (m, 6H), 7.25 (d, *J* = 9.4 Hz, 2H), 6.87 (d, *J* = 8.7 Hz, 2H), 5.47-5.44 (m, 1H), 4.97 (q, *J* = 5.8 Hz, 1H), 4.42 (s, 2H), 4.36-4.30 (m, 1H), 4.12 (td, *J* = 3.7, 6.3 Hz, 1H), 3.80-3.79 (m, 5H), 3.43 (t, *J* = 6.4 Hz, 2H), 2.49-2.47 (m, 2H), 2.18-2.11 (m, 4H), 2.06 (s, 3H), 1.96 (s, 3H), 1.70-1.63 (m, 2H), 1.57-1.50 (m, 2H), 1.03 (s, 9H); ^{13}C NMR δ 170.3, 170.2, 159.2, 135.7, 135.6, 133.5, 133.4, 130.8, 129.8, 129.3, 127.8, 113.9, 82.4, 81.5, 77.9, 75.0, 74.1, 73.3, 72.6, 69.6, 61.8, 55.3, 34.9, 29.0, 26.8, 25.7, 21.3, 21.2, 21.1, 19.3, 18.6; LRMS calculated for $C_{41}H_{52}O_8Si$ $[M+H]^+$ m/z 701.3, measured LC/MS (ESI) R_t 2.95 min, m/z 701.1 $[M+H]^+$.

Alcohols 4.23 and 4.28: To a solution of ether **4.22** (0.293 g, 0.418 mmol) in CH_2Cl_2 (3.2 mL) at 0 °C was added DDQ (0.142 g, 0.628 mmol) and water (0.17 mL). The resulting suspension was allowed to warm to room temperature and maintained for 3 h. The reaction mixture was filtered through a pad of Celite and the filtrated concentrated *in vacuo*. The residue was purified by flash column chromatography (gradient: 2:1 to 1:1 hexanes/EtOAc) to afford 0.220 g (91%) of alcohol **4.23** as a yellow to orange oil.

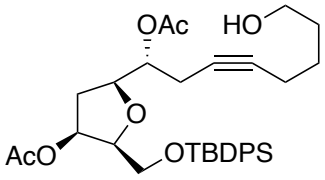

4.23: R_f 0.25 (2:1 hexanes/EtOAc); $[\alpha]^{23}_D$ +7.4 (*c* 1.0, $CHCl_3$); ^1H NMR (400 MHz, $CDCl_3$) δ 7.66-7.64 (m, 4H), 7.45-7.36 (m, 6H), 5.38-5.35 (m, 1H), 4.97-4.92 (m, 1H), 4.14-4.09 (m, 1H), 4.06 (td, *J* = 4.0, 6.3 Hz, 1H), 3.83 (d, *J* = 6.4 Hz, 2H), 3.65 (t, *J* = 6.4 Hz, 2H), 2.60-2.41 (m, 2H), 2.38 (ddd,

J = 5.9, 8.5, 14.5 Hz, 1H), 2.19-2.16 (m, 2H), 2.05 (s, 3H), 1.99 (s, 3H), 1.91 (ddd, J = 1.6, 4.5, 14.6 Hz, 1H), 1.69-1.63 (m, 2H), 1.59-1.51 (m, 2H), 1.03 (s, 9H); ^{13}C NMR (100 MHz, $CDCl_3$) δ 170.6, 170.4, 135.7, 135.6, 133.6, 133.4, 129.9, 127.9, 82.2, 82.1, 77.6, 75.6, 73.6, 73.2, 62.5, 61.8, 35.1, 31.9, 26.9, 25.2, 21.7, 21.19, 21.16, 19.3, 18.6; LRMS calculated for $C_{33}H_{44}O_7Si$ $[M+Na]^+$ m/z 603.3, measured LC/MS (ESI) R_t 2.25 min, m/z 602.9 $[M+Na]^+$.

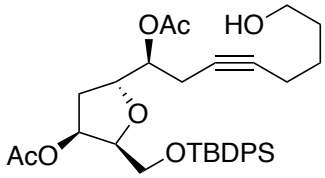

4.28: R_f 0.25 (2:1 hexanes/EtOAc); $[\alpha]^{23}_D$ +22.4 (*c* 1.0, $CHCl_3$); ^{1}H NMR (400 MHz, $CDCl_3$) δ 7.65-7.63 (m, 4H), 7.42-735 (m, 6H), 5.49-5.42 (m, 1H), 4.99 (q, J = 5.9 Hz, 1H), 4.34-4.28 (m, 1H), 4.13 (td, J = 3.8, 6.1 Hz, 1H), 3.80 (d, J = 6.2 Hz, 2H), 3.63 (t, J = 6.3 Hz, 2H), 2.55-2.41 (m, 2H), 2.22-2.11 (m, 4H), 2.07 (s, 3H), 1.97 (s, 3H), 1.67-1.60 (m, 2H), 1.57-1.50 (m, 2H), 1.03 (s, 9H); ^{13}C NMR (100 MHz, $CDCl_3$) δ 170.42, 170.37, 135.7, 133.5, 129.8, 127.8, 82.3, 81.5, 77.9, 75.3, 74.2, 73.4, 62.5, 61.8, 34.9, 31.9, 26.8, 25.1, 21.4, 21.2, 21.1, 19.3, 18.6; LRMS calculated for $C_{33}H_{44}O_7Si$ $[M+Na]^+$ m/z 603.3, measured LC/MS (ESI) R_t 2.26 min, m/z 602.9 $[M+Na]^+$.

Aldehydes 4.24 and 4.29: To a solution of primary alcohol **4.23** (2.8 g, 4.8 mmol) in CH_2Cl_2 (64 mL) was added DMP (4.1 g, 9.6 mmol). The solution was stirred for 1.5 h, quenched with a 1:1 solution of satd. aq. $NaHCO_3$ and $Na_2S_2O_3$ (4 mL) and allowed to stir for 10 min. The aqueous layer was extracted with Et_2O (3 x 75 mL). The combined organic extracts were washed with brine (75 mL), dried ($MgSO_4$), filtered and concentrated *in vacuo*. The residue was purified by flash chromatography (gradient 4:1 to 2:1 Hexanes: EtOAc) to afford 2.3 g (83 %) of aldehyde **4.24** as a colorless oil.

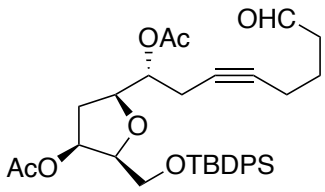

4.24: R_f 0.90 (2:1 hexanes/EtOAc); $[\alpha]^{23}_D$ +7.2 (*c* 2.0, $CHCl_3$); ^1H NMR (400 MHz, $CDCl_3$) δ 9.78 (s, 1H), 7.66-7.64 (m, 4H), 7.45-7.36 (m, 6H), 5.39-5.36 (m, 1H), 4.94-4.89 (m, 1H), 4.14-4.09 (m, 1H), 4.07 (td, *J* = 4.0, 6.3 Hz, 1H), 3.83 (d, *J* = 6.3 Hz, 2H), 2.59-2.43 (m, 4H), 2.38 (ddd, *J* = 5.9, 8.5, 14.5 Hz, 1H), 2.23-2.19 (m, 2H), 2.05 (s, 3H), 1.99 (s, 3H), 1.90 (ddd, *J* = 1.6, 4.5, 14.6 Hz, 1H), 1.79 (p, *J* = 7.0 Hz, 2H), 1.03 (s, 9H); ^{13}C NMR (100 MHz, $CDCl_3$) δ 202.1, 170.5, 170.2, 135.7, 135.6, 133.6, 133.4, 129.9, 127.9, 127.8, 82.2, 81.1, 77.4, 76.4, 73.5, 73.0, 61.8, 42.9, 35.1, 26.9, 21.6, 21.5, 21.2, 19.3, 18.3; LRMS calculated for $C_{33}H_{42}O_7Si$ $[M+H]^+$ m/z 579.3, measured LC/MS (ESI) R_t 1.07 min, m/z 579.0 $[M+H]^+$.

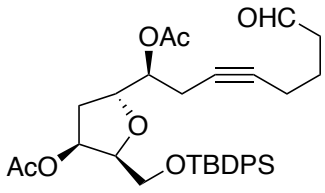

4.29: R_f 0.90 (2:1 hexanes/EtOAc); $[\alpha]^{23}_D$ +29.2 (*c* 1.0, $CHCl_3$); ^1H NMR (400 MHz, $CDCl_3$) δ 9.77 (s, 1H), 7.65-7.63 (m, 4H), 7.44-7.36 (m, 6H), 5.47-5.44 (m, 1H) 4.97 (q, *J* = 5.8 Hz, 1H), 4.33-4.28 (m, 1H), 4.12 (td, *J* = 3.8, 6.1 Hz, 1H), 3.80 (d, *J* = 6.2 Hz, 2H), 2.53 (t, *J* = 7.3 Hz, 2H), 2.49-2.48 (m, 2H), 2.21-2.18 (m, 2H), 2.15 (dd, *J* = 3.4, 7.8 Hz, 2H), 2.07 (s, 3H), 1.97 (s, 3H), 1.78 (p, *J* = 7.1 Hz, 2H), 1.03 (s, 9H); ^{13}C NMR (100 MHz, $CDCl_3$) δ 202.0, 170.32, 170.28, 135.7, 133.5, 129.9, 127.8, 81.6, 81.3, 77.8, 76.1, 74.2, 73.3, 61.8, 42.8, 35.0, 26.9, 21.42, 21.37, 21.2, 21.1, 19.3, 18.3; LRMS calculated for $C_{33}H_{42}O_7Si$ $[M+H]^+$ m/z 579.3, measured LC/MS (ESI) R_t 2.41 min, m/z 578.9 $[M+H]^+$.

Esters 4.25 and 4.30 To a solution of aldehyde **4.24** (172 mg, 0.297 mmol) in *t*-BuOH (1.49 mL) and 2-methyl-2-butene (0.94 mL, 8.9 mmol) was added $NaClO_2$ (62 mg, 0.68 mmol) and NaH_2PO_4 (71 mg, 0.59 mmol) in H_2O (0.23 mL). The resulting solution was maintained for 2 h, quenched

by addition of satd. aq. $Na_2S_2O_3$ (ca. 5-10 drops) and the aqueous layer was extracted with EtOAc (3 x 20 mL). The combined organic extracts were washed with brine (10 mL), dried ($MgSO_4$), filtered, and concentrated *in vacuo* to afford 191 mg of crude acid. The crude acid was dissolved in benzene (2.6 mL) and MeOH (0.64 mL). $TMSCHN_2$ (1.61 mL, 3.21 mmol, 2.0 M in hexanes) was added dropwise and the resulting solution maintained for 1 h, concentrated *in vacuo*. The residue was purified by flash column chromatography (2:1 hexanes/EtOAc) to afford 139 mg (77% over 2 steps) of ester **4.25** as a clear oil.

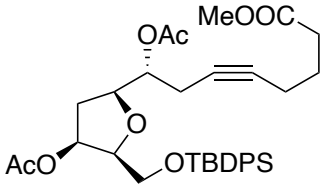

4.25: R_f 0.85 (2:1 hexanes/EtOAc); $[\alpha]^{23}_D$ +7.6 (*c* 1.0, $CHCl_3$); ^1H NMR (400 MHz, $CDCl_3$) δ 7.66-7.63 (m, 4H), 7.45-7.36 (m, 6H), 5.39-5.36 (m, 1H), 4.93-4.89 (m, 1H), 4.16-4.11 (m, 1H), 4.07 (td, *J* = 3.9, 6.3 Hz, 1H), 3.82 (d, *J* = 6.4 Hz, 2H), 3.66 (s, 3H), 2.59-2.44 (m, 2H), 2.43-2.34 (m, 3H), 2.22-2.18 (m, 2H), 2.05 (s, 3H), 1.99 (s, 3H), 1.90 (ddd, *J* = 1.7, 4.5, 14.6 Hz, 1H), 1.78 (p, *J* = 7.2 Hz, 2H), 1.03 (s, 9H); ^{13}C NMR (100 MHz, $CDCl_3$) δ 173.8, 170.5, 170.2, 135.7, 135.6, 133.6, 133.4, 129.9, 127.9, 127.8, 82.2, 81.2, 77.4, 76.1, 73.5, 73.0, 61.8, 51.7, 35.1, 32.9, 26.9, 24.2, 21.6, 21.2, 21.1, 19.3, 18.4; LRMS calculated for $C_{34}H_{44}O_8Si$ $[M+Na]^+$ m/z 631.3, measured LC/MS (ESI) R_t 1.19 min, m/z 631.0 $[M+Na]^+$.

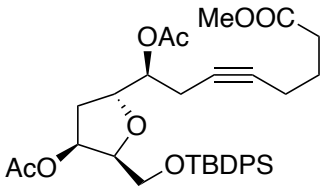

4.30: R_f 0.85 (2:1 hexanes/EtOAc); $[\alpha]^{23}_D$ +26.2 (*c* 1.0, $CHCl_3$); ^1H NMR (400 MHz, $CDCl_3$) δ 7.65-7.63 (m, 4H), 7.44-7.35 (m, 6H), 5.47-5.44 (m, 1H), 4.96 (q, *J* = 5.9 Hz, 1H), 4.34-4.29 (m, 1H), 4.12 (td, *J* = 3.7, 6.2 Hz, 1H), 3.80 (d, *J* = 6.2 Hz, 2H), 3.66 (s, 3H), 2.50-2.48 (m, 2H), 2.40 (t, *J* = 7.4 Hz, 2H), 2.21-2.14 (m, 4H), 2.07 (s, 3H), 1.97 (s, 3H), 1.77 (p, *J* = 7.2 Hz, 2H), 1.03 (s, 9H); ^{13}C

NMR (100 MHz, $CDCl_3$) δ 173.7, 170.31, 170.29, 135.7, 133.5, 129.9, 127.8, 81.6, 81.3, 77.8, 75.8, 74.2, 73.3, 61.8, 51.7, 35.0, 32.9, 26.9, 24.1, 21.4, 21.2, 21.1, 19.3, 18.3; LRMS calculated for $C_{34}H_{44}O_8Si$ $[M+Na]^+$ m/z 631.3, measured LC/MS (ESI) R_t 1.31 min, m/z 631.0 $[M+Na]^+$.

Alkenes 4.26 and 4.31: To a solution of alkyne **4.25** (122 mg, 0.200 mmol) in MeOH (4.0 mL) was added Lindlar catalyst (31 mg). The resulting suspension was purged with hydrogen for 10 min, placed under a 1 atm of hydrogen and stirred for 24 h. The reaction mixture was filtered through a plug of Celite and concentrated *in vacuo* to afford 120 mg (>95%) of alkene **4.26** as a clear oil.

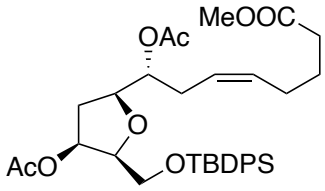

4.26: R_f 0.85 (2:1 Hexane: EtOAc); $[\alpha]^{23}_D$ +10.6 (*c* 1.0, $CHCl_3$); ^1H NMR (400 MHz, $CDCl_3$) δ 7.66-7.64 (m, 4H), 7.45-7.36 (m, 6H), 5.48-5.34 (m, 3H), 4.98-4.93 (m, 1H), 4.05-4.01 (m, 1H), 3.99-3.94 (m, 1H), 3.84 (d, *J* = 6.0 Hz, 2H), 3.64 (s, 3H), 2.39-2.32 (m, 3H), 2.28 (t, *J* = 7.5 Hz, 2H), 2.08-2.02 (m, 2H), 1.99 (s, 3H), 1.98 (s, 3H), 1.85 (ddd, *J* = 1.9, 5.2, 14.4 Hz, 1H), 1.66 (p, *J* = 7.5 Hz, 2H), 1.03 (s, 9H); ^{13}C NMR (100 MHz, $CDCl_3$) δ 174.1, 170.6, 170.4, 135.72, 135.65, 133.6, 133.5, 131.8, 129.9, 127.9, 125.2, 82.0, 78.3, 74.4, 73.6, 61.8, 51.6, 35.2, 33.6, 29.2, 26.9, 26.7, 24.9, 21.19, 21.18, 19.3; LRMS calculated for $C_{34}H_{46}O_8Si$ $[M+Na]^+$ m/z 633.3, measured LC/MS (ESI) R_t 2.55 min, m/z 632.9 $[M+Na]^+$.

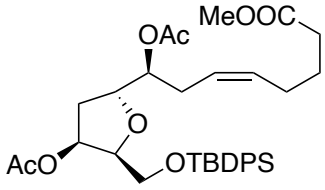

4.31: R_f 0.85 (2:1 hexanes/EtOAc); $[\alpha]^{23}_D$ +26.6 (*c* 1.0, $CHCl_3$); ^1H NMR (400 MHz, $CDCl_3$) δ 7.65-7.62 (m, 4H), 7.44-7.35 (m, 6H), 5.49-5.34 (m, 3H), 5.00-4.96 (m, 1H), 4.21-4.16 (m, 1H), 4.12 (td, *J* =

3.8, 6.4 Hz, 1H), 3.79 (d, J = 6.3 Hz, 2H), 3.65 (s, 3H), 2.37-2.25 (m, 4H), 2.13-2.05 (m, 4H), 2.03 (s, 3H), 1.96 (s, 3H), 1.71-1.63 (m, 2H), 1.03 (s, 9H); ^{13}C NMR (100 MHz, $CDCl_3$) δ 174.1, 170.5, 170.3, 135.70, 135.65, 133.6, 133.5, 131.8, 129.9, 127.8, 124.9, 81.5, 78.5, 74.7, 74.2, 61.8, 51.6, 35.0, 33.5, 29.0, 26.9, 26.7, 24.8, 21.2, 21.1, 19.3; LRMS calculated for $C_{34}H_{46}O_8Si$ $[M+Na]^+$ m/z 633.3, measured LC/MS (ESI) R_t 2.63 min, m/z 633.0 $[M+Na]^+$.

Alcohols 4.32 and 4.36: To a solution of silyl ether **4.26** (1.7 g, 2.7 mmol) in THF (27 mL) was added acetic acid (0.78 mL, 14 mmol), followed by a solution of TBAF (14 mL of 1.0 M THF, 14 mmol). The reaction mixture was maintained for 3 h, quenched with satd. Aq. ammonium chloride (25 mL). The aqueous layer was extracted with EtOAc (3 x 25 mL). The combined organic extracts were washed with brine, dried ($MgSO_4$), filtered and concentrated *in vacuo*. The crude residue was purified by flash chromatography (gradient: 1:1 to 1:2 hexanes/EtOAc) to afford 900 mg (90 %) of alcohol **4.32** as a clear oil.

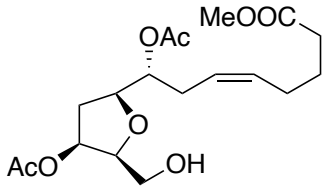

4.32: R_f 0.20 (1:1 hexanes/EtOAc); $[\alpha]^{23}_D$ -4.4 (*c* 1.0, $CHCl_3$); ^{1}H NMR (400 MHz, $CDCl_3$) δ 5.49-5.42 (m, 1H), 5.40-5.33 (m, 1H), 5.29-5.25 (m, 1H), 5.03-4.99 (m, 1H), 4.01-3.94 (m, 2H), 3.72 (dd, J = 6.4, 11.8 Hz, 1H), 3.64-3.60 (m, 4H), 2.39-2.27 (m, 5H), 2.08-2.04 (m, 5H), 2.02 (s, 3H), 1.89 (ddd, J = 2.9, 6.1, 14.1 Hz, 1H), 1.66 (p, J = 7.4 Hz, 2H); ^{13}C NMR (100 MHz, $CDCl_3$) δ 174.2, 171.1, 170.4, 131.8, 124.9, 81.8, 78.1, 74.1, 74.0, 61.1, 51.6, 34.6, 33.5, 29.0, 26.7, 24.7, 21.1, 21.0; LRMS calculated for $C_{18}H_{28}O_8$ $[M+Na]^+$ m/z 395.2, measured LC/MS (ESI) R_t 0.18 min, m/z 395.0 $[M+Na]^+$.

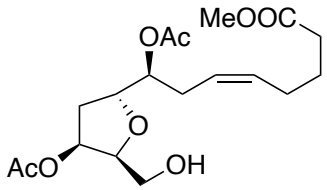

4.36: R_f 0.20 (1:1 hexanes/EtOAc); $[\alpha]^{23}_D$ -1.6 (*c* 1.0, $CHCl_3$); ^1H NMR (400 MHz, $CDCl_3$) δ 5.49-5.33 (m, 3H), 5.02-4.98 (m, 1H), 4.26-4.21 (m, 1H), 4.07 (td, *J* = 3.5, 6.0 Hz, 1H), 3.70 (dd, *J* = 6.2, 11.8 Hz, 1H), 3.64 (s, 3H), 3.53 (dd, *J* = 5.9, 11.8 Hz, 1H), 2.38-2.26 (m, 5H), 2.08-2.02 (m, 9H), 1.66 (p, *J* = 7.5 Hz, 2H); ^{13}C NMR (100 MHz, $CDCl_3$) δ 174.1, 171.2, 170.5, 131.9, 124.8, 82.1, 78.2, 74.8, 74.4, 60.8, 51.6, 34.6, 33.5, 28.9, 26.7, 24.7, 21.2, 21.0; LRMS calculated for $C_{18}H_{28}O_8$ $[M+Na]^+$ m/z 395.2, measured LC/MS (ESI) R_t 0.19 min, m/z 395.0 $[M+Na]^+$.

General procedure for enones 4.34 and 4.38: To a solution of alcohol **4.32** (70 mg, 0.19 mmol) in CH_2Cl_2 (2.2 mL) was added $NaHCO_3$ (19 mg, 0.23 mmol) and DMP (96 mg, 0.23 mmol). The resulting suspension was maintained at for 2 h. The reaction mixture was quenched with a 1:1 mixture of satd. aq. $Na_2S_2O_3$ and $NaHCO_3$ (2 mL) and stirred until a clear solution was obtained. The aqueous layer was extracted with Et_2O (3 x 10 mL). The combined organic extracts were washed with brine (10 mL), dried ($MgSO_4$), filtered, and concentrated *in vacuo*. The residue was flushed through a plug of silica gel (2:1 hexanes/EtOAc) to afford 51 mg of crude aldehyde **4.33**. To a solution of ketophosphonate (61 mg, 0.28 mmol) in THF (1.4 mL) at 0 °C was added NaHMDS (0.28 mL, 0.28 mmol). The resulting suspension was stirred for 30 min, **4.33** (51 mg, 0.14 mmol) in THF (0.70 mL) was added dropwise. The resulting solution was maintained for 2 h then the reaction was quenched with satd. aq. NH_4Cl (4 mL). The aqueous layer was extracted with EtOAc (3 x 10 mL). The combined organic extracts were washed with brine (10 mL), dried ($MgSO_4$), filtered, and concentrated *in vacuo*. The residue was purified by flash column chromatography (gradient: 4:1 to 2:1 hexanes/EtOAc) to afford 42 mg (48% over 2 steps) enone **4.34** as a clear oil.

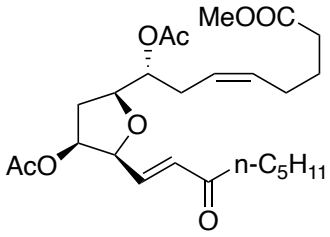

4.34: R_f 0.4 (2:1 hexanes/EtOAc); $[\alpha]^{23}_D$ -25.2 (*c* 0.5, $CHCl_3$); ^1H NMR (400 MHz, $CDCl_3$) δ 6.67 (dd, *J* = 5.1, 16.0 Hz, 1H), 6.32 (dd, *J* = 1.3, 16.0 Hz, 1H), 5.52-5.33 (m, 3H), 5.09-5.05 (m, 1H), 4.52-4.50 (m, 1H), 4.06-4.01 (m, 1H), 3.65 (s, 3H), 2.53 (t, *J* = 7.4 Hz, 2H), 2.44-2.37 (m, 3H), 2.30 (t, *J* = 7.5 Hz, 2H), 2.11-2.04 (m, 5H), 2.00 (s, 3H), 1.96 (ddd, *J* = 2.7, 6.0, 14.2 Hz, 1H), 1.72-1.65 (m, 2H), 1.60 (m, *J* = 7.3 Hz, 2H), 1.34-1.26 (m, 4H), 0.88 (t, *J* = 6.9 Hz, 3H); ^{13}C NMR (100 MHz, $CDCl_3$) δ 200.3, 174.1, 170.5, 170.4, 139.1, 132.0, 131.1, 124.9, 80.9, 78.4, 74.8, 73.9, 51.6, 40.8, 34.7, 33.5, 31.5, 29.1, 26.8, 24.8, 23.9, 22.6, 21.2, 21.0, 14.0; LRMS calculated for $C_{25}H_{38}O_8$ $[M+H]^+$ m/z 467.3, measured LC/MS (ESI) R_t 0.78 min, m/z 466.0 $[M+H]^+$.

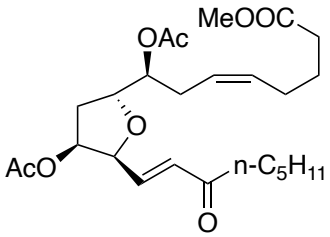

4.38: R_f 0.40 (2:1 hexanes/EtOAc); $[\alpha]^{23}_D$ -1.2 (*c* 1.0, $CHCl_3$); ^1H NMR (400 MHz, $CDCl_3$) δ 6.62 (dd, *J* = 4.9, 16 Hz, 1H), 6.33 (d, *J* = 16 Hz, 1H), 5.50-5.34 (m, 3H), 5.04-5.00 (m, 1H), 4.65-4.64 (m, 1H), 4.32-4.27 (m, 1H), 3.64 (s, 3H), 2.50 (t, *J* = 7.4 Hz, 2H), 2.37-2.26 (m, 3H), 2.13-2.03 (m, 6H), 1.99 (s, 3H), 1.73-1.64 (m, 2H), 1.62-1.55 (m, 2H), 1.31-1.23 (m, 6H), 0.87 (t, *J* = 6.9 Hz, 3H); ^{13}C NMR (100 MHz, $CDCl_3$) δ 200.3, 174.0, 170.4, 170.2, 139.6, 132.0, 130.9, 124.7, 80.9, 78.7, 75.6, 74.4, 51.6, 40.6, 34.6, 33.5, 31.5, 29.1, 26.7, 24.8, 23.9, 22.6, 21.2, 21.0, 14.0; LRMS calculated for $C_{25}H_{38}O_8$ $[M+H]^+$ m/z 467.3, measured LC/MS (ESI) R_t 0.89 min, m/z 467.0 $[M+H]^+$.

General procedure for Luche reduction to 4.35 and 4.39 To a solution of enone **4.34** (42 mg, 0.090 mmol) in MeOH (2.3 mL) was added $CeCl_3 \cdot 7H_2O$ (40 mg, 0.11 mmol) followed by $NaBH_4$ (3 mg, 0.09 mmol). The resulting solution was maintained at for 1 h and concentrated *in vacuo*. The residue was purified by flash column chromatography (1:1 hexanes / EtOAc) to afford 30 mg (71%) of **4.35** as a clear oil.

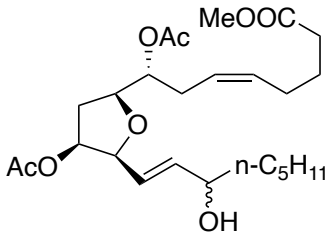

4.35: R_f 0.3 (1:1 hexanes/EtOAc); ^{1}H NMR (400 MHz, $CDCl_3$) δ 5.84-5.76 (m, 1H), 5.69-5.61 (m, 1H), 5.51-5.37 (m, 2H), 5.26-5.23 (m, 1H), 5.07-5.02 (m, 1H), 4.35-4.32 (m, 1H), 4.11 (m, J = 6.5 Hz, 1H), 3.98 (dt, J = 6.3, 8.1 Hz, 1H), 3.66 (s, 3H), 2.46-2.35 (m, 3H), 2.31 (t, J = 7.5 Hz, 2H), 2.11-2.04 (m, 8H), 1.91 (ddd, J = 2.6, 6.0, 14.2 Hz, 1H), 1.69 (m, J = 7.5 Hz, 2H), 1.54-1.46 (m, 2H), 1.29 (m, 6H), 0.88 (t, J = 6.5 Hz, 3H); ^{13}C NMR (100 MHz, $CDCl_3$) δ 174.2, 170.6, 170.51, 170.45 (isomers), 137.8, 137.7 (isomers), 131.8, 125.1, 124.9, 124.7 (isomers), 82.2, 82.1 (isomers), 78.04, 77.99 (isomers), 75.09, 75.06 (isomers), 74.4, 72.4, 72.2 (isomers), 51.7, 37.24, 37.20 (isomers), 34.9, 33.6, 31.90, 31.87 (isomers), 29.1, 26.8, 25.2, 24.9, 22.7, 21.23, 21.19, 21.1 (isomers), 14.2; LRMS calculated for $C_{25}H_{40}O_8$ $[M+Na]^+$ m/z 491.3, measured LC/MS (ESI) R_t 0.79 min, m/z 491.0 $[M+Na]^+$.

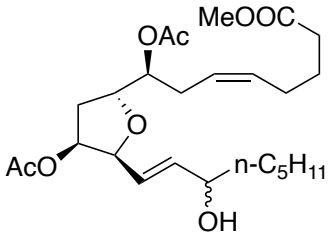

4.39: R_f 0.3 (1:1 hexanes/EtOAc); ^{1}H NMR (400 MHz, $CDCl_3$) δ 5.82-5.74 (m, 1H), 5.64-5.56 (m, 1H), 5.49-5.32 (m, 3H), 5.00-4.96 (m, 1H), 4.47-4.46 (m, 1H), 4.28-4.23 (m, 1H), 4.12-4.05 (m, 1H), 3.65 (s, 3H), 2.40-2.25 (m, 4H), 2.17-2.00 (m, 10H), 1.71-1.64 (m, 2H), 1.50-1.44 (m, 2H), 1.28-1.24 (m, 6H), 0.87 (t, J = 6.6 Hz, 3H); ^{13}C NMR (100 MHz, $CDCl_3$) δ 174.1,

170.5, 170.4, 170.3 (isomers), 137.61, 137.58 (isomers), 131.9, 125.2, 125.0, 124.9 (isomers), 82.02, 81.99 (isomers), 78.2, 76.0, 74.74, 74.72 (isomers), 72.4, 72.2 (isomers), 51.7, 37.2, 34.8, 33.6, 31.90, 31.86 (isomers), 29.09, 29.06 (isomers), 26.8, 25.2, 24.8, 22.7, 21.3, 21.15, 21.10 (isomers), 14.2; LRMS calculated for $C_{25}H_{40}O_8$ $[M+Na]^+$ m/z 491.3, measured LC/MS (ESI) R_t 1.42 min, m/z 491.0 $[M+Na]^+$.

General procedure for lipase resolution of C15 epimers: To a solution of a 1:1 mixture of C15 secondary alcohols **4.35** (56 mg, 0.12 mmol) in vinyl acetate (1.2 mL) in a microwave vial was added powered 4Å molecular sieves (56 mg) followed by Lipase Amano AK (390 mg). The microwave vial was sealed and heated at 40 °C for 7-8 days. The mixture was cooled to room temperature, filtered through a plug of Celite and washed with EtOAc (3 x 10 mL). The filtrate was concentrated *in vacuo* and the residue purified by flash chromatography (gradient: 4:1 to 2:1 hexanes/EtOAc) to afford 26 mg (43 %) of **4.40** and 24 mg (43 %) of **4.41**, both as yellow oils. Stereochemical assignment of was based on NMR analysis of Mosher esters derived from secondary alcohols at C15.

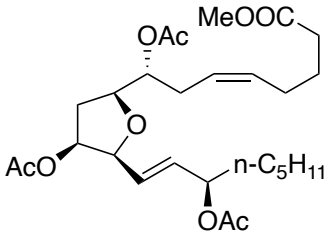

4.40: R_f 0.8 (1:1 hexanes/EtOAc); $[\alpha]^{23}_D$ +4.2 (*c* 1.0, $CHCl_3$); ^{1}H NMR (400 MHz, $CDCl_3$) δ 5.70 (dd, *J* = 6.0, 15.7 Hz, 1H), 5.62 (dd, *J* = 5.9, 15.7 Hz, 1H), 5.50-5.37 (m, 2H), 5.27-5.21 (m, 2H), 5.08-5.03 (m, 1H), 4.33 (t, *J* = 5.1 Hz, 1H), 4.00-3.95 (m, 1H), 3.66 (s, 3H), 2.41-2.32 (m, 3H), 2.31 (t, *J* = 7.5 Hz, 2H), 2.11-2.03 (m, 11H), 1.91 (ddd, *J* = 2.7, 6.2, 14.1 Hz, 1H), 1.68 (m, *J* = 7.5 Hz, 2H), 1.62-1.51 (m, 2H), 1.27 (m, 6H), 0.88 (m, 3H); ^{13}C NMR (100 MHz, $CDCl_3$) δ 174.1, 170.48, 170.45, 170.3, 132.4, 131.8, 126.9, 125.1, 81.8, 78.1, 74.8, 74.1, 73.9,

51.6, 34.7, 34.4, 33.6, 31.7, 29.1, 26.8, 24.9, 24.8, 22.6, 21.4, 21.2, 21.0, 14.1; LRMS calculated for $C_{27}H_{42}O_9$ $[M+Na]^+$ m/z 533.3, measured LC/MS (ESI) R_t 1.81 min, m/z 533.0 $[M+Na]^+$.

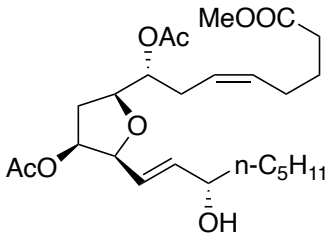

4.41: R_f 0.3 (1:1 hexanes/EtOAc); $[\alpha]^{23}_D$ -6.0 (*c* 0.5, $CHCl_3$); ^1H NMR (400 MHz, $CDCl_3$) δ 5.84 (ddd, *J* = 0.8, 6.1, 15.6 Hz, 1H), 5.66 (ddd, *J* = 1.0, 6.6, 15.6 Hz, 1H), 5.51-5.37 (m, 2H), 5.26-5.23 (m, 1H), 5.07-5.02 (m, 1H), 4.36-4.33 (m, 1H), 4.15-4.10 (m, 1H), 3.98 (dt, *J* = 6.3, 8.1 Hz, 1H), 3.66 (s, 3H), 2.44-2.34 (m, 3H), 2.31 (t, *J* = 7.5 Hz, 2H), 2.11-2.04 (m, 8H), 1.91 (ddd, *J* = 2.6, 5.9, 14.2 Hz, 1H), 1.69 (m, *J* = 7.5 Hz, 2H), 1.53-1.48 (m, 2H), 1.30-1.28 (m, 6H), 0.90-0.87 (m, 3H); ^{13}C NMR (100 MHz, $CDCl_3$) δ 174.2, 170.6, 170.4, 137.7, 131.8, 125.1, 124.7, 82.1, 78.0, 75.1, 74.4, 72.2, 51.7, 37.2, 34.9, 33.6, 31.9, 29.1, 26.8, 25.2, 24.9, 22.7, 21.22, 21.19, 14.2; LRMS calculated for $C_{25}H_{40}O_8$ $[M+Na]^+$ m/z 491.3, measured LC/MS (ESI) R_t 0.83 min, m/z 491.0 $[M+Na]^+$.

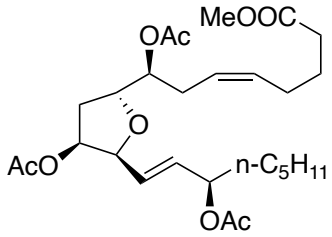

4.42: R_f 0.8 (1:1 Hexane: EtOAc); $[\alpha]^{23}_D$ +28.0 (*c* 0.25, $CHCl_3$); ^1H NMR (400 MHz, $CDCl_3$) δ 5.71 (dd, *J* = 6.4, 16.0 Hz, 1H), 5.59 (dd, *J* = 6.0 16.0 Hz, 1H), 5.50-5.34 (m, 3H), 5.23 (q, *J* = 6.5 Hz, 1H), 5.00 (dt, *J* = 5.4, 7.3, Hz, 1H), 4.49-4.46 (m, 1H), 4.29-4.24 (m, 1H), 3.66 (s, 3H), 2.42-2.29 (m, 4H), 2.19-2.02 (m, 13H), 1.68 (m, *J* = 7.5 Hz, 2H), 1.62-1.49 (m, 2H), 1.27-1.26 (m, 6H), 0.89-0.85 (m, 3H); ^{13}C NMR (100 MHz, $CDCl_3$) δ 174.1, 170.5, 170.30, 170.26, 132.2, 131.9, 127.2, 124.9, 81.8, 78.3, 75.7, 74.7, 73.9, 51.6, 34.6, 34.4, 33.5, 31.7, 29.1, 26.8, 24.9, 24.8, 22.6, 21.4, 21.3, 21.0, 14.1; LRMS calculated for $C_{27}H_{42}O_9$ $[M+Na]^+$ m/z 533.3, measured LC/MS (ESI) R_t 1.01 min, m/z 533.0 $[M+Na]^+$.

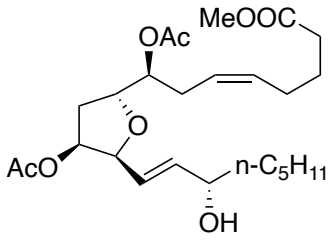

4.43: R_f 0.3 (1:1 Hexane: EtOAc); $[\alpha]^{23}_D$ +14.4 (*c* 0.17, $CHCl_3$) ^1H NMR (400 MHz, $CDCl_3$) δ 5.81 (dd, *J* = 6.1, 15.6, 1H), 5.63 (dd, *J* = 6.6, 15.6 Hz, 1H), 5.51-5.32 (m, 3H), 5.00 (dt, *J* = 5.4, 7.2 Hz, 1H), 4.48 (dd, *J* = 3.6, 6.6 Hz, 1H), 4.29-4.24 (m, 1H), 4.11 (q, *J* = 6.2 Hz, 1H), 3.66 (s, 3H), 2.43-2.35 (m, 2H), 2.31 (t, *J* = 7.5 Hz, 2H), 2.16-2.03 (m, 10H), 1.69 (m, *J* = 7.5 Hz, 2H), 1.63-1.56 (m, 2H), 1.32-1.27 (m, 6H), 0.88 (t, *J* = 6.6 Hz, 3H); ^{13}C NMR (100 MHz, $CDCl_3$) δ 174.1, 170.5, 170.4, 137.6, 131.9, 125.0, 124.9, 82.0, 78.2, 76.0, 74.8, 72.2, 51.7, 37.2, 34.8, 33.6, 31.9, 29.1, 26.8, 25.2, 24.8, 22.7, 21.3, 21.2, 14.2; LRMS calculated for $C_{25}H_{40}O_8$ $[M+Na]^+$ m/z 491.3, measured LC/MS (ESI) R_t 1.45 min, m/z 491.0 $[M+Na]^+$.

General procedure for Δ^{13}-9-Isofuran methyl esters To a solution of either triacetate **4.40** or diacetate **4.41** (20 mg) in MeOH (1 mL) was added K_2CO_3 (ca. 5-10 mg). The mixture was maintained for 3 h and quenched with 1 N HCl (ca. 5-10 drops). The mixture was diluted with water (1 mL), and EtOAc (1 mL), extracted with EtOAc (3 x 2 mL), combined organic extracts dried (Na_2SO_4), filtered and concentrated *in vacuo*. The residue was purified by flash column chromatography (EtOAc) to afford 15 mg (>90%) of Δ^{13}-9-Isofuran methyl ester as colorless oil.

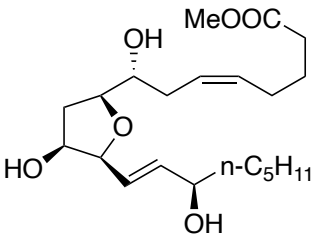

4.44: R_f 0.3 (EtOAc); $[\alpha]^{23}_D$ +13.2 (*c* 0.5, $CHCl_3$); ^1H NMR (400 MHz, $CDCl_3$) δ 5.84 (dd, *J* = 6.9, 15.6 Hz, 1H), 5.73 (dd, *J* = 5.4, 15.6 Hz, 1H), 5.51-5.43 (m, 2H), 4.19-4.10 (m, 3H), 4.05 (q, *J* = 6.8 Hz, 1H), 3.90-3.86 (m, 1H), 3.67 (s, 3H), 2.32 (t, *J* = 7.4 Hz, 2H), 2.28-2.01 (m, 6H), 1.70 (m, *J* = 7.4 Hz, 2H), 1.56-1.43 (m, 2H), 1.28-1.27 (m, 6H), 0.89-0.85 (m, 3H); ^{13}C NMR (100 MHz, $CDCl_3$) δ 174.2, 136.6, 131.4, 126.6, 126.3, 83.2, 80.3, 72.9, 72.4, 71.9, 51.7, 36.7,

34.2, 33.6, 32.3, 31.9, 26.9, 25.4, 24.8, 22.7, 14.2; LRMS calculated for $C_{21}H_{36}O_6$ $[M+Na]^+$ m/z 407.3, measured LC/MS (ESI) R_t 0.42 min, m/z 407.6 $[M+Na]^+$.

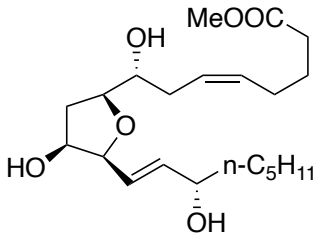

4.45: R_f 0.3 (EtOAc); $[\alpha]^{23}_D$ +16.0 (*c* 0.25, $CHCl_3$); ^1H NMR (400 MHz, $CDCl_3$) δ 5.89-5.80 (m, 2H), 5.54-5.41 (m, 2H), 4.16-4.08 (m, 4H), 3.90-3.86 (m, 1H), 3.67 (s, 3H), 2.32 (t, *J* = 7.3 Hz, 2H), 2.31-2.02 (m, 6H), 1.70 (m, *J* = 7.3 Hz, 2H), 1.56-1.50 (m, 2H), 1.29-1.27 (m, 6H), 0.88 (t, *J* = 6.7 Hz, 3H); ^{13}C NMR (100 MHz, $CDCl_3$) δ 174.2, 137.9, 132.0, 126.0, 125.9, 84.1, 80.4, 73.0, 72.2, 72.1, 51.7, 37.0, 34.4, 33.5, 32.1, 31.9, 26.8, 25.3, 24.8, 22.7, 14.2; LRMS calculated for $C_{21}H_{36}O_6$ $[M+Na]^+$ m/z 407.3, measured LC/MS (ESI) R_t 0.41 min, m/z 407.4 $[M+Na]^+$.

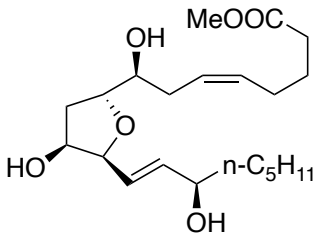

4.46: R_f 0.3 (EtOAc); $[\alpha]^{23}_D$ +16.8 (*c* 0.5, $CHCl_3$); ^1H NMR (400 MHz, $CDCl_3$) δ 5.91 (dd, *J* = 6.0, 15.6 Hz, 1H), 5.75 (dd, *J* = 6.0, 15.6 Hz, 1H), 5.53-5.44 (m, 2H), 4.46-4.44 (m, 1H), 4.33-4.32 (m, 1H), 4.27 (ddd, *J* = 3.8, 6.0, 9.8 Hz, 1H), 4.16 (q, *J* = 6.1 Hz, 1H), 3.90-3.85 (m, 1H), 3.67 (s, 3H), 2.32 (t, *J* = 7.4 Hz, 2H), 2.19-2.07 (m, 5H), 1.97 (dd, *J* = 6.0, 13.0 Hz, 1H), 1.70 (m, *J* = 7.5 Hz, 2H), 1.57-1.51 (m, 2H), 1.40-1.27 (m, 6H), 0.88 (t, *J* = 6.7 Hz, 3H); ^{13}C NMR (100 MHz, $CDCl_3$) δ 174.3, 137.6, 131.6, 126.1, 125.7, 83.5, 80.7, 74.2, 72.3, 72.2, 51.7, 37.3, 34.6, 33.6, 31.9, 30.9, 26.8, 25.3, 24.9, 22.7, 14.2; LRMS calculated for $C_{21}H_{36}O_6$ $[M+Na]^+$ m/z 407.3, measured LC/MS (ESI) R_t 0.29 min, m/z 407.4 $[M+Na]^+$.

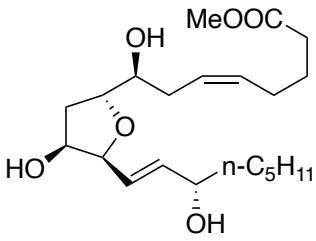

4.47: R_f 0.3 (EtOAc); $[\alpha]^{23}_D$ +10.2 (*c* 1.0, $CHCl_3$); ^{1}H NMR (400 MHz, $CDCl_3$) δ 5.90 (dd, *J* = 6.2, 15.6 Hz, 1H), 5.77 (dd, *J* = 6.2, 15.6 Hz, 1H), 5.53-5.44 (m, 2H), 4.47-4.45 (m, 1H), 4.35-4.33 (m, 1H), 4.27 (ddd, *J* = 3.8, 6.0, 9.8 Hz, 1H), 4.18 (q, *J* = 6.1 Hz, 1H), 3.90-3.85 (m, 1H), 3.67 (s, 3H), 2.32 (t, *J* = 7.4 Hz, 2H), 2.20-2.07 (m, 5H), 1.97 (dd, *J* = 6.0, 13.1 Hz, 1H), 1.70 (m, *J* = 7.4 Hz, 2H), 1.57-1.52 (m, 2H), 1.30-1.28 (m, 6H), 0.88 (t, *J* = 6.8 Hz, 3H); ^{13}C NMR (100 MHz, $CDCl_3$) δ 174.3, 137.6, 131.7, 126.1, 126.0, 83.7, 80.8, 74.3, 72.4, 72.2, 51.7, 37.4, 34.5, 33.6, 31.9, 31.0, 26.8, 25.3, 24.9, 22.7, 14.2; LRMS calculated for $C_{21}H_{36}O_6$ $[M+Na]^+$ m/z 407.3, measured LC/MS (ESI) R_t 0.29 min, m/z 407.5 $[M+Na]^+$.

General procedure for Δ^{13}-9-Isofurans To a solution of Δ^{13}-9-Isofuran methyl ester (7 mg, 0.018 mmol) in THF (0.5 mL) was added LiOH (54 μL, 0.054 mmol, 1 M in water). The mixture was maintained for 8 h, then quenched with KH_2PO_4 (X mL, 1 M in water) then HCl (X mL, 1 M in water). The aqueous layer was extracted with EtOAc (4 x 20 mL). The combined organic extracts were washed with brine, dried (Na_2SO_4), filtered, and concentrated in vacuo to afford 7 mg (>95%) of Δ^{13}-9-Isofuran as a colorless oil**.**

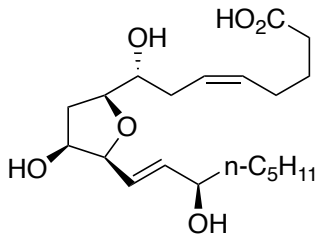

3.68: R_f 0.2 (EtOAc); $[\alpha]^{23}_D$ +6.4 (*c* 0.25, $CHCl_3$); ^{1}H NMR (400 MHz, $CDCl_3$) δ 5.86 (dd, *J* = 6.6, 15.6 Hz, 1H), 5.76 (dd, *J* = 5.7, 15.6 Hz, 1H), 5.51-5.44 (m, 2H), 4.20-4.18 (m, 1H), 4.14-4.08 (m, 3H), 3.90-3.87 (m, 1H), 2.36 (t, *J* = 7.0 Hz, 2H), 2.26-2.01 (m, 6H), 1.75-1.69 (m, 2H), 1.58-1.47 (m, 2H), 1.28-1.27 (m, 6H), 0.89-0.86 (m, 3H) ;^{13}C NMR (150 MHz, $CDCl_3$) δ 177.7, 136.8, 131.7, 126.3 (x2), 83.3, 80.4, 72.9, 72.6, 72.1, 36.7, 34.4, 33.1, 32.0, 31.9, 26.5,

25.4, 24.4, 22.7, 14.2; LRMS calculated for $C_{20}H_{34}O_6$ $[M+Na]^+$ m/z 393.2, measured LC/MS (ESI) R_t 0.17 min, m/z 393.4 $[M+Na]^+$.

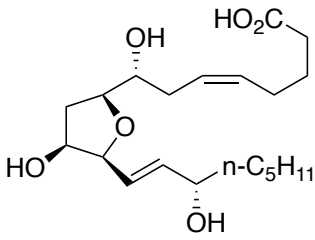

3.69: R_f 0.2 (EtOAc); $[\alpha]^{23}_D$ +13.6 (*c* 0.25, $CHCl_3$); ^1H NMR (400 MHz, $CDCl_3$) δ 5.86-5.79 (m, 2H), 5.54-5.42 (m, 2H), 4.19-4.09 (m, 4H), 3.90-3.86 (m, 1H), 2.36 (t, *J* = 6.8 Hz, 2H), 2.26-2.01 (m, 6H), 1.75-1.67 (m, 2H), 1.65-1.46 (m, 2H), 1.29-1.28 (m, 6H), 0.89-0.86 (m, 3H); ^{13}C NMR (100 MHz, $CDCl_3$) δ 177.8, 137.7, 132.0, 126.12, 126.06, 84.1, 80.5, 73.2, 72.2, 72.1, 36.9, 34.3, 33.0, 32.1, 31.9, 26.5, 25.3, 24.5, 22.7, 14.2; LRMS calculated for $C_{20}H_{34}O_6$ $[M+Na]^+$ m/z 393.2, measured LC/MS (ESI) R_t 0.17 min, m/z 393.4 $[M+Na]^+$.

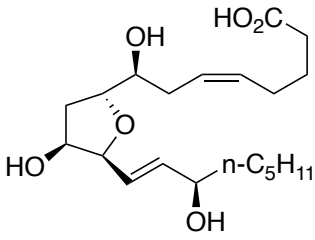

4.6: R_f 0.2 (EtOAc); $[\alpha]^{23}_D$ +8.8 (*c* 0.25, $CHCl_3$); ^1H NMR (400 MHz, $CDCl_3$) δ 5.88 (dd, *J* = 6.1, 15.7 Hz, 1H), 5.74 (dd, *J* = 6.0, 15.7 Hz, 1H), 5.49 (m, 2H), 4.46-4.44 (m, 1H), 4.34-4.33 (m, 1H), 4.28-4.24 (m, 1H), 4.17-4.12 (m, 1H), 3.90-3.85 (m, 1H), 2.36 (t, *J* = 6.9 Hz, 2H), 2.20-2.10 (m, 5H), 1.98 (dd, *J* = 6.2, 13.2 Hz, 1H), 1.71 (p, *J* = 7.2 Hz, 2H), 1.58-1.47 (m, 2H), 1.29-1.27 (m, 6H), 0.90-0.87 (m, 3H); ^{13}C NMR (100 MHz, $CDCl_3$) δ 177.8, 137.1, 131.4, 126.4, 126.0, 83.4, 80.7, 74.3, 72.5, 72.3, 37.1, 34.5, 33.1, 31.9, 31.0, 26.5, 25.3, 24.5, 22.8, 14.2; LRMS calculated for $C_{20}H_{34}O_6$ $[M+Na]^+$ m/z 393.2, measured LC/MS (ESI) R_t 0.14 min, m/z 393.4 $[M+Na]^+$.

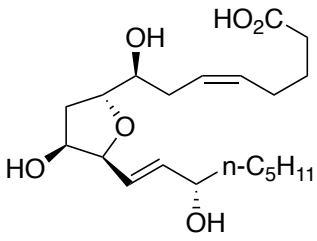

4.7: R_f 0.2 (EtOAc); $[\alpha]^{23}_D$ +8.8 (*c* 0.25, $CHCl_3$); ^1H NMR (400 MHz, $CDCl_3$) δ 5.84 (dd, *J* = 5.6, 15.7 Hz, 1H), 5.78 (dd, *J* = 6.2, 15.7 Hz, 1H), 5.52-5.44 (m, 2H), 4.45-4.43 (m, 1H), 4.35-4.33 (m, 1H), 4.29-4.24 (m, 1H), 4.18-4.13 (m, 1H), 3.89-3.85 (m, 1H), 2.37-2.32 (m, 2H), 2.22-2.09 (m, 5H), 2.01-1.95 (m, 1H), 1.73-1.69 (m, 2H), 1.56-1.51 (m, 2H), 1.29-1.25 (m, 6H), 0.90-0.87 (m, 3H); ^{13}C NMR (100 MHz, $CDCl_3$) δ 177.8, 137.2, 131.4, 126.6, 126.4, 83.8, 80.8, 74.6, 72.4, 72.3, 37.1, 34.3, 33.1, 31.9, 31.0, 26.5, 25.3, 24.5, 22.7, 14.2; LRMS calculated for $C_{20}H_{34}O_6$ $[M+Na]^+$ m/z 393.2, measured LC/MS (ESI) R_t 0.15 min, m/z 393.5 $[M+Na]^+$.

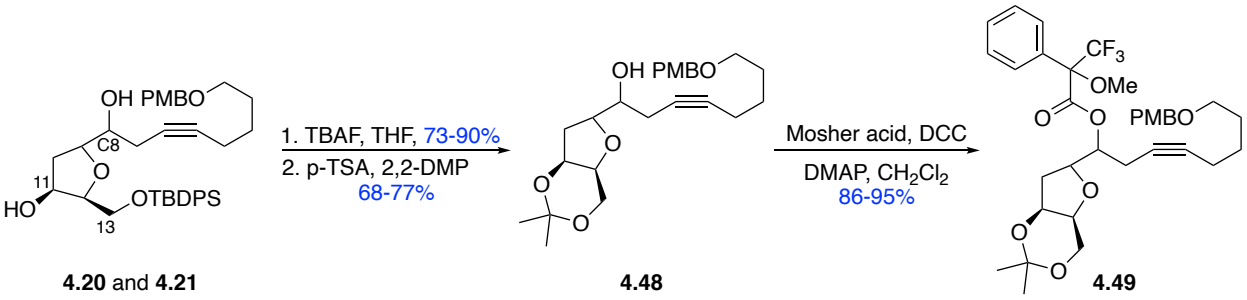

4.20 and **4.21** **4.48** **4.49**

4.48: To a solution of diol **4.21** (67 mg, 0.11 mmol) in THF (2.2 mL) was added TBAF (0.13 mL, 1.0 M in hexanes). The resulting solution was stirred for 2 h then concentrated *in vacuo*. The residue was purified by flash column chromatography (gradient: 2:1 to 1:1 hexanes/EtOAc) to afford the desired triol in 73-90% yield as a clear oil. To a solution of the triol (37 mg, 0.10 mmol) in 2,2-dimethoxypropane (0.98 mL) was added p-TSA (cat). The resulting solution was stirred for 72 h then quenched with NEt_3 (ca. 2-3 drops) and concentrated *in vacuo*. The residue was purified by flash column chromatography (gradient: 4:1 to 2:1 hexanes/EtOAc) to afford acetonide **4.48** in 68-77% yield as a clear oil.

Mosher ester 4.49: To a solution of **4.48** (14 mg, 0.033 mmol) in CH_2Cl_2 (0.52 mL) was added α-methoxy-α–trifluoromethylphenylacetic acid (24 mg, 0.10 mmol), DCC (21 mg, 0.10 mmol), and 4-dimethylaminopyridine (13 mg, 0.10 mmol). The resulting solution was maintained for 48-72 h, filtered through a cotton plug, concentrated *in vacuo*, and the residue purified by flash column chromatography (2:1 hexanes/EtOAc) to afford Mosher ester **4.49** in 86-95% yield as a clear oil.

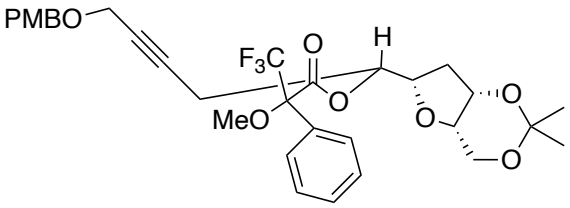

4.49a: R_f 0.8 (1:1 hexanes/EtOAc); ^{1}H NMR (400 MHz, $CDCl_3$) δ 7.62-7.61 (m, 2H), 7.39-7.37 (m, 3H), 7.24 (d, *J* = 8.5 Hz, 2H), 6.87 (d, *J* = 8.5 Hz, 2H), 5.32-5.27 (m, 1H), 4.40 (s, 2H), 4.30-4.28 (m, 1H), 4.20 (td, *J* = 3.0, 8.6 Hz, 1H), 4.02 (dd, *J* = 3.2, 13.0 Hz, 1H), 3.90 (dd, *J* = 2.0, 13.0 Hz, 1H), 3.80 (s, 3H), 3.68-3.67 (m, 1H), 3.63-3.61 (m, 3H), 3.41 (t, *J* = 6.3 Hz, 2H), 2.91-2.71 (m, 2H), 2.17-2.13 (m, 2H), 2.08-2.01 (m, 1H), 1.76-1.73 (m, 1H), 1.69-1.62 (m, 2H), 1.57-1.51 (m, 2H), 1.40 (s, 3H), 1.39 (s, 3H).

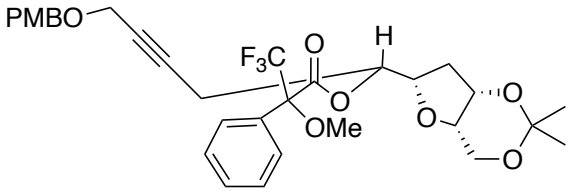

4.49b: R_f 0.8 (1:1 hexanes/EtOAc); ^{1}H NMR (400 MHz, $CDCl_3$) δ 7.60-7.58 (m, 2H), 7.39-7.37 (m, 3H), 7.25 (d, *J* = 8.5 Hz, 2H), 6.87 (d, *J* = 8.5 Hz, 2H), 5.30-5.26 (m, 1H), 4.41 (s, 2H), 4.37-4.35 (m, 1H), 4.28-4.23 (m, 1H), 4.04 (dd, *J* = 3.4, 13.0 Hz, 1H), 3.92 (dd, *J* = 2.2, 13.0 Hz, 1H), 3.80 (s, 3H), 3.71-3.70 (m, 1H), 3.56 (s, 3H), 3.40 (t, *J* = 6.4 Hz, 2H), 2.86-2.67 (m, 2H), 2.26-2.19 (m, 1H), 2.06-2.02 (m, 2H), 1.71-1.68 (m, 1H), 1.64-1.57 (m, 2H), 1.49-1.43 (m, 2H), 1.41 (s, 3H), 1.36 (s, 3H).

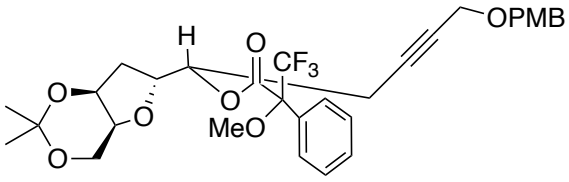

4.49c: R_f 0.8 (1:1 hexanes/EtOAc); ^{1}H NMR (400 MHz, $CDCl_3$) δ 7.58-7.55 (m, 2H), 7.44-7.36 (m, 3H), 7.26 (d, *J* = 8.6 Hz, 2H), 6.87 (d, *J* = 8.6 Hz, 2H), 5.38-5.33 (m, 1H), 4.64-4.59 (m, 1H), 4.45 (s, 2H), 4.38-4.37 (m, 1H), 3.98-3.88 (m, 2H), 3.80 (s, 3H), 3.50 (s, 3H), 3.45 (t, *J* = 6.4 Hz, 2H), 3.42 (m, 1H), 2.59-2.48 (m, 2H), 2.10-2.05 (m, 3H), 2.02-1.95 (m, 1H), 1.69-1.62 (m, 2H), 1.54-1.46 (m, 2H), 1.42 (s, 3H), 1.38 (s, 3H).

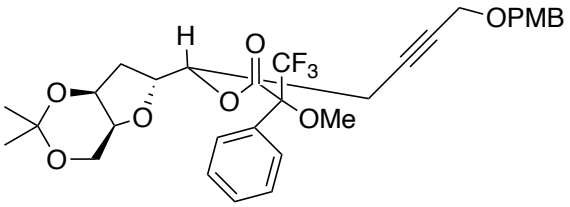

4.49d: R_f 0.8 (1:1 hexanes/EtOAc); ^{1}H NMR (400 MHz, $CDCl_3$) δ 7.60-7.58 (m, 2H), 7.38-7.36 (m, 3H), 7.25 (d, *J* = 8.6 Hz, 2H), 6.87 (d, *J* = 8.6 Hz, 2H), 5.38-5.34 (m, 1H), 4.48-4.43 (m, 2H), 4.41 (s, 2H), 4.28-4.27 (m, 1H), 3.86-3.75 (m, 5H), 3.62 (s, 3H), 3.43 (t, *J* = 6.3 Hz, 2H), 3.26-3.24 (m, 1H), 2.65-2.49 (m, 2H), 2.15-2.11 (m, 2H), 1.96-1.92 (m, 1H), 1.89-1.82 (m, 1H), 1.69-1.62 (m, 2H), 1.57-1.49 (m, 2H), 1.38 (s, 3H), 1.35 (s, 3H).

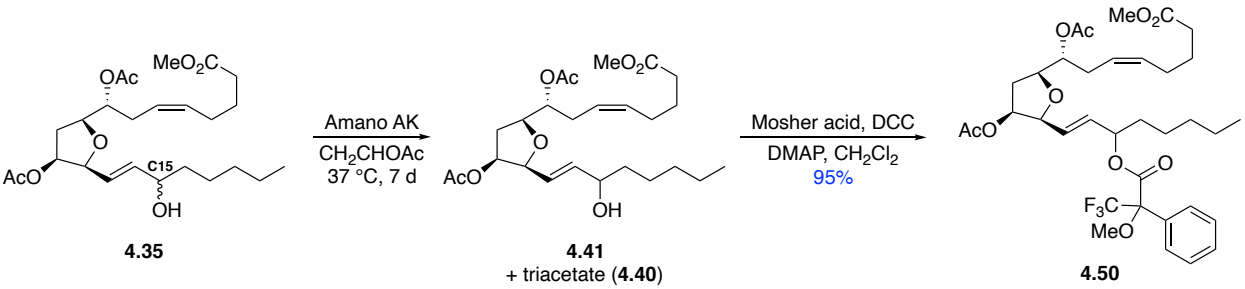

4.35 → **4.41** + triacetate (**4.40**) → **4.50**

Mosher ester 4.50: To a solution of allylic alcohol **4.41** (2.7 mg, 0.0057 mmol) in CH_2Cl_2 (0.5 mL), was added S-MPTA (4 mg, 0.018 mmol), DCC (3.7 mg, 0.018 mmol) and DMAP (2.2 mg, 0.018 mmol). The reaction mixture was maintained for 14 h. CH_2Cl_2 (1 mL) was added to the reaction mixture, the solution was filtered and concentrated. The crude mixture was purified by

flash chromatography (gradient: 9:1 Hexanes: EtOAc) to afford 3.7 mg (95 %) of the desired mosher ester.

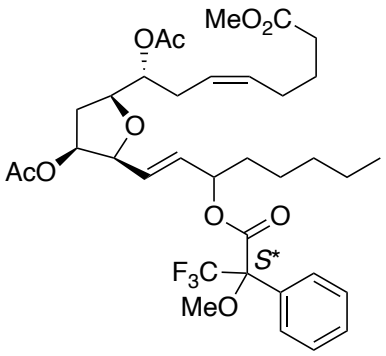

4.50a: R_f 0.4 (4:1 hexanes/EtOAc); ^{1}H NMR (400 MHz, $CDCl_3$) δ 7.51-7.49 (m, 2H), 7.41-7.38 (m, 3H), 5.83-5.67 (m, 2H), 5.51-5.37 (m, 3H), 5.28-5.24 (m, 1H), 5.08-5.04 (m, 1H), 4.36-4.33 (m, 1H), 4.01-3.96 (m, 1H), 3.66 (s, 3H), 3.53 (s, 3H), 2.42-2.27 (m, 5H), 2.11-1.99 (m, 8H), 1.95-1.89 (m, 1H), 1.72-1.58 (m, 4H), 1.27-1.20 (m, 6H), 0.88-0.82 (m, 3H).

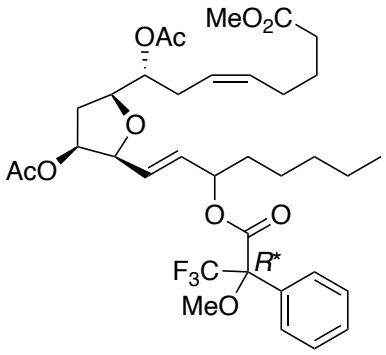

4.50b: R_f 0.4 (4:1 hexanes/EtOAc); ^{1}H NMR (400 MHz, $CDCl_3$) δ 7.52-7.47 (m, 2H), 7.40-7.37 (m, 3H), 5.77-5.61 (m, 2H), 5.51-5.37 (m, 3H), 5.30-5.23 (m, 1H), 5.08-5.02 (m, 1H), 4.39-4.30 (m, 1H), 4.02-3.95 (m, 1H), 3.66 (s, 3H), 3.54 (s, 3H), 2.42-2.29 (m, 5H), 2.09-2.01 (m, 8H), 1.94-1.88 (m, 1H), 1.72-1.65 (m, 4H), 1.36-1.22 (m, 6H), 0.89-0.82 (m, 3H).

References

(51) Takamura, H. *Tetrahedron Lett.* **2018**, *59*, 955–966.

(52) Davis, R. W.; Allweil, A.; Tian, J.; Brash, A. R.; Sulikowski, G. A. *Tetrahedron Lett.* **2018**, *59*, 4571–4573.

(53) Mash, E. A.; Nelson, K. A.; Van Deusen, S.; Hemperly, S. B. *Org. Synth.* **1990**, *68*, 92.

(54) Mukai, C.; Kim, J. S.; Uchiyama, M.; Sakamoto, S.; Hanaoka, M. *J. Chem. Soc. Perkin 1* **1998**, No. 17, 2903–2916.

(55) Huang, Z.; Negishi, E. *Org. Lett.* **2006**, *8* (17), 3675–3678.

(56) Cacchi, S.; Morera, E.; Ortar, G. *Tetrahedron Lett.* **1985**, *26*, 1109–1112.

(57) Chehade, K. A. H.; Kiegiel, K.; Isaacs, R. J.; Pickett, J. S.; Bowers, K. E.; Fierke, C. A.; Andres, D. A.; Spielmann, H. P. *J. Am. Chem. Soc.* **2002**, *124*, 8206–8219.

(58) Barnych, B.; Rand, A. A.; Cajka, T.; Lee, K. S. S.; Hammock, B. D. *Org. Biomol. Chem.* **2017**, *15*, 4308–4313.

(59) Dess, D. B.; Martin, J. C. *J. Org. Chem.* **1983**, *48*, 4155–4156.

(60) Schafroth, M. A.; Zuccarello, G.; Krautwald, S.; Sarlah, D.; Carreira, E. M. *Angew. Chem. Int. Ed.* **2014**, *53*, 13898–13901.

(61) Dale, J. A.; Mosher, H. S. *J. Am. Chem. Soc.* **1973**, *95*, 512–519.

(62) Hoye, T. R.; Jeffrey, C. S.; Shao, F. *Nat. Protoc.* **2007**, *2*, 2451–2458.

Appendix 1

Spectra Relevant to Chapter 4

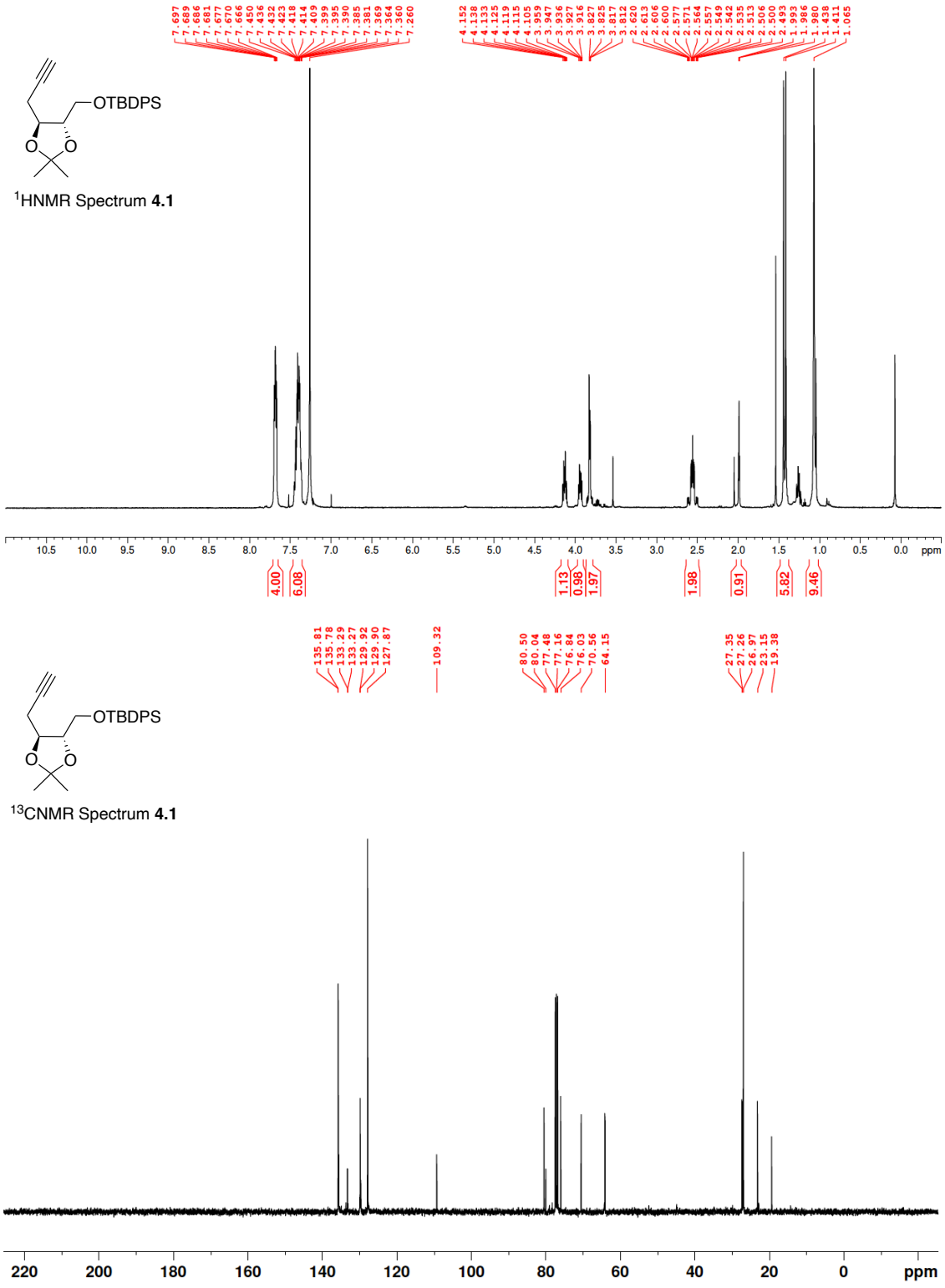

Figure A.1 ^{1}H NMR (400 MHz, $CDCl_3$) and ^{13}C NMR (100 MHz, $CDCl_3$) of **4.1**.

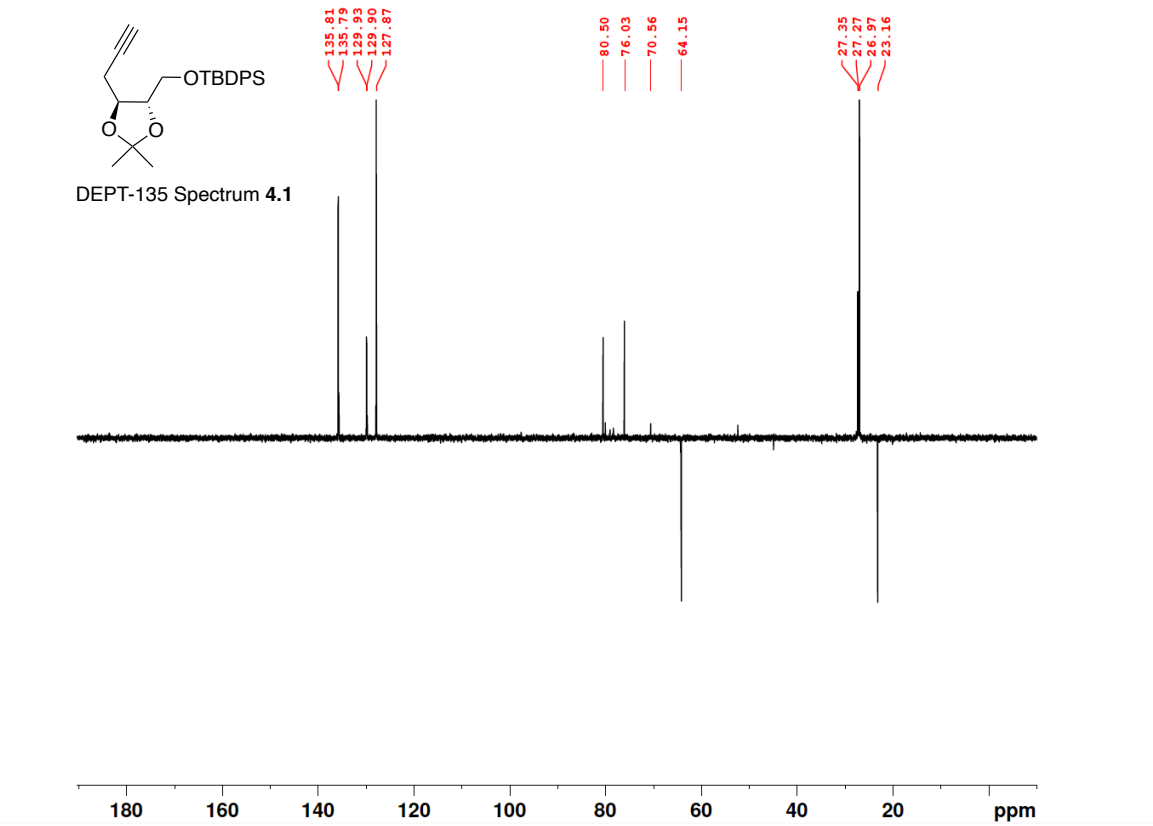

Figure A.2 DEPT-135 (100 MHz, $CDCl_3$) of **4.1**.

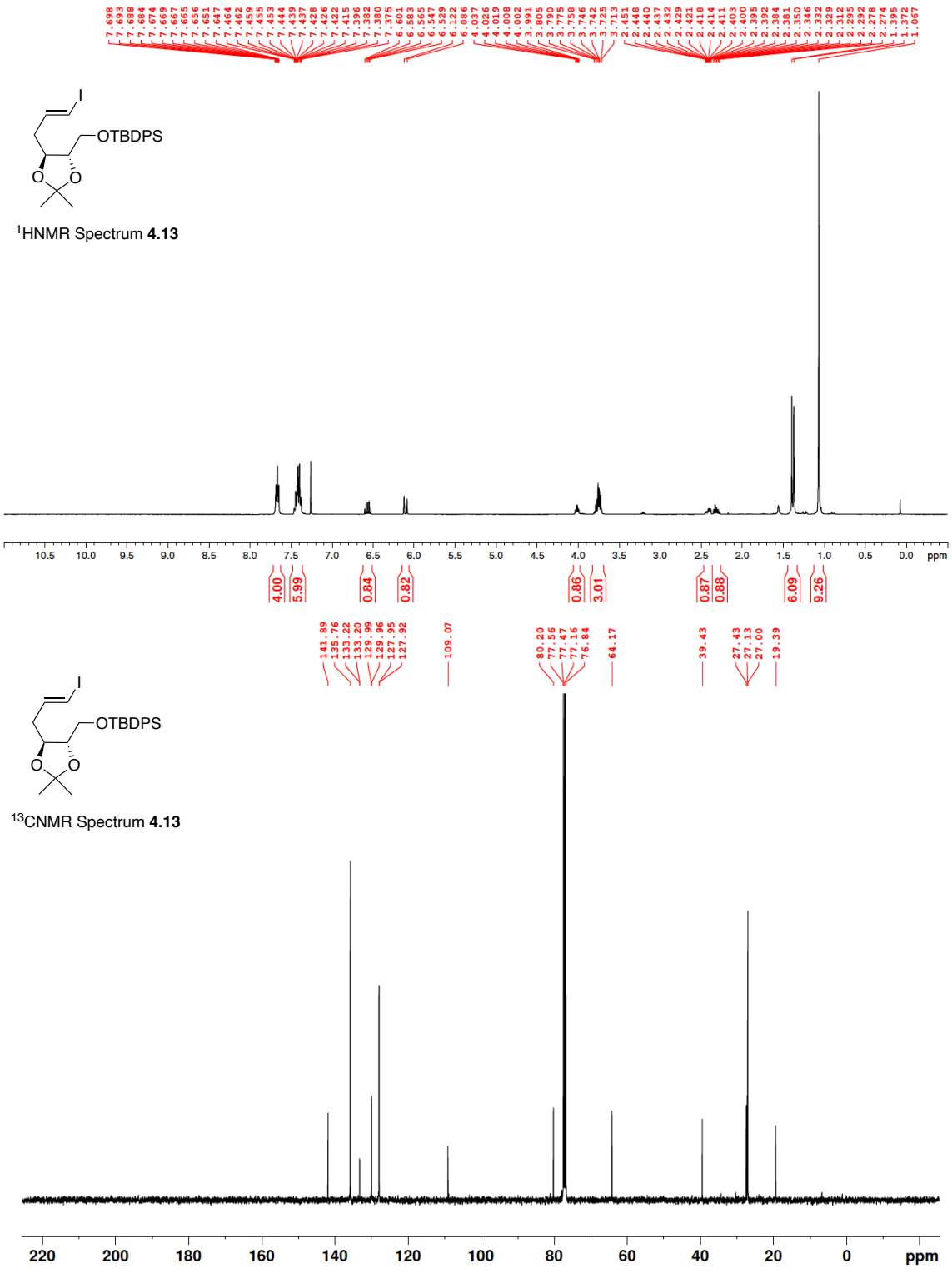

Figure A.3 ^{1}H NMR (400 MHz, $CDCl_3$) and ^{13}C NMR (100 MHz, $CDCl_3$) of **4.13**.

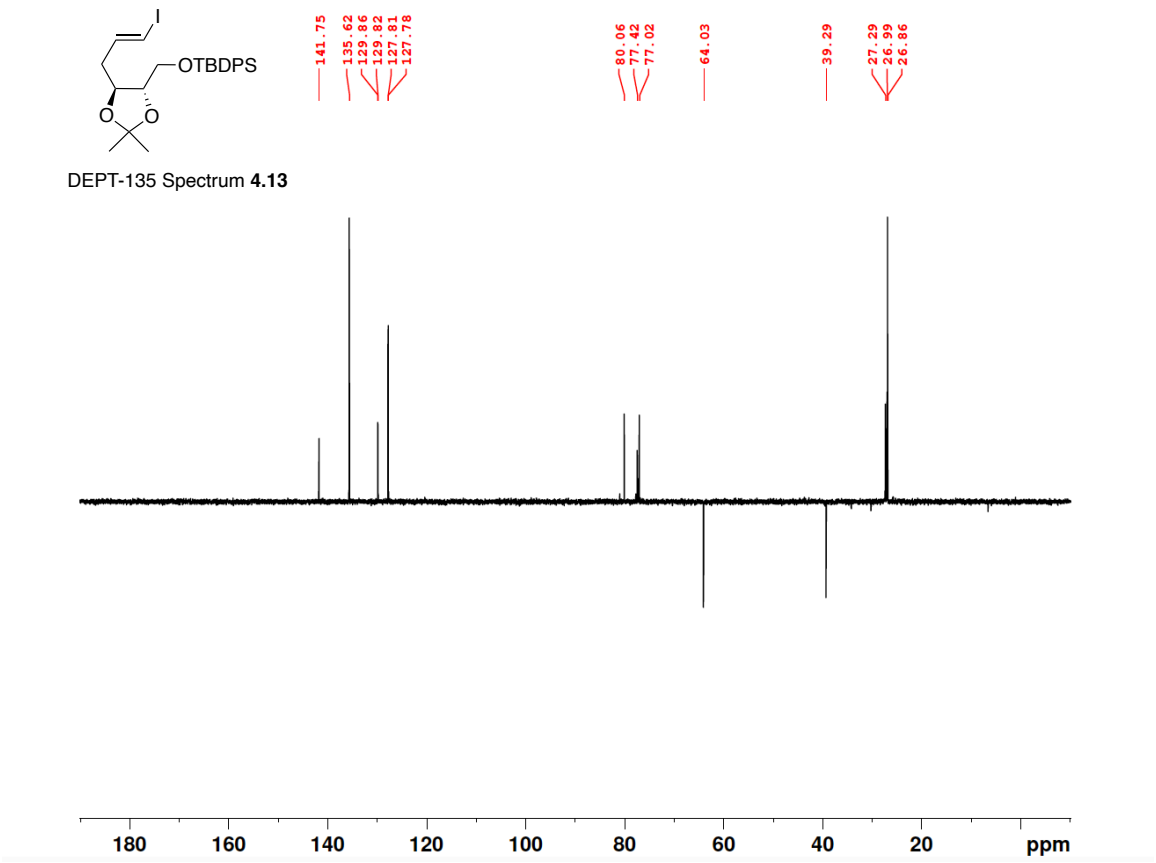

Figure A.4 DEPT-135 (100 MHz, $CDCl_3$) of **4.13**.

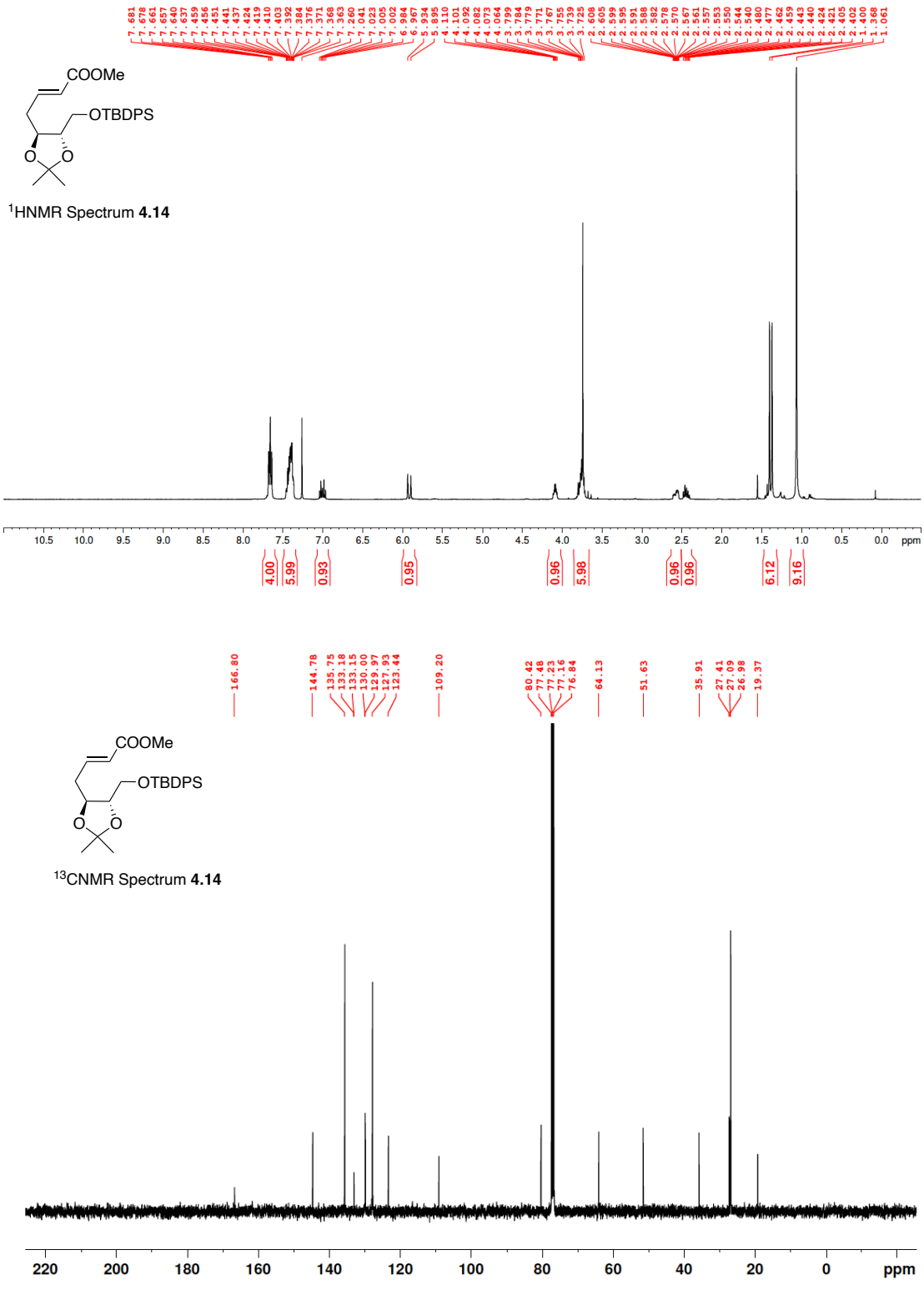

Figure A.5 ^{1}H NMR (400 MHz, $CDCl_3$) and ^{13}C NMR (100 MHz, $CDCl_3$) of **4.14**.

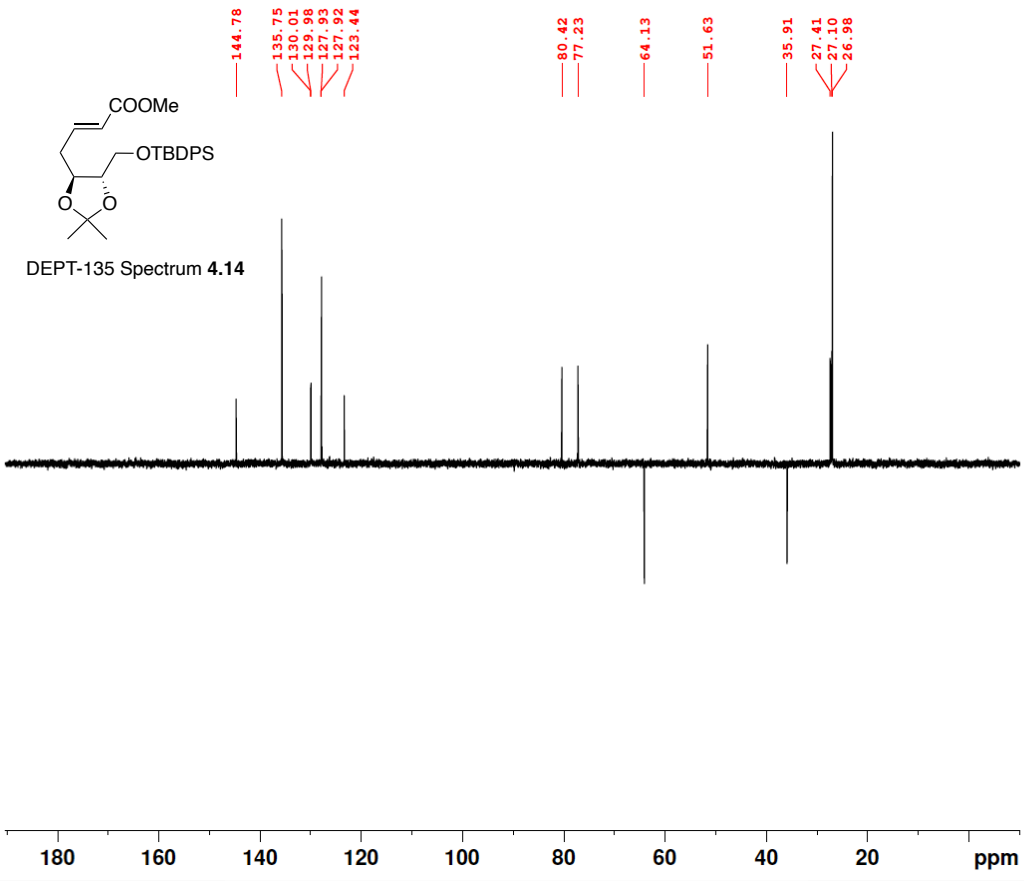

Figure A.6 DEPT-135 (100 MHz, $CDCl_3$) of **4.14**.

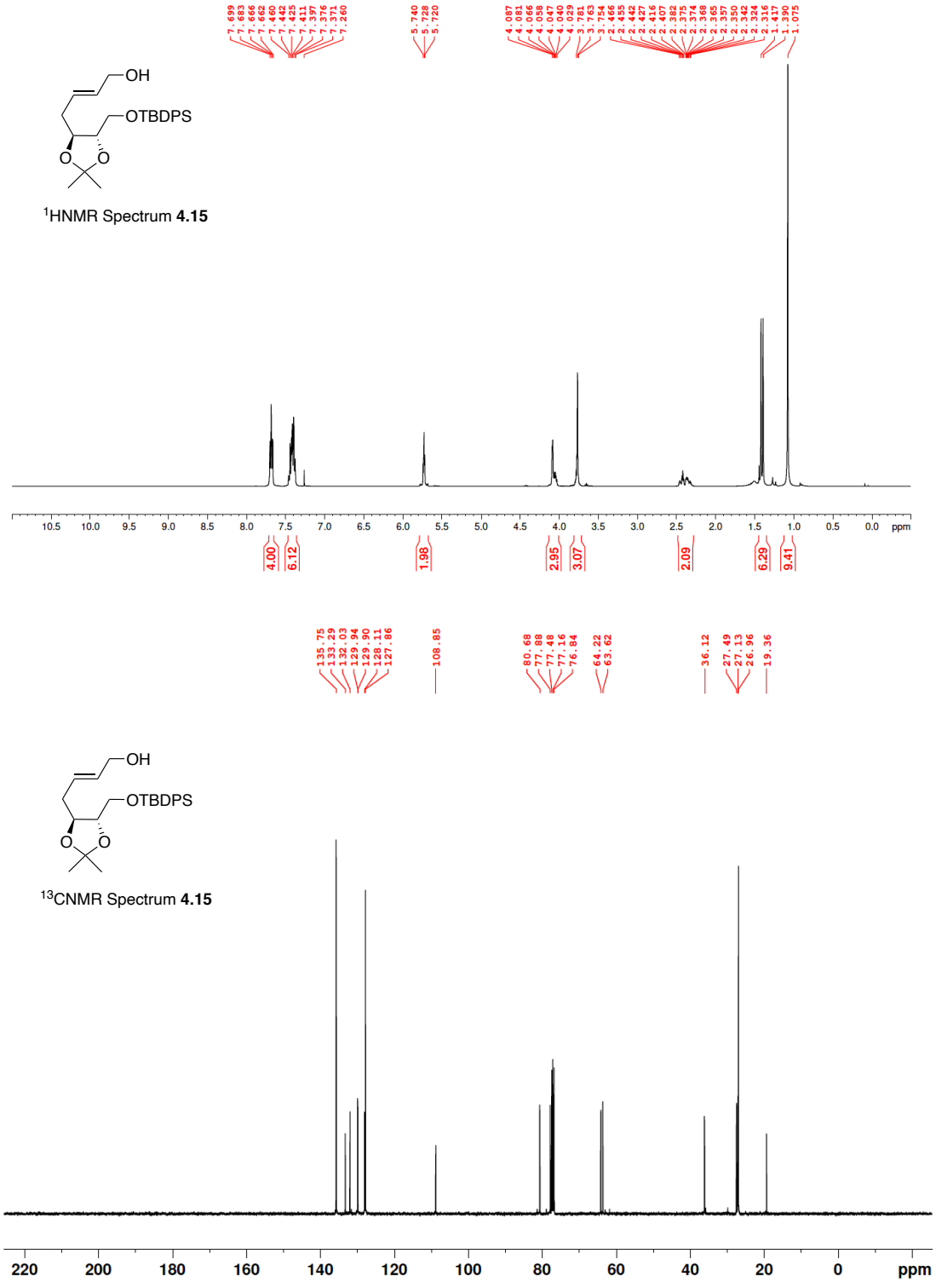

Figure A.7 ^{1}H NMR (400 MHz, $CDCl_3$) and ^{13}C NMR (100 MHz, $CDCl_3$) of **4.15**.

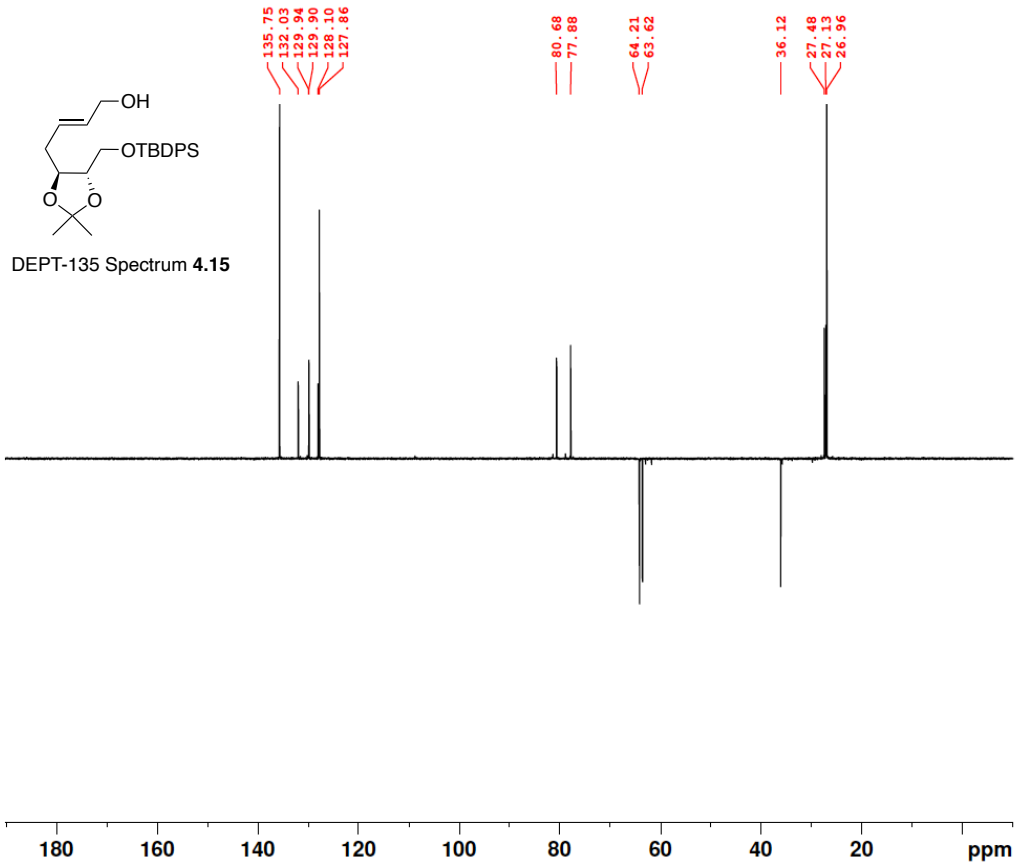

Figure A.8 DEPT-135 (100 MHz, $CDCl_3$) of **4.15**.

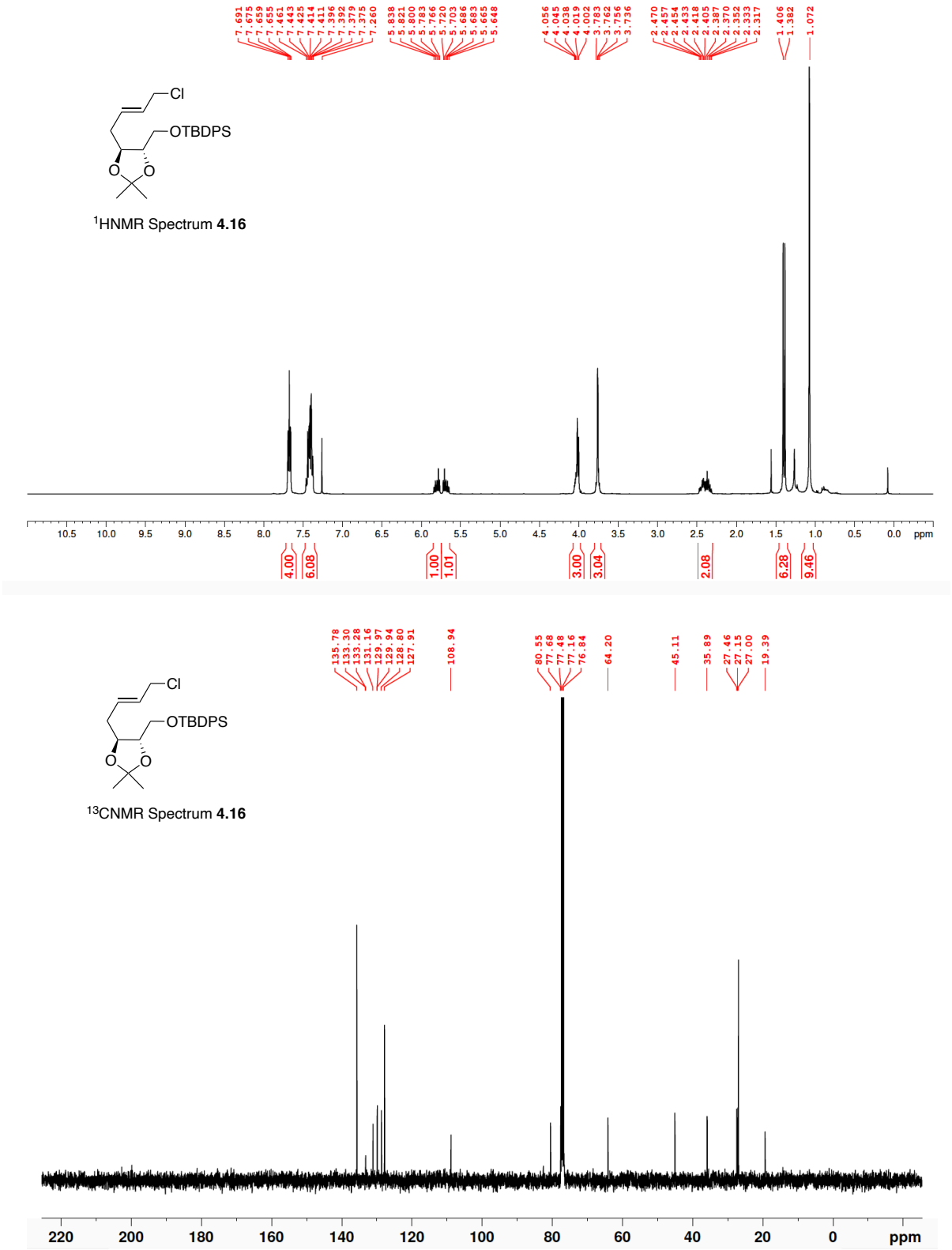

Figure A.9 ^{1}H NMR (400 MHz, $CDCl_3$) and ^{13}C NMR (100 MHz, $CDCl_3$) of **4.16**.

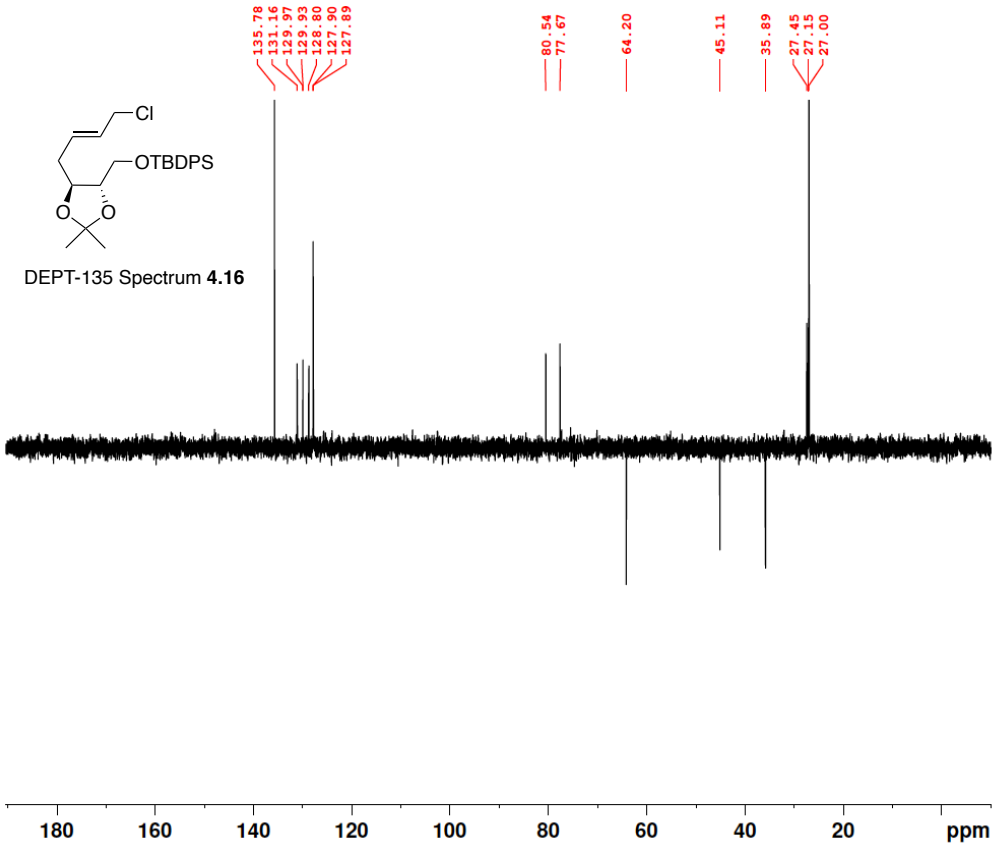

Figure A.10 DEPT-135 (100 MHz, $CDCl_3$) of **4.16**.

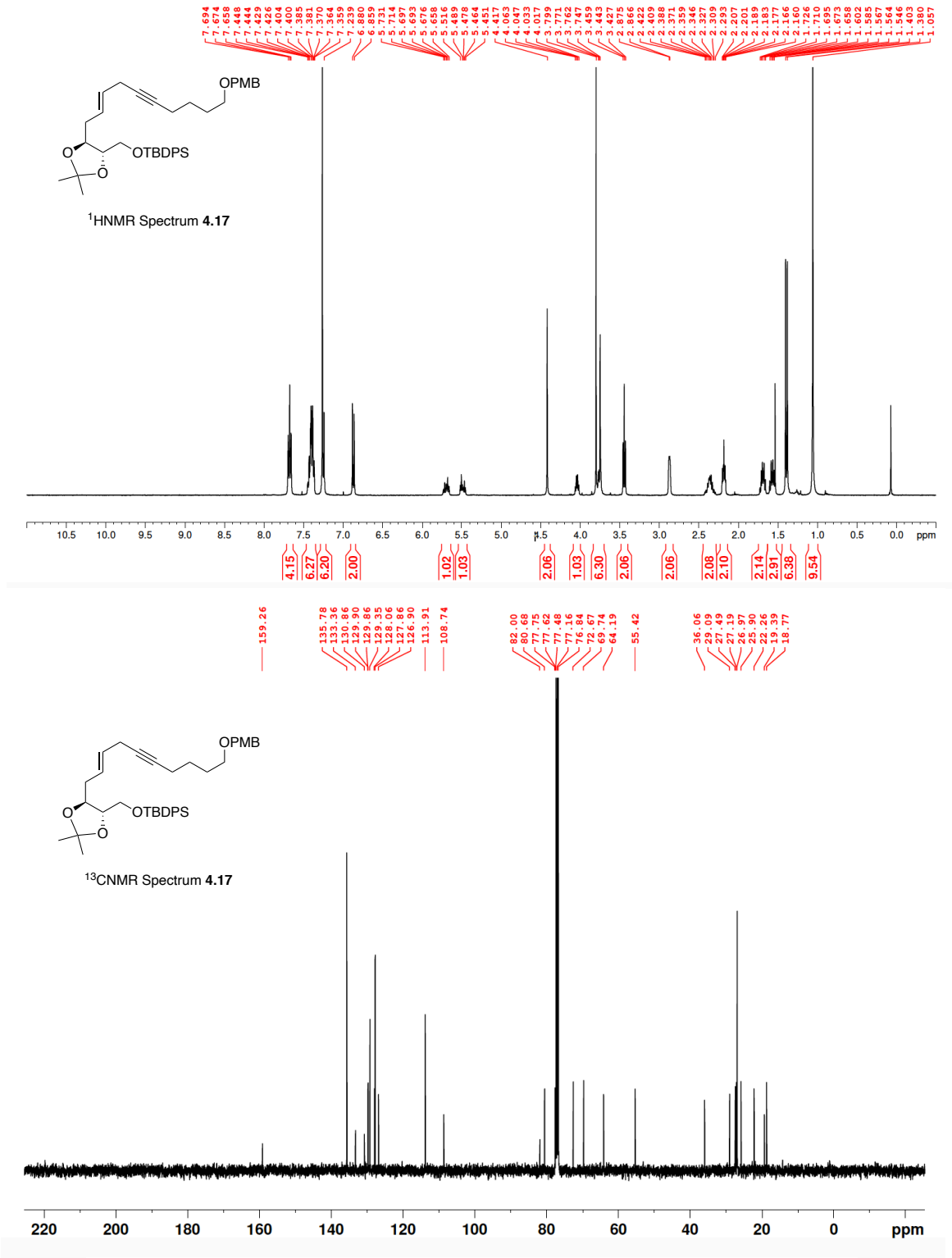

Figure A.11 ^{1}H NMR (400 MHz, $CDCl_3$) and ^{13}C NMR (100 MHz, $CDCl_3$) of **4.17**.

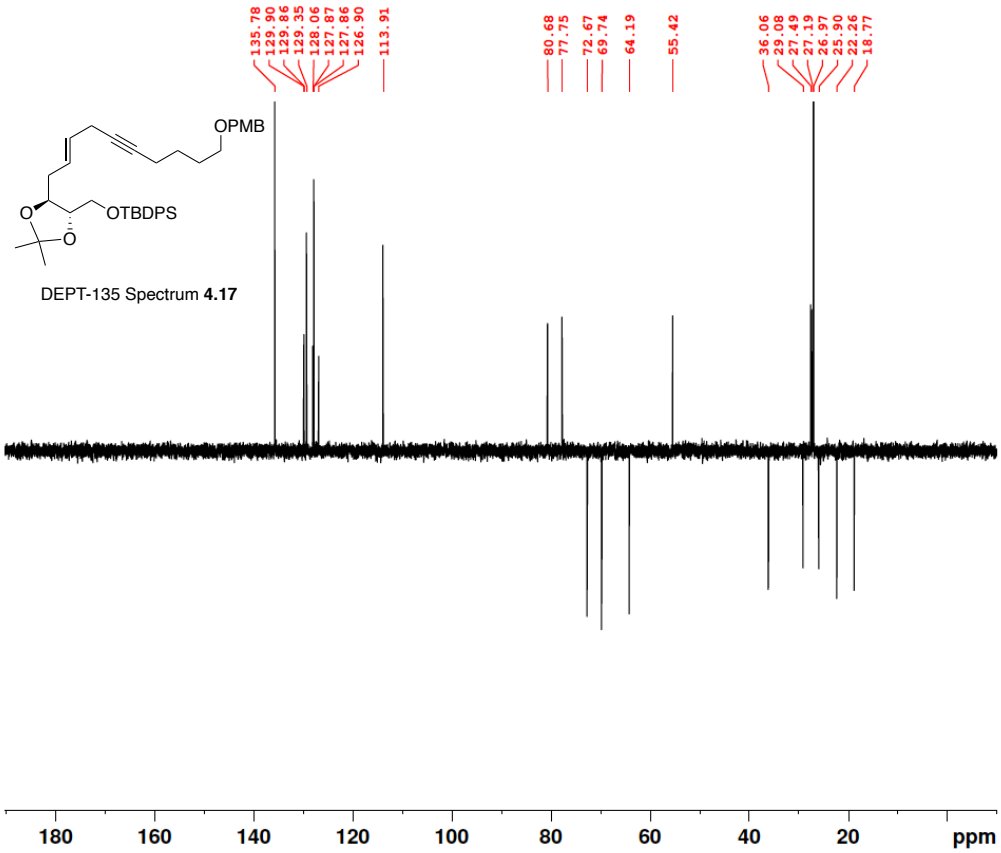

Figure A.12 DEPT-135 (100 MHz, $CDCl_3$) of **4.17**.

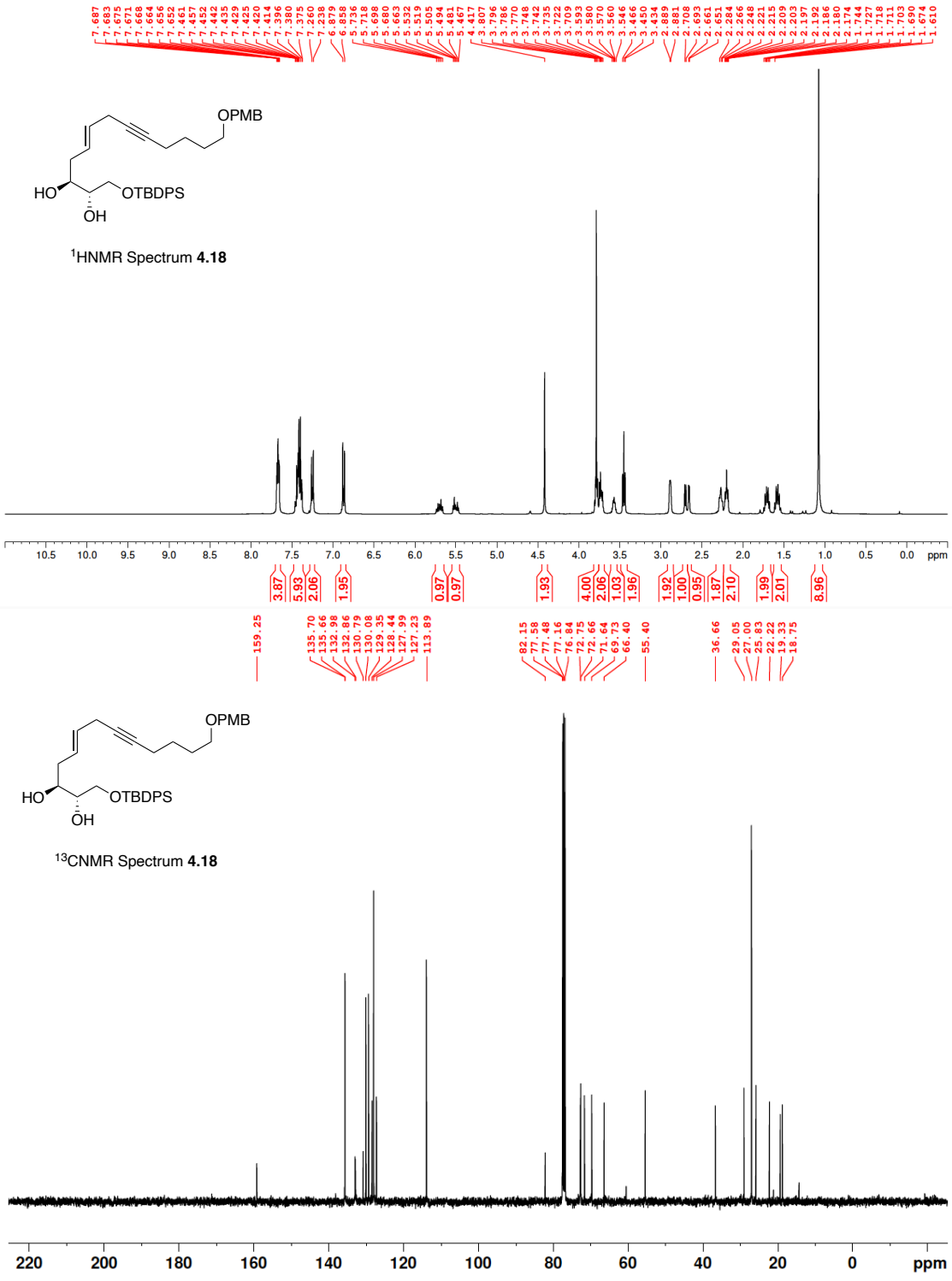

Figure A.13 ^{1}H NMR (400 MHz, $CDCl_3$) and ^{13}C NMR (100 MHz, $CDCl_3$) of **4.18**.

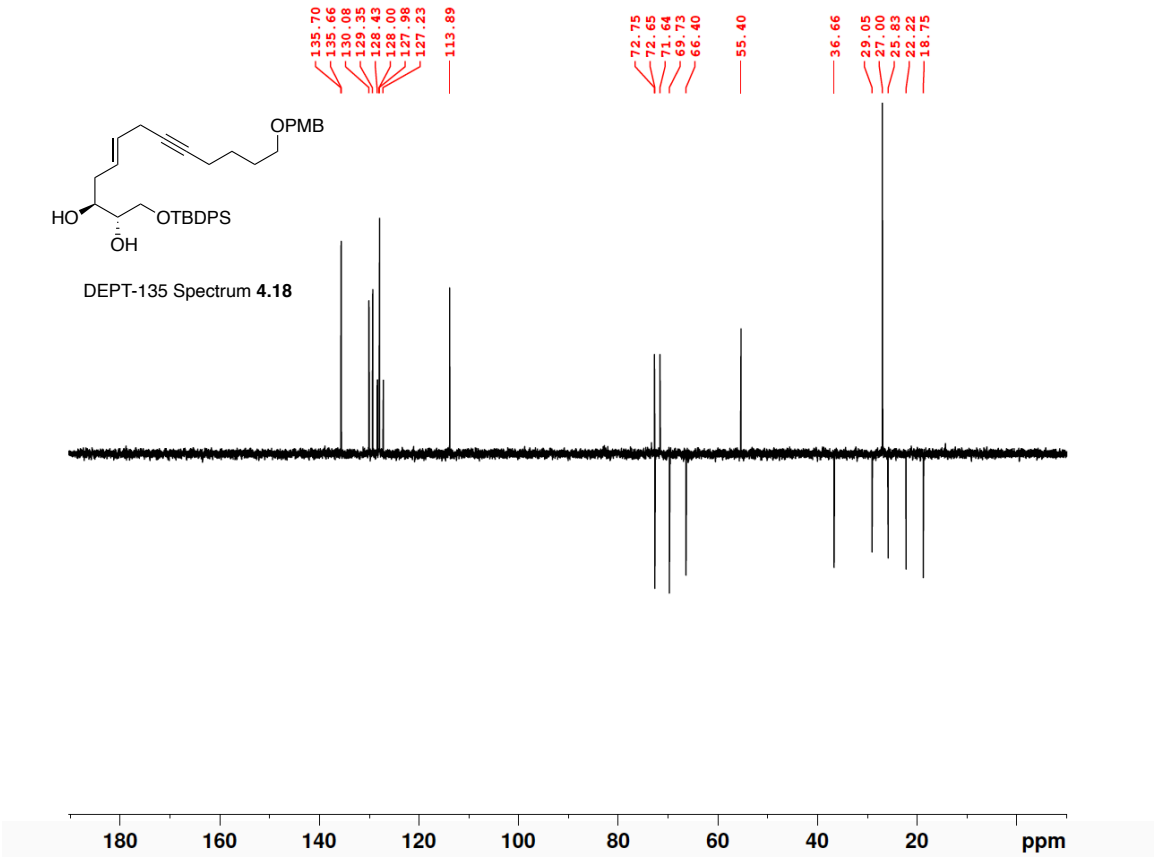

Figure A.14 DEPT-135 (100 MHz, $CDCl_3$) of **4.18**.

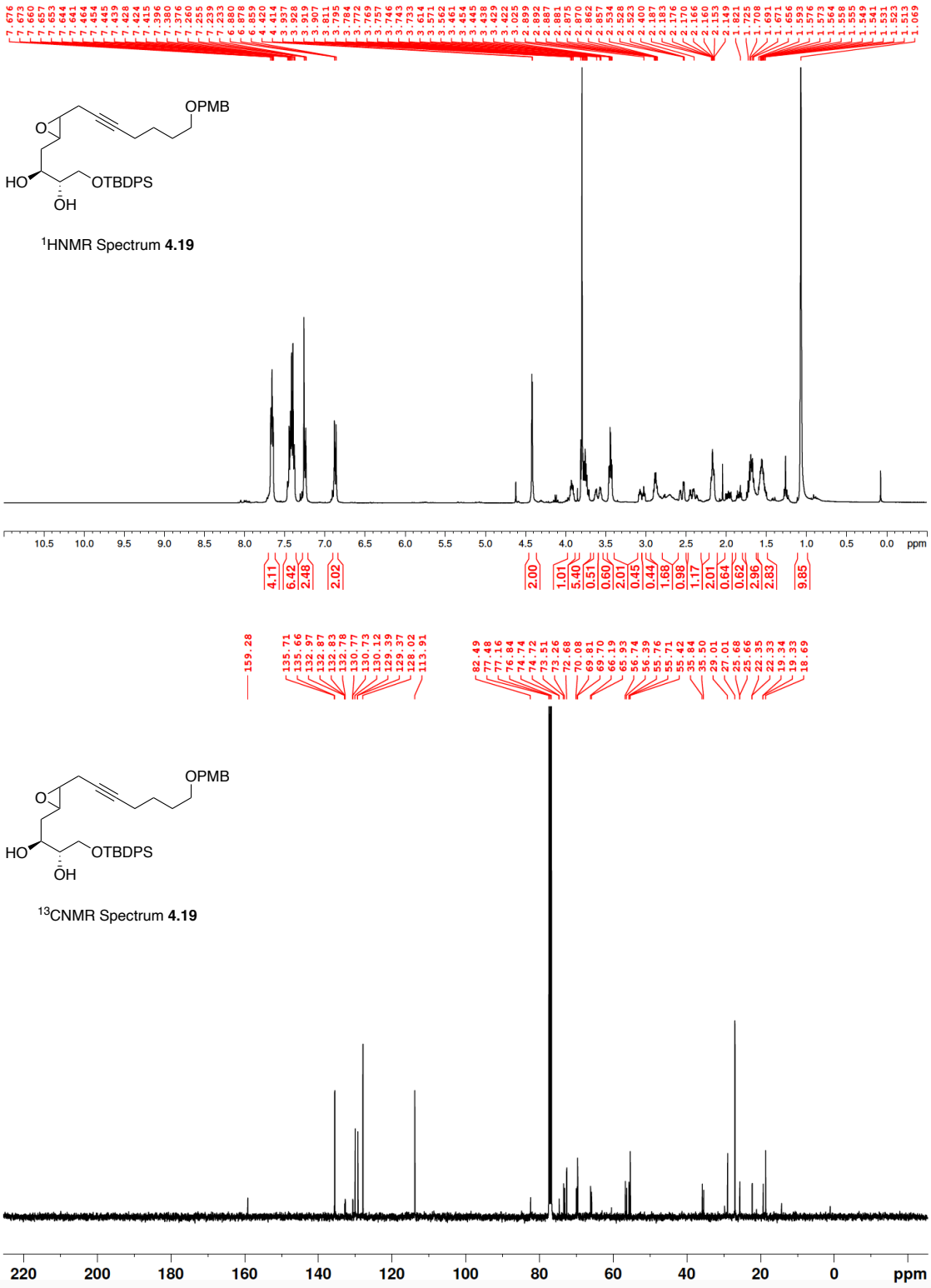

Figure A.15 ^{1}H NMR (400 MHz, $CDCl_3$) and ^{13}C NMR (100 MHz, $CDCl_3$) of **4.19**.

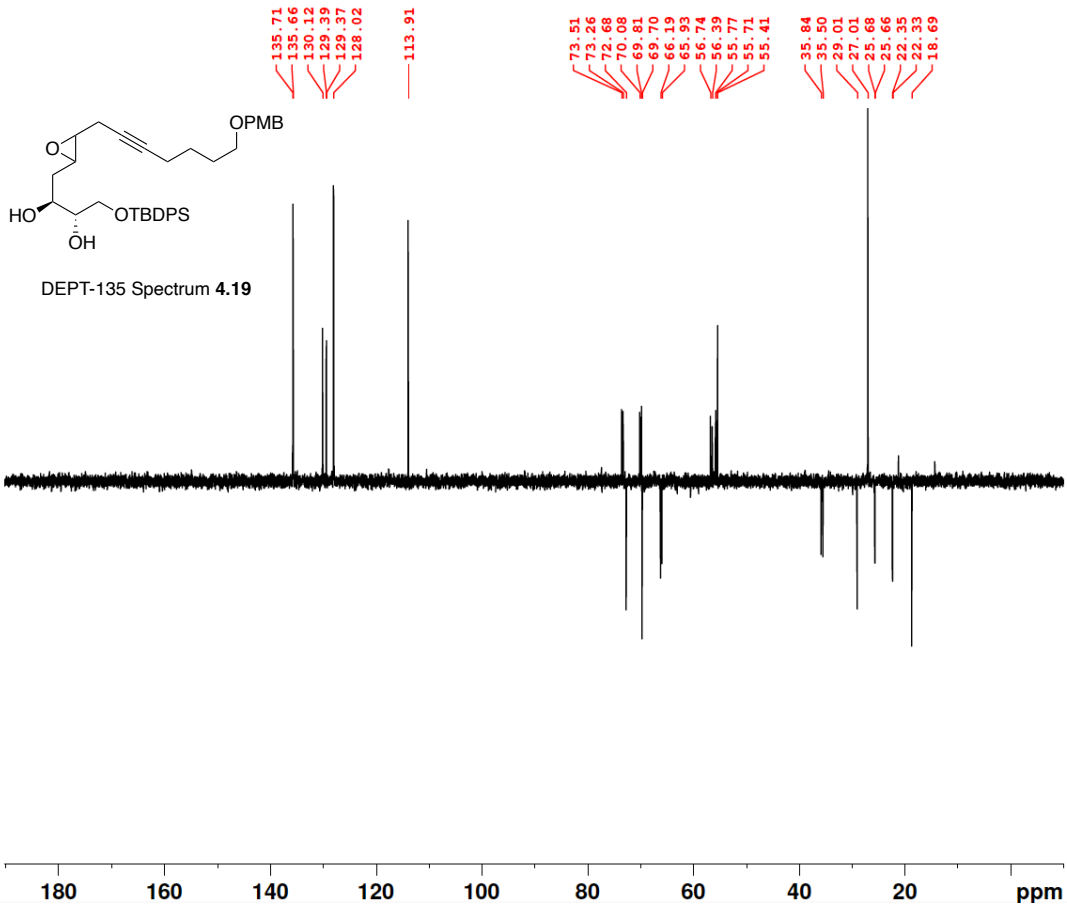

Figure A.16 DEPT-135 (100 MHz, $CDCl_3$) of **4.19**.

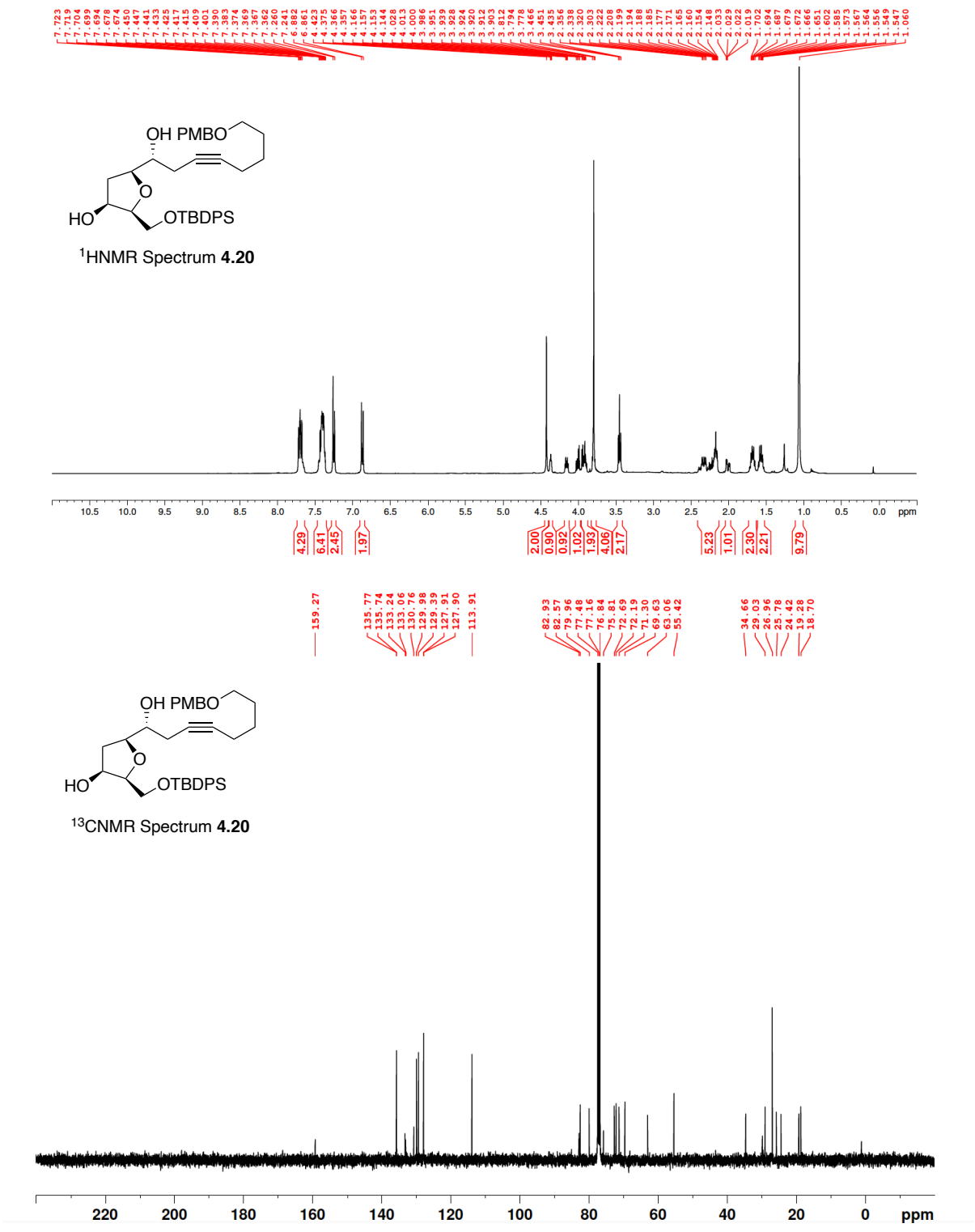

Figure A.17 ^{1}H NMR (400 MHz, $CDCl_3$) and ^{13}C NMR (100 MHz, $CDCl_3$) of **4.20**.

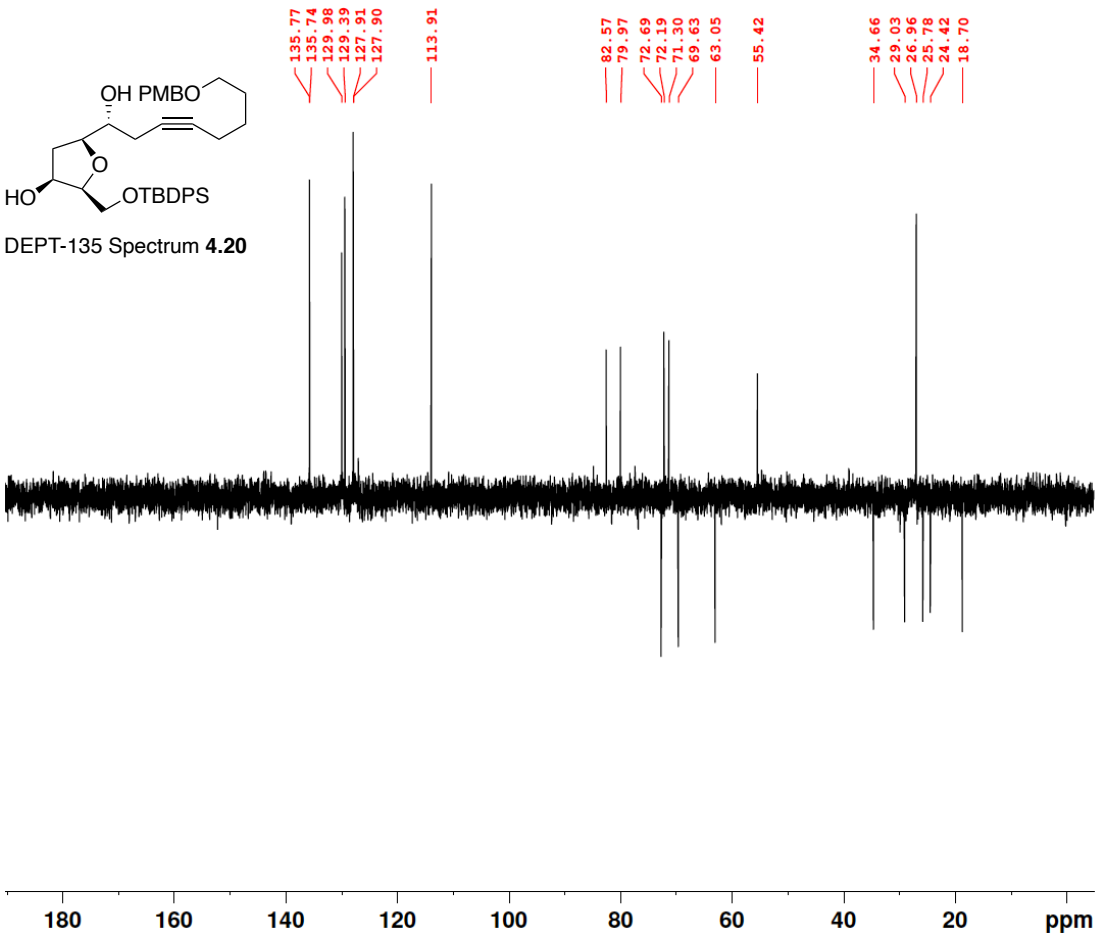

Figure A.18 DEPT-135 (100 MHz, $CDCl_3$) of **4.20**.

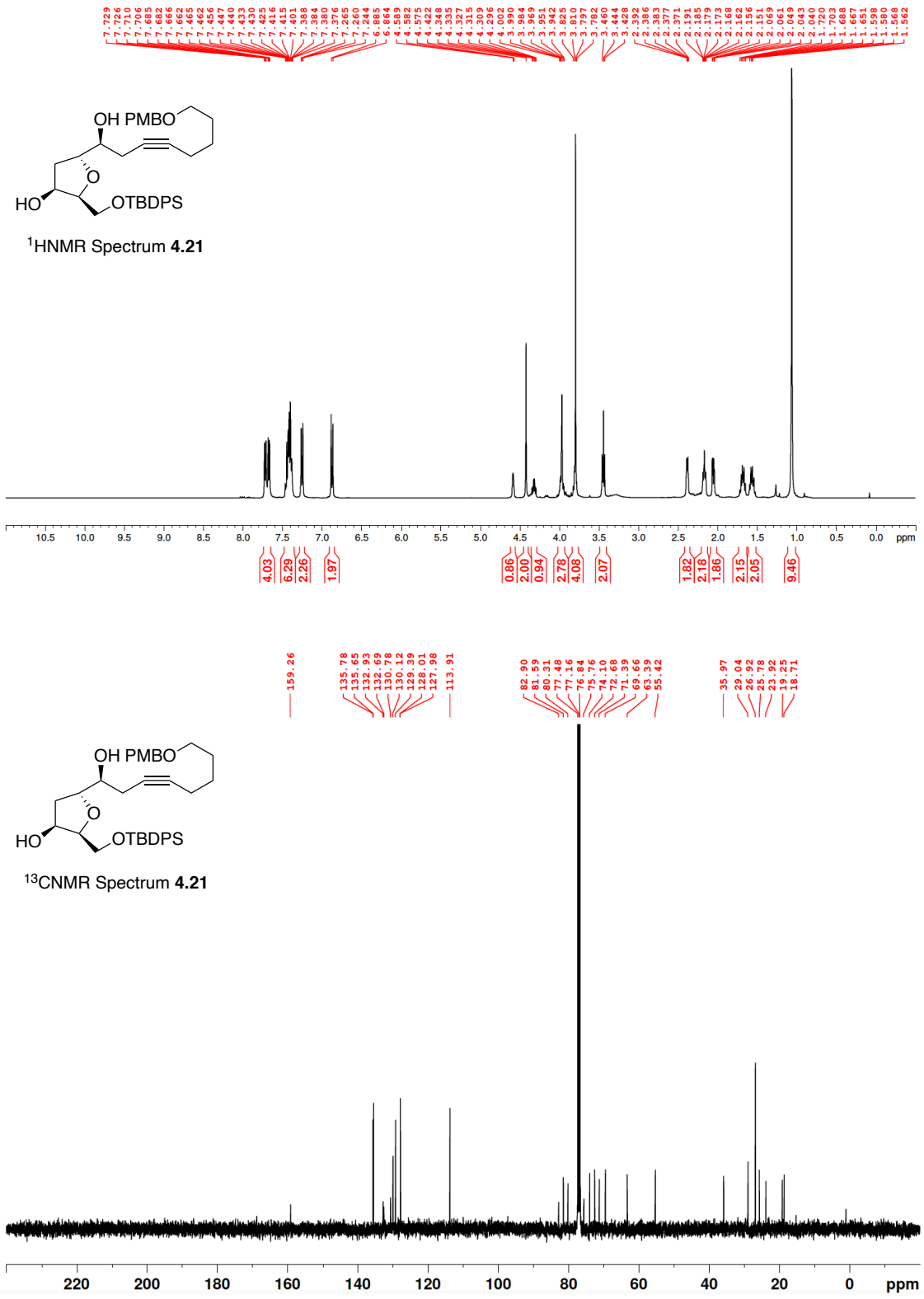

Figure A.19 ^{1}H NMR (400 MHz, $CDCl_3$) and ^{13}C NMR (100 MHz, $CDCl_3$) of **4.21**.

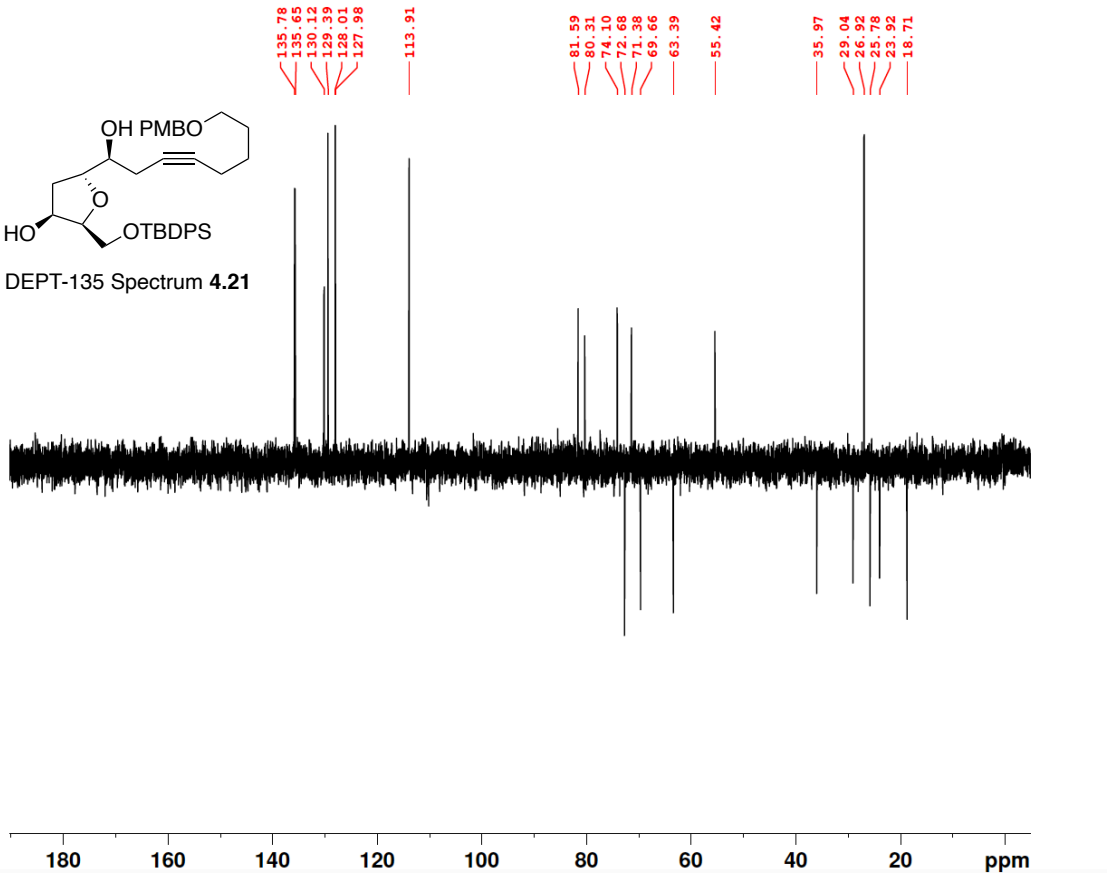

Figure A.20 DEPT-135 (100 MHz, $CDCl_3$) of **4.21**.

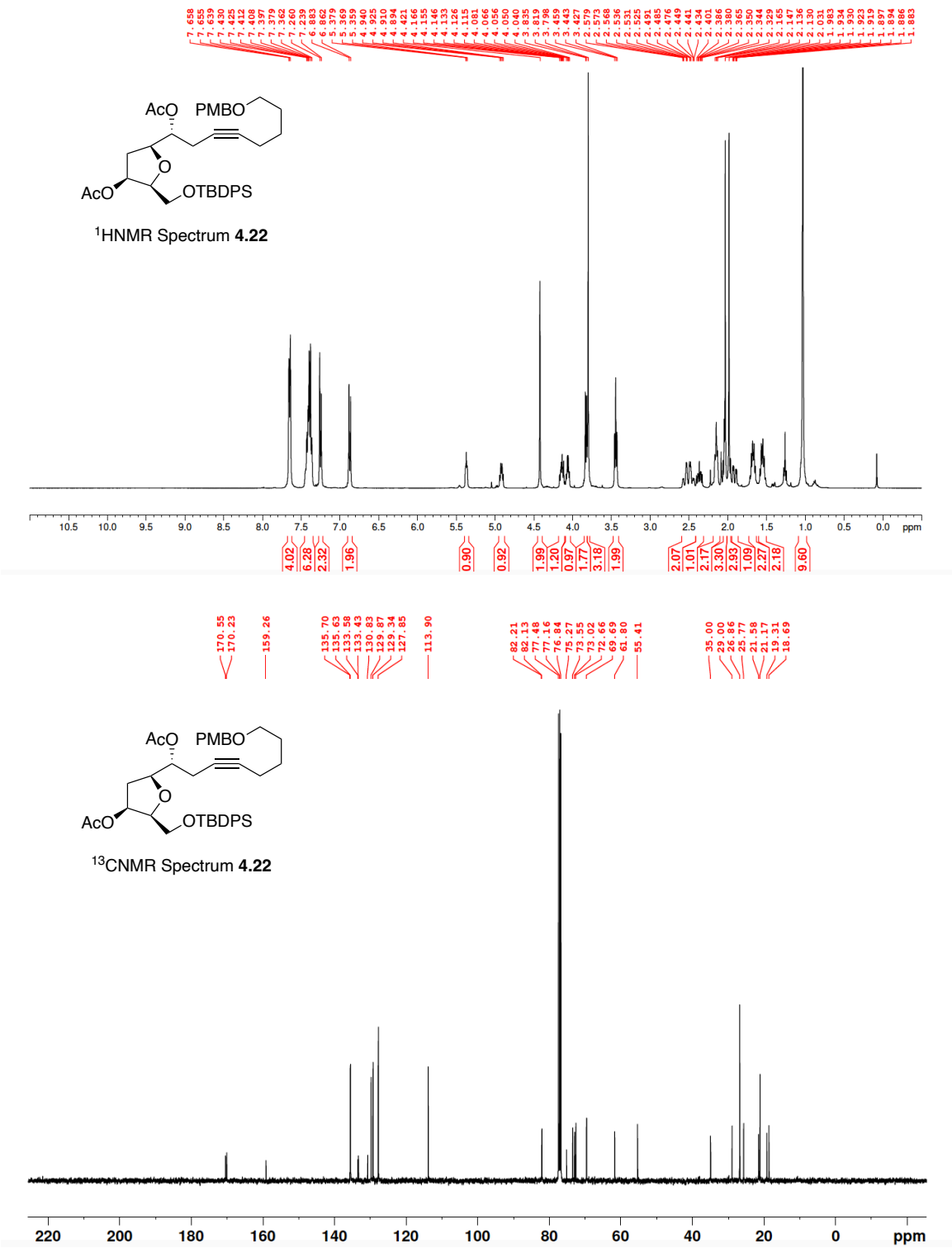

Figure A.21 ^{1}H NMR (400 MHz, $CDCl_3$) and ^{13}C NMR (100 MHz, $CDCl_3$) of **4.22**.

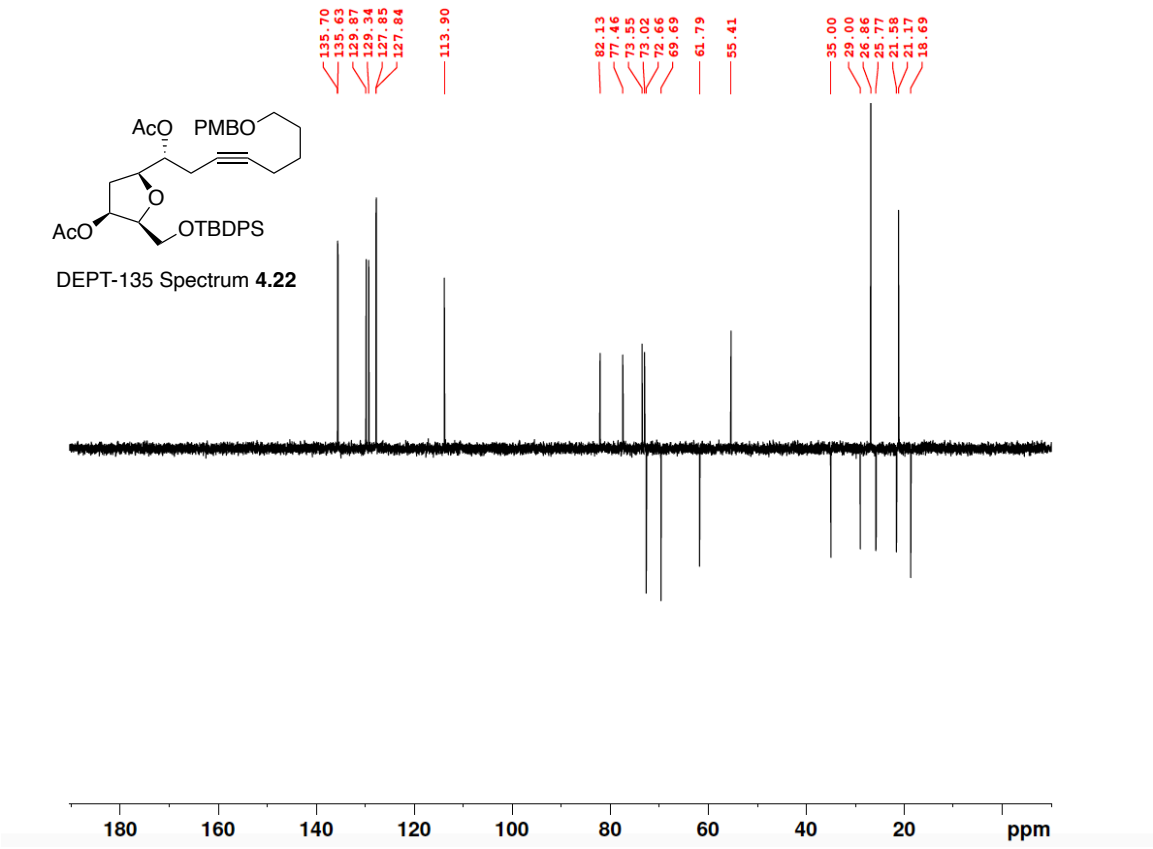

Figure A.22 DEPT-135 (100 MHz, $CDCl_3$) of **4.22**.

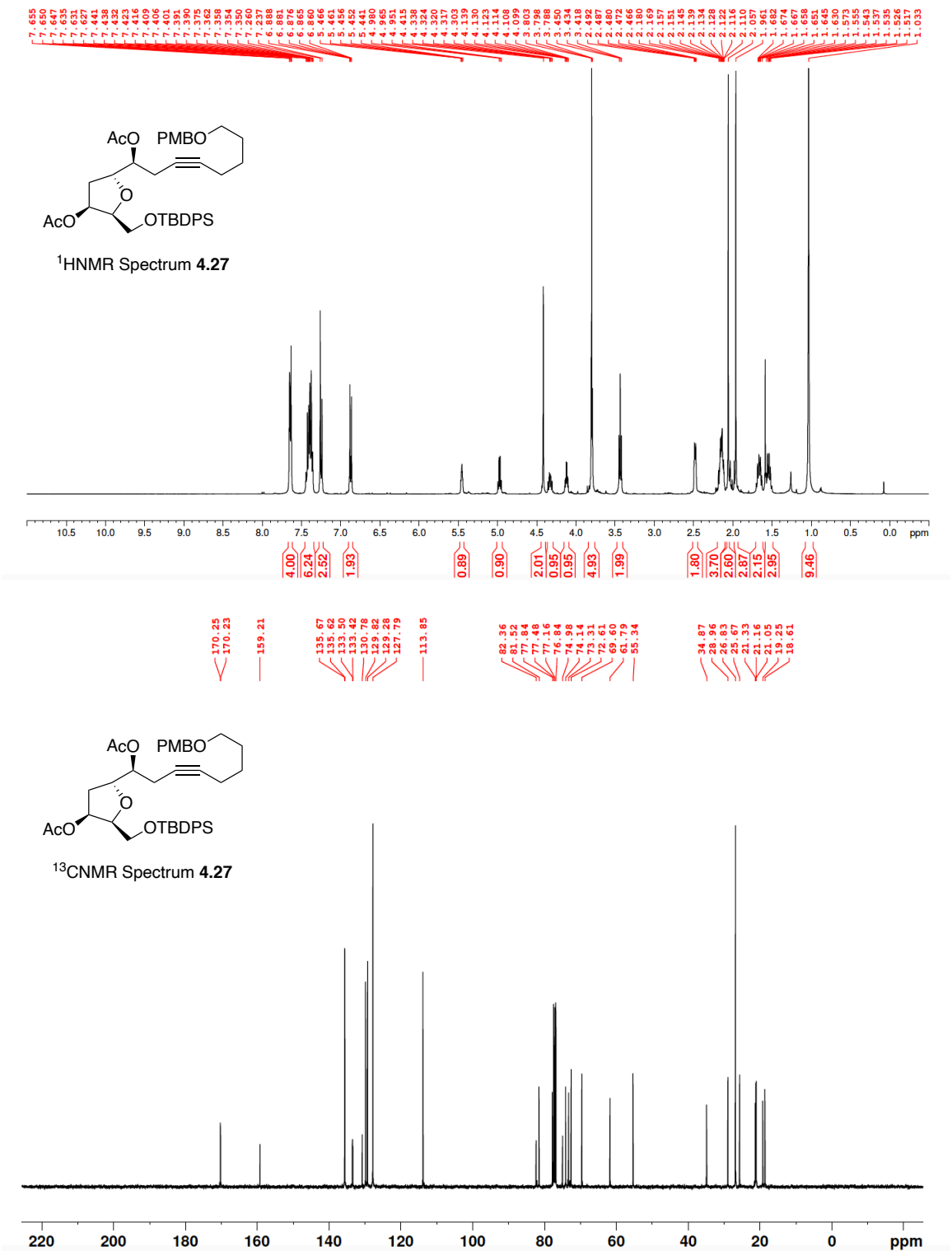

Figure A.23 ^{1}H NMR (400 MHz, $CDCl_3$) and ^{13}C NMR (100 MHz, $CDCl_3$) of **4.27**.

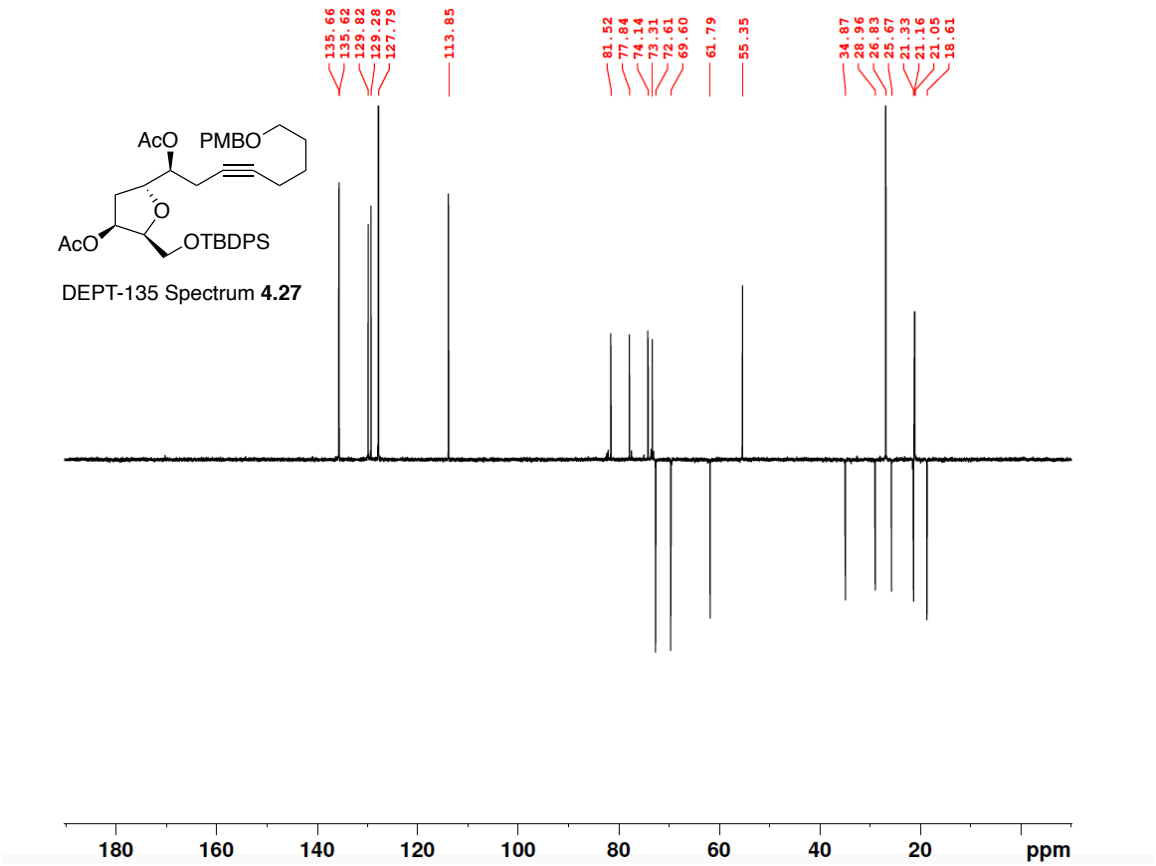

Figure A.24 DEPT-135 (100 MHz, $CDCl_3$) of **4.27**.

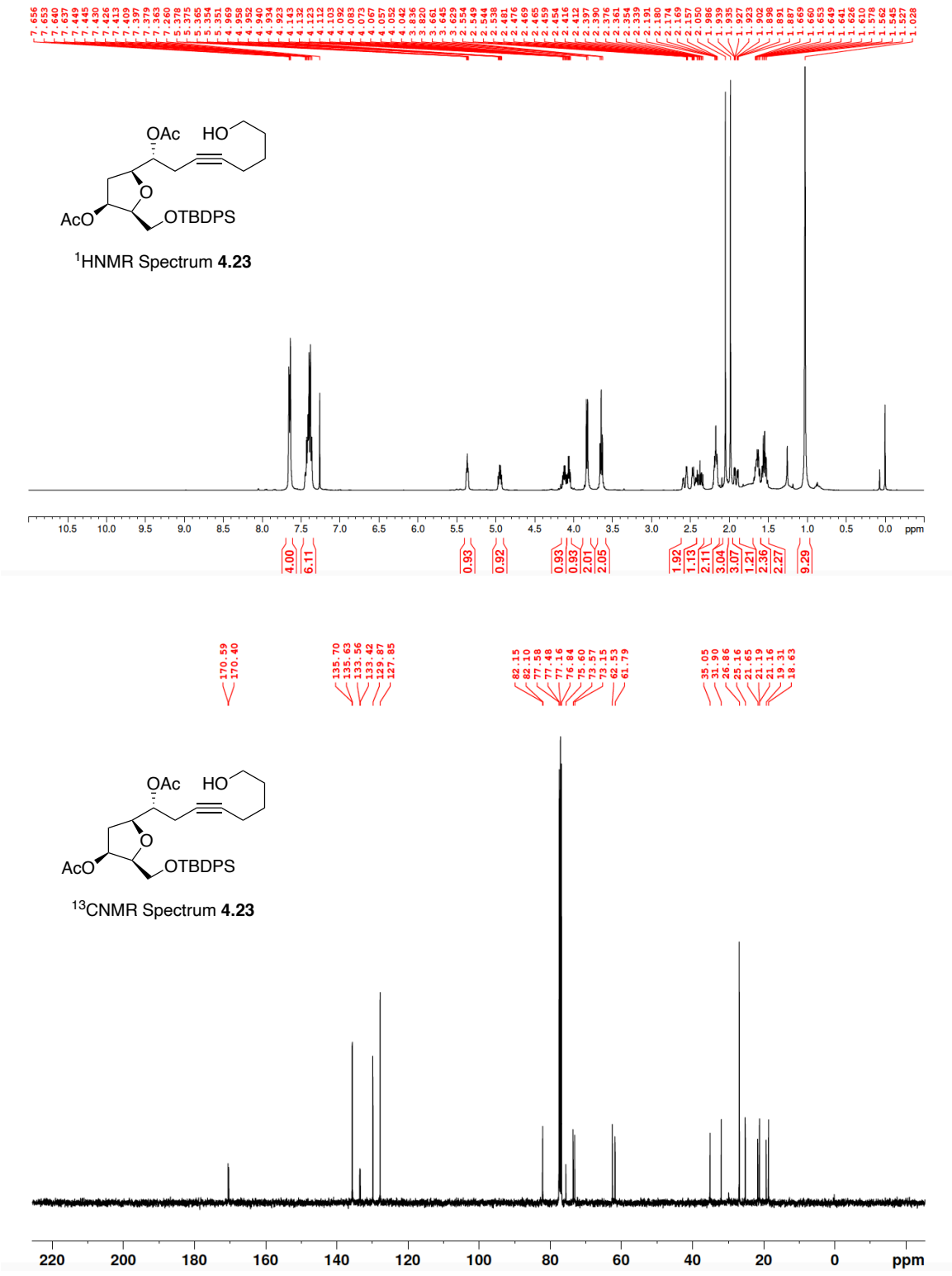

Figure A.25 ^{1}H NMR (400 MHz, $CDCl_3$) and ^{13}C NMR (100 MHz, $CDCl_3$) of **4.23**.

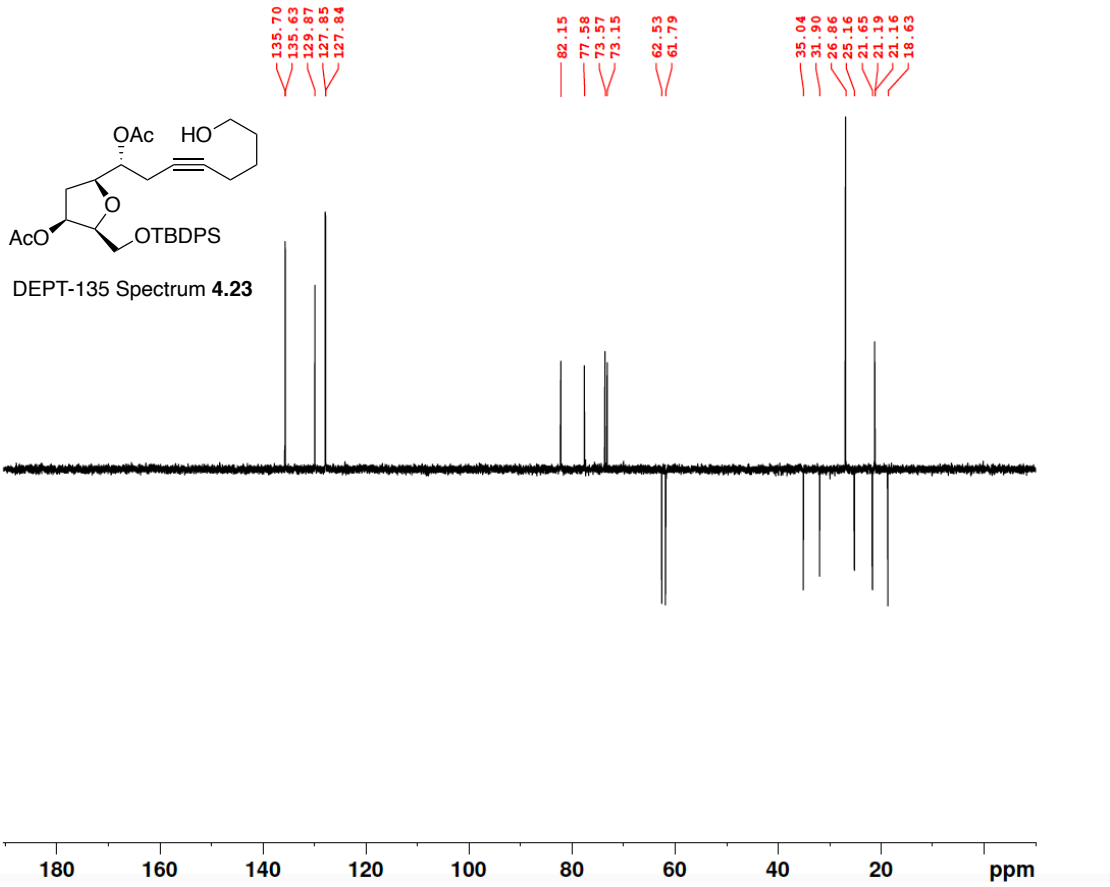

Figure A.26 DEPT-135 (100 MHz, $CDCl_3$) of **4.23**.

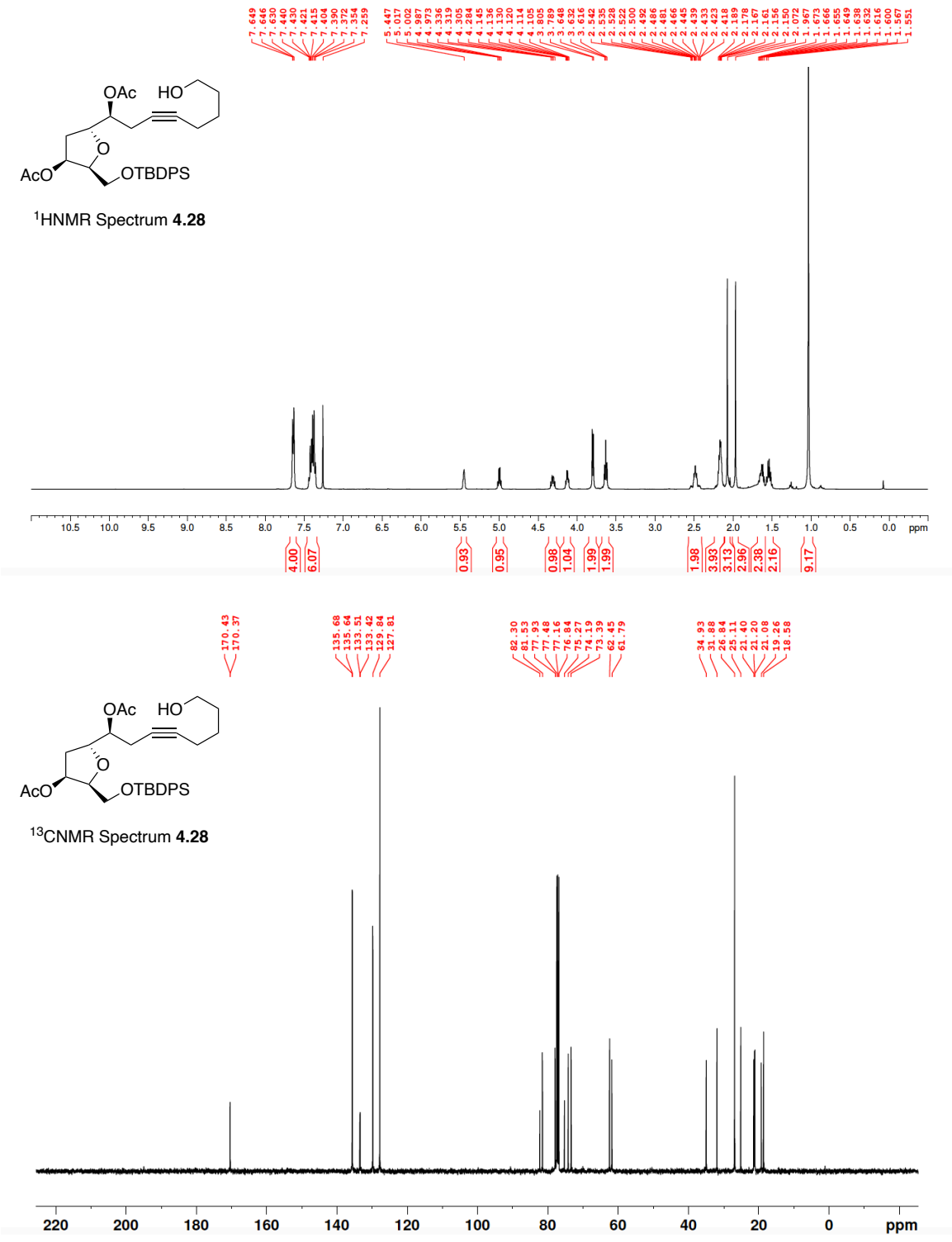

Figure A.27 ^{1}H NMR (400 MHz, $CDCl_3$) and ^{13}C NMR (100 MHz, $CDCl_3$) of **4.28**.

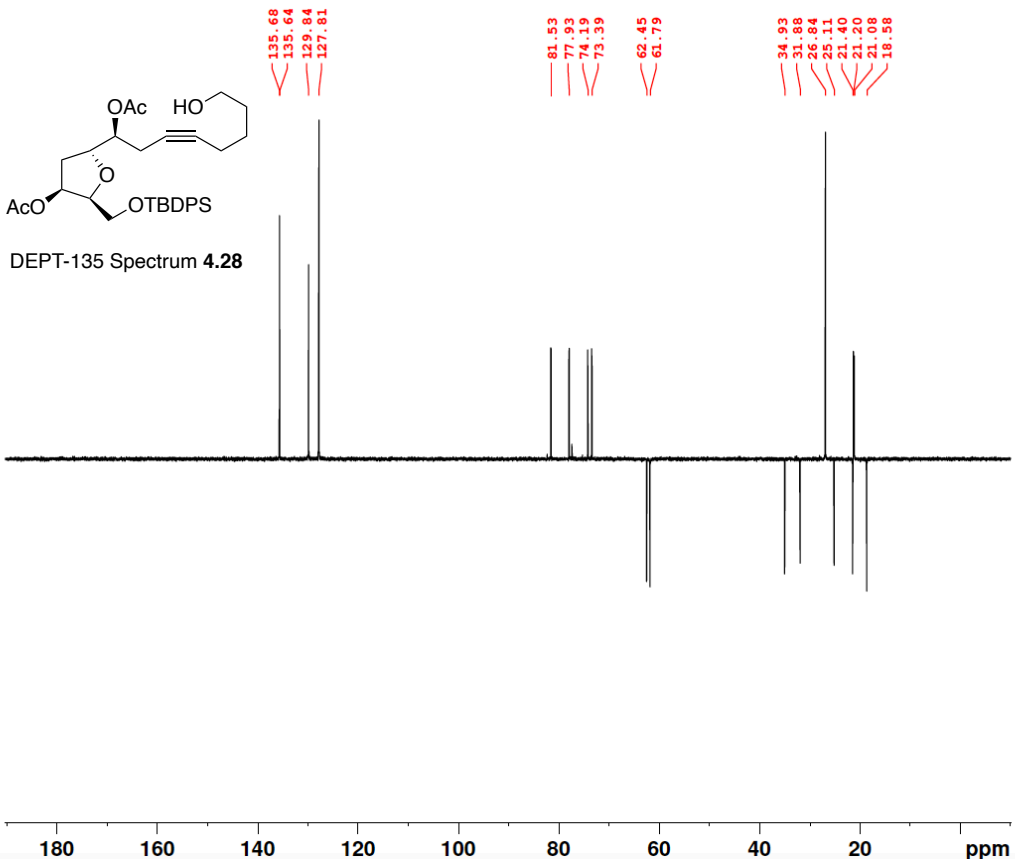

Figure A.28 DEPT-135 (100 MHz, $CDCl_3$) of **4.28**.

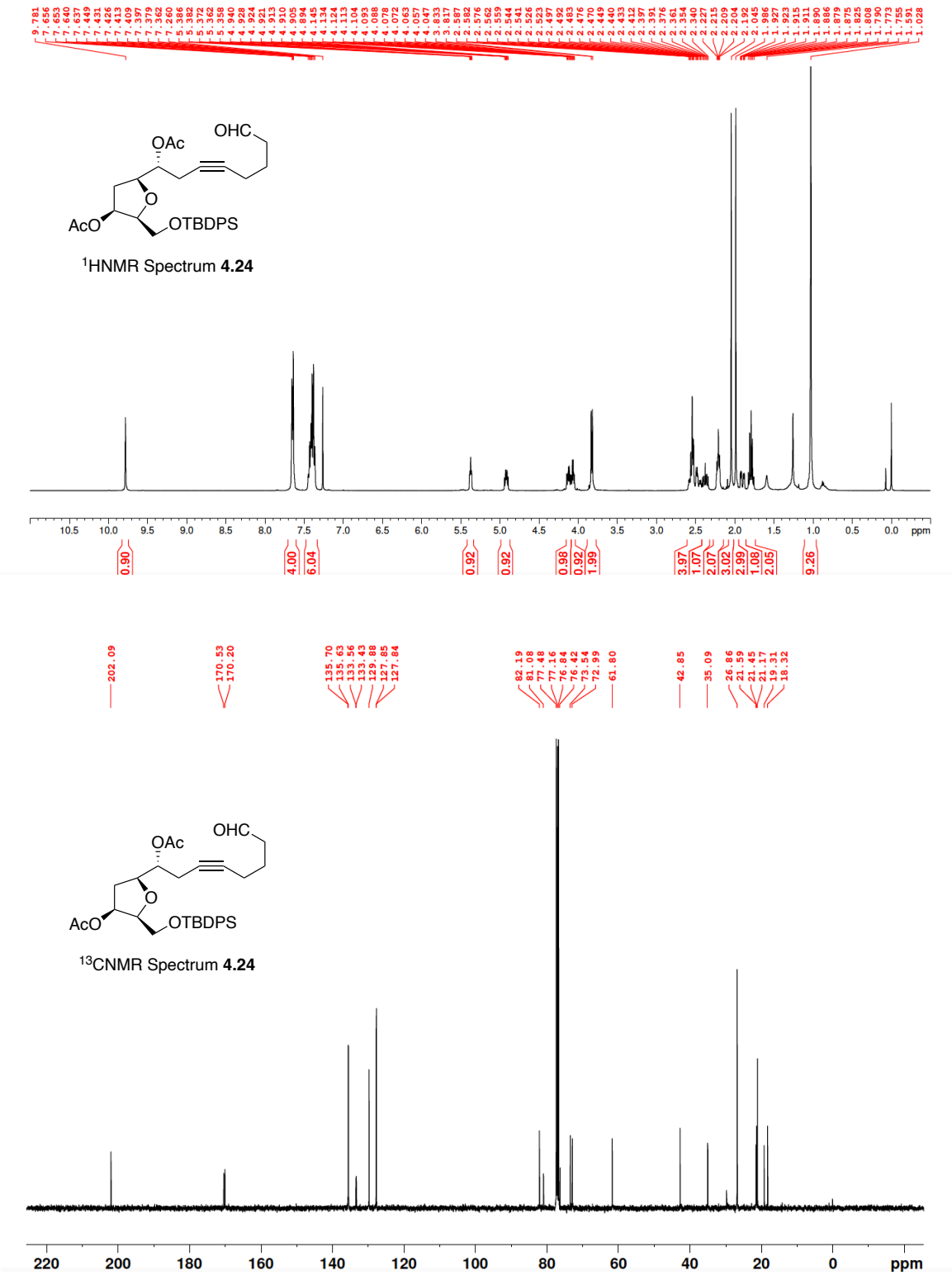

Figure A.29 ^{1}H NMR (400 MHz, $CDCl_3$) and ^{13}C NMR (100 MHz, $CDCl_3$) of **4.24**.

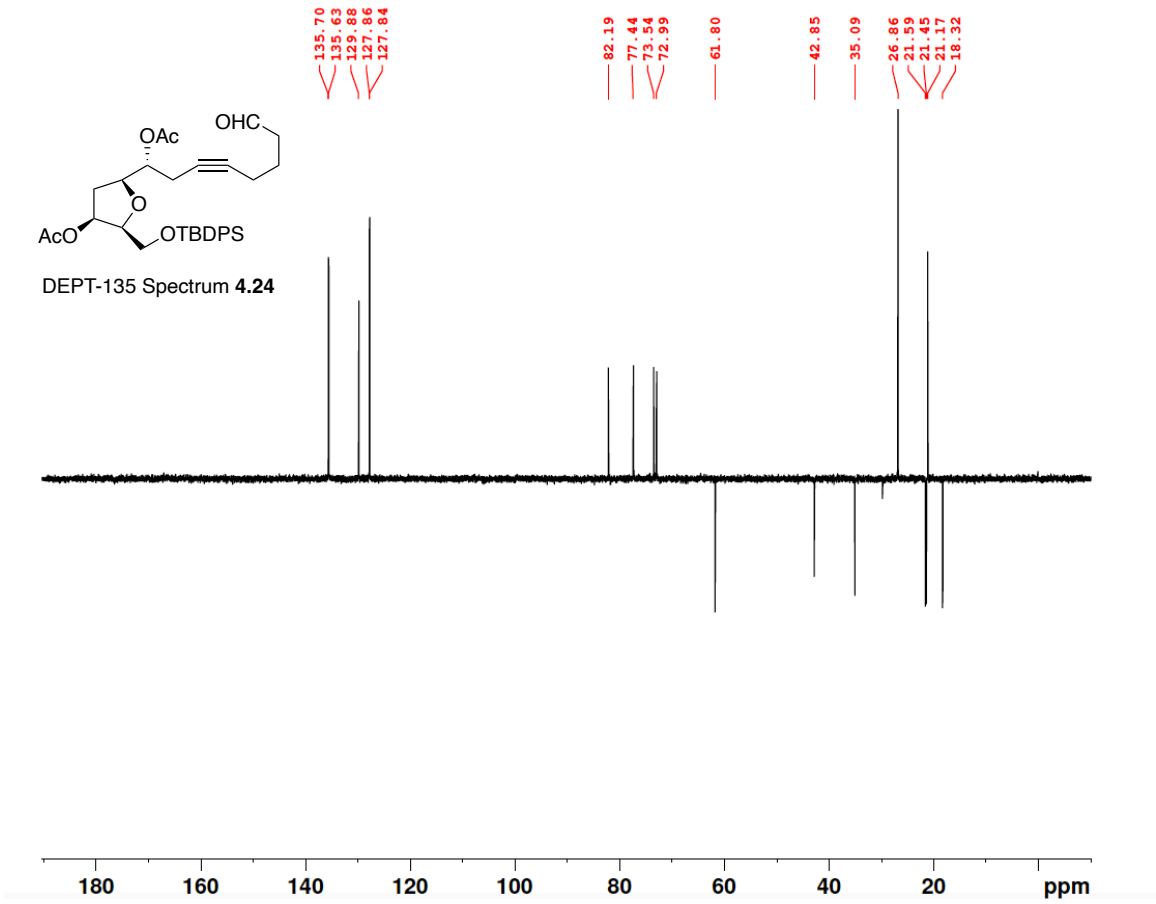

Figure A.30 DEPT-135 (100 MHz, $CDCl_3$) of **4.24**.

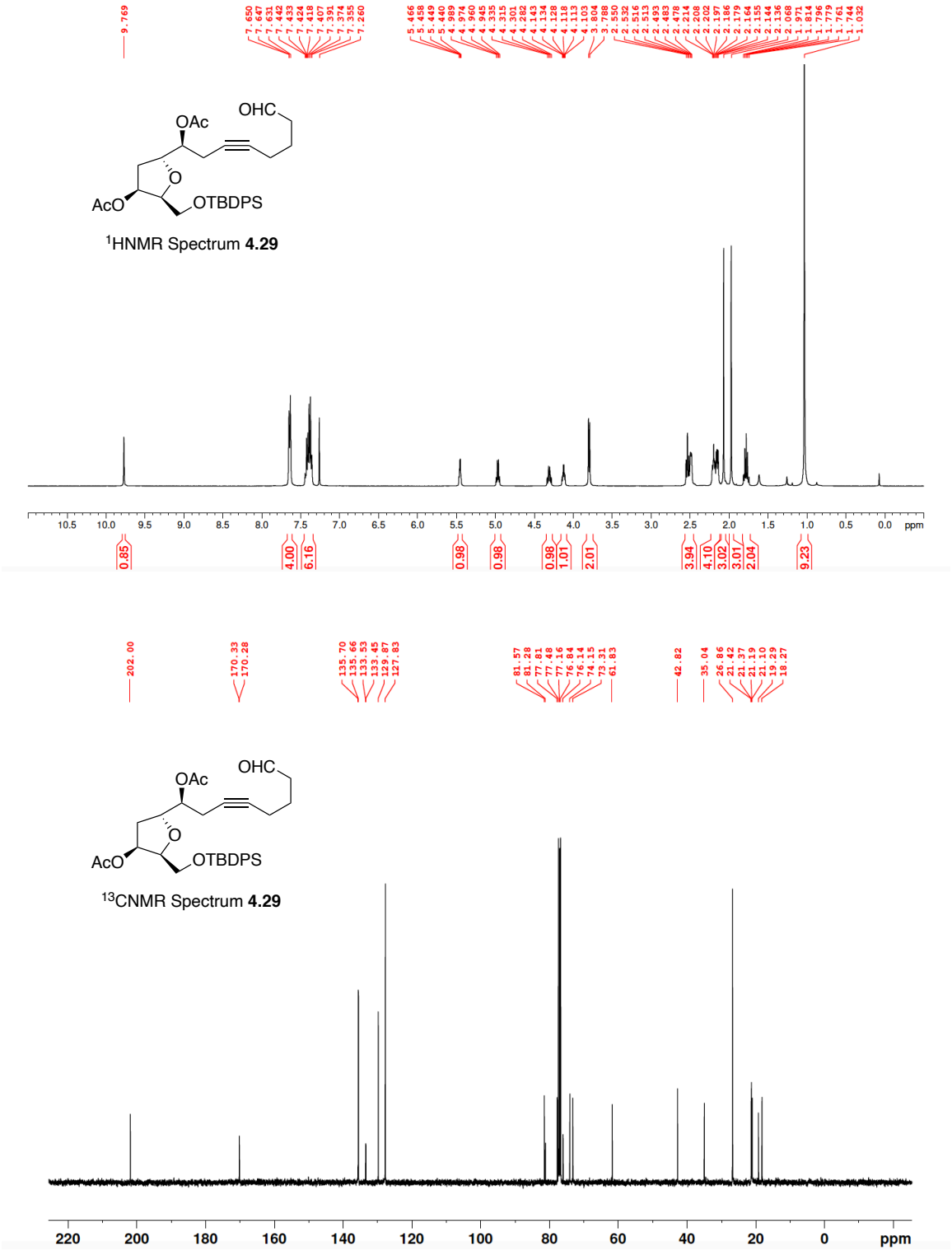

Figure A.31 ^{1}H NMR (400 MHz, $CDCl_3$) and ^{13}C NMR (100 MHz, $CDCl_3$) of **4.29**.

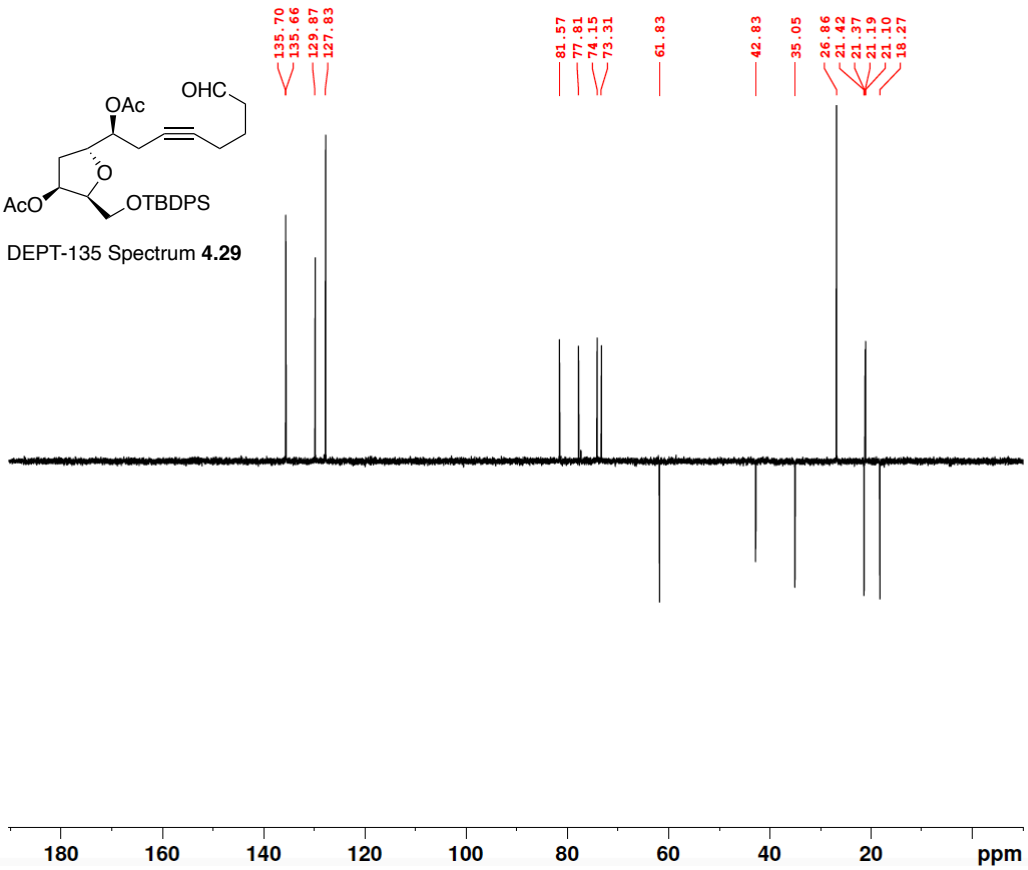

Figure A.32 DEPT-135 (100 MHz, $CDCl_3$) of **4.29**.

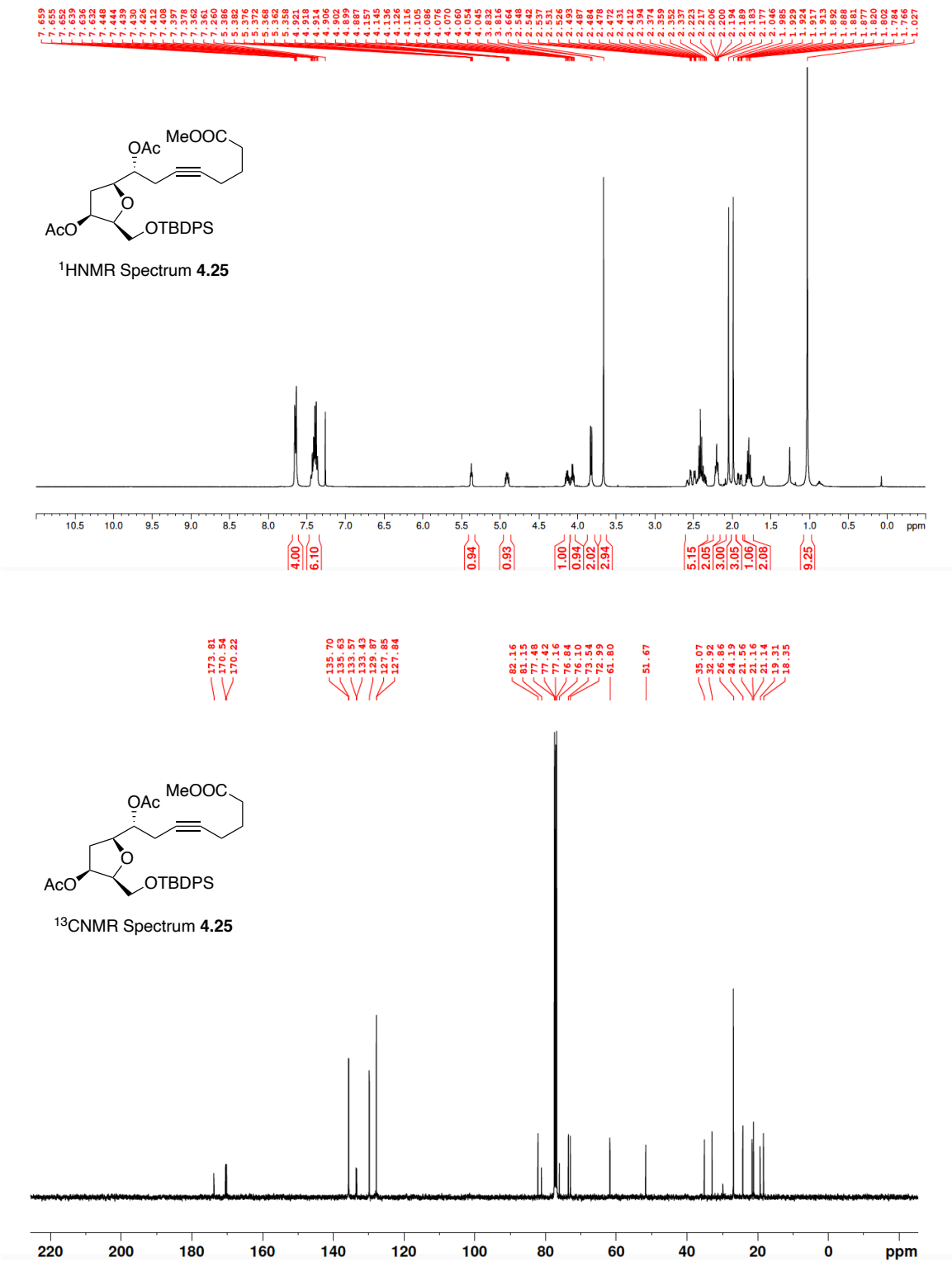

Figure A.33 ^{1}H NMR (400 MHz, $CDCl_3$) and ^{13}C NMR (100 MHz, $CDCl_3$) of **4.25**.

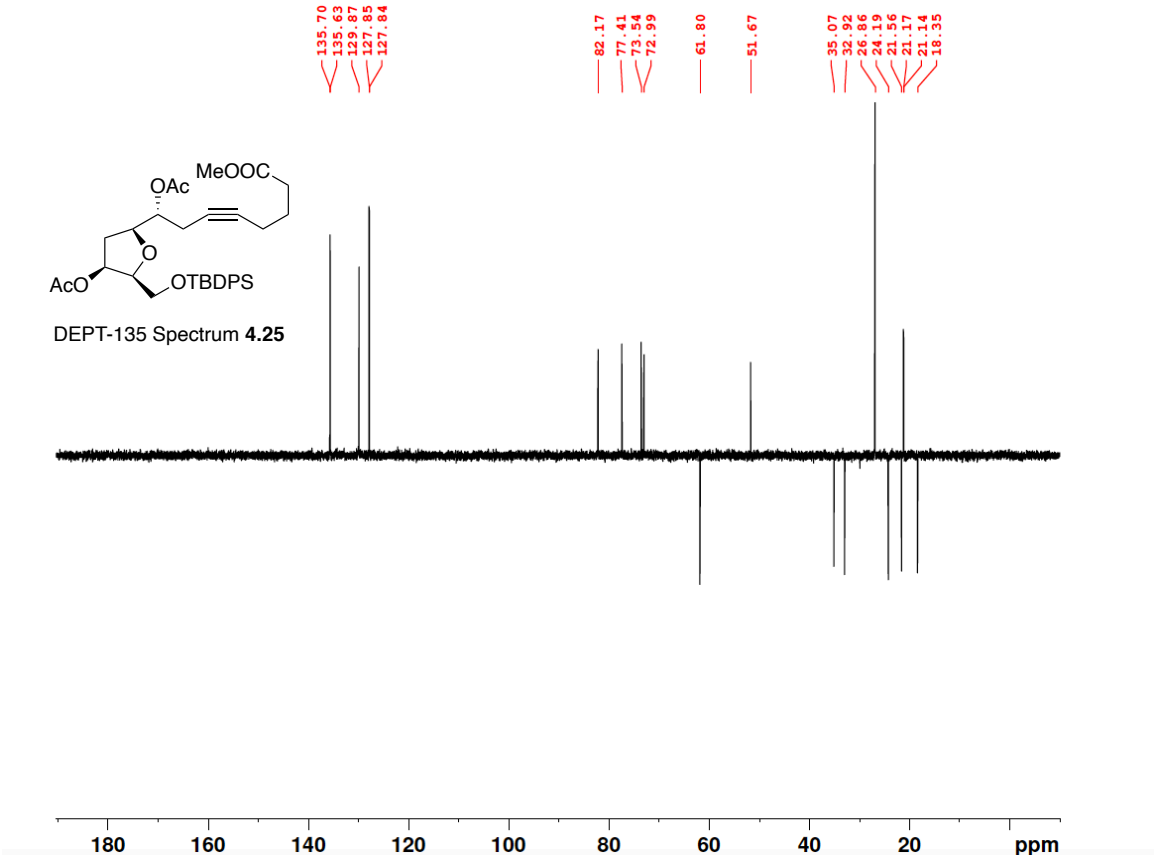

Figure A.34 DEPT-135 (100 MHz, $CDCl_3$) of **4.25**.

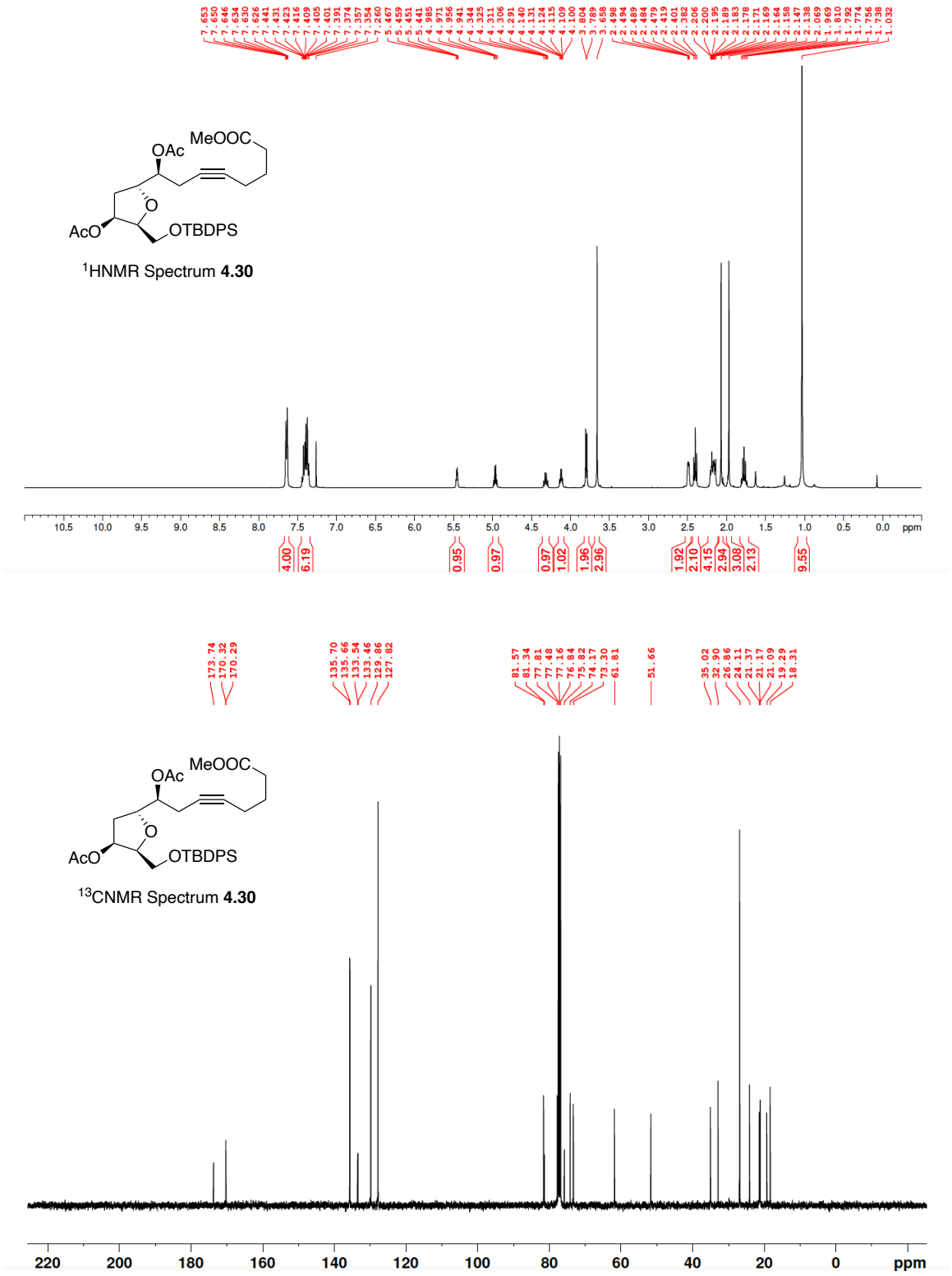

Figure A.35 ^{1}H NMR (400 MHz, $CDCl_3$) and ^{13}C NMR (100 MHz, $CDCl_3$) of **4.30**.

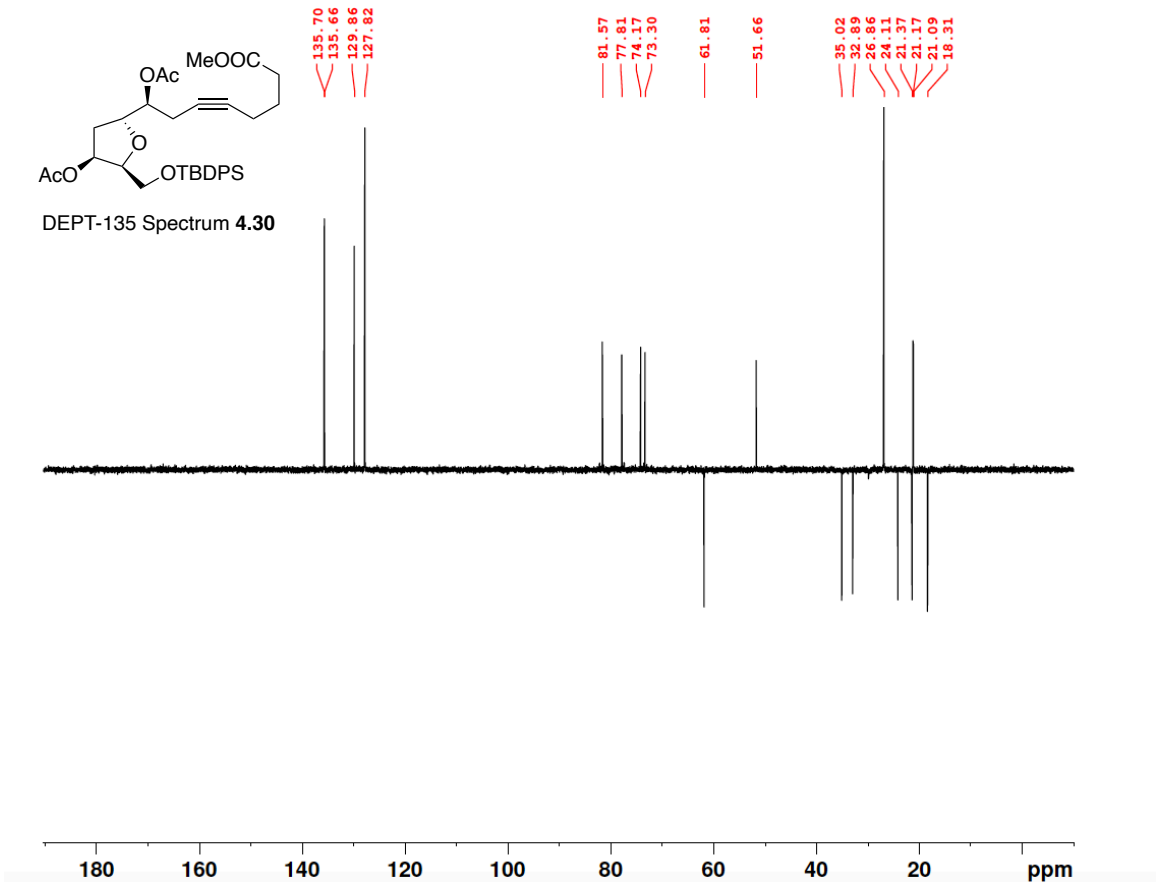

Figure A.36 DEPT-135 (100 MHz, $CDCl_3$) of **4.30**.

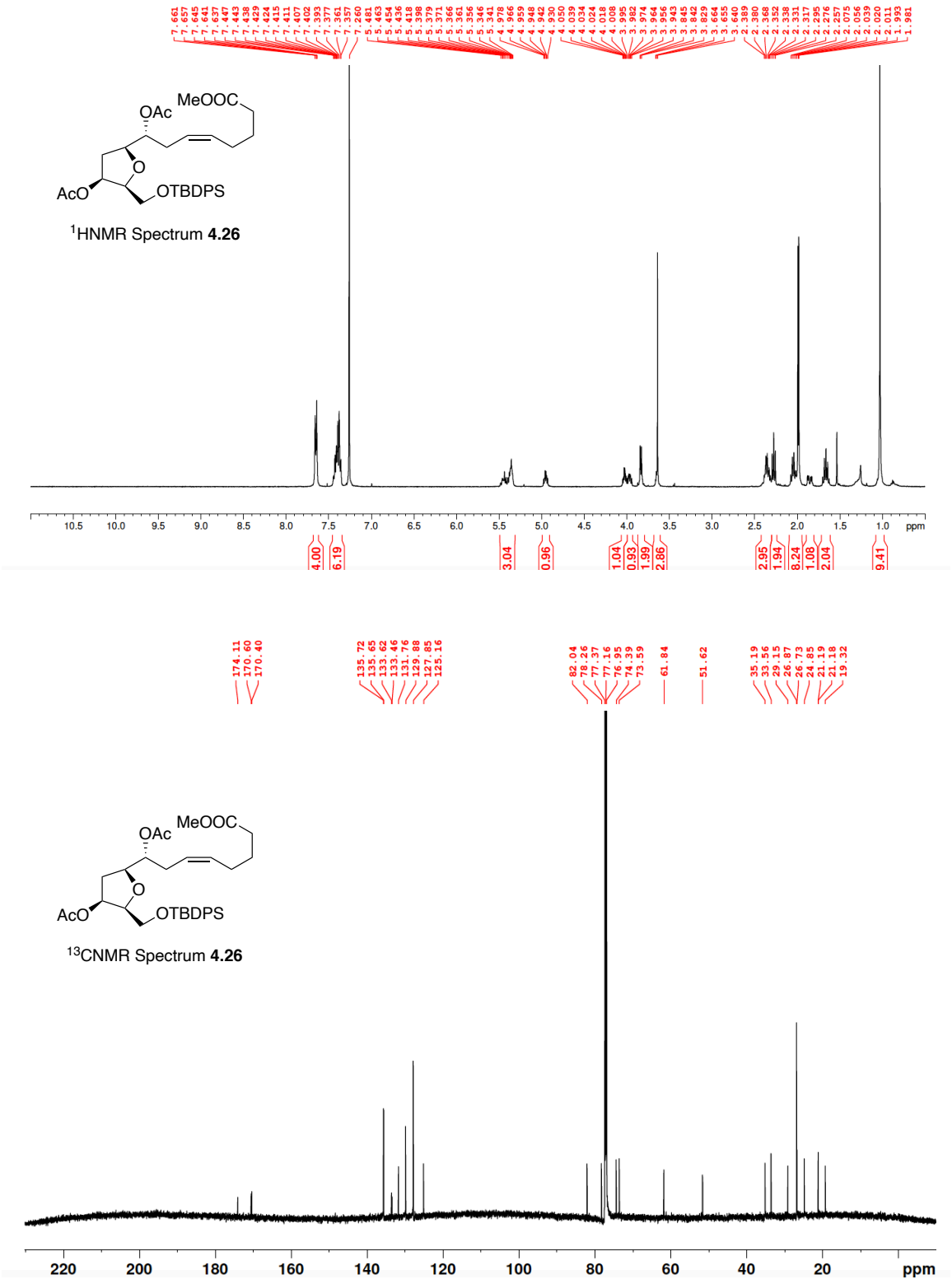

Figure A.37 ^{1}H NMR (400 MHz, $CDCl_3$) and ^{13}C NMR (100 MHz, $CDCl_3$) of **4.26**.

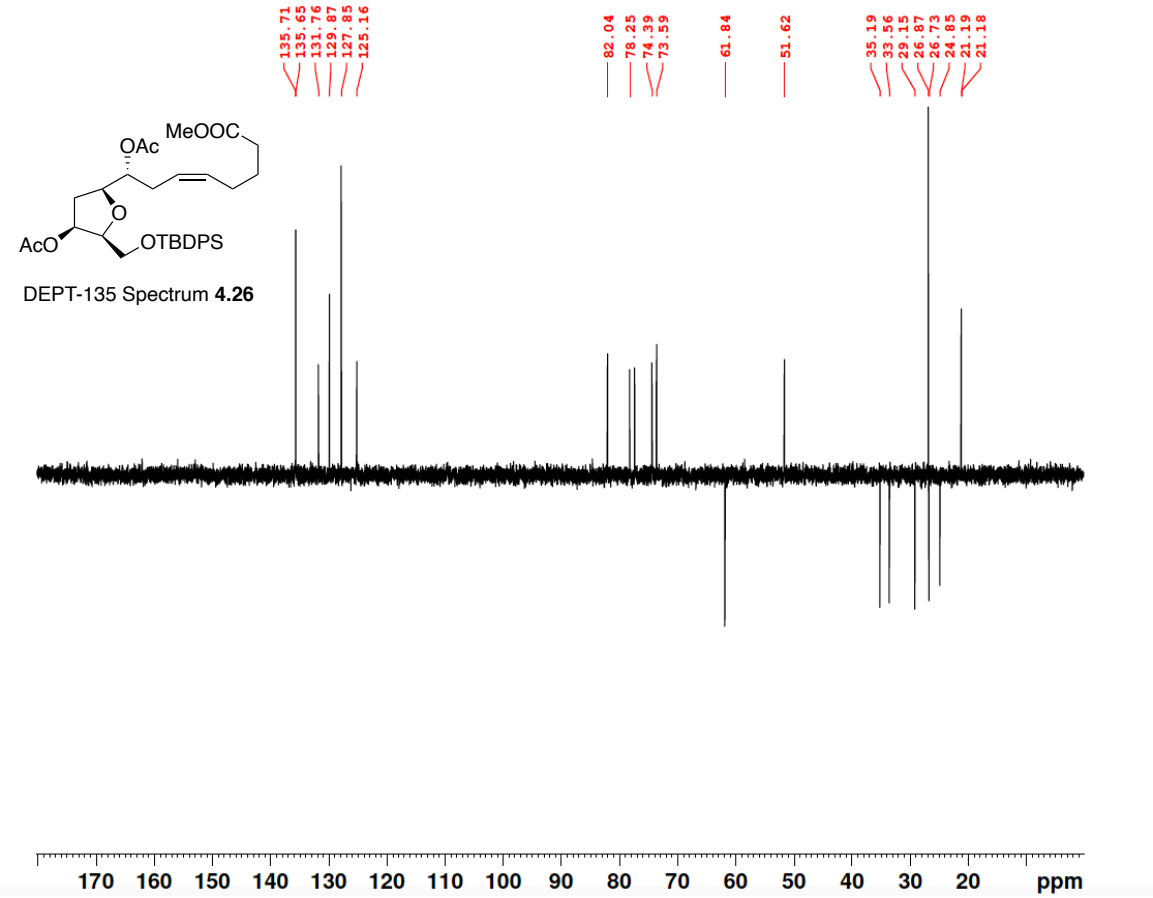

Figure A.38 DEPT-135 (100 MHz, $CDCl_3$) of **4.26**.

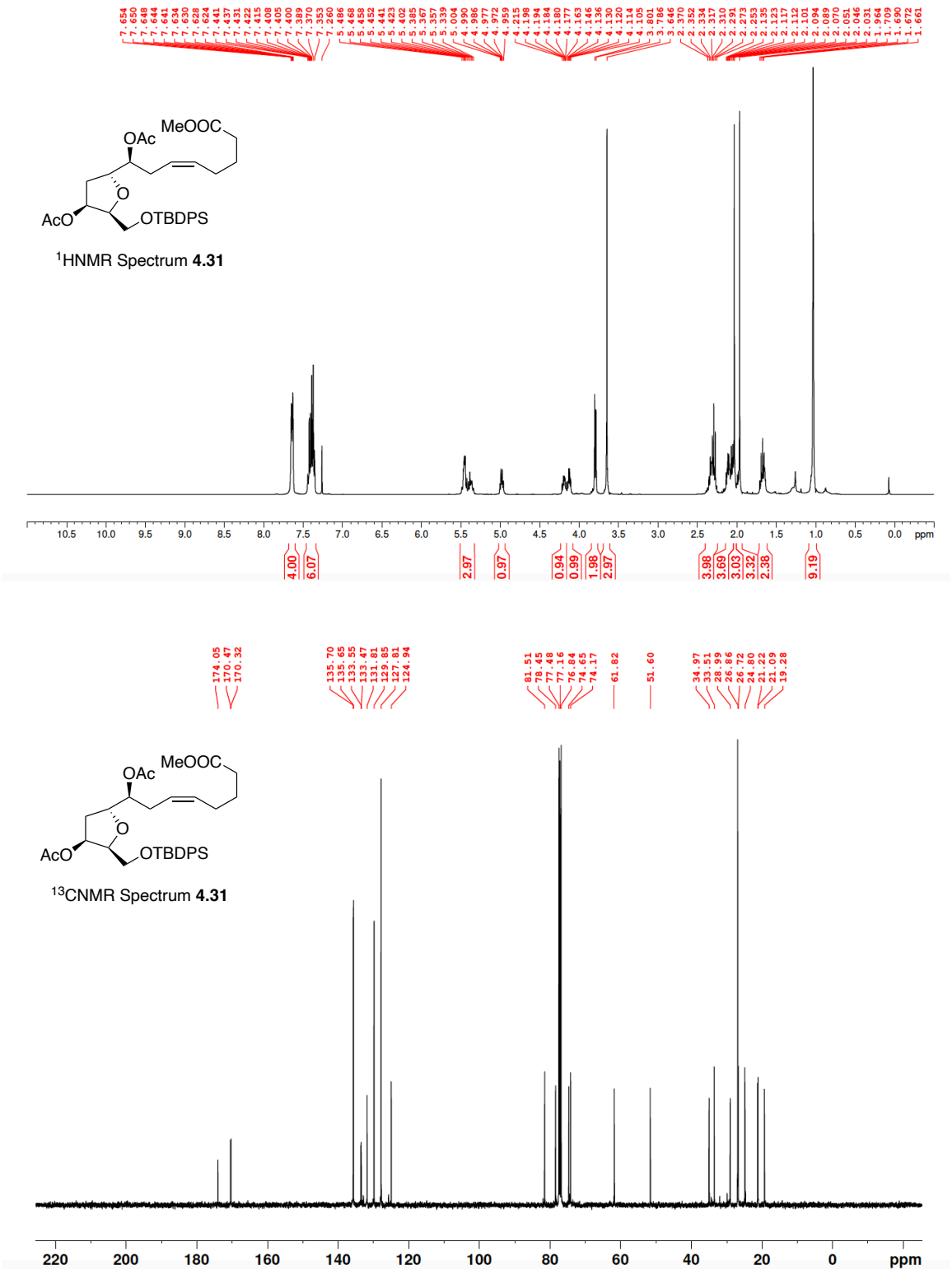

Figure A.39 ^{1}H NMR (400 MHz, $CDCl_3$) and ^{13}C NMR (100 MHz, $CDCl_3$) of **4.31**.

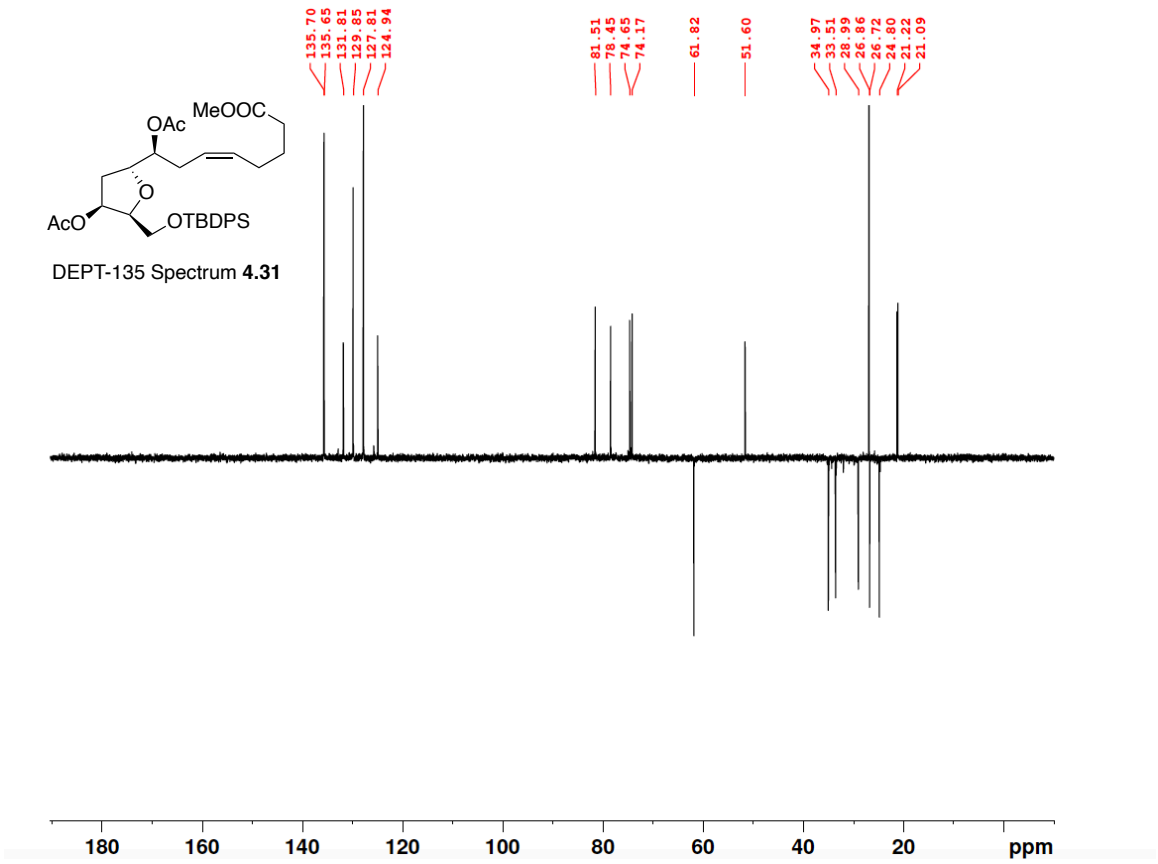

Figure A.40 DEPT-135 (100 MHz, $CDCl_3$) of **4.31**.

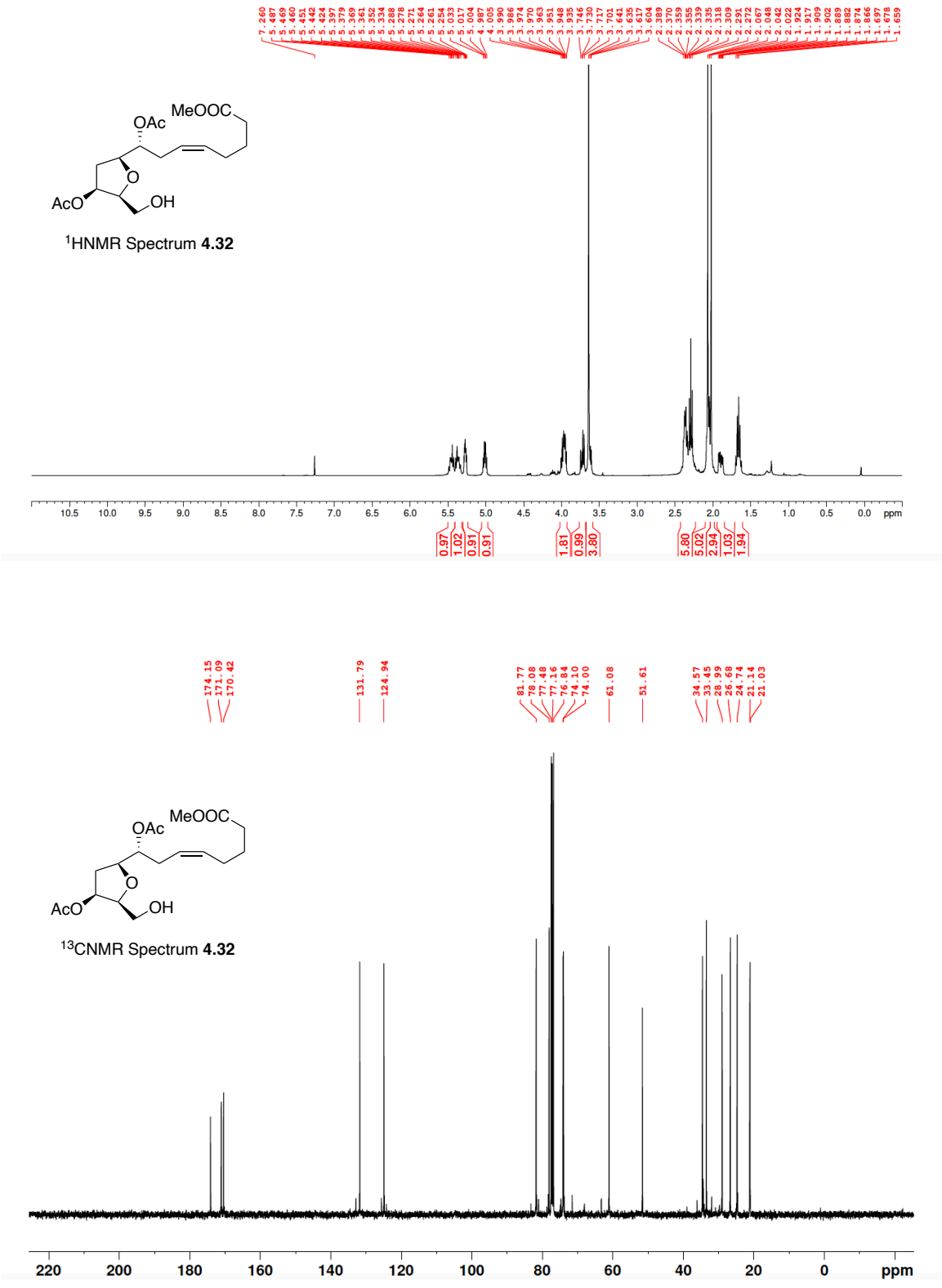

Figure A.41 ^{1}H NMR (400 MHz, $CDCl_3$) and ^{13}C NMR (100 MHz, $CDCl_3$) of **4.32**.

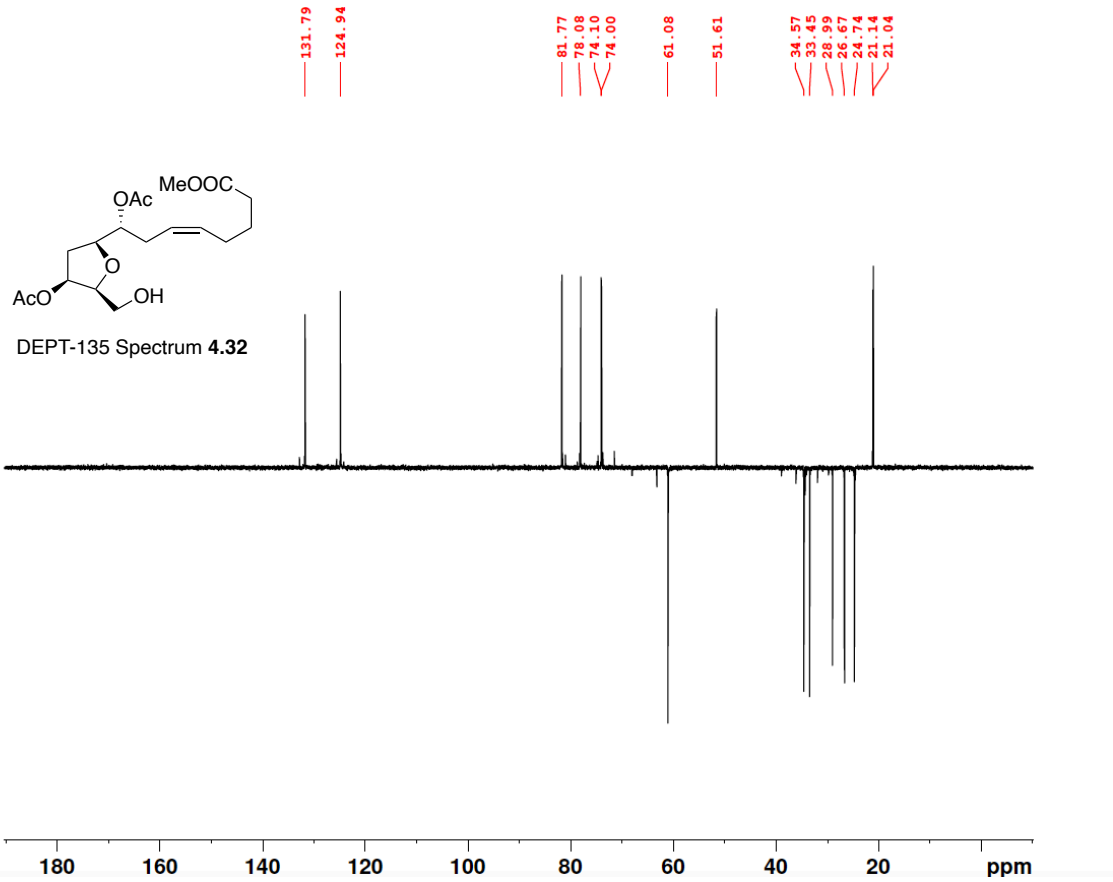

Figure A.42 DEPT-135 (100 MHz, $CDCl_3$) of **4.32**.

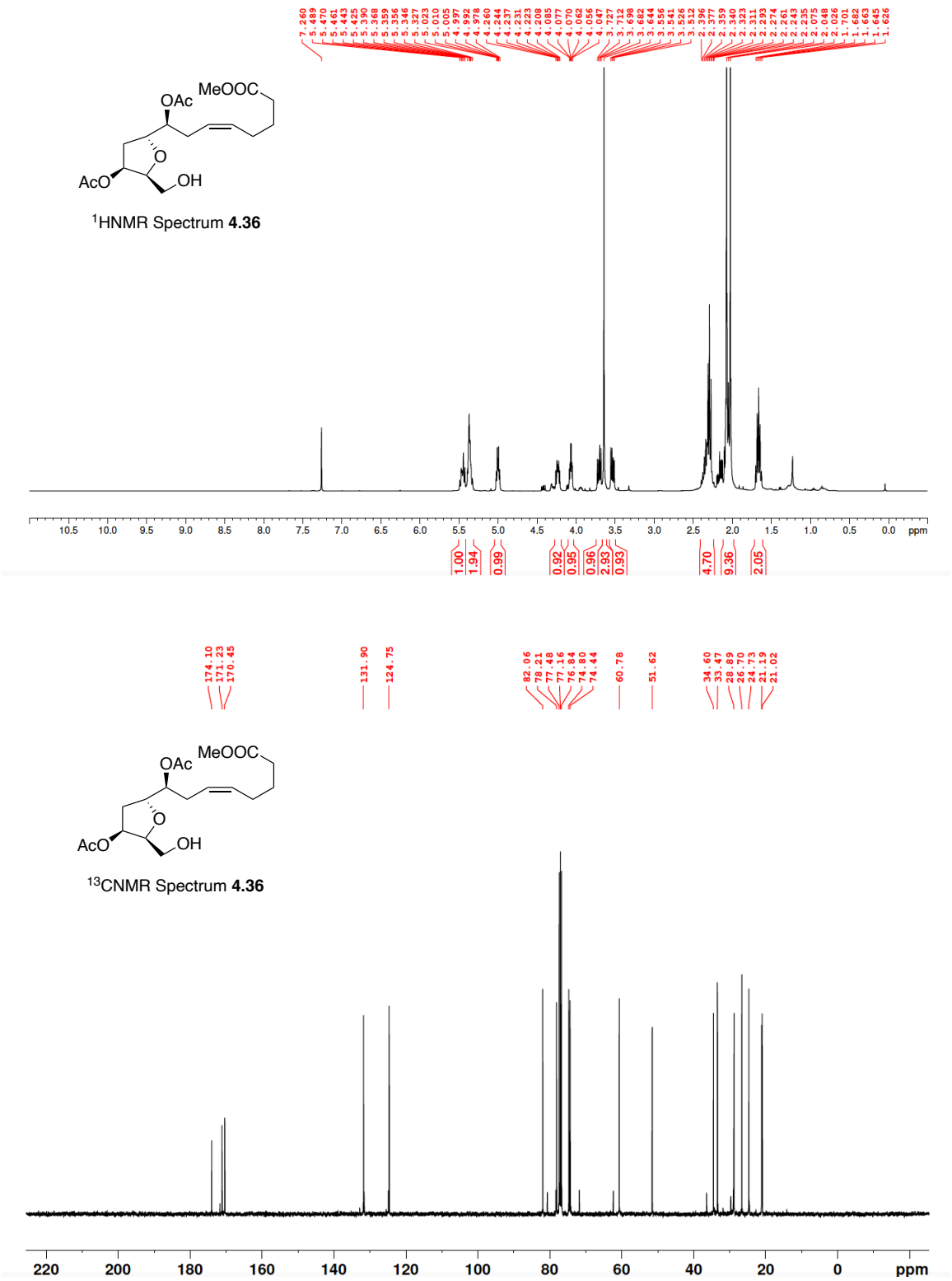

Figure A.43 ^{1}H NMR (400 MHz, $CDCl_3$) and ^{13}C NMR (100 MHz, $CDCl_3$) of **4.36**.

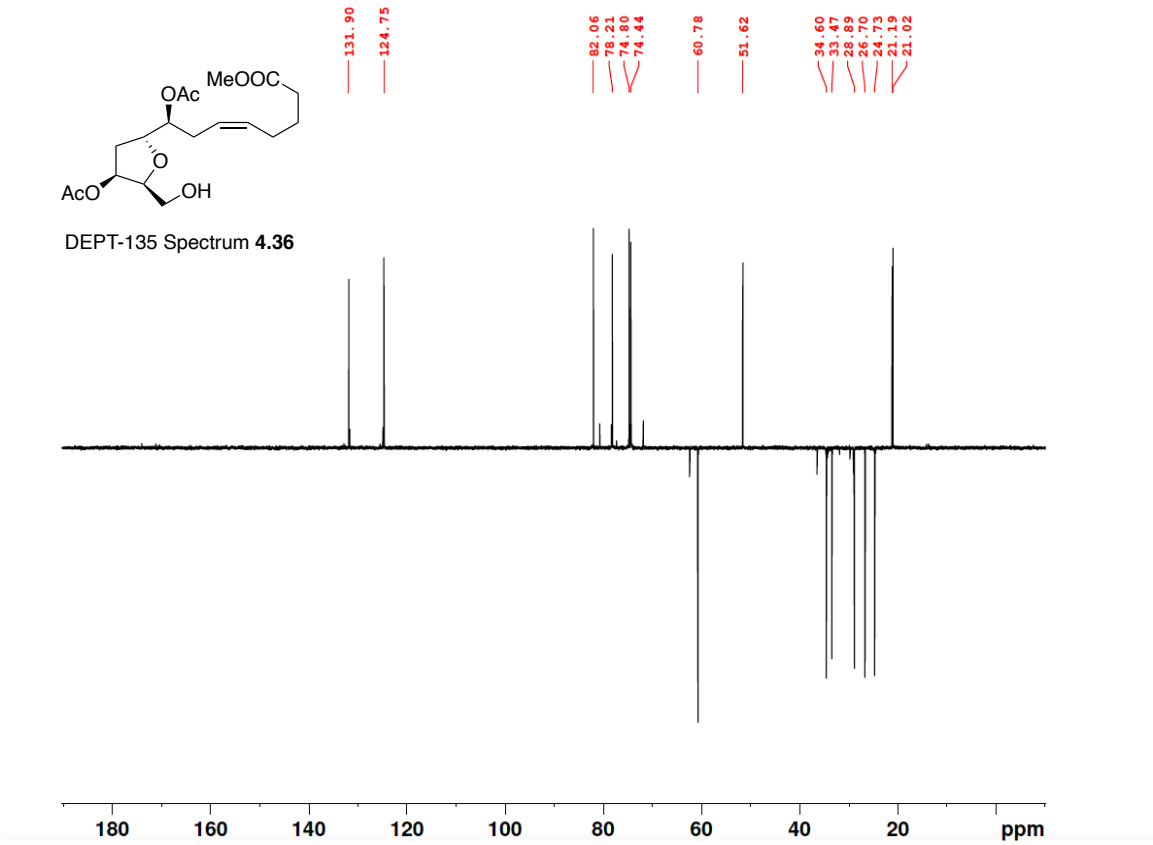

Figure A.44 DEPT-135 (100 MHz, $CDCl_3$) of **4.36**.

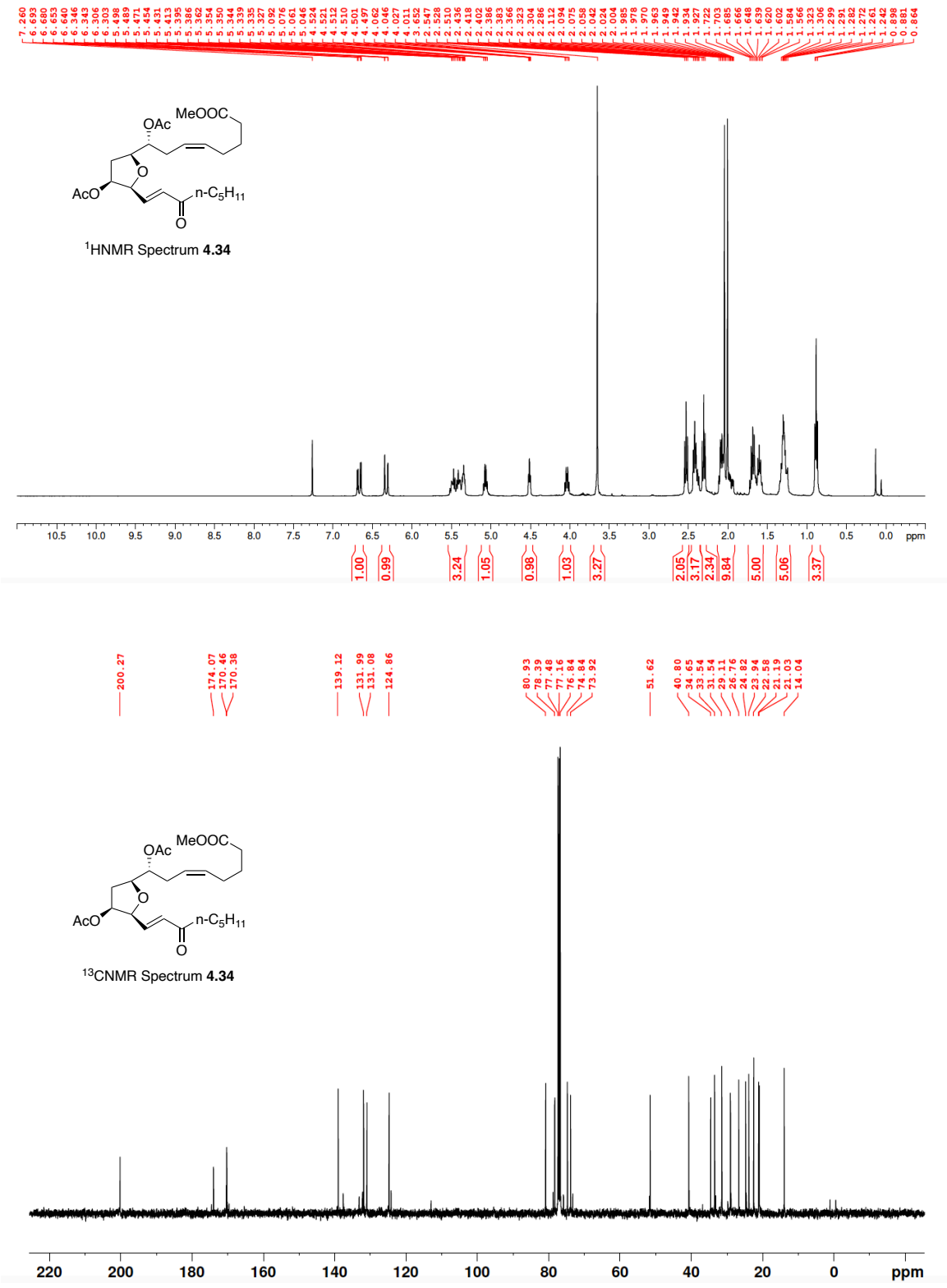

Figure A.45 ^{1}H NMR (400 MHz, $CDCl_3$) and ^{13}C NMR (100 MHz, $CDCl_3$) of **4.34**.

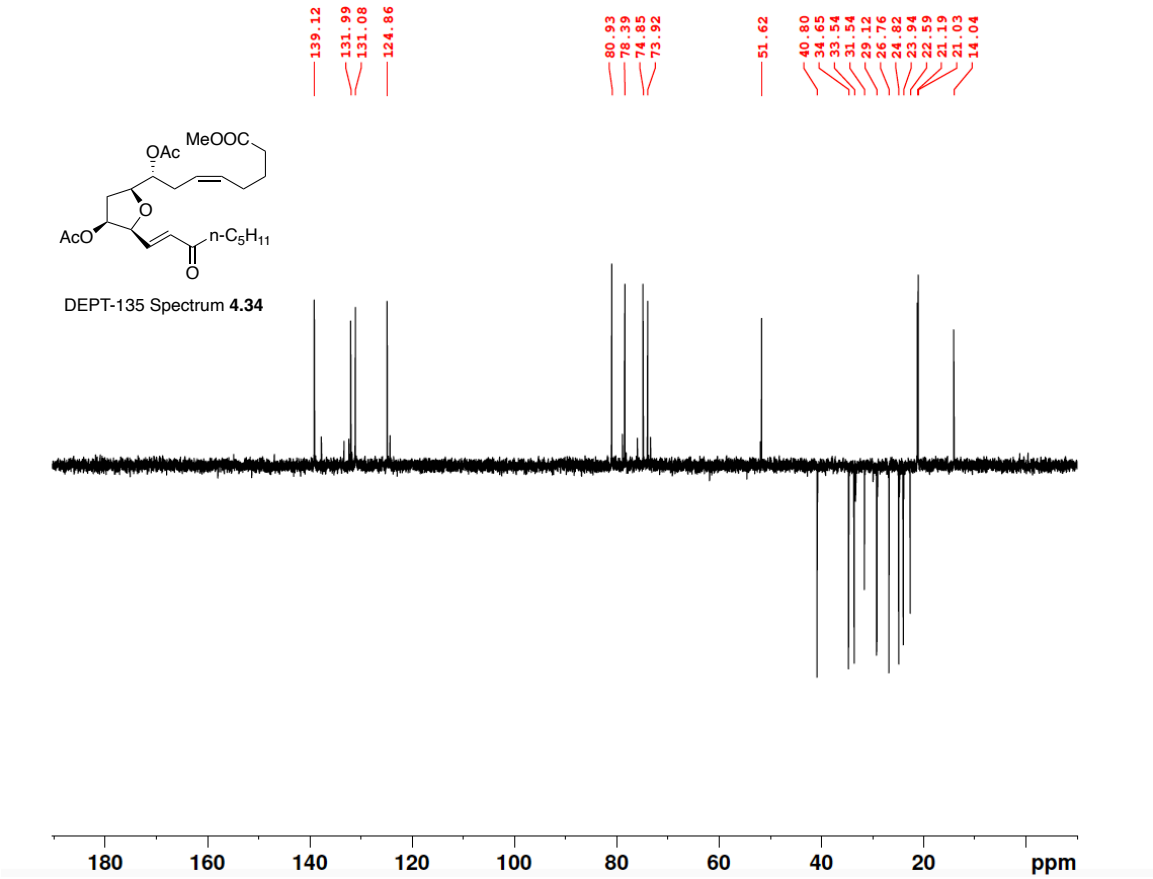

Figure A.46 DEPT-135 (100 MHz, $CDCl_3$) of **4.34**.

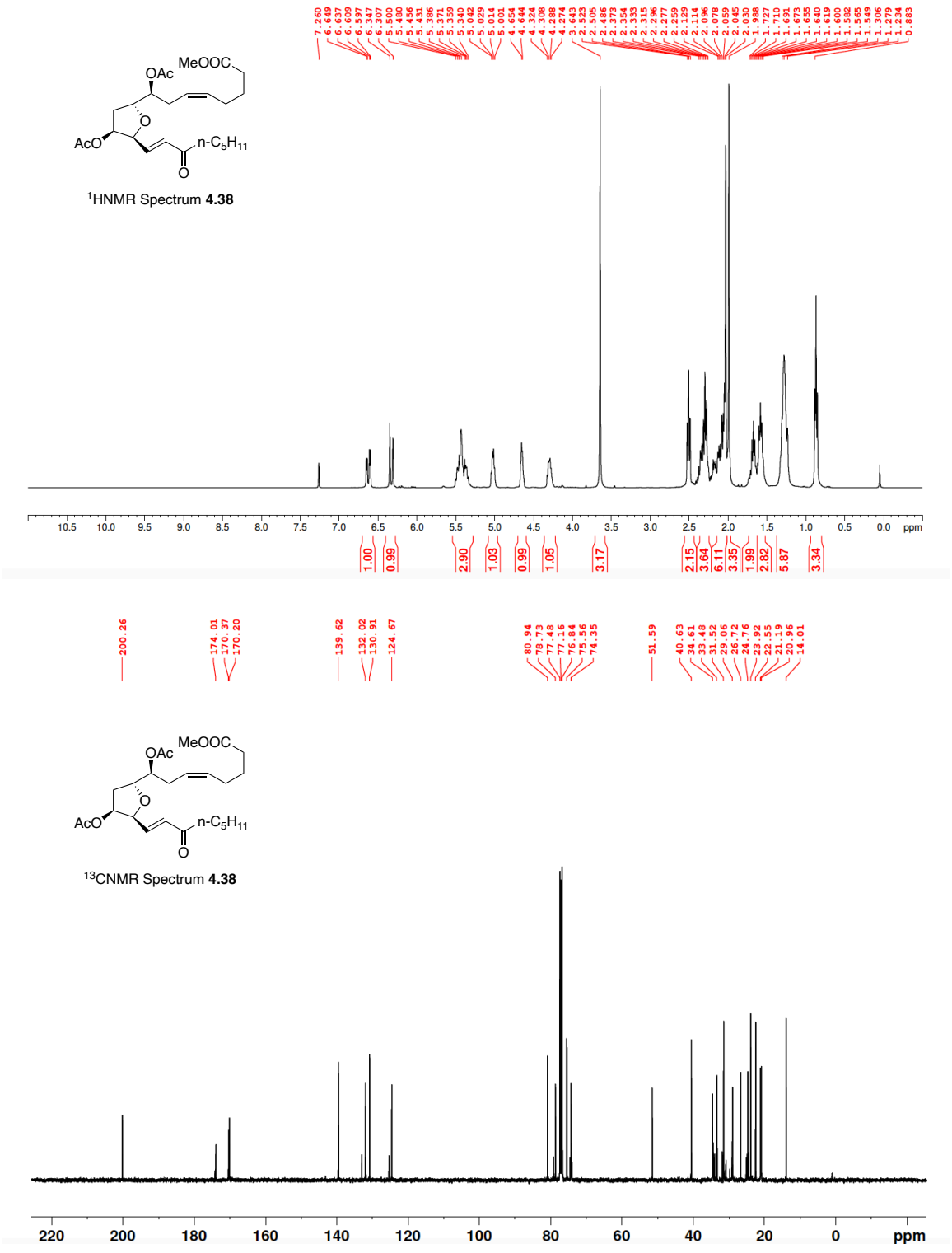

Figure A.47 ^{1}H NMR (400 MHz, $CDCl_3$) and ^{13}C NMR (100 MHz, $CDCl_3$) of **4.38**.

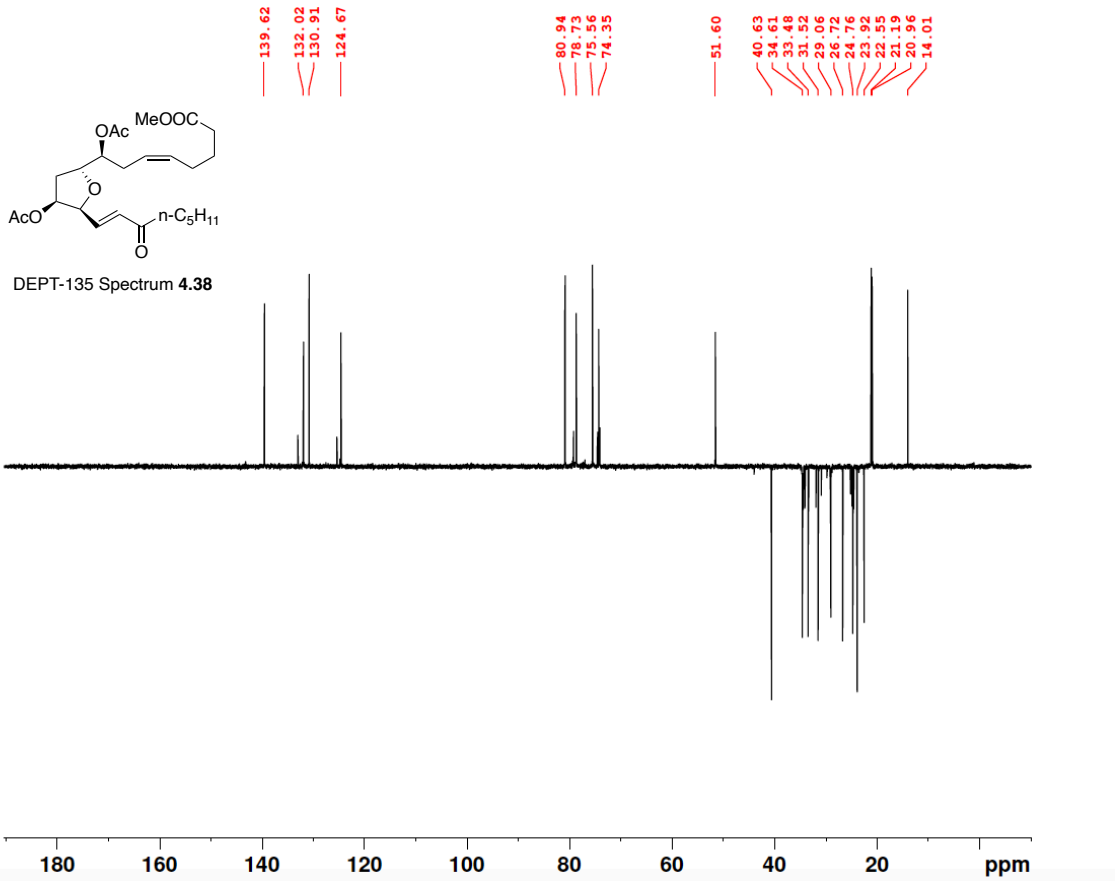

Figure A.48 DEPT-135 (100 MHz, $CDCl_3$) of **4.38**.

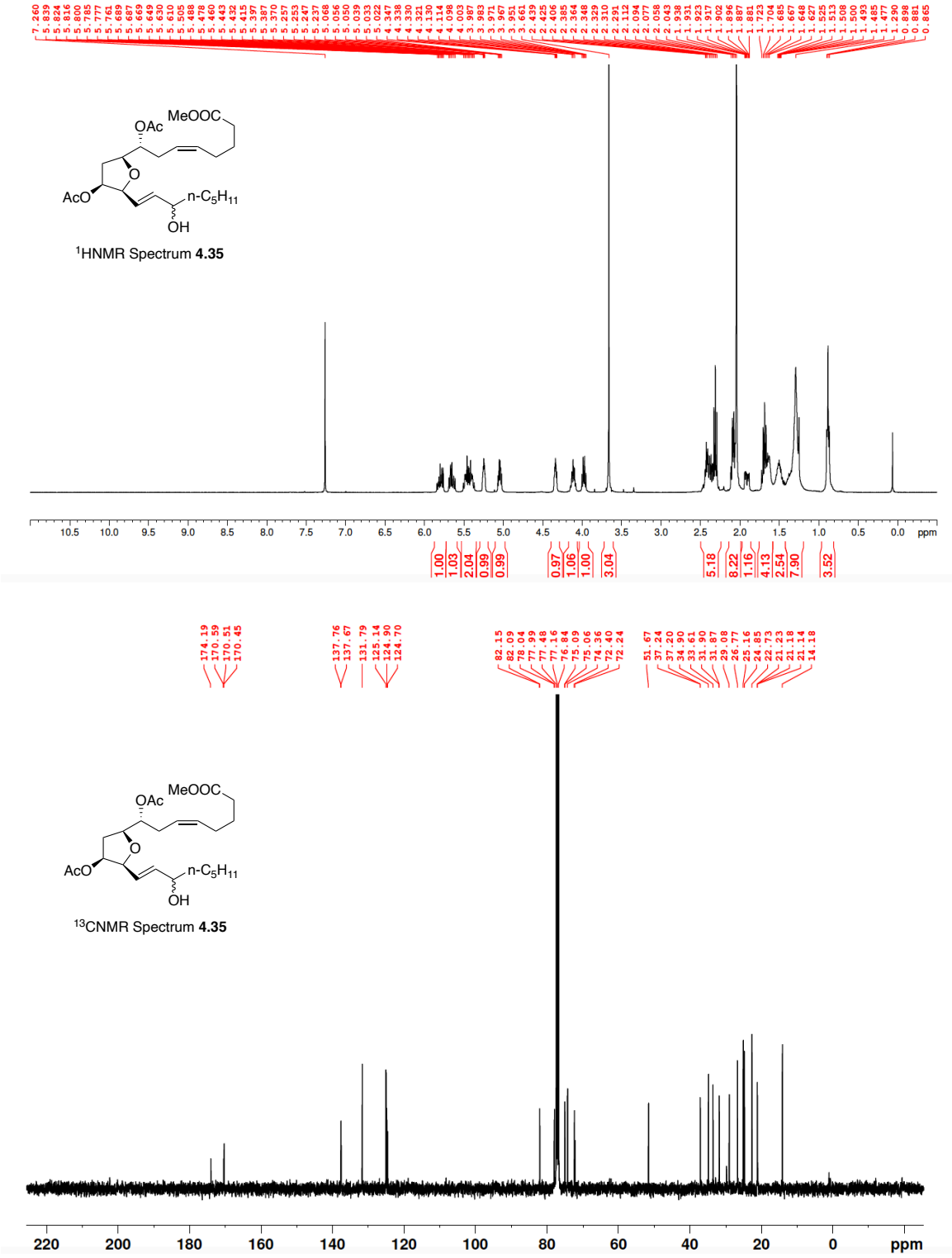

Figure A.49 ^{1}H NMR (400 MHz, $CDCl_3$) and ^{13}C NMR (100 MHz, $CDCl_3$) of **4.35**.

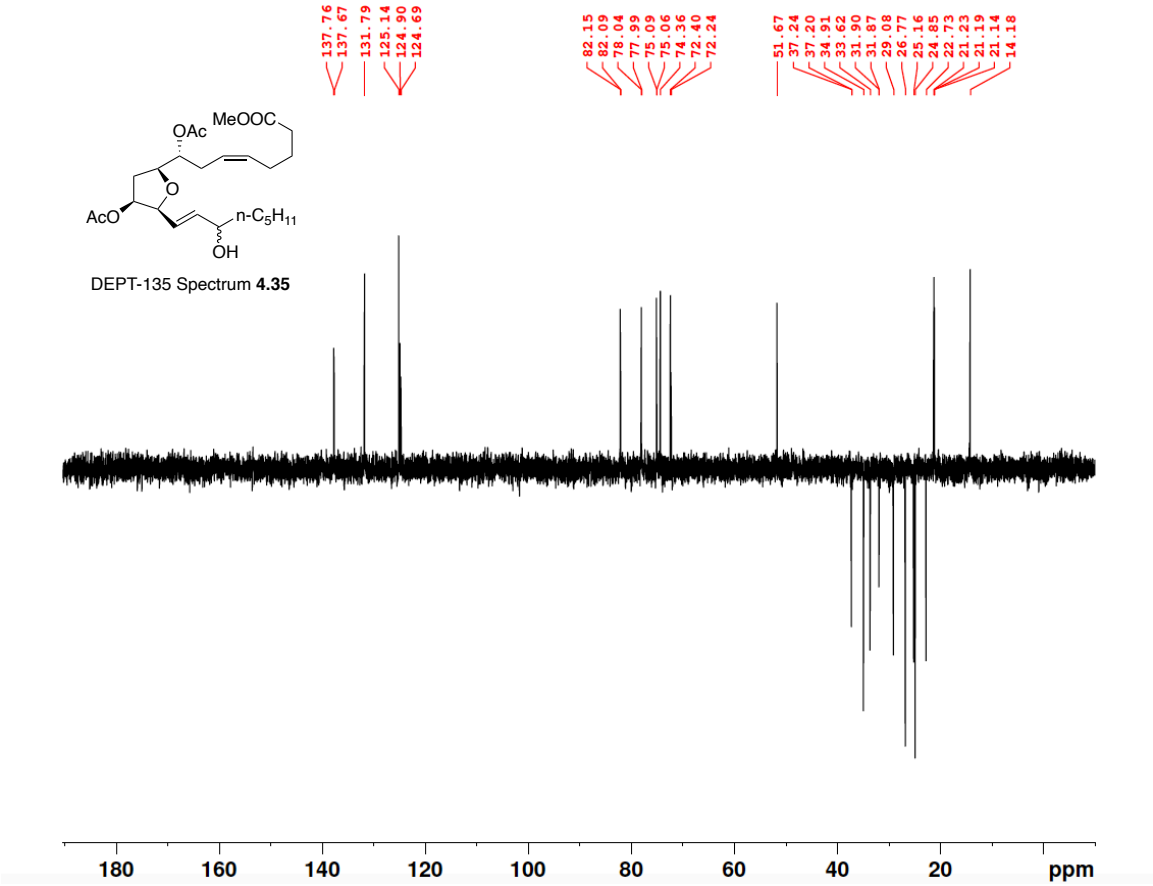

Figure A.50 DEPT-135 (100 MHz, $CDCl_3$) of **4.35**.

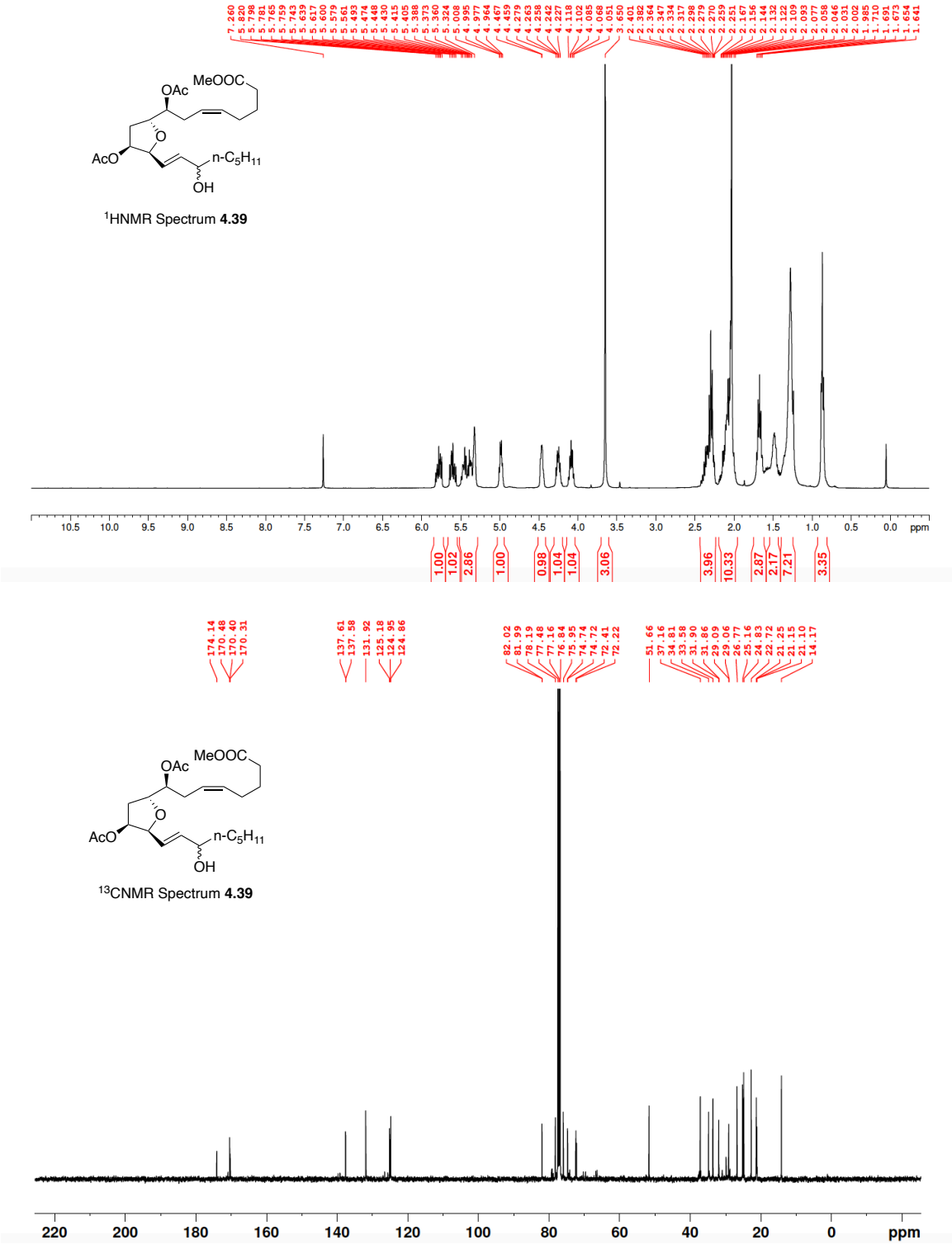

Figure A.51 ^{1}H NMR (400 MHz, $CDCl_3$) and ^{13}C NMR (100 MHz, $CDCl_3$) of **4.39**.

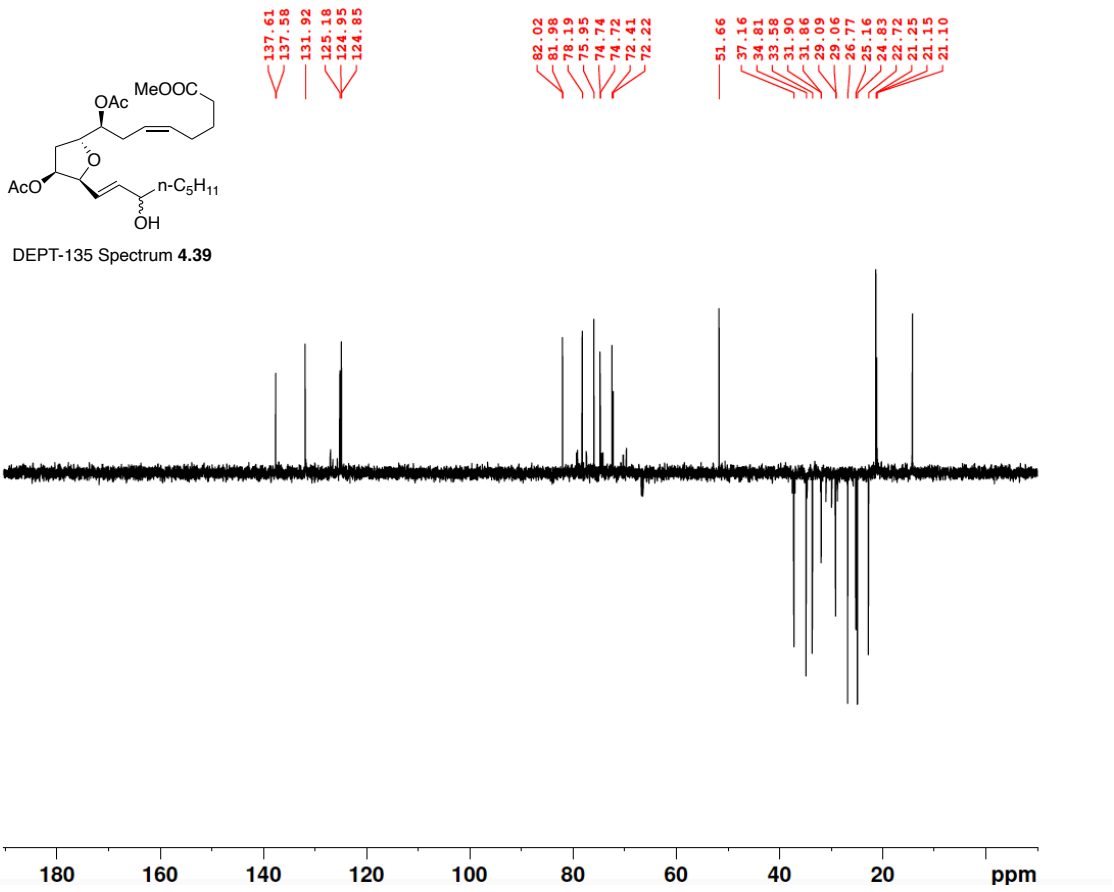

Figure A.52 DEPT-135 (100 MHz, $CDCl_3$) of **4.39**.

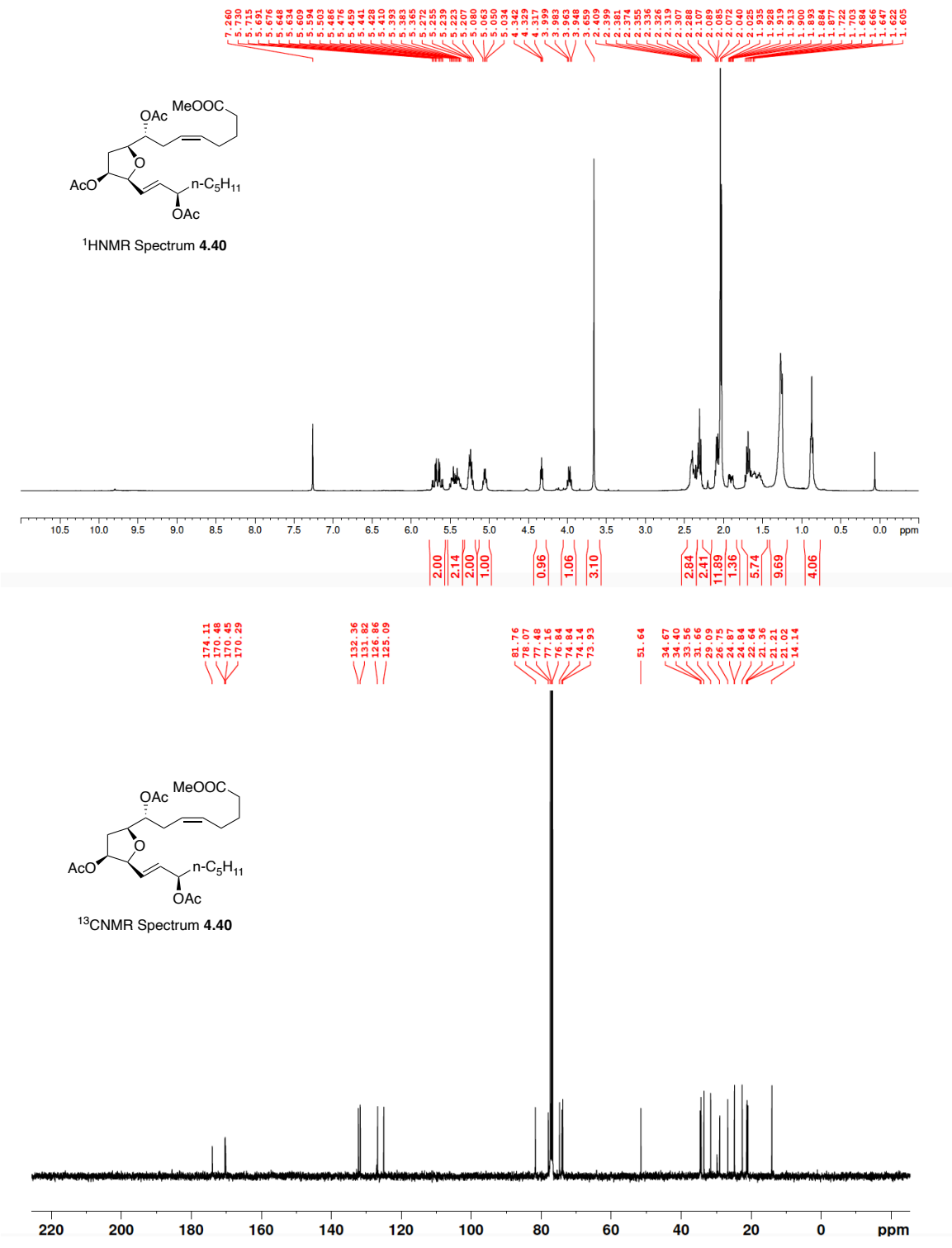

Figure A.53 ^{1}H NMR (400 MHz, $CDCl_3$) and ^{13}C NMR (100 MHz, $CDCl_3$) of **4.40**.

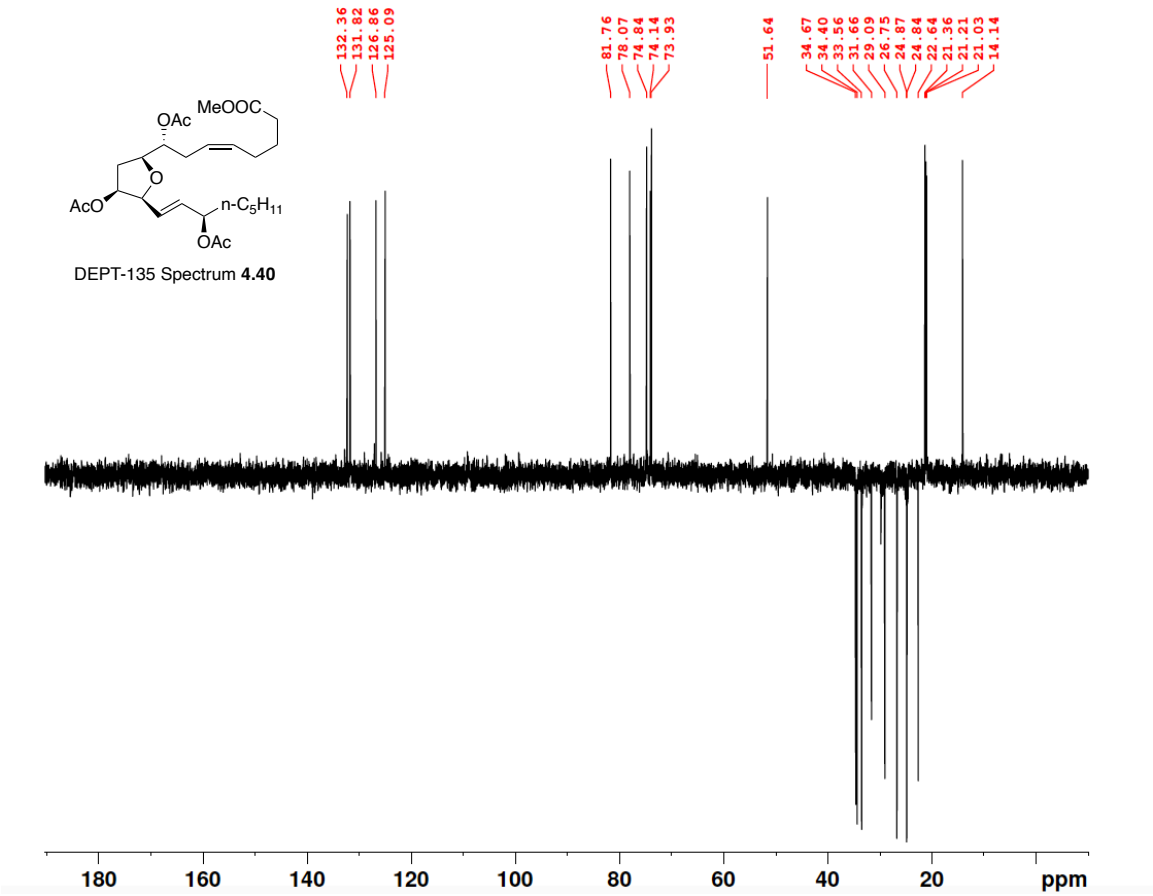

Figure A.54 DEPT-135 (100 MHz, $CDCl_3$) of **4.40**.

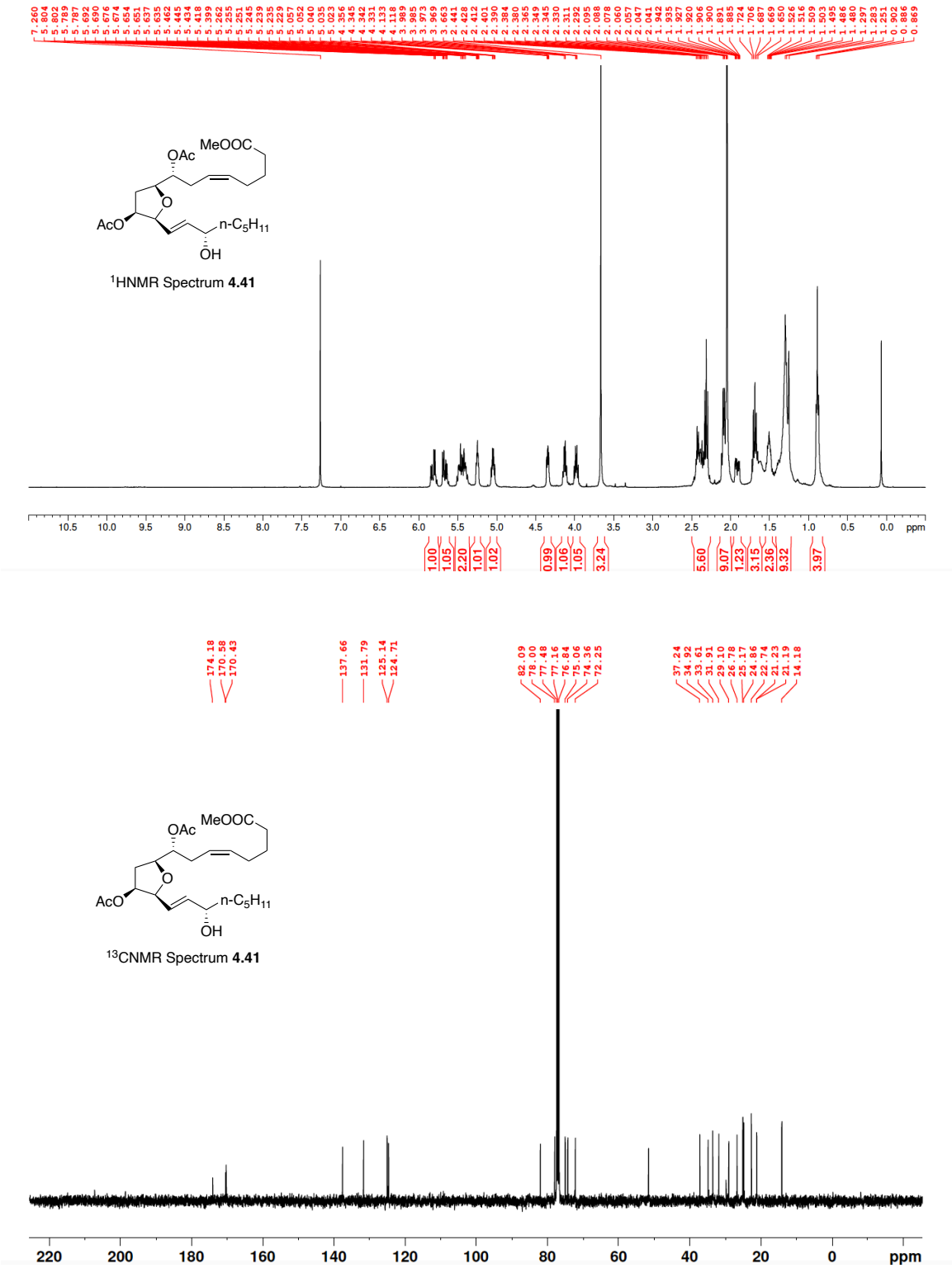

Figure A.55 ^{1}H NMR (400 MHz, $CDCl_3$) and ^{13}C NMR (100 MHz, $CDCl_3$) of **4.41**.

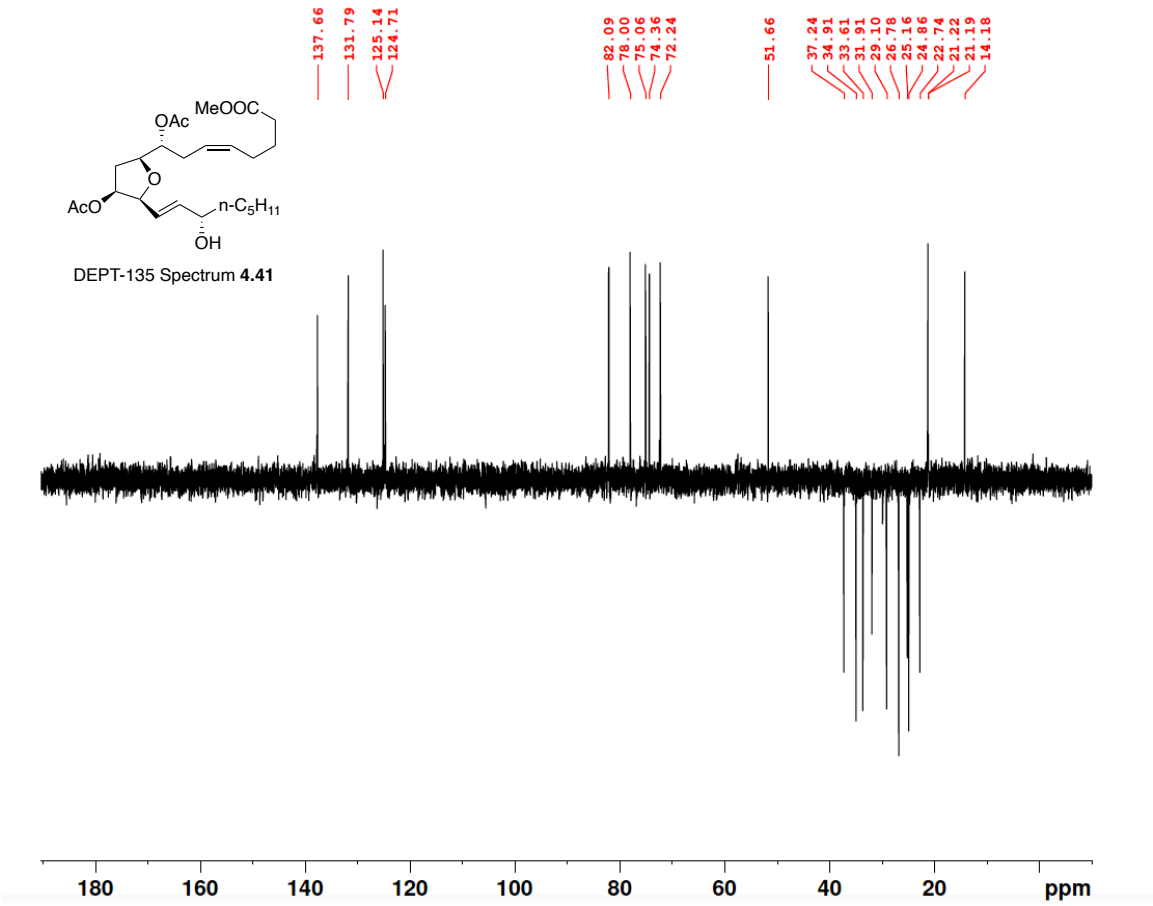

Figure A.56 DEPT-135 (100 MHz, $CDCl_3$) of **4.41**.

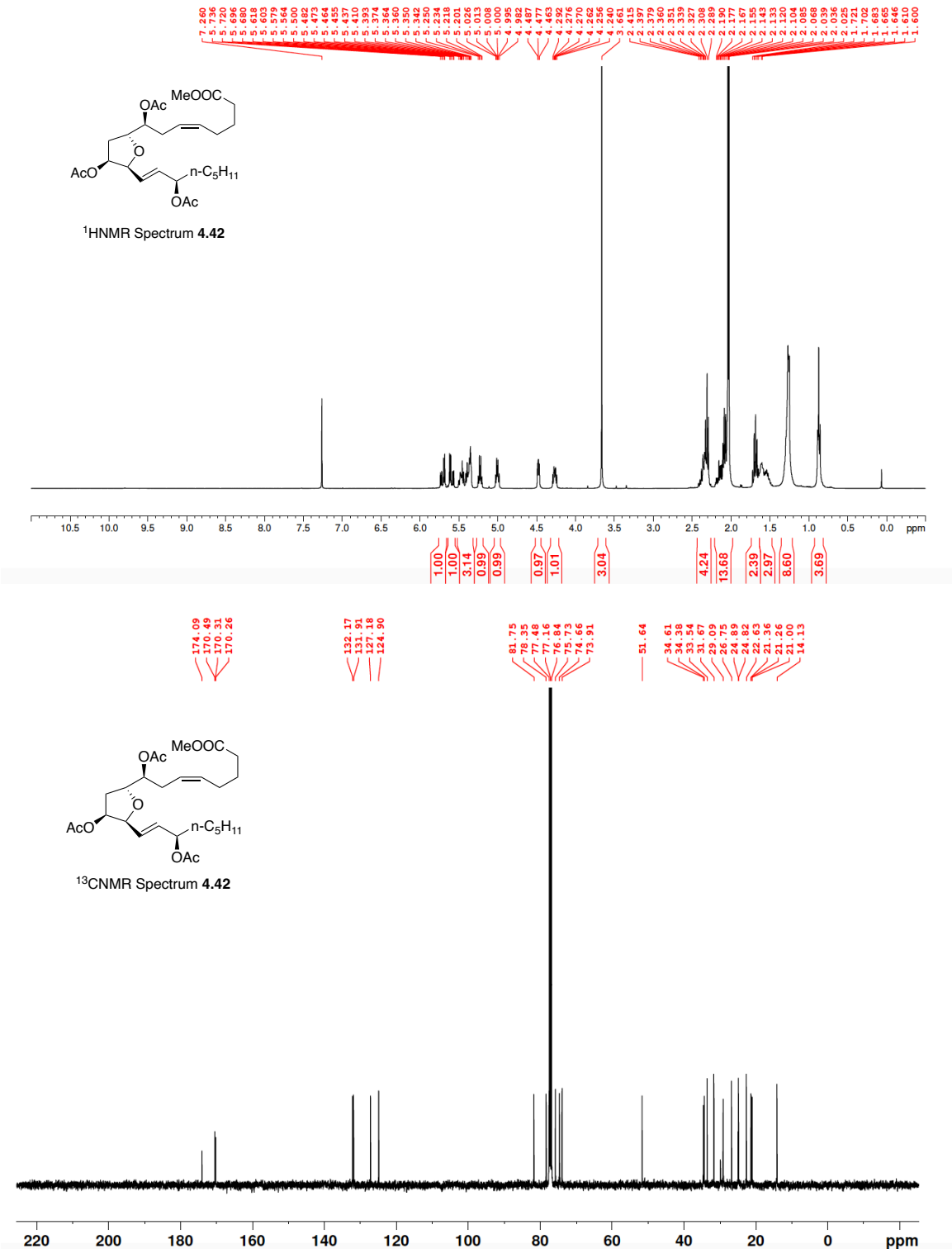

Figure A.57 ^{1}H NMR (400 MHz, $CDCl_3$) and ^{13}C NMR (100 MHz, $CDCl_3$) of **4.42**.

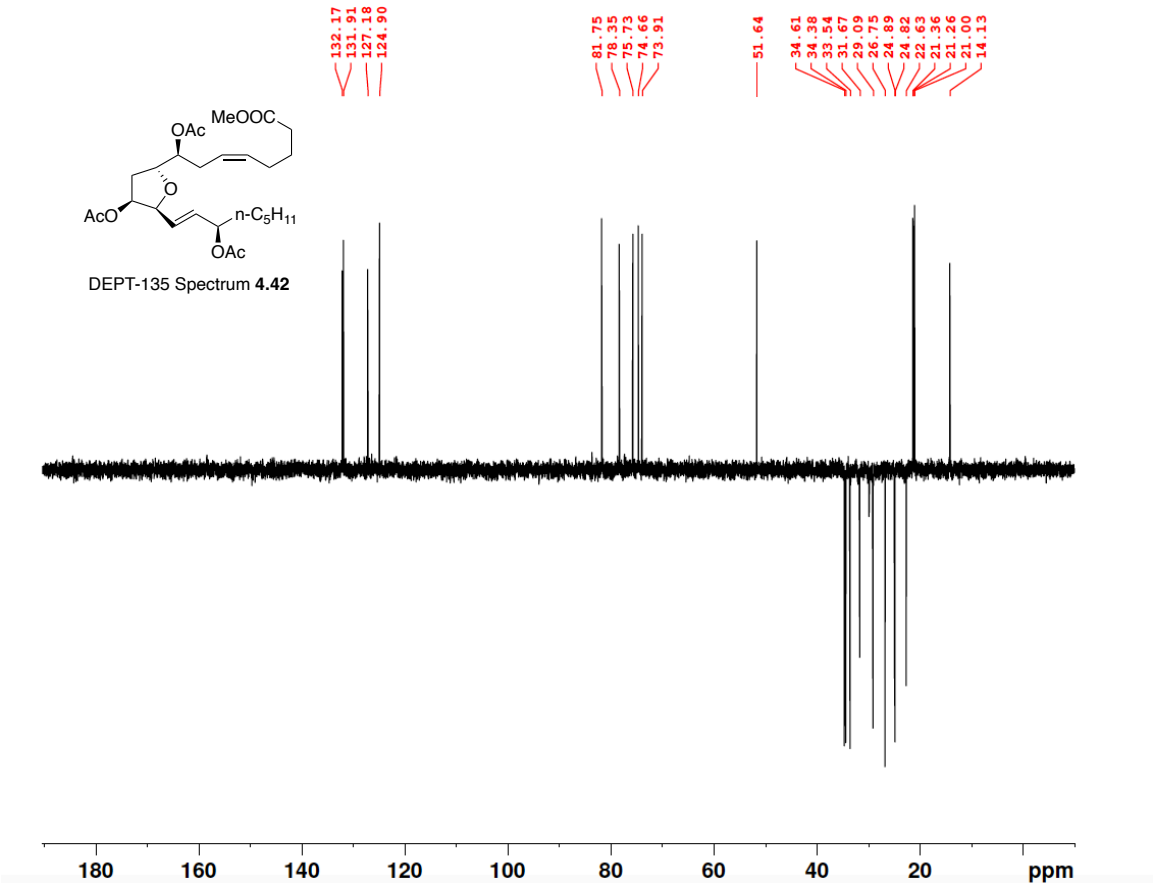

Figure A.58 DEPT-135 (100 MHz, $CDCl_3$) of **4.42**.

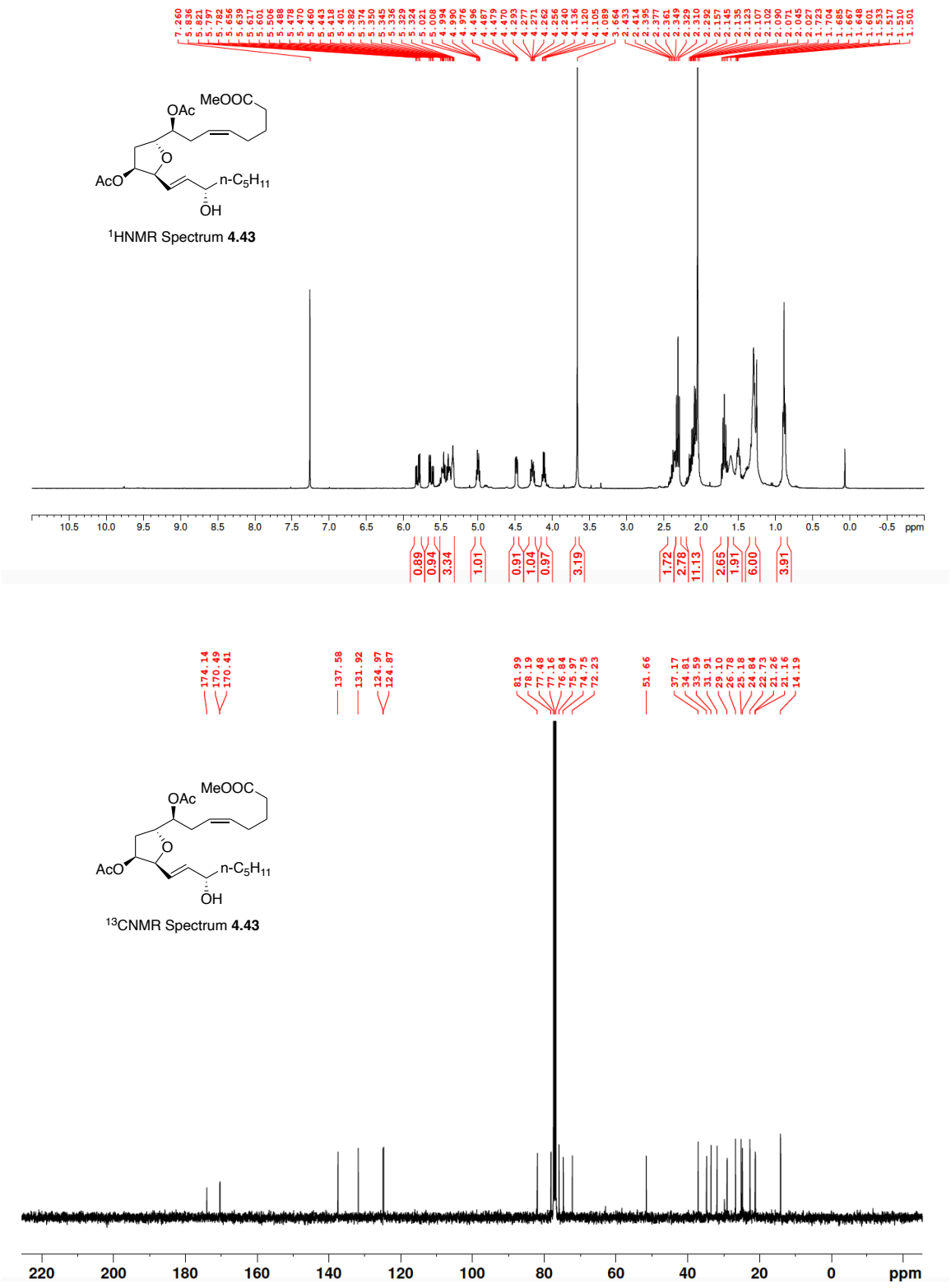

Figure A.59 ^{1}H NMR (400 MHz, $CDCl_3$) and ^{13}C NMR (100 MHz, $CDCl_3$) of **4.43**.

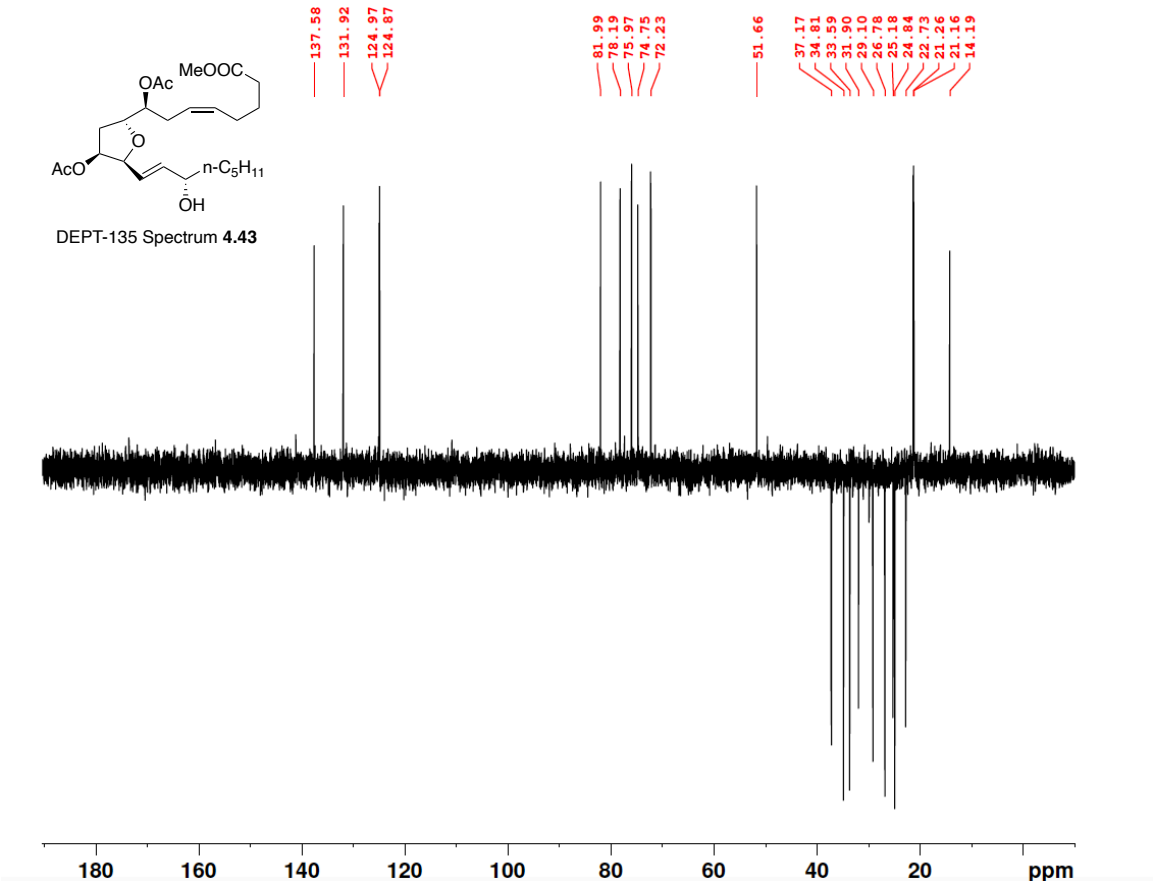

Figure A.60 DEPT-135 (100 MHz, $CDCl_3$) of **4.43**.

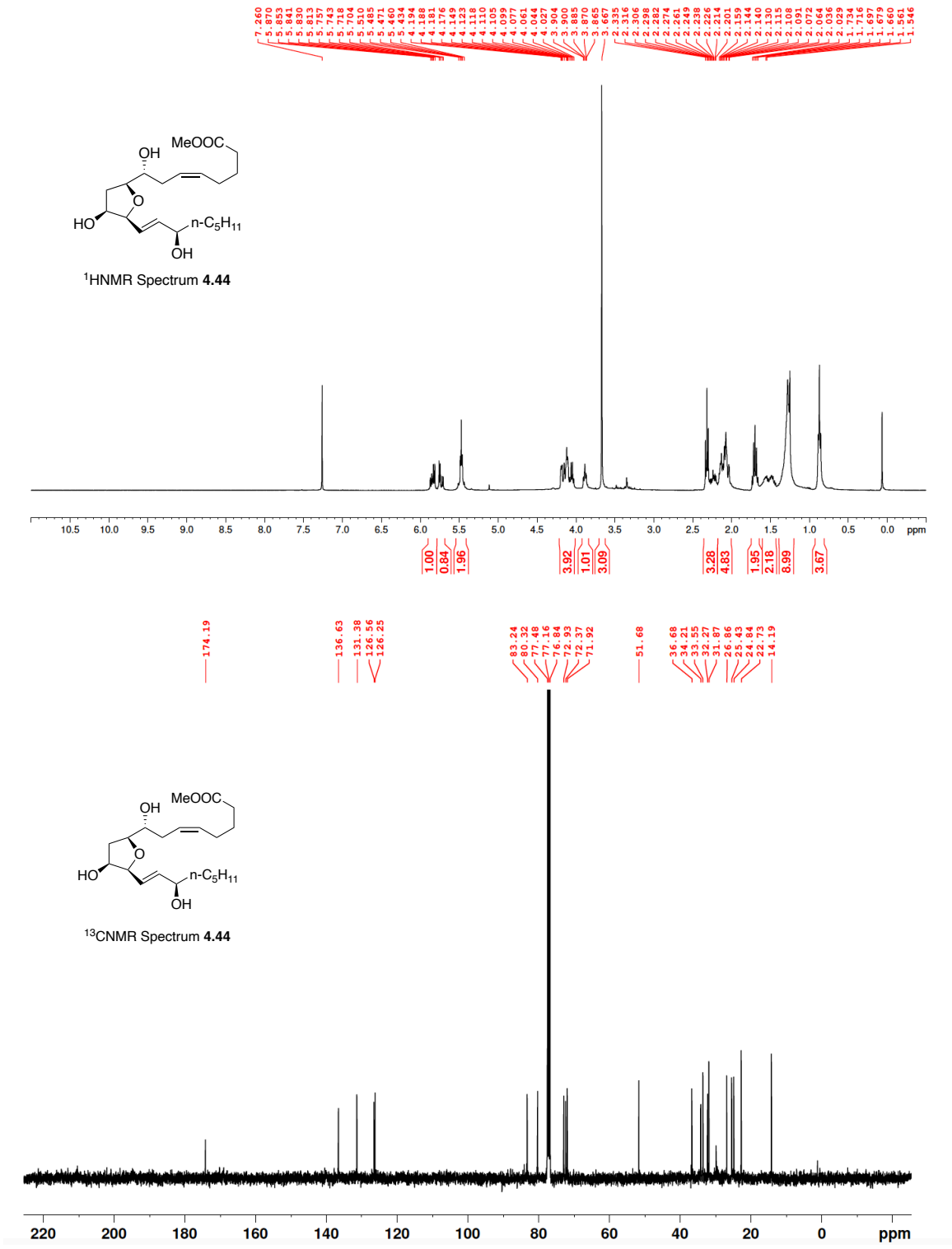

Figure A.61 ^{1}H NMR (400 MHz, $CDCl_3$) and ^{13}C NMR (100 MHz, $CDCl_3$) of **4.44**.

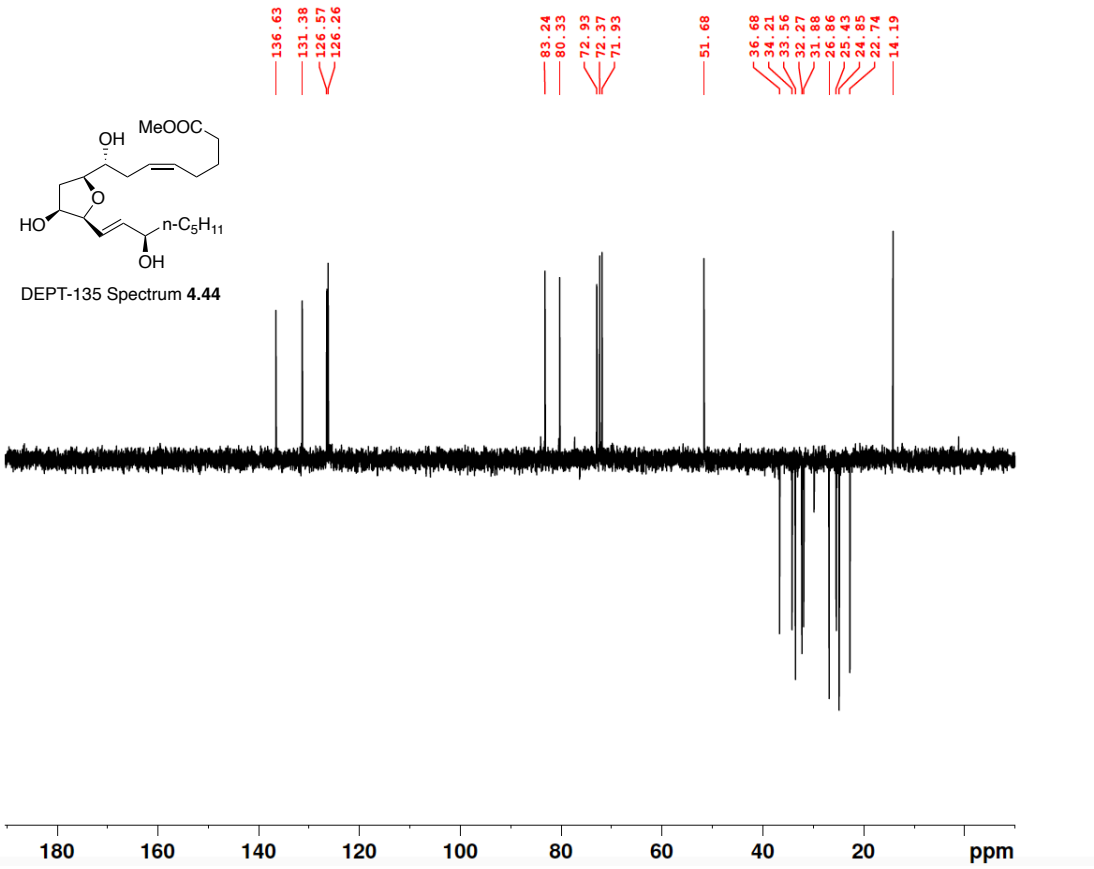

Figure A.62 DEPT-135 (100 MHz, $CDCl_3$) of **4.44**.

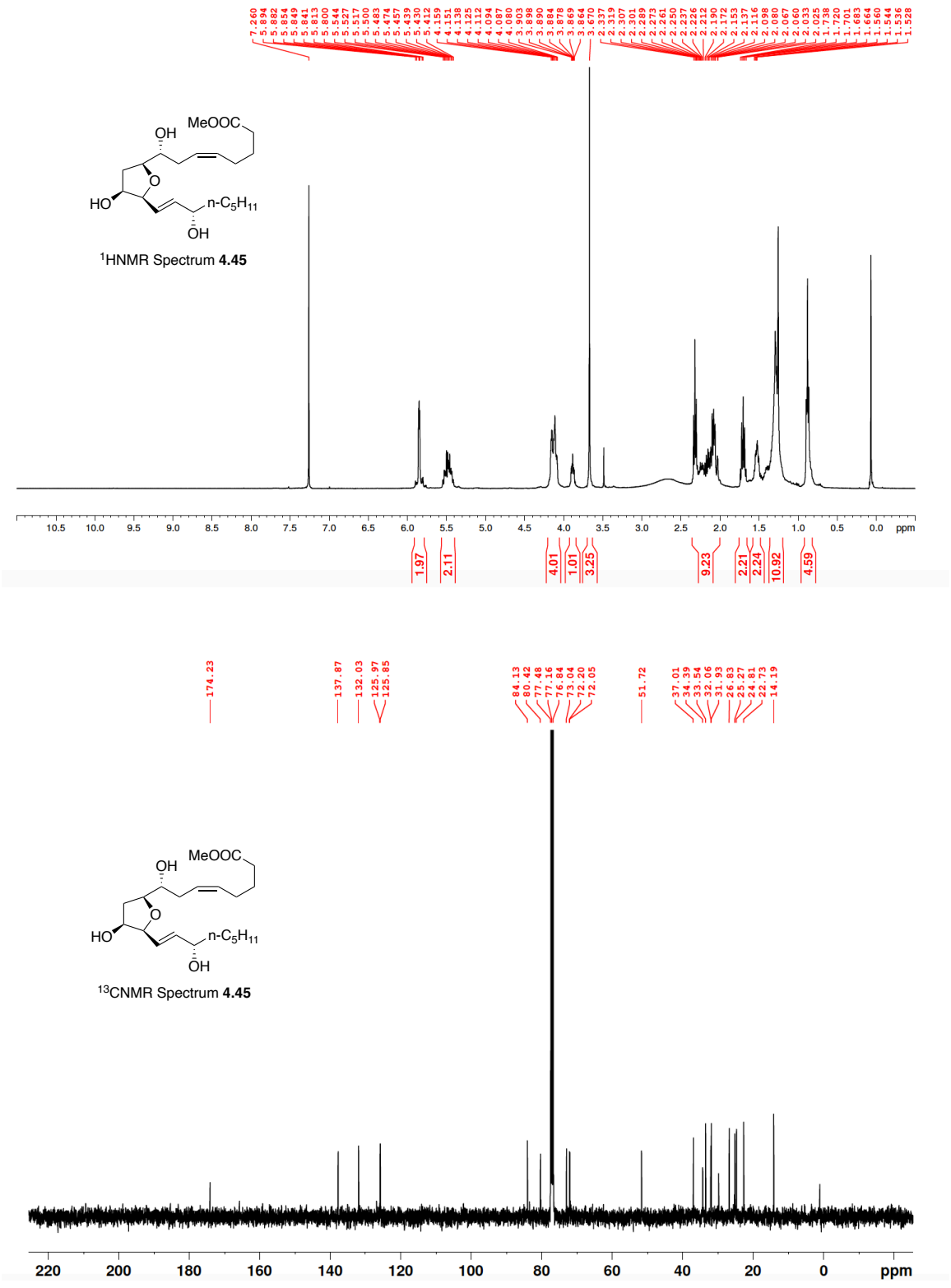

Figure A.63 ^{1}H NMR (400 MHz, $CDCl_3$) and ^{13}C NMR (100 MHz, $CDCl_3$) of **4.45**.

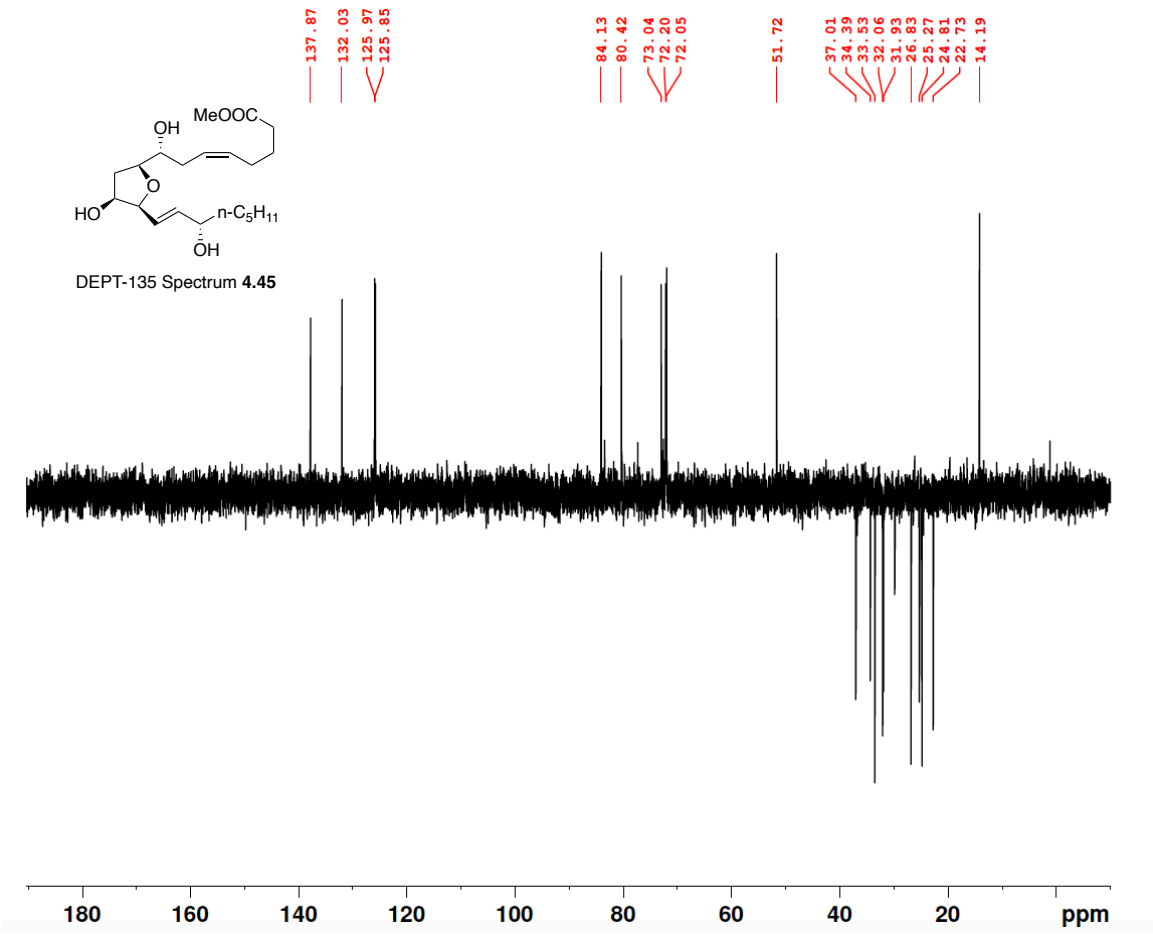

Figure A.64 DEPT-135 (100 MHz, $CDCl_3$) of **4.45**.

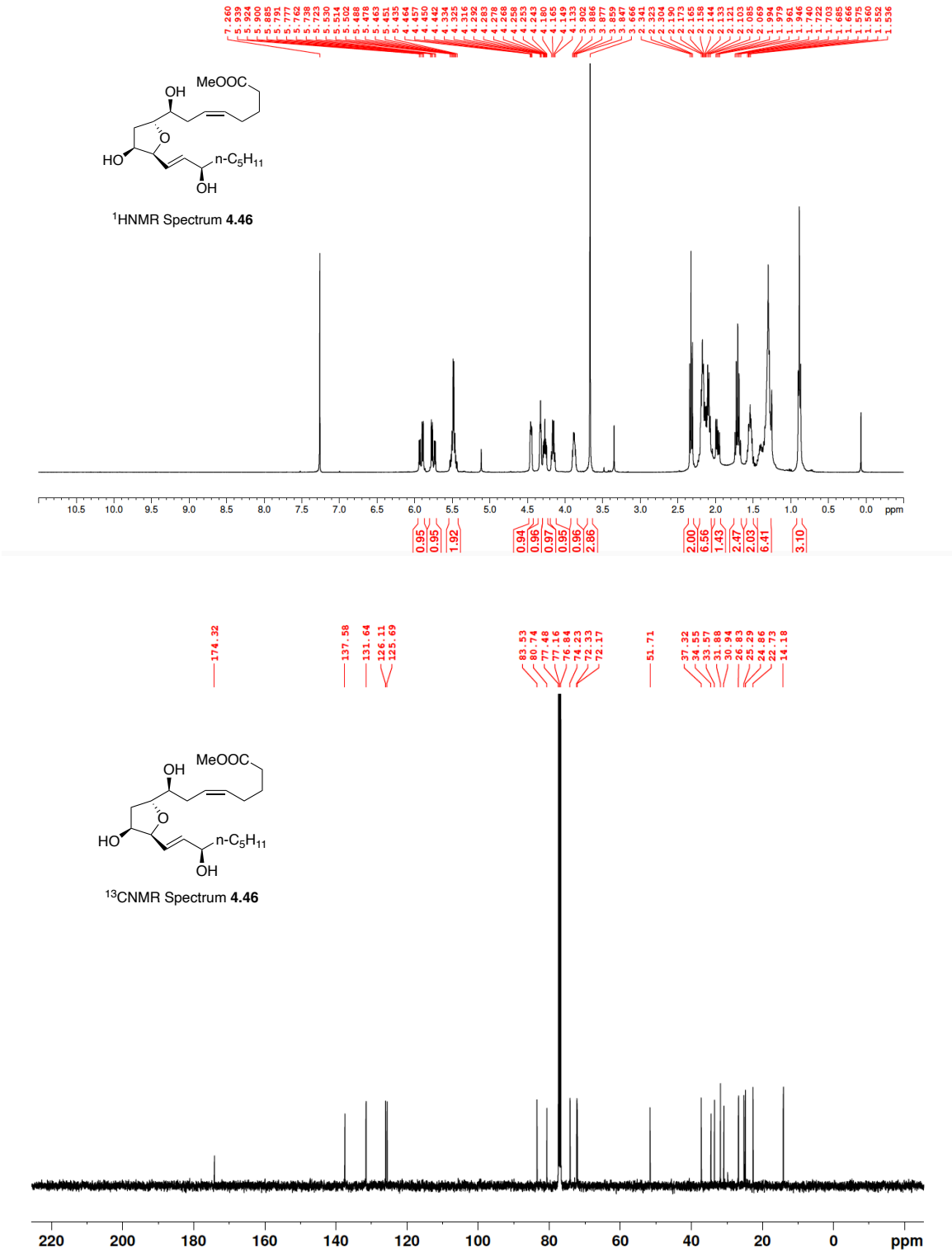

Figure A.65 ^{1}H NMR (400 MHz, $CDCl_3$) and ^{13}C NMR (100 MHz, $CDCl_3$) of **4.46**.

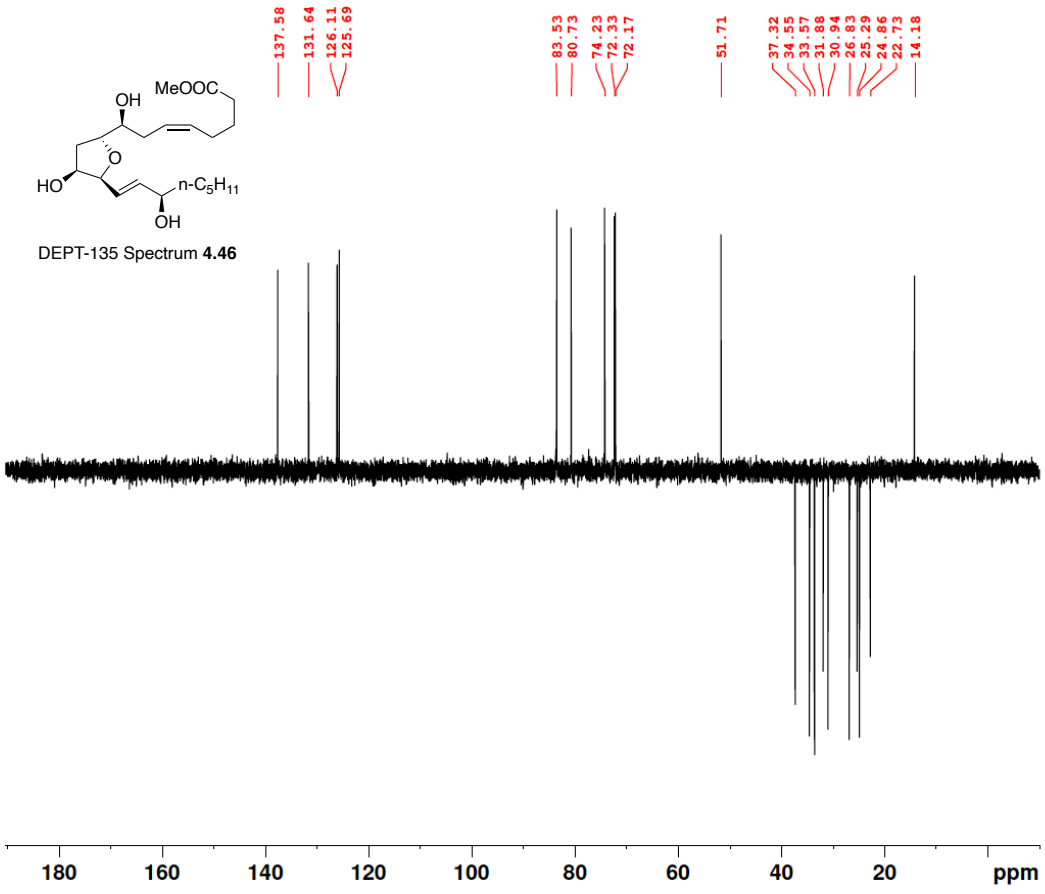

Figure A.66 DEPT-135 (100 MHz, $CDCl_3$) of **4.46**.

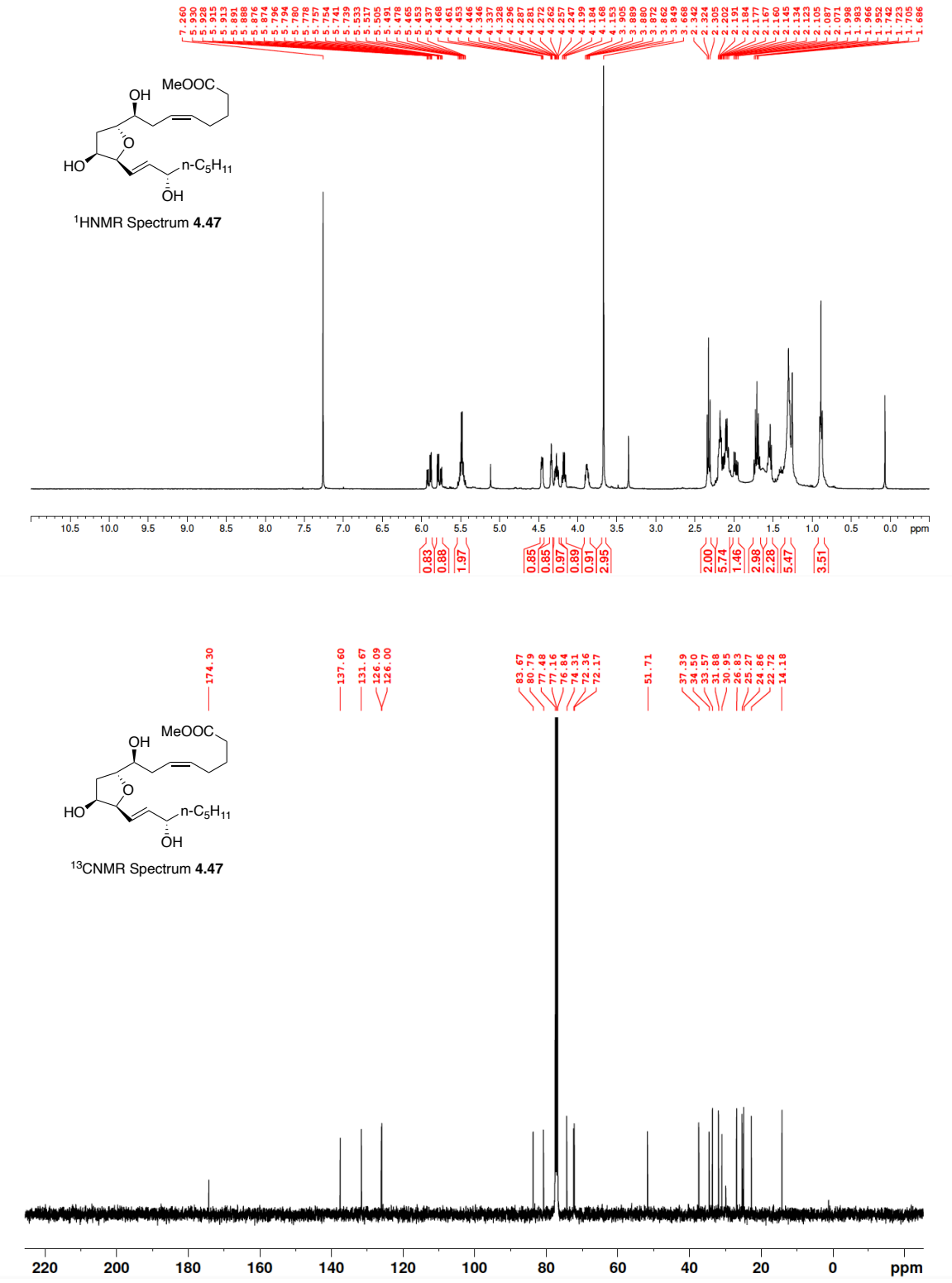

Figure A.67 ^{1}H NMR (400 MHz, $CDCl_3$) and ^{13}C NMR (100 MHz, $CDCl_3$) of **4.47**.

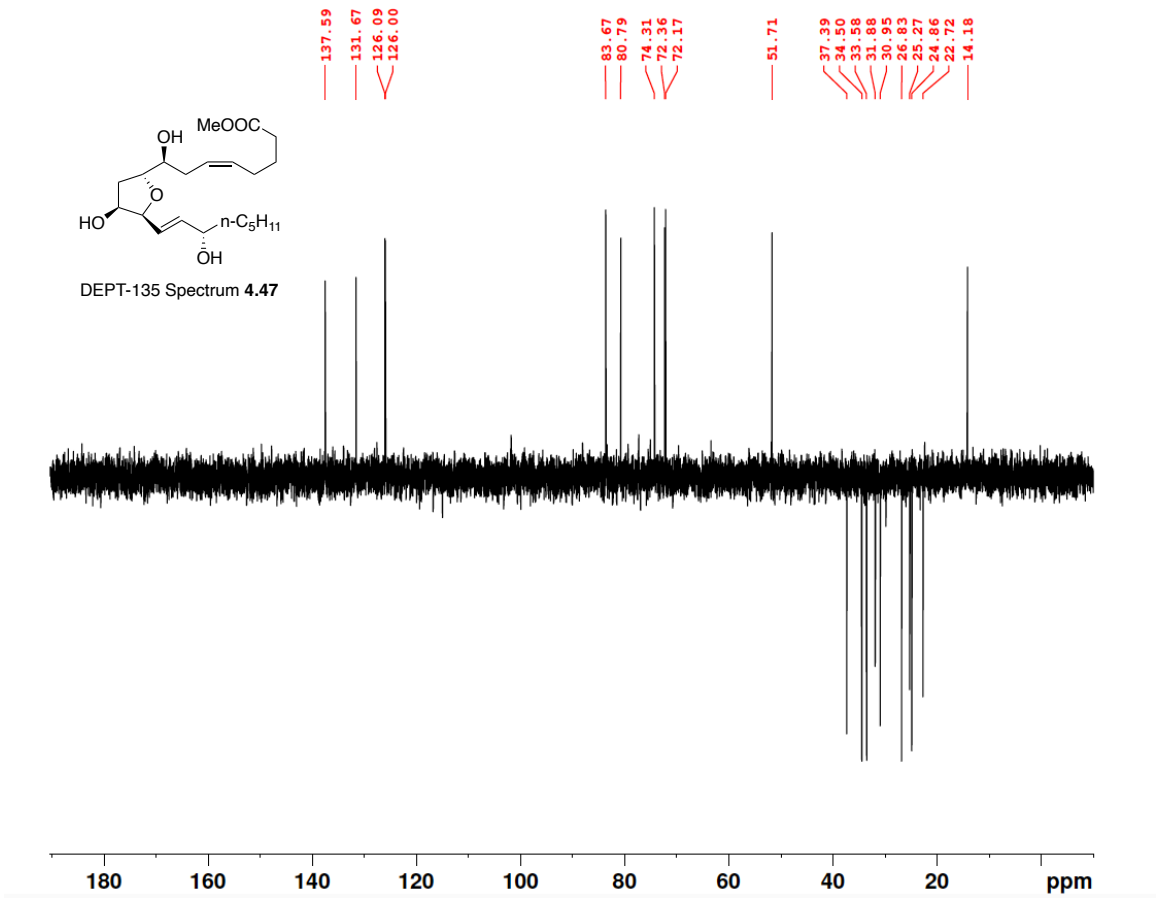

Figure A.68 DEPT-135 (100 MHz, $CDCl_3$) of **4.47**.

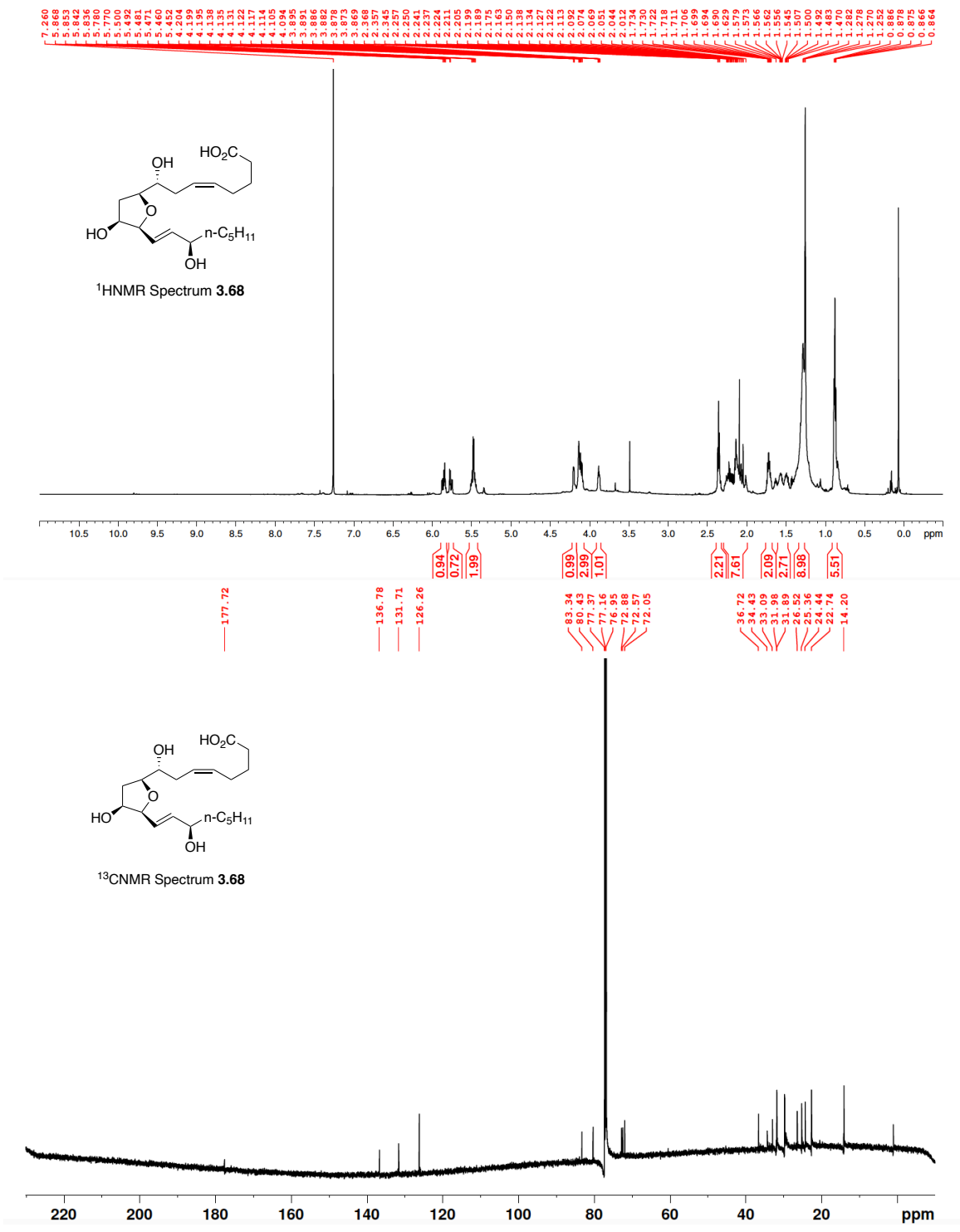

Figure A.69 ^{1}H NMR (400 MHz, $CDCl_3$) and ^{13}C NMR (100 MHz, $CDCl_3$) of **3.68**.

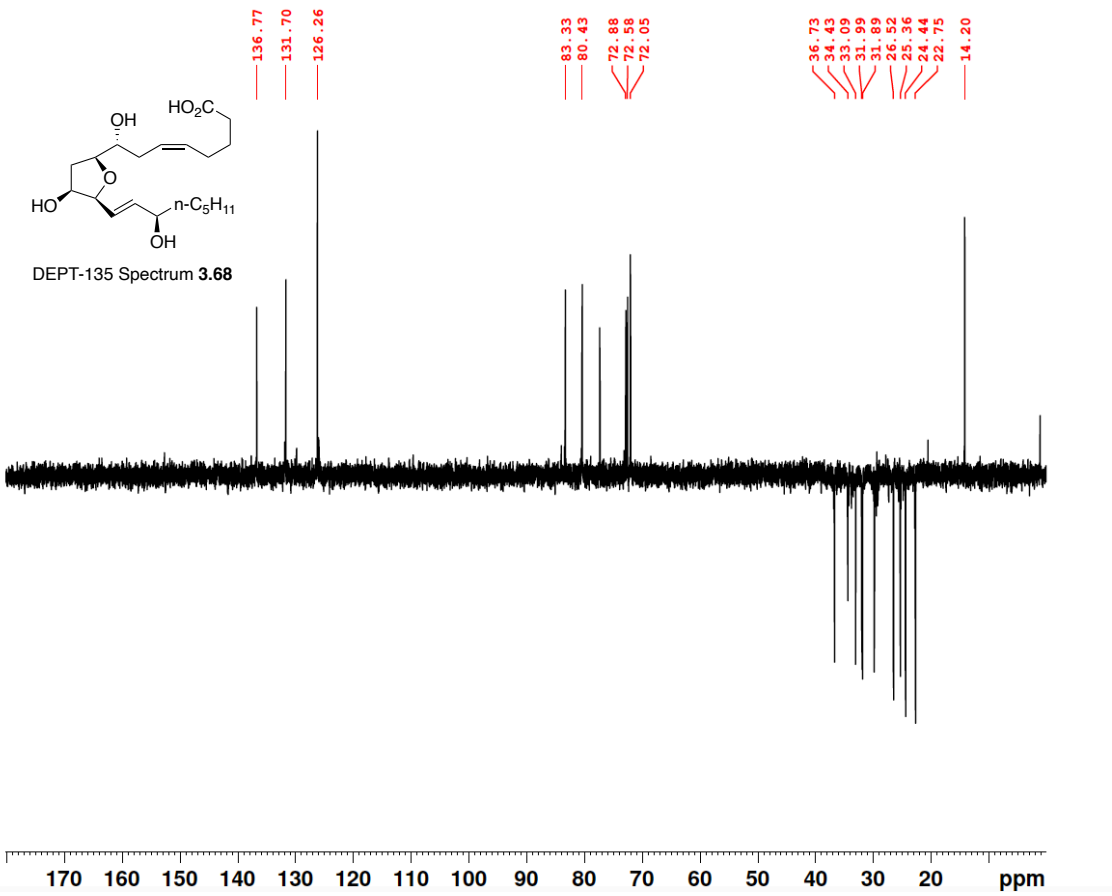

Figure A.70 DEPT-135 (100 MHz, $CDCl_3$) of **3.68**.

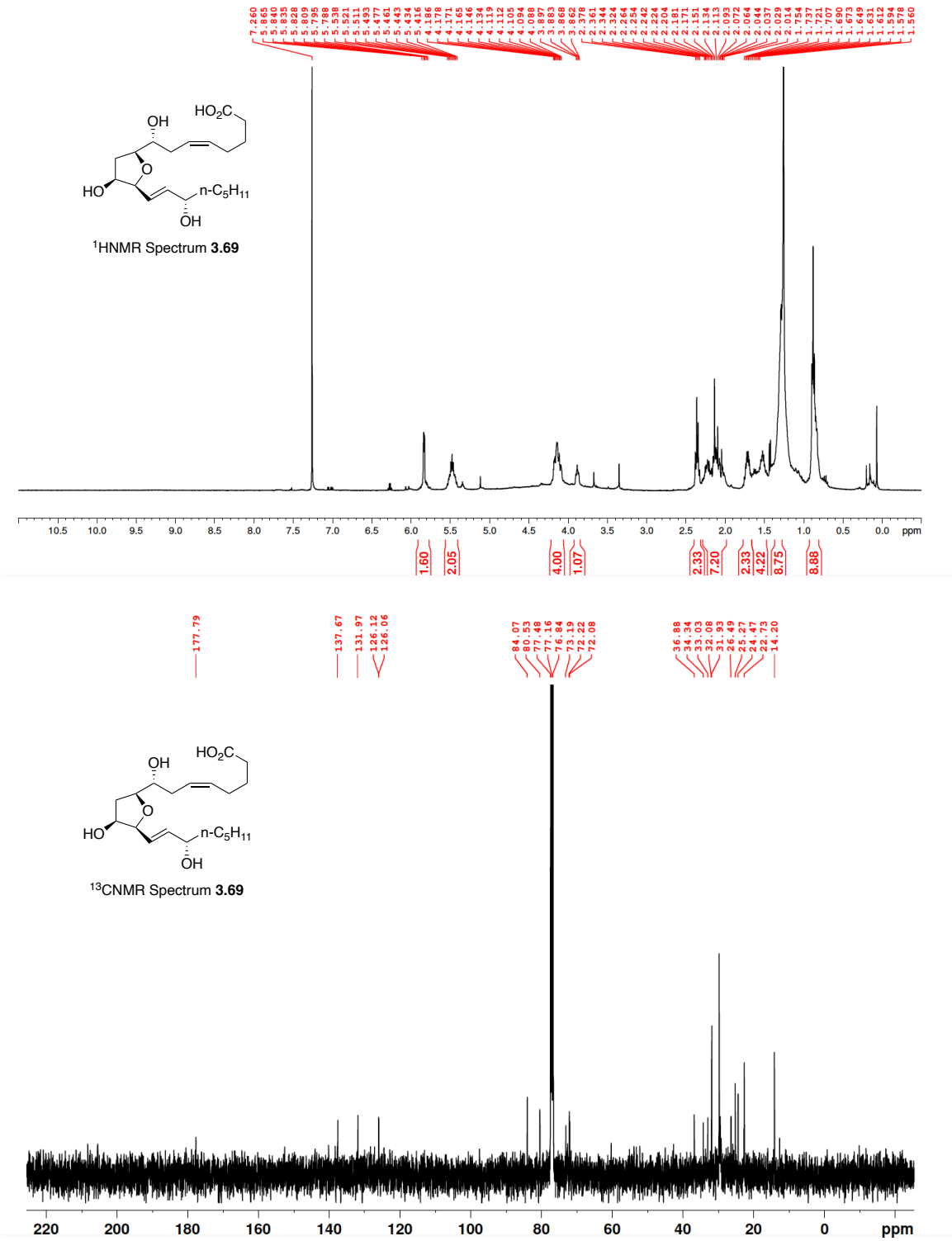

Figure A.71 ^{1}H NMR (400 MHz, $CDCl_3$) and ^{13}C NMR (100 MHz, $CDCl_3$) of **3.69**.

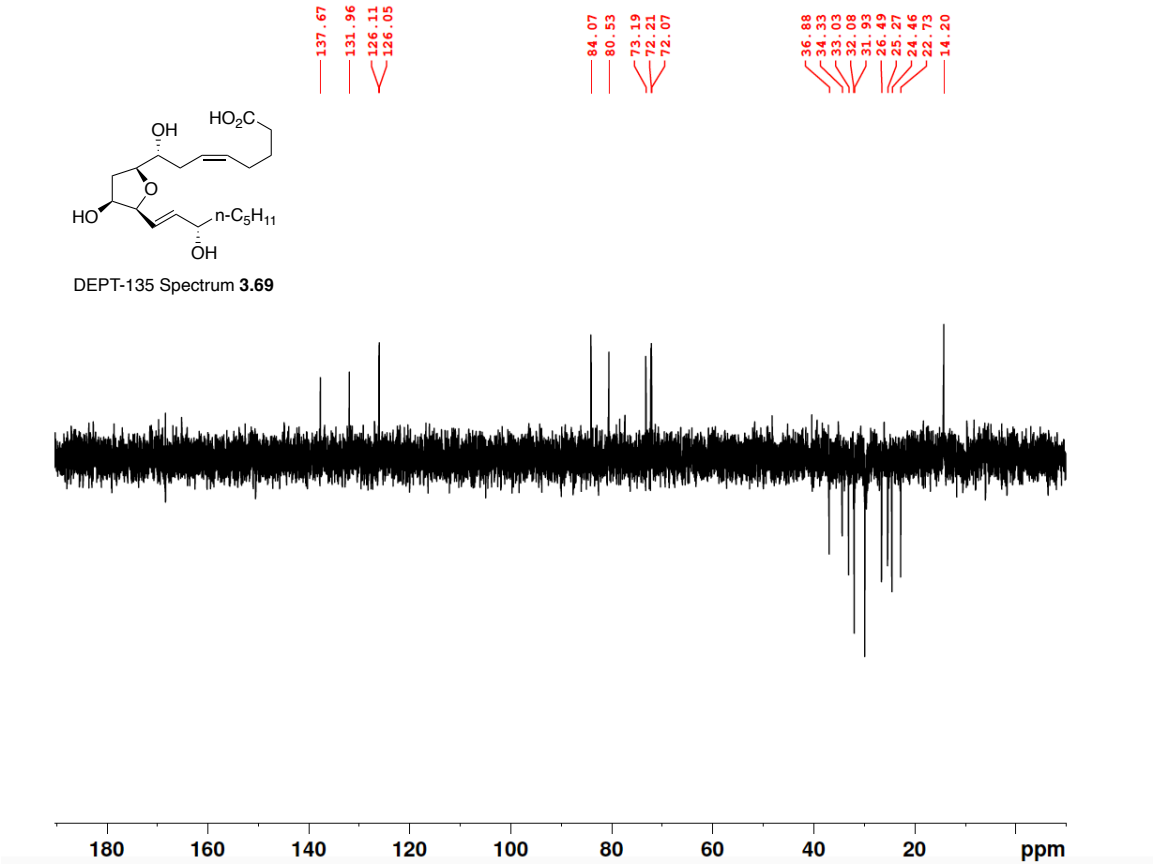

Figure A.72 DEPT-135 (100 MHz, $CDCl_3$) of **3.69**.

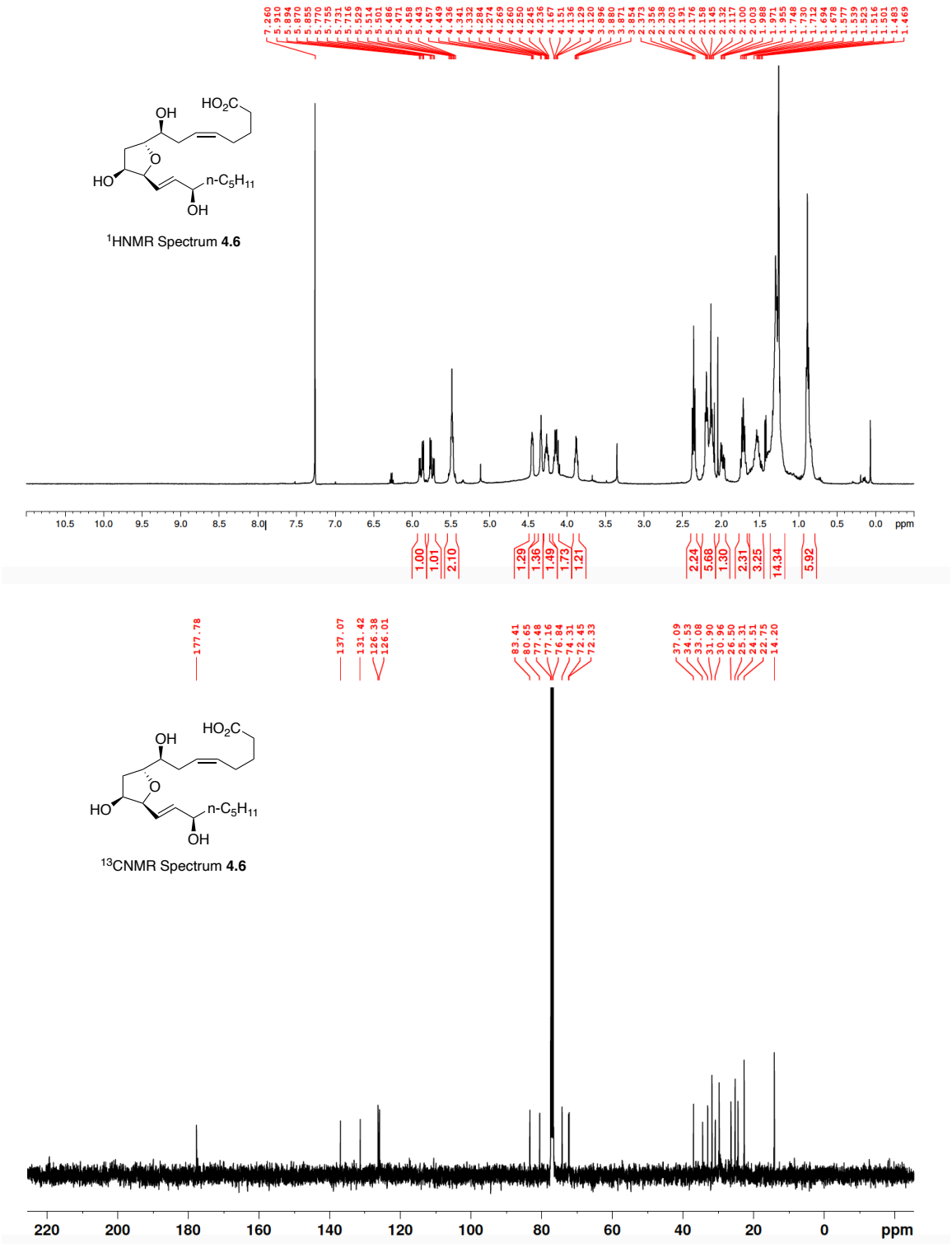

Figure A.73 ^{1}H NMR (400 MHz, $CDCl_3$) and ^{13}C NMR (100 MHz, $CDCl_3$) of **4.6**.

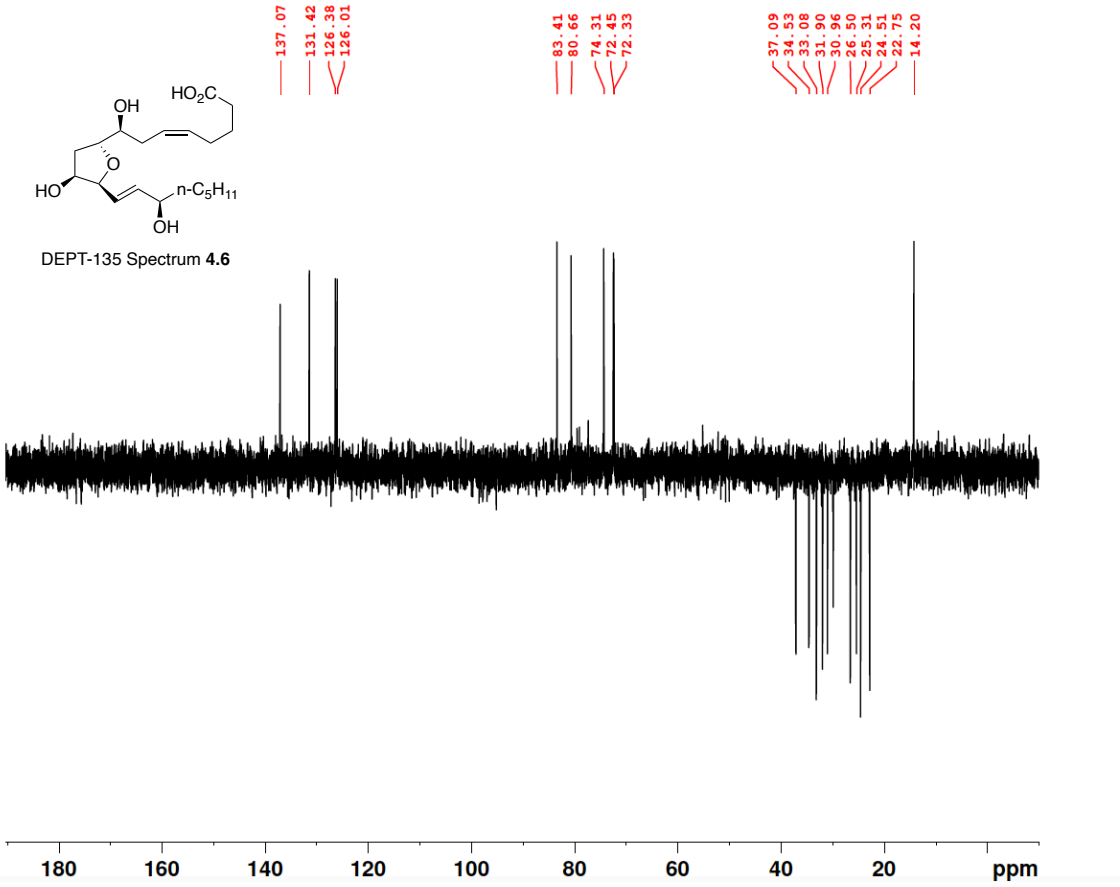

Figure A.74 DEPT-135 (100 MHz, $CDCl_3$) of **4.6**.

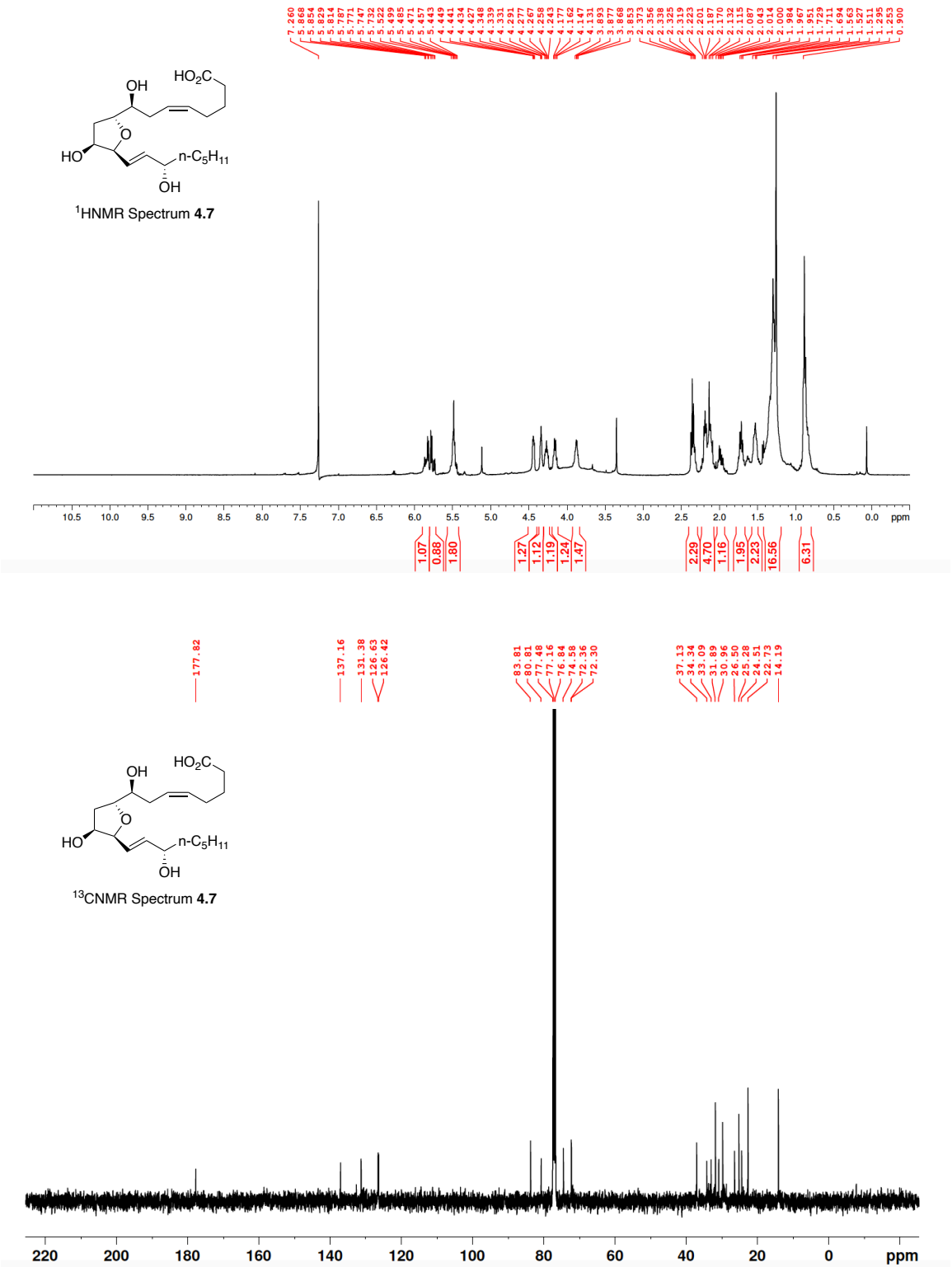

Figure A.75 ^{1}H NMR (400 MHz, $CDCl_3$) and ^{13}C NMR (100 MHz, $CDCl_3$) of **4.7**.

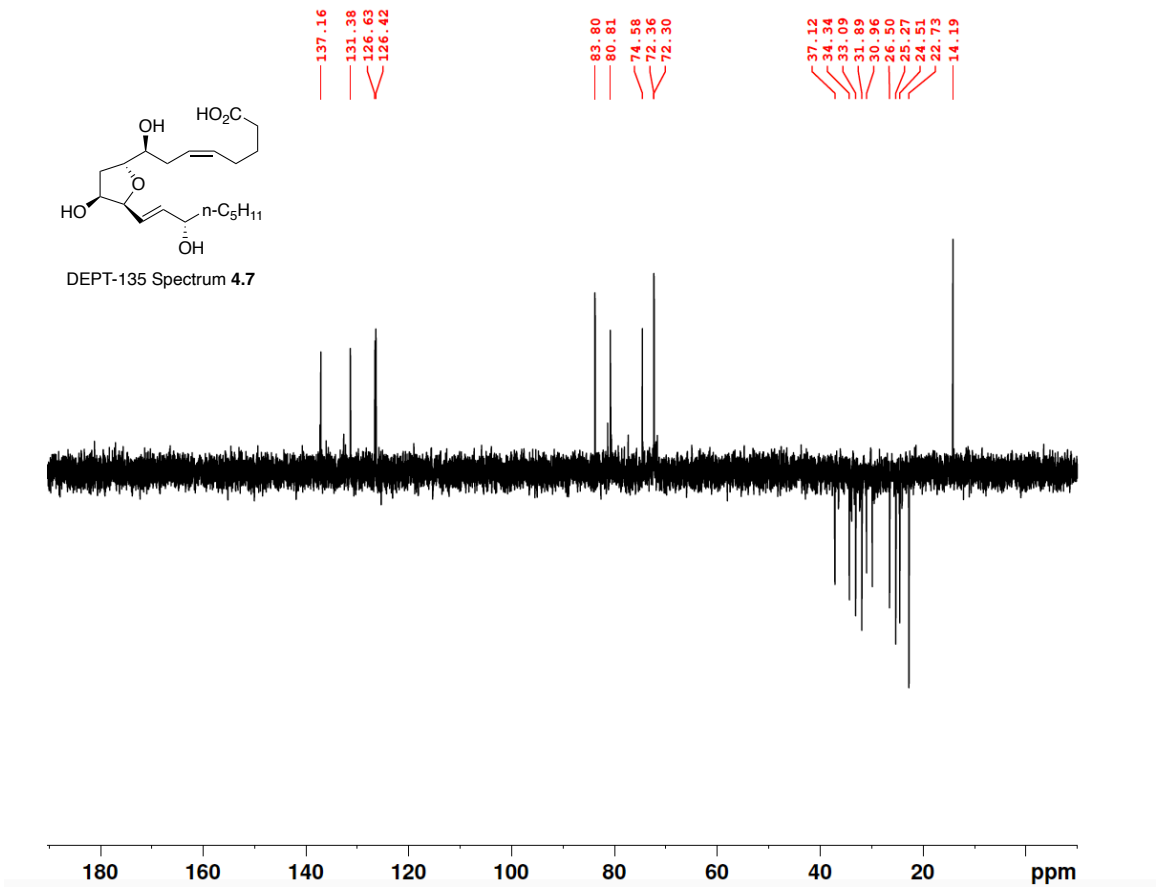

Figure A.76 DEPT-135 (100 MHz, $CDCl_3$) of **4.7**.

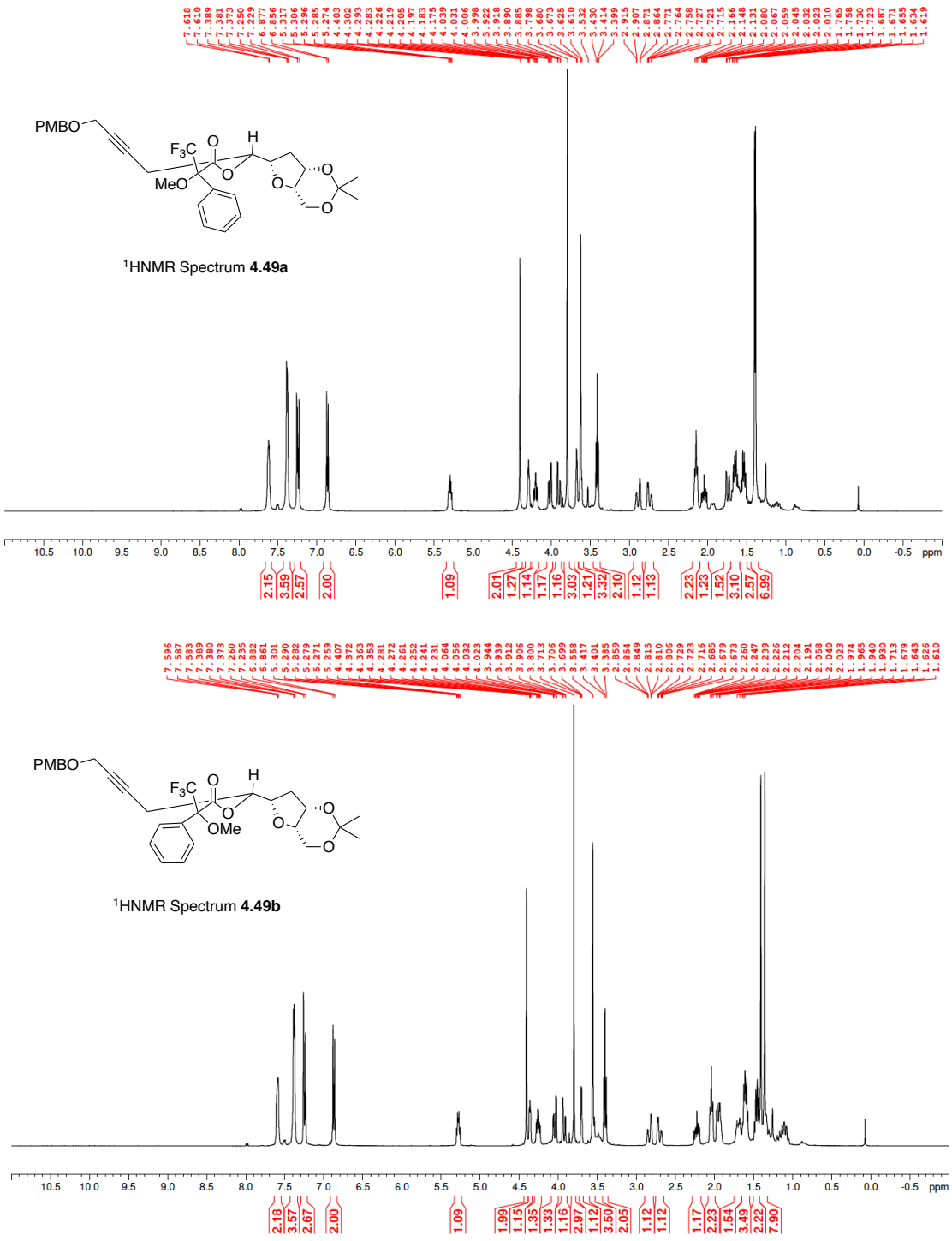

Figure A.77 ^{1}H NMR (400 MHz, $CDCl_3$) of **4.49a** and **4.49b**.

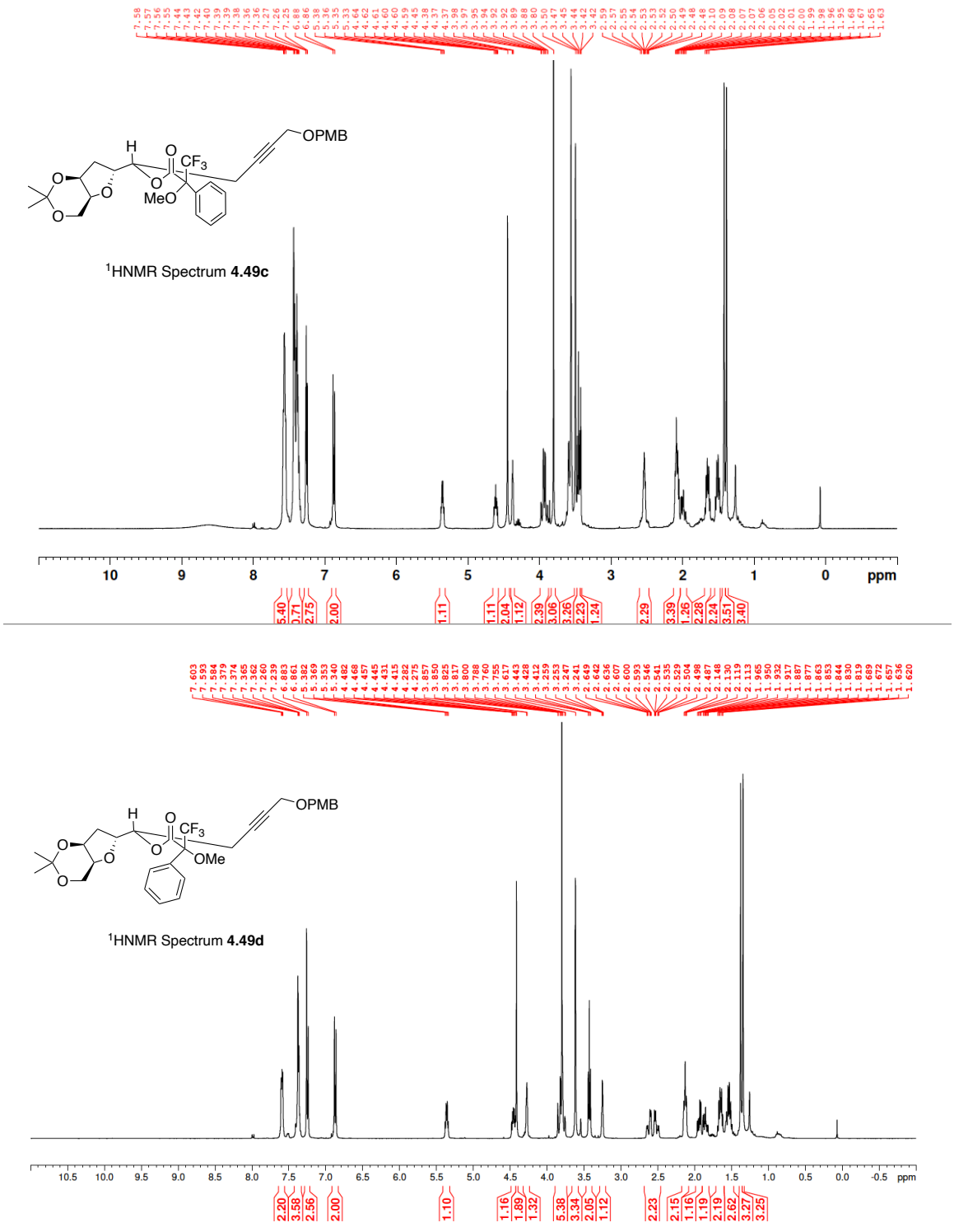

Figure A.78 ^{1}H NMR (400 MHz, $CDCl_3$) of **4.49c** and **4.49d**.

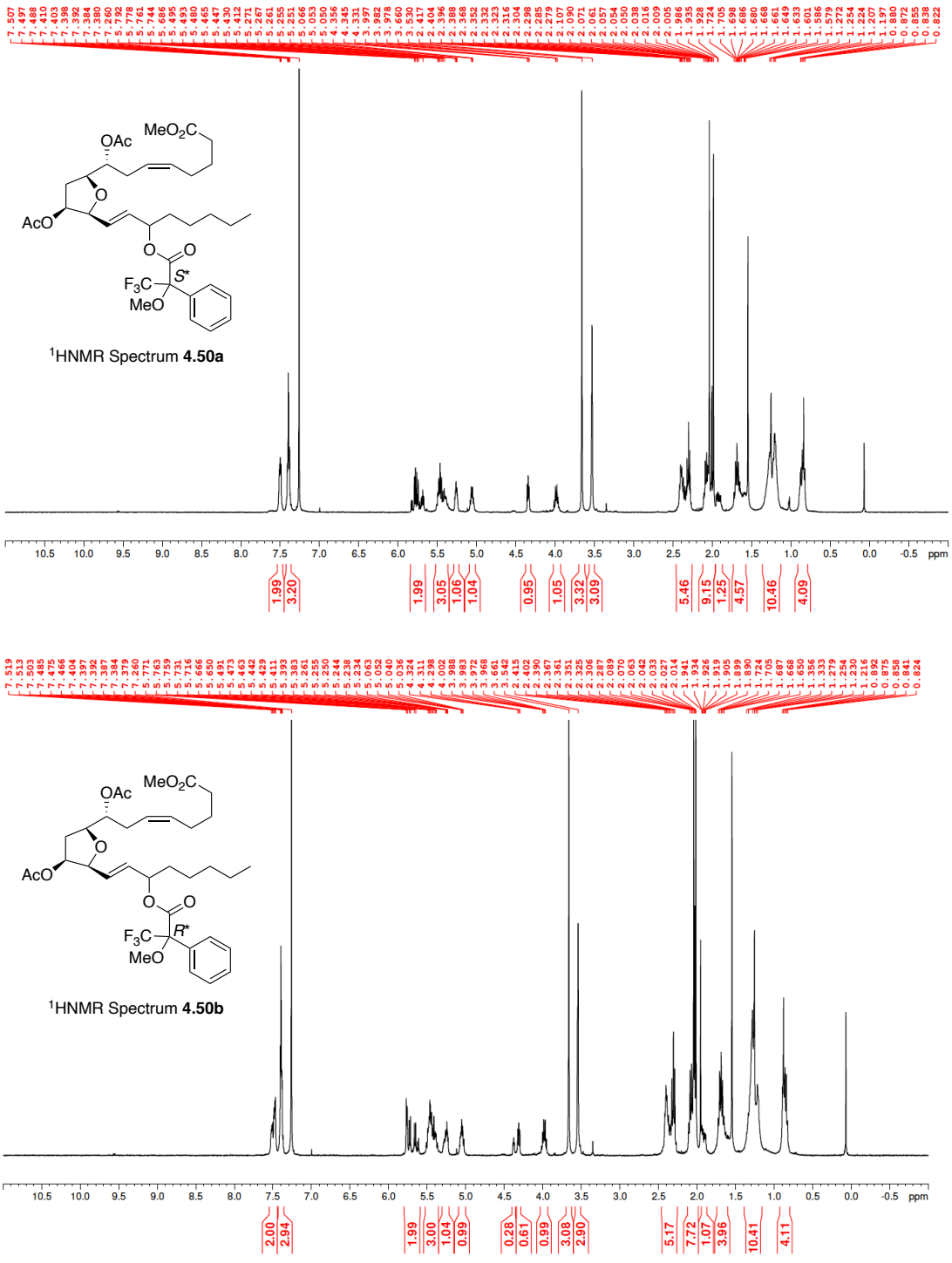

Figure A.79 ^{1}H NMR (400 MHz, $CDCl_3$) of **4.50a** and **4.50b**.